

**OPERATIONAL RISK ASSESSMENT OF OIL AND GAS PIPELINES
SUBJECTED TO INTERNAL CORROSION**

by

Uyen Dao

A thesis submitted to the School of Graduate Studies
in partial fulfillment of the requirements for the degree of

Doctor of Philosophy

Faculty of Engineering & Applied Science

Memorial University of Newfoundland

March 2023

St. John's

Newfoundland, Canada

Dedication

*This research is dedicated to my Dad Anh Chen Dao and my Mom Thi Mach Kieu
who always give me unconditional love and sacrificed everything for my arrival
on this earth and cherished me to become the person I am.*

I am truly blessed to have you both in my life!

ABSTRACT

Oil and gas transportation by pipelines serves as the primary means and the failure of pipelines is another fundamental concern. Under harsh operating conditions, oil and gas pipelines are vital infrastructures facing multiple damages, which increases the risk of metal degradation. Thus, the integrity of the pipeline is crucial to avoid various types of safety accidents at all levels which may cause fatality and substantial economic loss.

To specify, oil and gas pipelines are mostly made of steel or stainless steel and are operated in harsh environmental conditions, due to the susceptibility of metallic characteristics of pipelines' materials to corrosion, oil and gas pipelines are easily corroded. Thus, offshore oil and gas pipelines are facing a high rate of failures due to corrosion. The cost of corrosion-induced asset failure is rising, despite the vast investment in corrosion mitigation and control.

Internal corrosion poses an integrity threat to oil and gas transportation, especially in harsh offshore environments. Internal corrosion including under-deposit corrosion (UDC), microbiologically influenced corrosion (MIC), localized corrosion, uniform corrosion, and erosion is considered one of the major contributing causes of pipeline failures in both onshore and offshore oil and gas industries, leading to significant financial losses. Predicting the internal corrosion rate is essential to ensure asset integrity and cost-effective transportation of oil and gas through pipelines. The study serves as an early warning guide for the integrity management of pipelines against internal corrosion. The work found that pipeline failures are caused by deposition parameters and microbial activities are predicted to be more frequent and dangerous than other factors. UDC and microbiologically influenced corrosion under deposits (UD-MIC) are found to be key contributors to pipeline system failure in the energy, marine, and petroleum industries. The operating parameters, environmental factors, material composition, microbial activity, and deposition parameters are major risk factors. The biotic factors also play a significant role in metal degradation in offshore domains, which enrich

the UDC propagation and formation. Previous studies have not explored the interdependencies of such risk factors. Therefore, it is necessary to develop the probabilistic relationships among prevalent influencing risk factors of UDC and UDC-MIC and define their dependencies. This research seeks to study the complex interactions, controlling parameters, and characteristics that lead to UDC-induced failures. It is followed by analyzing the integrity of pipelines and proposing potential management solutions.

More importantly, with the blooming of alternative energy. Hydrogen, a clean and emission-free fuel is considered a promising energy for the future. Hydrogen blending into existing natural gas pipelines is large-scale and low-cost for hydrogen transportation by pipelines that have the potential to spontaneously ignite Hydrogen leaks. Thus, safety for hydrogen pipelines is necessary to understand when we are talking about the hydrogen industry.

The safety of blended hydrogen pipelines is also studied using the physics and mechanistic approach of hydrogen and pipeline degradation. Understanding the relationship between corrosion rate and hydrogen pipeline degradation can help ensure the safety of blended hydrogen pipelines. This work is also expected to explore further and assess how predictive maintenance can help increase the safety of hydrogen pipelines.

Acknowledgment

First, I would like to express my deep appreciation to my supervisor Dr. Faisal Khan. He has been supervising my doctoral research thesis during the COVID-19 pandemic. It is Dr. Khan who gave me this opportunity to fulfill my childhood dream and provided me with the chance to pursue my Ph.D. program under his supervision. This was a turning point to significantly change my knowledge over the past few years and my career in the future.

Dr. Khan's profound knowledge and rigorous academic philosophy have deeply nurtured and influenced me. I am grateful for all his patience, dedication, and sacrifice for our success. It is a great pleasure to have worked under his supervision.

I genuinely acknowledge my co-supervisors. I sincerely thank Dr. Yahui Zhang for his valuable contribution. He is always available to provide his support, encouragement, and mentorship whenever needed. His critical comments and motivational feedback are precious support for me and this thesis. I wholeheartedly thank Dr. Zaman Sajid who guided my thesis and shared his precious knowledge and skills with me. I am grateful to acknowledge his patience to explain and learn new knowledge with me. I received the foremost help from them in any situation and any time even at midnight on weekends and holidays.

I also would like to express my heartiest gratitude to the *late Prof. Ha Nguyen* at the University of Saskatchewan for all his precious support from the beginning I came to Canada. I really appreciate his time to share his knowledge and advice with me. I will always keep in mind his encouragement and his valuable lessons in both academic work and in life.

I extend a special appreciation to the Faculty of Engineering and Applied Science, School of Graduate Studies of the Memorial University, Centre for Risk, Integrity, and Safety Engineering

(CRISE), at Memorial University. I am grateful to acknowledge the Ministry of Education and Training for supporting me with the Vietnam International Education Development Scholarship (VIED). I would like to extend a special appreciation to the Hanoi University of Mining and Geology (HUMG) for encouraging me to fulfill my program.

I want to extend my heartiest appreciation to my family. With a constant source of love, concern, support, and strength, they always motivate me to achieve a higher degree. To my friends and colleagues, you have all contributed through your encouraging words during the period of my Ph.D. journey. My sincere appreciation also goes to Mr. Trung Tran, Dr. Hai H. Ngo, Dr. Rioshar Yarveysy, Dr. Shams Anwar, Dr. Sidum Adumene, Dr. Amer Aborig, Dr. Mohammad Yazdi, and Dr. Mohammed Taleb.

Table of Contents

<i>ABSTRACT</i>	<i>iii</i>
<i>CHAPTER 1</i>	<i>1</i>
<i>1 Introduction</i>	<i>1</i>
1.1 Background and Motivation.....	1
1.2 Research Objectives	5
1.3 Contributions and novelties.....	7
1.4 Thesis organization	9
1.5 Co-authorship Statement.....	12
<i>CHAPTER 2</i>	<i>13</i>
<i>2 Literature review</i>	<i>13</i>
2.1 Internal corrosion in a pipeline system	13
2.2 Under deposit corrosion susceptibility analysis	14
2.3 Under deposit corrosion failure characteristics	16
2.4 Under deposit corrosion risk assessment	18
2.5 Blended hydrogen pipelines risk assessment	19
2.6 Current state of knowledge and gaps	21
<i>CHAPTER 3</i>	<i>23</i>
<i>3 Modeling and Analysis of Internal Corrosion Induced Failure of Oil and Gas Pipelines</i>	<i>23</i>
3.1 Preface.....	23
3.2 Abstract	23
3.3 Introduction.....	24
3.4 Research Methodology.....	27
3.5 Results and Discussions	35
3.6 Conclusions	50
3.7 Appendix.....	51
<i>CHAPTER 4</i>	<i>65</i>
<i>4 A Bayesian approach to under-deposit corrosion assessment in oil and gas pipelines</i>	<i>65</i>
4.1 Preface.....	65
4.2 Abstract	65
4.3 Introduction	66
4.4 The Proposed Model	70
4.5 Model results	73

4.6	Discussions.....	85
4.7	Conclusions.....	105
4.8	Appendixes.....	106
<i>CHAPTER 5.....</i>		<i>113</i>
5	<i>Dynamic Bayesian network model to study under-deposit corrosion</i>	<i>113</i>
5.1	Preface.....	113
5.2	Abstract.....	113
5.3	Introduction.....	114
5.4	Literature review.....	116
5.5	Dynamic Bayesian Network (DBN) for Asset Failure Analysis.....	119
5.6	The applications of DBN – an industrial case study.....	121
5.7	The Analysis Methodology.....	121
5.8	Results and Discussion.....	128
5.9	Conclusions.....	141
5.10	Appendix.....	143
<i>CHAPTER 6.....</i>		<i>150</i>
6	<i>Risk assessment of oil and gas pipelines failure in Vietnam</i>	<i>150</i>
6.1	Preface.....	150
6.2	Abstract.....	150
6.3	Introduction.....	151
6.4	Risk analysis of natural gas pipeline operation.....	152
6.5	Methodology.....	154
6.6	Results and discussions.....	157
6.7	Conclusions.....	159
6.8	Appendix.....	162
<i>CHAPTER 7.....</i>		<i>164</i>
7	<i>Safety Analysis of Blended Hydrogen Pipelines using Dynamic Object-oriented Bayesian Network.....</i>	<i>164</i>
7.1	Preface.....	164
7.2	Abstract.....	164
7.3	Introduction.....	165
7.4	The proposed model.....	174
7.5	Results and Discussion.....	181
7.6	Conclusions.....	192

7.7 Appendix	193
CHAPTER 8.....	196
8.1 Summary	196
8.2 Conclusions	198
8.3 Recommendations	199
9 References	200

List of Figures

<i>Figure 1. 1: Interrelationship among key influencing factors causing pipelines' failure.....</i>	<i>4</i>
<i>Figure 1. 2: Research flowchart.....</i>	<i>9</i>
<i>Figure 1. 3: The organization of the thesis and the relevant publications.....</i>	<i>11</i>
<i>Figure 3. 1: A schematic view of the proposed research methodology.....</i>	<i>28</i>
<i>Figure 3. 2: A graphical representation of a DOOBN.....</i>	<i>31</i>
<i>Figure 3. 3: A Bayesian subnetwork model for UDC.....</i>	<i>36</i>
<i>Figure 3. 4: A Bayesian subnetwork for uniform corrosion.....</i>	<i>38</i>
<i>Figure 3. 5: Bayesian network for localized corrosion.....</i>	<i>40</i>
<i>Figure 3. 6: A Bayesian subnetwork model for erosion.....</i>	<i>41</i>
<i>Figure 3. 7: A Bayesian subnetwork model for MIC.....</i>	<i>42</i>
<i>Figure 3. 8: A Bayesian subnetwork model for asset failure of a gas pipeline.....</i>	<i>43</i>
<i>Figure 3. 9: OOBN for asset failure due to internal corrosion of oil and gas pipeline.....</i>	<i>44</i>
<i>Figure 3. 10: A DOOBN indicating the asset failure over time due to internal corrosion.....</i>	<i>45</i>
<i>Figure 3. 11: Variations of three scenarios over time in the study.....</i>	<i>46</i>
<i>Figure 3. 12: Accuracy of the proposed model for each time step.....</i>	<i>48</i>
<i>Figure 3. 13: Validation of the DOOBN model in this study</i>	<i>49</i>
<i>Figure 4. 1: Overview of the UDC effective corrosion rate model for oil and gas pipelines</i>	<i>71</i>

<i>Figure 4. 2: The inert deposit susceptibility submodel</i>	<i>74</i>
<i>Figure 4. 3: The deposit permeability aspect of the UDC model.....</i>	<i>75</i>
<i>Figure 4. 4: Reactive deposit susceptibility submodel</i>	<i>76</i>
<i>Figure 4. 5: Organic deposit impact submodel.....</i>	<i>77</i>
<i>Figure 4. 6: Influence diagram for the galvanic corrosion due to parasitic inhibitor loss mechanism</i>	<i>78</i>
<i>Figure 4. 7: Influence diagram of the under-deposit galvanic cell mechanism's components.....</i>	<i>79</i>
<i>Figure 4. 8: Overview of factors influencing UDC</i>	<i>80</i>
<i>Figure 4. 9: Overview of the UD-MIC BN's influence diagram</i>	<i>81</i>
<i>Figure 4. 10: The deposition susceptibility assessment submodel</i>	<i>84</i>
<i>Figure 4. 11: The pipeline's seabed elevation profile and the defect densities on pipe joints, adapted from (El-Raghy et al., 2000).....</i>	<i>86</i>
<i>Figure 4. 12: Results of effective corrosion rates assessment of the Gulf of Suez crude pipeline failure.....</i>	<i>88</i>
<i>Figure 4. 12: Results of effective corrosion rates assessment of the Gulf of Suez crude pipeline failure.....</i>	<i>89</i>
<i>Figure 4. 13: Pipeline elevation profile obtained from MFL tool adapted from (H. Mansoori et al., 2017).....</i>	<i>92</i>
<i>Figure 4. 14: Wet gas pipeline effective UDC rate assessment</i>	<i>93</i>
<i>Figure 4. 15: Overview of the UDC BN implementing information from the subsea water injection pipeline failure.....</i>	<i>96</i>
<i>Figure 4. 16: Overview of BN evaluating effective corrosion rates for the crude product traps</i>	<i>98</i>
<i>Figure 4. 17: Inspected pipeline segment's schematic.....</i>	<i>100</i>
<i>Figure 4. 18: Overview of the BN implementation of the tie-in spool area</i>	<i>103</i>

<i>Figure 4. 18: Overview of the BN implementation of the tie-in spool area</i>	104
<i>Figure 5. 1(a):A static BN</i>	120
<i>Figure 5. 2: A schematic view of the methodology for the case study</i>	122
<i>Figure 5. 3: The corroded pipe dimensions</i>	125
<i>Figure 5. 4: A framwork of the MSC process</i>	127
<i>Figure 5. 5: BN model of UDC asset failure for subsea pipelines</i>	130
<i>Figure 5. 6: DBN results for pipe failure (PoF), simulation developed in Genie Software</i>	135
<i>Figure 5. 7: CDF of PoF</i>	137
<i>Figure 5. 8: Comparison of dynamic Bayesian Network and Industrial data</i>	138
<i>Figure 5. 9: Correlation of MCS parameters in the UDC model</i>	140
<i>Figure 5. 10: Results of sensitivity analysis</i>	141
<i>Figure 6. 1: FT of the underwater pipelines</i>	161
<i>Figure 7. 1: Hydrogen production and delivery</i>	166
<i>Figure 7. 2: The structure of equipment in a pressurization station</i>	169
<i>Figure 7. 3: Structure of a hydrogen pipeline transport system</i>	170
<i>Figure 7. 4: Hydrogen-associated degradation mechanisms</i>	172
<i>Figure 7. 5: Proposed methodology for hydrogen transportation mechanism</i>	175
<i>Figure 7. 6: A graphical representation of a DOOBN</i>	177
<i>Figure 7. 7: Fault tree of hydrogen degradation mechanism</i>	179
<i>Figure 7. 8: Hydrogen release OOBN model</i>	181
<i>Figure 7. 9: Hydrogen blistering (HB) submodel</i>	183
<i>Figure 7. 10: Hydrogen corrosion cracking (SCC) submodel</i>	184
<i>Figure 7. 11: Hydrogen embrittlement (HE) submodel</i>	186
<i>Figure 7. 12: Corrosion fatigue (CF) submodel</i>	187

<i>Figure 7. 13: Material failure submodel</i>	187
<i>Figure 7. 14: Operational failure submodel</i>	188
<i>Figure 7. 15: Hydrogen release submodel</i>	189
<i>Figure 7. 16: Chances of hydrogen release over time</i>	190
<i>Figure 7. 17: Results of sensitivity analysis</i>	191

List of Tables

<i>Table 1. 1: Research objectives and tasks</i>	6
<i>Table 3. 1: OOBN for asset failure due to internal corrosion of oil and gas pipeline</i>	51
<i>Table 3. 2: Case history parameters in the DOOBN model</i>	62
<i>Table 3. 3: The operational summarized data of the gas pipeline during six years</i>	64
<i>Table 4. 1: The effective corrosion rates assessed using data with different levels of uncertainty</i> .	90
<i>Table 4. 2: Effective UDC rates and their respective probabilities of occurrence</i>	94
<i>Table 4. 3: The BN representing the subsea water injection pipeline’s case history</i>	95
<i>Table 4. 4: Effective UDC rates based on information from the wet crude product traps case study</i>	99
<i>Table 4. 5: Six-year-long data summary statistics for the export gas</i>	101
<i>Table 4. 6: Overview of the corrosion features identified</i>	101
<i>Table 4. 7: Overview of the effective UDC rates simulated for two points on the pipeline segment</i>	102
<i>Table 4. 8: The node descriptions and discretization ranges of the UDC susceptibility model</i>	106
<i>Table 4. 9: Deposit permeability submodel descriptions and discretization ranges</i>	106
<i>Table 4. 10: Reactive deposit susceptibility submodel’s nodes, states, and discretization values</i> .	107
<i>Table 4. 11: The organic deposit’s inhibiting impact submodel components</i>	107
<i>Table 4. 12: Details of the galvanic corrosion due to parasitic inhibitor loss mechanism’s submodel</i>	108
<i>Table 4. 13: The under deposit galvanic cell mechanism’s node properties and discretization</i> ...	108
<i>Table 4. 14: The UD-MIC submodel's properties</i>	109
<i>Table 4. 15: Case history parameters as implemented in the model</i>	110
<i>Table 5. 1: Details of parameters and their associated distributions in MCS</i>	127
<i>Table 6. 1: List all the primary events for the construction of the FT</i>	162
<i>Table 6. 2: Probability of Top and Intermediate events</i>	163
<i>Table 7. 1: The basic events for hydrogen release</i>	180

Nomenclature

Acronyms

UDC	Under deposit corrosion
(D)BN	(Dynamic) Bayesian network
(D)OBN	(Dynamic) Object-oriented Bayesian network
MIC	Microbiologically influenced corrosion
SRB	Sulfate-reducing bacteria
SRA	Sulfate-reducing archaea
APB	Acid-producing bacteria
MA	Methanogenic archaea
DAG	Directed acyclic graphs
CPTs	Conditional probability tables
P(U)	Probability distribution
ROC	receiver operating characteristic
AUROC	Area under the receiver operating characteristic
MEG	mono-ethylene glycol
SAW	Submerged arc-welded
MCS	Monte Carlo simulation
P _{CO2}	Partial pressure of CO ₂
FTA	Fault tree analysis

PDF	Probability density function
CB	Crystal Ball software
LPG	Liquefied petroleum gas
CCR	Catalytic reforming
PDH	Propane dehydrogenation
H2NG	Hydrogen and natural gas
HE	Hydrogen embrittlement
HB	Hydrogen blistering
SCC	Stress-corrosion cracking
HELP	Hydrogen-enhanced localized plasticity
HEDE	Hydrogen-enhanced decohesion
HSC	Hydrogen stress cracking
CF	Corrosion fatigue

Variables, parameters, and Functions

P_F	Failure pressure of pipeline
LSF	Limit state function
Pop	Operating pressure
$M(T)$	The length correction factor
t	Wall thickness (mm)
f_u	Tensile strength (Mpa)
d(T)	Defect depth at time T
D	Pipe outer diameter (mm)

d_{mean}	Defect depth or loss in wall thickness
c_d	Radial corrosion growth
c_L	Axial corrosion growth
d_p	The predicted maximum pit depth
OD	Outer diameter
CDF	Cumulative density function
$P(U E)$	Conditional probability of even E

CHAPTER 1

1 Introduction

1.1 Background and Motivation

Energy is considered a modern industry and the sustainable development of the economy. Energy consumption has increased rapidly in recent years, leading to significant energy demand growth. Thus, achieving a high energy production rate has gained much attention. Therefore, transportation of oil and gas through pipelines has increased, as are safety concerns. Pipelines serve as the primary means of oil and gas transportation, and the failure of pipelines is another primary concern. Material and weld failure are among the leading causes of pipeline failures globally (Qiao et al., 2017; Y. Yang et al., 2017).

Under harsh operating conditions, oil and gas pipelines are vital infrastructures facing corrosion-related damages, which increase the risk of metal degradation. The oil, gas, and chemical industry statistics indicate that 70% of all mechanical integrity failures are related to piping. In addition to causing significant economic loss when pipelines are damaged, corrosion poses a significant environmental threat (Fan et al., 2022; Koch, 2017; Mazumder et al., 2020).

In the operation of pipelines, oil, and gas pipelines are threatened by internal corrosion, particularly in the stringent offshore environment. Numerous elements affect the rusting mechanism, which has detrimental environmental repercussions that are many-sided. Despite the massive investments in corrosion reduction and control, the cost of corrosion-related asset failure is rising.

The issue with today's oil and gas pipelines is that they are vulnerable to external environmental elements, including nature. On the other hand, external, operational, and environmental factors contribute significantly to metal degradation in offshore pipeline corrosion.

As for the pipeline operating in high temperatures, the cold day and night temperature differences are more significant. Corrosion of oil and gas pipelines can be triggered by acid-alkali, rain, and

snow, which impacts the regular transportation of oil and gas resources. Although the pipeline maintenance managers have made specific preliminary preparations, corrosion might still impair the pipeline before it is used for transportation. Oil and gas pipelines are susceptible to corrosion because they are long-term buried below and exposed to variations in temperature, moisture, and the natural environment. Other factors leading to pipeline corrosion are material selection, construction technology, and construction methods (Lu et al., 2020; Schmitt et al., 2009). Besides, various chemical substances are present in oil and gas resources, and chemical components are more diverse and complex. For instance, collisions between the hydrogen sulfide element found in oil and gas resources will bring about certain chemical reactions during transportation. It results in the crystal lattice of the interior of oil and gas pipelines changes, which significantly reduces the pipeline's corrosion resistance.

Several internal driving mechanisms affect pipeline integrity, such as erosion, localized corrosion, uniform corrosion, UDC, and MIC. Unlike uniform corrosion, pitting is more detrimental. It is because of challenges in its detection, estimate, and deterrence. Complex driving mechanisms of UDC and MIC limit their monitoring, assessment, and management. UDC is one of the severe types of localized degradation connected with devastating consequences. Several studies have proposed that UDC poses a far-reaching threat to the integrity of carbon steel pipelines in the oil and gas sector (Almahamedh, 2015; H. Mansoori et al., 2017). Thus, exploring and investigating the UDC mechanism can help industries to develop an asset integrity framework for their offshore oil and gas operations.

Corrosion creates severe safety and integrity challenges in offshore and onshore industrial sectors. It is noted for its involvement in comprehensive corrosion failure and the related outcomes. UDC in pipelines has been reported as a pivotal contributor to sudden system failure across the energy,

oil, gas, and marine industries, described as corrosion occurring beneath while close to deposits on a steel surface (Suarez et al., 2019; Tajallipour et al., 2011). The nature of the environmental, characteristic, and operational factors could further enhance the high rate of degradation of the steel pipelines (Adumene et al., 2020; Okoro et al., 2022; Shekari et al., 2017b; Yazdi, Khan, & Abbassi, 2022).

UDC is stochastic and uncertain; therefore, there are challenges in assessing it. Some researchers have attempted to understand UDC behaviour; for example, see (Almahamedh, 2015; Brown & Moloney, 2017; Kagarise et al., 2017; Vera et al., 2012). However, no literature captures mechanistic, experiential, quantitative risk, and probabilistic models and the knowledge of the phenomenon and its mechanisms is still growing. Limited and insufficient understanding of UDC stochastic behaviour may result in improper integrity management tools to deal with corroded oil and gas pipelines. Furthermore, interdependencies among different risk factors are unknown. Therefore, it is crucial to investigate the interrelationship among the corrosion influencing factors, shown in Fig 1.1, such as environmental factors, materials composition, operational factors, and deposit-related factors, and their effects on the failure characteristics of oil and gas pipeline systems.

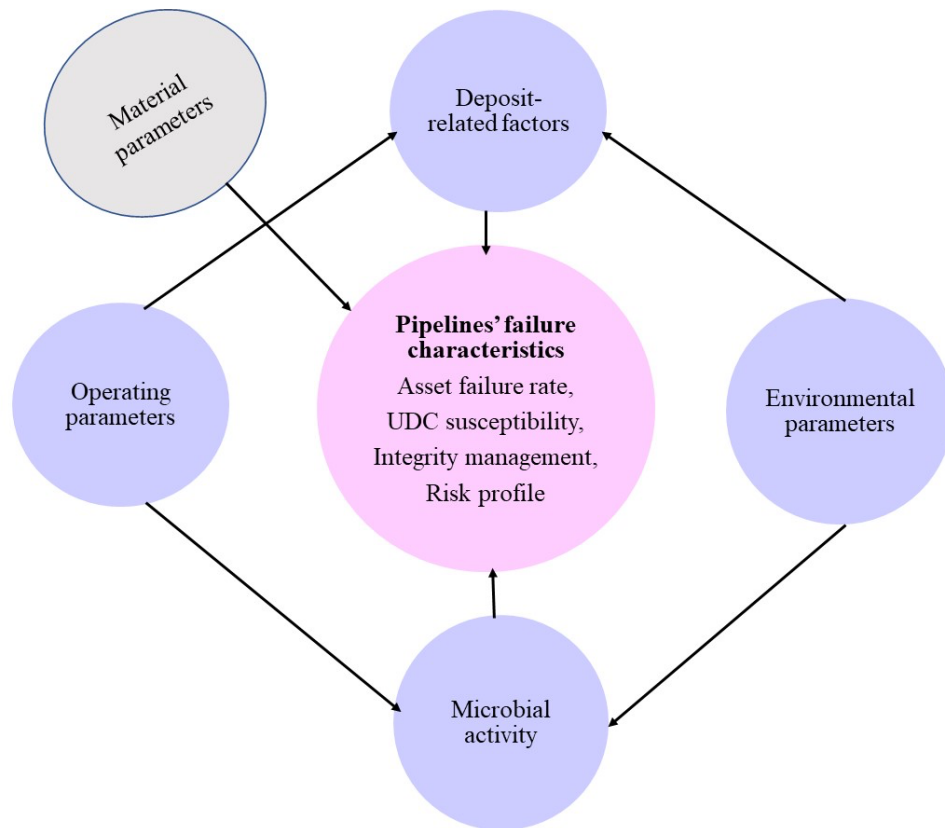


Figure 1. 1: Interrelationship among key influencing factors causing pipelines' failure

It demands further research investigations to understand the behavior of internal corrosion and UDC, particularly corresponding failure probabilities, and the development of a risk-based integrity assessment for corroding oil and gas pipelines.

The existing models cannot correctly capture the non-linear effects of the physio-chemical parameters on the UDC rate and the failure probability prediction simultaneously. Moreover, they also do not capture the collective impact of the damage-causing mechanisms and conditions leading to UDC on the degradation rates. Few related pieces of literature (Kuang & Cheng, 2015; Qin et al., 2015; X. Wang & Melchers, 2017) only estimated the effect of multi-failure modes' dependencies on the remaining strength of pipelines affected by UDC.

Predicting failure using a regression model and comparing these results with a probabilistic model can help to reach the theoretical and practical aspects of UDC. A thorough review of the existing literature reveals that they cannot capture the stochastic and dynamic nature of UDC failures of oil and gas pipelines for a risk-based integrity assessment. This study is performed to fill such research gaps.

In addition to oil and gas pipelines, hydrogen transportation faces multiple safety challenges (X. Li et al., 2020; J. Liu et al., 2021; Witkowski et al., 2017). A cost-effective way is to study the feasibility of using current oil and gas pipelines for hydrogen transportation. Therefore, this study also proposes a methodological framework for safe hydrogen transport using the existing infrastructure of oil and gas pipelines. Based on the risk assessment of the conditional pipelines (Fang et al., 2019; PHMSA, 2017; W. Wang et al., 2021), the proposed methodological framework utilizes the physics and mechanistic approach of hydrogen-associated degradation in pipelines. In addition to providing safety guidelines, the model also highlights that controlling the corrosion rate can help ensure the safety of blended hydrogen pipelines.

1.2 Research Objectives

The primary research objectives of this thesis are to develop a risk assessment methodology for the failure of oil and gas pipelines due to UDC, then map that into the safety of hydrogen pipelines.

This thesis attempts to answer the following questions:

- i. How do different risk factors interact in corrosion mechanisms and affect asset integrity?
- ii. What are key performance indicators that ensure pipeline integrity over time?
- iii. How can industrial practices of asset damage due to corrosion be compared to theoretical knowledge of corrosion?
- iv. How can existing oil and gas pipelines transport hydrogen fuel safely?

With these research questions in mind, the objectives of this research are:

- i. To illustrate different corrosion behavior and identify the potential internal corrosion modes in the system.
- ii. To develop a novel UDC rate model.
- iii. To develop a novel probabilistic model for operational risk assessment for pipeline failure characteristics.
- iv. To develop the probabilistic correlations among the main risk factors.
- v. To develop a dynamic risk of hydrogen pipelines through existing pipeline infrastructure.

Table 1.1 presents the corresponding tasks performed to achieve these objectives.

Table 1. 1: Research objectives and tasks

Objective	Task
To illustrate different corrosion behavior and identify the potential internal corrosion modes in the system.	Task 1: Develop a DOOBN model to present interactions of risk factors in internal corrosion.
To develop a novel UDC rate model.	Task 2: Proposing a BN model to predict the UDC rate.
To develop a novel probabilistic model for operational risk assessment for pipeline failure characteristics.	Task 3: Proposing a BN model to assess susceptibility to UDC and estimate failure probability.

<p style="text-align: center;">To develop the probabilistic correlations among the main risk factors.</p>	<p>Task 4: Develop a DOOBN model to assess the asset failure probability. It also proposes a model to study oil and gas asset failure.</p>
<p style="text-align: center;">To develop a dynamic risk of hydrogen pipelines through existing pipeline infrastructure.</p>	<p>Task 5: Providing a DOOBN model to study the mechanisms and physics of failure with hydrogen-associated degradation.</p>

1.3 Contributions and novelties

The contributions and novelty of this research are developing probabilistic models for different corrosion mechanisms based on theoretical knowledge and comparing them to industrial practices.

The highlights of contributions are as below:

1. A novel failure assessment model for internal corrosion: the model identifies interdependencies among influencing risk factors and their probabilistic correlations. The model is validated using filed data, and an early warning guide for the integrity management of pipelines is developed.
2. A state-of-the-art Bayesian network (BN) model is proposed: the model assesses susceptibility and under-deposit corrosion rate using new and improved susceptibility and expected corrosion rate tools. Model applications are illustrated using four case studies of pipeline failures due to UDC, and results are validated using a sweet gas pipeline case study.
3. An innovative, dynamic operational safety assessment model for multiple UDC defects interactions: a probabilistic framework for corrosion mechanism is proposed based on available mechanisms and theory. Operationalization of the framework is shown using an

industrial case study. The model indicates the difference in regression and the BN approach predicting failure.

4. A risk assessment model for natural gas release: a fault tree analysis (FTA) and fuzzy theory are integrated into the methodology. The model investigates key factors causing asset failure and the release of natural gas.
5. A dynamic model to study the mechanisms and physics of failure of the hydrogen-blended pipeline is proposed: the proposed model explains how low-strength steel is less susceptible compared to high-strength steel pipes for hydrogen-induced failure. The model can study the impacts of moisture, internal stress, and loss of metal ductility on the safety of blended hydrogen pipelines.

Fig. 1.2 summarizes the research roadmap for this thesis.

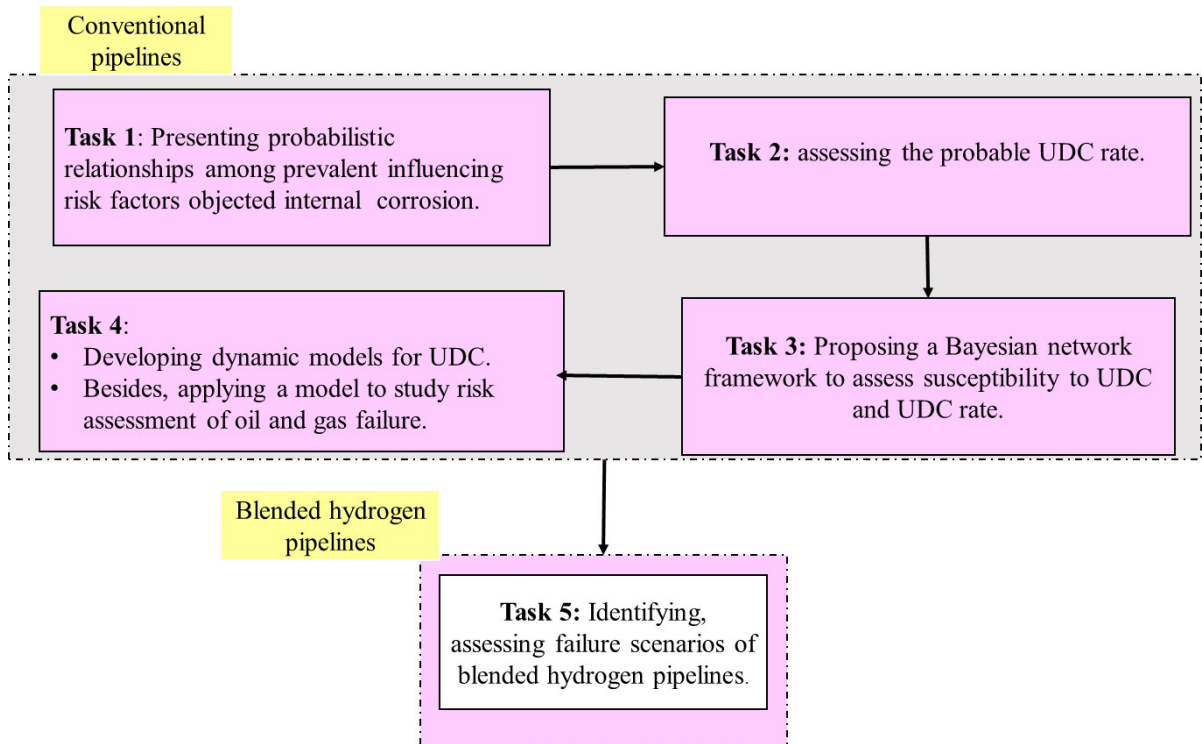


Figure 1. 2: Research flowchart

1.4 Thesis organization

The thesis is written in the format of manuscripts. The four peer-reviewed journal papers and one international conference paper are the primary outcomes of this work and are presented in this thesis. The organization of this thesis is sketched in Figure 1.3. The introduction and literature review are presented in Chapters 1 and 2. Chapters 3 to 7 present technical articles, and finally, Chapter 8 concludes this thesis and provides recommendations for future work. Further details are discussed below:

Chapter 1 shows this thesis’s motivations, objectives, and novel contributions. It also provides an outline of how this thesis is organized.

Chapter 2 presents a systematic literature review available and identifies the research gap. The systematic literature review discusses internal corrosion, under-deposit corrosion analysis susceptibility, and available studies on integrity analysis leading to asset failures of oil and gas pipelines. It also identifies literature on risk assessment of blended hydrogen pipelines.

Chapter 3 covers in-depth modeling and analysis of internal corrosion for oil and gas pipelines. A dynamic object-oriented Bayesian network (DOOBN) is developed to represent the probabilistic relationships among influencing risk factors and define their dependencies. This chapter is published in *Reliability Engineering and System Safety* journal.

Chapter 4 proposes a Bayesian approach to UDC assessment and its susceptibility analysis. This chapter has been submitted to *the Journal of Process Safety and Environmental Protection* and is under review.

Chapter 5 provides a dynamic model of UDC over time. The proposed model is based on a theoretical perspective, and a comparison is made to industry practices. The chapter is published in *the Journal of Reliability Engineering and System Safety*.

Chapter 6 proposes a risk assessment for oil and gas pipelines by constructing a fault tree analysis (FTA) to determine the most significant hazards that lead to failure events. Risk profiles at varying degrees of asset damage are developed using stochastic analysis. This chapter is published in the *International Journal of Engineering and Technology*.

Chapter 7 provides a dynamic model to study the mechanisms and physics of failure of the hydrogen-blended pipeline. It is based on a comprehensive understanding of the risks of conventional pipelines for hydrogen transportation and proposes a new model for safe hydrogen transportation. It has been submitted to *the Internal Journal of Hydrogen Energy* and is Decision in Process.

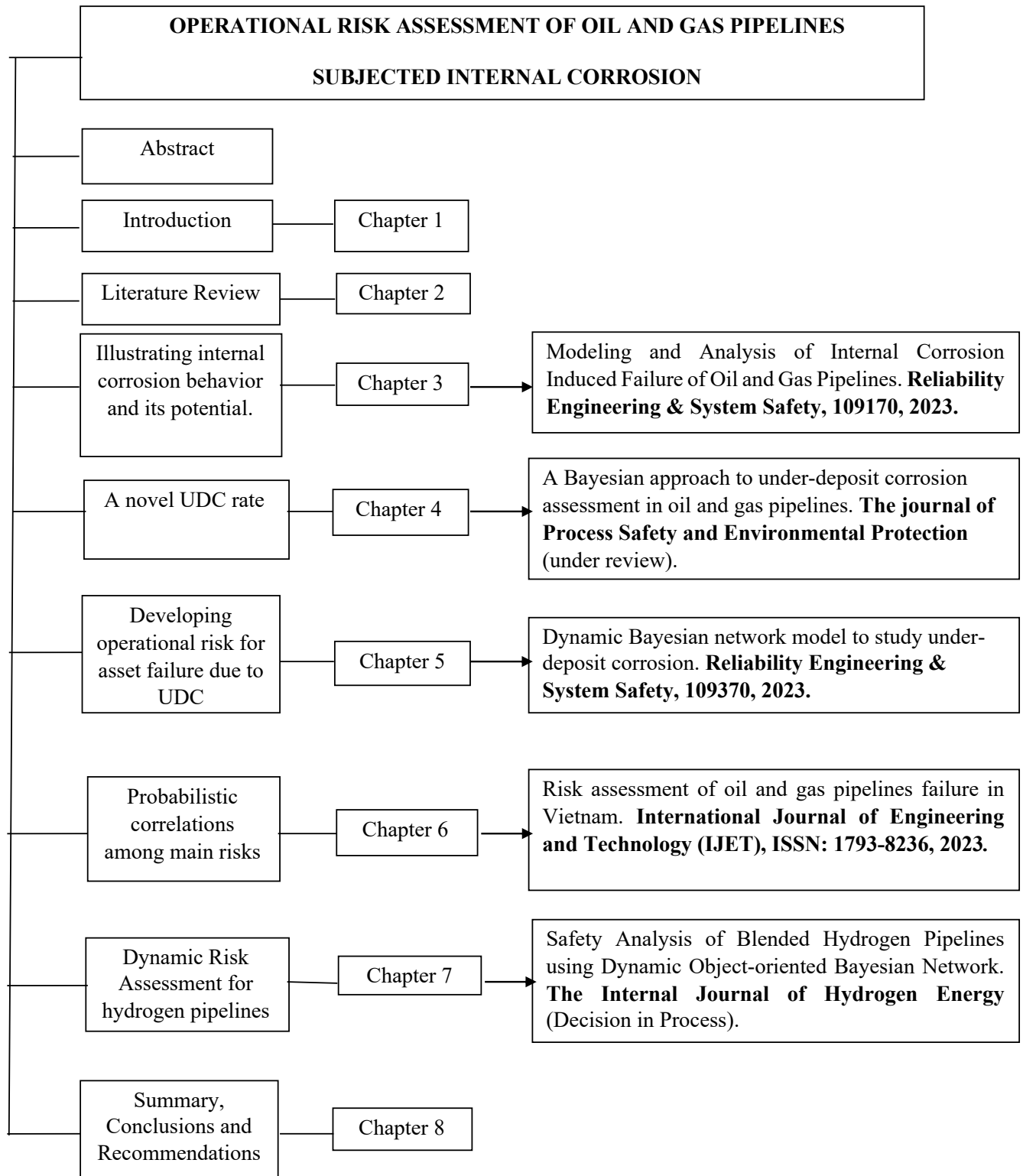


Figure 1. 3: The organization of the thesis and the relevant publications

1.5 Co-authorship Statement

I am the primary author of this thesis under the direct supervision of Dr. Faisal Khan and the co-supervision of Dr. Yahui Zhang and Dr. Zaman Sajid. This thesis consists of five main tasks following by five papers. I developed and discussed a conceptual understanding of the model presented and its potential applications; Carried out the literature review; Performed and wrote the initial drafts of all papers, performed analysis, and developed models in software; Reviewing and editing the manuscripts based on feedback from co-authors and journal reviewers. Subsequently, co-authors revised and edited the drafts. Dr. Faisal Khan formulated the project, granted the research question; Helped me develop the research concept, methodology, and models; Guidance in data analysis, and re-organizing and review of the manuscripts and thesis. Drs. Yahui Zhang and Zaman Sajid provided revise drafts and analyze software use and testing models; Review of the manuscripts and thesis. Details of the contributions of each author are acknowledged at the start of Chapters 3 to 7.

CHAPTER 2

2 Literature review

2.1 Internal corrosion in a pipeline system

Transportation using pipelines is the most effective mode for large-scale plans. A pipeline system consists of a pipeline, cathodic protection stations, a pipeline communication system, various types of valves, an automatic monitoring system, and dispatching. Due to the susceptibility of metallic characteristics to corrosion, oil, and gas pipelines are easily corroded, and leakage accidents bring serious safety risks to the operation of equipment as well as human life.

UDC, MIC, localized corrosion, uniform corrosion, and erosion are the five main types of internal corrosion, causing pipeline failures. When applying the case study to determine the probability of occurrence, the available literature (Papavinasam et al., 2010; Shabarchin & Tesfamariam, 2016; Thodi et al., 2013; Y. Yang et al., 2017) show that they have not been reviewed to assess their credibility or feasibility the models. Thus, a Bayesian network assessing the probability of various types of internal corrosion (susceptibility model) based on the parameters above is in need.

UDC, is known as a serving type of pitting corrosion, which is complicated to detect, predict, and prevent (Bhandari et al., 2015; Shekari et al., 2017a; J. Zhao, 2014). Thus, oil and gas pipelines suffering from UDC are one of the most dangerous modes for asset integrity. UDC describes the growth and spread of corrosion beneath or close to accumulated deposits as a result of the relation of various deposit-related factors with microbial activities. Under-deposit corrosion (UDC) is a stochastic deterioration process, influenced and sparked by deposit-related variables and microbial activity. Understanding the multiple mechanisms of the UDC process is vital to address the complicated development of deposition parameters and bacteria activities.

From the available literature, the understanding of the UDC mechanisms is currently restricted (Obot, 2021a; Place et al., 2009). Thus, the important risk factors that interact to cause UDC have not been examined in the models of this study. The literature suggests that these interactions could change the potential of corrosion and make the pipeline systems vulnerable to UDC (Hou et al., 2018). UDC causes minor surface excavations that ultimately lead to the pipelines being perforated. This mutualistic group aggressively modifies and complicates the electrochemical reaction, which causes a rapid rate of deterioration. Under prolonged exposure, oil and gas pipeline systems affected by UDC may encounter complicated and unpredictable failure processes. UDC has been extensively reported as annually causing the loss of billions of dollars (Mahidashti et al., 2020; Z. B. Wang et al., 2022).

As a result, it required to have better knowledge UDC propagation and formation mechanisms through a robust rate-based prediction of pipeline failures due to UDC in the service life the of pipeline system. This serves as an early warning guide for the integrity management of pipelines. Hydrogen blended with natural gas is a large-scale modern way for future transportation by pipelines. A blended hydrogen pipeline has the potential to spontaneously ignite hydrogen leaks. Hence, stress corrosion cracking (SCC) in hydrogen pipelines is a result of a combination of tensile strains and many corrosion processes (Cheng, 2007; Djukic et al., 2015; Witkowski et al., 2017; Zvirko et al., 2016). As a result, blended hydrogen pipelines that is infrequently exposed during prolonged periods is normally unaffected.

2.2 Under deposit corrosion susceptibility analysis

The development of water and particles in the pipelines' six o'clock position is often what causes UDC to occur (Allan et al., 2012; Arabnejad et al., 2015). The terrain and the pipeline's construction both contribute to the deposit-related conditions. Conditions promoting various

corrosion deterioration and preventing mechanisms may present beneath the deposits. Models using UDC are better to incorporate UD-MIC because of the extensive co-occurrence of UDC and MIC under the deposits. Probabilistic models are necessary because of the UDC phenomena's complexity, uncertainty, and the unique conditions that cause it to occur.

In order to reflect the mechanisms driving the highest rates, this model seeks to incorporate the UDC and UD-MIC rates to compute the UDC rate. The combination of the deposition susceptibility and the mechanism presenting the dangerous threat provides an effective UDC rate. An anode, a cathode, and an electrolyte containing a reducible species that connects the electrodes are required for the corrosion (Ameh et al., 2017). When zones with various electrochemical potentials occur beneath or near the deposits, the metallic surfaces of metal pipelines can react as cathode and anode (Han et al., 2013; Pang, Wang, Emori, et al., 2021). Thus, the component missing from an electrochemical cell is the electrolyte, which creates the connection between the two electrodes. The co-existence of solid deposits and the electrolyte is what causes the susceptibility to UDC.

The critical velocity parameter, which indicates the flow's capability to remove deposited solids, implies that velocities less than those required in the physician's assessment will result in a deposition. It is believed that the accumulation of such particles that have been moist with micro-water is what allows corrosion to develop straight away following over-bends in large-diameter heavy crude oil pipelines.

Although available literature related to UDC has not been applied to modeling UDC, most cases of UDC occurrence are associated with MIC. Thus, a proposed model is applied based on used tools for modeling MIC from previous literature (Kamil et al., 2021; Taleb-berrouane et al., 2018). (X. Li, Jia, et al., 2022) has investigated the propagation characteristic of MIC and used the

proposed model to estimate the degradation of MIC as well as its susceptibility. Based on the similar characteristic MIC from the available literature, it is crucial to capture a model by combining the UDC and UD-MIC rates to reflect mechanisms causing the highest rates.

2.3 Under deposit corrosion failure characteristics

Failures due to UDC pose devastating issues in the operations of oil and gas pipelines. Several systems that suffered UDC have resulted in catastrophic failures (Durnie et al., 2005; El-Raghy et al., 2000; Ilman, 2014; Skovhus et al., 2017). Existing literature says that there is limited information and knowledge about UDC characteristics direct to the failure of pipeline systems. Additionally, it is more difficult to forecast failure probabilities due to the random and unstable nature of UDC generation and dissemination. The difficulty of the corrosion induced UDC failure prediction is also affected by the characterized multidimensional influencing parameters. Deposits are frequently linked to UDC because of their remarkable capacity to adsorb corrosion. Thereby, the associated failure of subsea pipelines suffering from UDC is still a concern across multiple characteristics of deposits and bacteria. The phases that make up a solid deposit are frequently divided into organic, inorganic, and mixed deposits (X. Chen et al., 2015; H. He et al., 2015). There have been observations of complex solid mixes of sand, clay, wax, asphaltenes, hydrates, and corrosion products forming in subsea pipelines. These deposits present a wide range of structures and compositions, which makes them extremely difficult to analyze and mitigate (Al-Yaari, 2011; Chawla et al., 2012; Kagarise et al., 2017). The formation processes of these deposits are not well known, and their precise definition is unclear.

The deterioration rate, failure probability, and intricate interactions between the key influencing parameters determine a system's failure characteristic when the system is affected by UDC. The

UDC characteristic of the system is degradation rate, probability of failure, thickness loss, defect depth, and multidimensional interactions between the UDC factors.

Regarding risk analysis of pipeline systems under UDC, many researchers have recently suggested experimental and analytical models. (Shukla & Naraian, 2017) investigated the failure characteristics of subsea water injection pipeline steel which failed in year three of operation condition because of UDC after four years of service. This study investigated how corrosion-influencing parameters affect the corrosion rate and flow velocities below less than those necessary for restraining the deposits and weakly attached corrosion product layers. Measurements of the polarization curve for various exposure days and wall thickness loss of metal both caused the failure asset. Similarly, (Alabbas & Mishra, 2013) experimentally studied a high-pressure crude oil pipeline that failed after being in service for two years of operation due to bacterial activity in the presence of inert deposits and active corrosion products. It can be observed that the most likely corrosion rates to be observed are between 1-5mm/year, which is the result of microbial activities and UDC mechanisms. (El-Raghy et al., 2000) presented a case history of a subsea pipeline with no bacterial activity or indication of scaling or organic deposits. The failures occurred as five leaks, all in the six o'clock position. The study revealed that failure characteristics are mostly due to deficiencies in the corrosion monitoring program. The study concluded that in the long term, system failure shows non-linear features of biocide treatment and microbial monitoring programs. Considering the capability of this model, it is post-failure-based and failed to capture the effects of the dominant influential parameters in a dynamic manner in order to estimate the failure probability and loss thickness. In addition, the integration of the chemical parameters, deposition parameters, and microbial activities on failure characteristics on failure characteristic was not studied.

2.4 Under deposit corrosion risk assessment

The deterioration of pipeline systems due to UDC causes failure with associated consequences. Based on the characteristics of corroding pipelines under UDC, it is of considerable significance to carry out safety assessment and analysis. In the oil and gas industries, it is necessary to implement risk assessments on pipelines to prevent all forms of safety mishaps at all levels and improve operational safety.

Available literature hardly ever contains risk-based models, especially for UDC-induced failures. Thus, comprehensive knowledge of stochastic characteristics and complex failure behavior is necessarily applied for risk assessment of systems suffering UDC.

Plus, failure assessment would be a dissolution of the pipeline material into the electrochemical environment, decreasing the pipeline strength. In order to reduce operational and design risks in pipelines, this will serve as well-informed guidance. (Katerina & Gubner, 2010; Winters et al., 1993) proposed risk-based mitigation and testing methods for performance and UDC monitoring in field operations. Similar to this, (Alamri, 2020; Suarez et al., 2019) scaled the UDC risk level according to the concentrations of CO₂, sodium chloride (salt), and hydrogen sulfide in subsea pipelines. Deposits can impact corrosion rates by creating micro-environments with different environmental parameters from the bulk fluid (J. Li et al., 2022). The model only provides a diagnostic risk-based monitoring capability via key performance indicators; it does not quantitatively predict the risk of UDC-induced system failure under various operating parameters. Furthermore, (Askari et al., 2019; Skovhus et al., 2017) introduced a quantitative estimation model of the probability of failure (PoF) for a subsea facility under UDC. For a credible danger possibility projection on the system's integrity after inspection, they proposed screening assessment criteria. Based on the chosen criteria, by combining the settlement potential, oxygen ingress, rate of metal

breakdown, availability, and UDC mitigation effectiveness, they determined the PoF. However, the proposed approach captures the effects of the screening parameters to formulate the PoF levels, which range from very high to high, high to medium, medium to low, and low to very low). The risk indicators were structured and expressed qualitatively by a logic diagram with a characterized path number.

- i. Calculating the failure probability of asset (pipeline) over a period (before and after launching in-line inspection and cleaning tools);
- ii. Repairing the defect if required;
- iii. Optimizing the periodic schedule of in-line inspection tools to determine the defects and corresponding sizes of the defects;
- iv. Manipulating operational parameters;
- v. Using chemical compounds to prevent deposits, bacteria as well as applying coating and cathodic protection;
- vi. Providing an early warning guide to prevent oncoming evolution of pipelines' failure.

2.5 Blended hydrogen pipelines risk assessment

The performance of pipeline appliances will be impacted by differences in an H2NG blend's thermo-physical properties. Depending on the form in which it is transported, hydrogen can be gaseous, liquid, or solid; high-pressure gaseous hydrogen is now the most widely used and environmentally benign mode of transportation. The most effective way to move a lot of material is through pipelines, which may be used for distribution over short distances as well as long distances. Large-diameter, high-pressure long-distance transmission pipeline that is mostly used to move high-pressure hydrogen between the hydrogen station and the hydrogen producing unit. The transport of low- and medium-pressure hydrogen between both the hydrogen station and the

end user is the primary purpose of the second low-pressure and small-diameter pipeline (Erdener et al., 2022).

The proportion of hydrogen in the blended pipelines was found to determine the transient overpressure, which increased the internal load and circumferential stress on the pipe wall thickness. Additionally, the hydrogen pipelines' damages were seen to increase as overpressure grew, therefore safety considerations were applied to assure the security of the blended H₂NG pipelines' processes. Different characteristics in pipeline transportation are caused by differences in the thermophysical properties of methane (CH₄) and hydrogen, which also have an impact on flow and heat transfer attributes.

Furthermore, it is necessary to assess the influence of a hydrogen fraction on the transport process in order to ensure the practicality, safety, and cost-effectiveness of using an existing natural gas pipeline to transfer a blended H₂NG pipeline.

Although there have been multiple simulations of the flow in a blended pipeline, the majority of previous models assumed that natural gas was made exclusively of CH₄. However, in practice, natural gas also contains other gases like CH₄, ethane (C₂H₆), and propane (C₃H₈). Depending on the gas sources that are accessible, its composition changes.

A particular pipeline network's actual gas composition may be related to the impact of a hydrogen fraction. As a result, when modeling the pipe flow and analyzing the influence on hydrogen injection, simulations should be based on real-world circumstances.

Many researchers pointed out that the design, construction, and operational characteristics of H₂ pipes would be familiar to those of natural gas pipelines. Thus, it is useful to first understand the information on these aspects of natural gas pipelines.

Hydrogen transportation faces multiple safety challenges (Yoo et al., 2021). In the following sections, a methodology for the safety development of the current infrastructure of hydrogen transportation is proposed. To evaluate how existing natural gas transportation pipelines can be used for hydrogen transportation, the safety of hydrogen transportation is a crucial problem that requires further attention. Based on the risk assessment of conditional pipelines a safety analysis model is proposed using the physics and mechanistic approach of hydrogen-associated degradation. Notably, the model highlights that controlling the corrosion rate can help ensure the safety of blended hydrogen pipelines.

The risk assessment of blended hydrogen pipelines is to identify, assess and evaluate failure scenarios of hydrogen transportation through conventional pipeline by fulfilling the following gaps:

- i. Lack of a detailed understanding of all possible mechanisms of hydrogen degradation in hydrogen pipeline blending into existing gas pipelines;
- ii. There is no any dynamic model to estimate likelihood of blended pipeline failure risk in operating and composition of existing gas pipelines over time.

2.6 Current state of knowledge and gaps

Risk-based integrity assessment due to UDC induced failure demands a deeper comprehension of stochastic behavior displayed by UDC and its influential parameters, which subsequently influence failure prediction. Thus, an effective risk assessment requires the establishment of a dynamic model. The dynamic framework will be able to capture the UDC's time-dependent behavior and its key characteristics to forecast complicated failure causes, failure propensity, and failure-related outcomes.

The limitations in the current UDC susceptibility, failure, and risk-based models in literature are revealed through a thorough analysis below:

- (i) With regard to the non-linear interactions among corrosion-affecting factors, the models are not dynamically designed to estimate the UDC rate;
- (ii) Current models cannot foresee the failure probability. Furthermore, given the monitoring operating parameter and the deposit-related characteristics, the future defect depth distribution cannot be assessed;
- (iii) No theoretical framework exists to clarify how multiple risk variables that affect UDC are interrelated;
- (iv) The models are able to anticipate the effects of several UDC flaws only on the basis of corroding system's strength loss and safe operating pressure;
- (v) Lack of a comparison the performance and results of the probabilistic framework model with industrial data using a stochastic approach (Monte Carlo Simulation (MCS));
- (vi) The models could not capture the dynamic interactions between numerous failure mechanisms and random corrosion factors on the pipeline system's safety and reliability during operation;
- (vii) There are insufficient dynamic quantitative risk-based models to investigate how time-dependent UDC influences the likelihood of failure and what that means for risk profiling in the context of numerous failure modes and deposition factors;
- (viii) There is no any blended hydrogen pipeline' risk assessment so far.

CHAPTER 3

3 Modeling and Analysis of Internal Corrosion Induced Failure of Oil and Gas Pipelines

3.1 Preface

*A version of this chapter has been published in the **Reliability Engineering & System Safety**, 109170, 2023. I am the primary author along with the Co-authors, Zaman Sajid, Faisal Khan, Yahui Zhang, and Trung Tran. I wrote original draft, Software, Review & editing, and developed the Methodology, Formal analysis, Conceptualization, Data curation. I prepared the first draft of the manuscript and subsequently revised the manuscript based on the co-authors' and peer review feedback.*

Co-author Zaman Sajid provided support in Writing – review & editing, Supervision, Software, Methodology, Formal analysis, Data curation. Co-author Faisal Khan helped in writing – review & editing, Supervision, Methodology, Formal analysis, Conceptualization. Co-author Yahui Zhang provided fundamental assistance in Writing – review & editing, Supervision, Methodology, Formal analysis. Co-author Trung Tran provided fundamental assistance in Writing – review & editing, Methodology, Formal analysis, Data curation. The co-authors also contributed to the review and revision of the manuscript.

3.2 Abstract

Internal corrosion is a complex phenomenon that includes under-deposit corrosion (UDC), microbially influenced corrosion (MIC), erosion, and localized and uniform corrosion mechanisms. For robust risk management of pipelines, there is a need to study the interactions of risk factors in internal corrosion. It is necessary to monitor the variations of corrosion risk factors and assess the pipeline's failure likelihood as a function of time. A Dynamic Object-Oriented

Bayesian network (DOOBN) model is developed for this purpose. The DOOBN model has helped represent the probabilistic relationships among prevalent influencing risk factors and define their conditional dependencies. There are 94 risk factors considered for the different internal corrosion mechanisms. Results show that the probability of UDC occurrence for a given pipeline is 58%, while MIC is 48%. The study also confirms the increase in asset failure rate with the rise in internal corrosion. Results of model validation show that model is 93.22% accurate. The study serves as an early warning guide for the integrity management of pipelines against internal corrosion.

Keywords: Internal corrosion; Asset Integrity; MIC; UDC; Dynamic Object-Oriented Bayesian network.

3.3 Introduction

Internal corrosion poses an integrity threat to oil and gas transportation, especially in harsh offshore environments. Multiple factors influence the corrosion mechanism and cause multi-dimensional and adverse environmental effects. The cost of corrosion-induced asset failure is rising, despite the vast investment in corrosion mitigation and control. For instance, the US spent about \$2.5 trillion on corrosion control and management. Different driving mechanisms in internal corrosion cause corrosion, for example, UDC, MIC, localized corrosion, uniform corrosion, and corrosion due to erosion. UDC and MIC have been reported as key contributors to sudden pipeline system failure in marine, energy, and petroleum industries (Adumene et al., 2022). Both corrosion types' complex driving mechanisms result in unpredictable characteristics that limit their monitoring and control. Studies have identified that the multiphase pipeline failures resulted in a loss of \$203 million in 2017 due to internal corrosion (PHMSA, 2017). As a result, predicting the internal corrosion rate is essential to ensure asset integrity and cost-effective transportation of oil and gas through pipelines (Khan et al., 2021).

The corrosion mechanism of UDC is a result of deposits, including sand, particles, and debris, transported along with the fluid during oil and gas operations. Under specific operational conditions, these particles accumulate and form deposits at the pipeline's six o'clock position. Depending on the terrain and other operating parameters, water may also be collected in pipeline sections. In the presence of water, these deposits create isolated local micro-environments with characteristics vastly different from those of the transported fluid (Jawwad and Mohamed, 2020). In addition to these conditions, the deposits prevent the corrosion products from dispersing. The collected metallic corrosion products may also worsen the corrosion progress. The deposits in pipelines are classified according to their sources and porosity. The active deposits are metallic corrosion products separated from the pipe wall and are transported until they are deposited on the pipeline surface. The active deposits include the heavy and large molecules in the crude oil, such as wax, asphaltene, etc. The co-existence of these deposit types in pipelines could further complicate the UDC mechanism.

Despite advanced studies to understand the complex mechanisms of both UDC and MIC, there are still failure cases due to these corrosion mechanisms. These mechanisms depend on environmental, operational, microbial, and deposit-related risk factors. The association of under-deposit and microbial corrosion could further complicate the prediction of the corrosion mechanism. The formation of solid deposits provides rich conditions for microbes to grow. Microbes and deposits usually have complex relationships (Suarez et al., 2019). Thus, addressing biofilm formation and deposit factors in the UDC process is crucial to understanding its mechanism. We currently have limited knowledge of the mechanism of UDC based on the existing literature (Kagarise et al., 2017). The current models have not studied the interactions of the critical risk factors which lead to UDC.

Uniform corrosion spreads on the whole surface of a corrosive metal pipeline and weakens its integral strength. A pipeline's weak integral strength can lead to its failure, and a pipeline failure can halt the fluid transportation system. Therefore, uniform corrosion can pose a considerable loss. This corrosion is influenced by CO₂, temperature, O₂ content, H₂S, pH, water wetting, and the presence of Fe²⁺ and Fe³⁺ in pipelines. Dissolving CO₂ in solution leads to the formation of carbonic acid, which catalyzes uniform corrosion in steel pipelines.

In contrast, high partial pressure of CO₂ can form FeCO₃ on a steel surface. This phenomenon will, in turn, decrease the probability of uniform corrosion in steel assets. H₂S is also a weak acid gas and can directly cause corrosion (Liu et al., 2022).

The pH of flowing fluid inside a pipe can significantly contribute to localized corrosion. A high pH value can decrease FeCO₃ solubility and, therefore, can increase the precipitation rate. This process can also lead to quicker development of protective films and thus can reduce the corrosion rate (Sliem et al., 2021). A high temperature can accelerate pH in localized corrosion and increase the precipitation rate of FeCO₃. Based on the solubility of passive films, the temperature can affect localized corrosion. In the case of low pH, typically, passive films do not form, and a temperature rise can lead to high corrosion rates, but at a higher pH, the precipitation rate will increase with an increase in temperature, thus accelerating localized corrosion (Alamri, 2020). Besides crevice corrosion, pitting is the manifestation of localized corrosion due to many different corrosion mechanisms (Calabokis et al., 2021). Unlike uniform corrosion, pitting is more dangerous due to its difficult detection, prediction, and prevention. According to a study (Heidary & Groth, 2021), pitting in carbon steel starts due to the breakdown of product films on a metal surface. In sweet systems, the holes due to pitting are tiny yet have sharp edges. Pitting is a form of localized

corrosion in an environment containing chloride. Localized corrosion results in small excavations of the metal surface, ultimately causing perforation of the affected piping or equipment.

Erosion is the physical removal of wall material by the flowing process fluids. In corrosive conditions where solids are present, erosion corrosion can occur. In systems where the corrosion products provide some protection from corrosion, solid particles can remove these corrosion product films, exposing the fresh metal surface to erosion (Andreini et al., 2019). A related corrosion mechanism is a flow-induced corrosion, in which the fluid is the erosive component (Zheng et al., 2022). The mechanism for erosion involves continuous water flow that removes protective film. A protective film could be a corrosion inhibitor of metal oxide from forming on the surface of the metal. Erosion corrosion can lead to rapid failure. As regards corrosion inhibitors, a rule of thumb is that these inhibitors are generally ineffective once gas velocities exceed 20m/s and liquid velocities 8m/s. Above these velocities, the inhibitor is stripped from the pipe wall. High water cuts due to flow can also abolish the protective layer, increasing the corrosion rate inside a pipeline. The dominant influencing factors for internal corrosion were described in detail by (Askari et al., 2019) and are divided into five main threats: uniform corrosion, localized corrosion, erosion, MIC, and UDC.

3.4 Research Methodology

The proposed methodology of this study consists of five steps, as shown in Fig.3.1. The application of the model is presented using an actual case study.

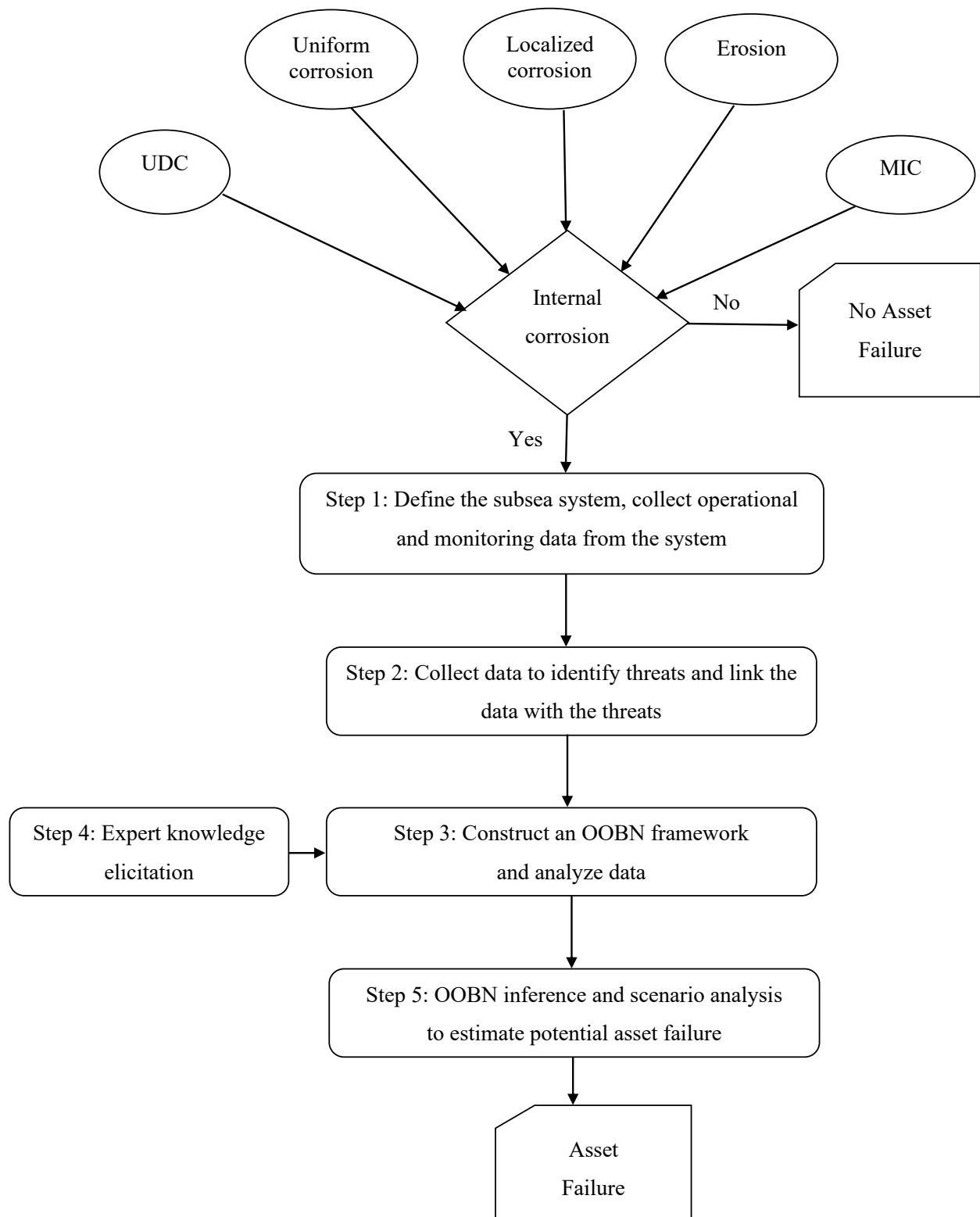


Figure 3. 1: A schematic view of the proposed research methodology

Dynamic Object-Oriented Bayesian Network (DOOBN) Model

BNs are directed acyclic graphs (DAG). Nodes on a BN model represent risk factors, while causal relationships among risk factors are indicated by arcs (J. Kim et al., 2020). The strength of linkages among nodes is represented in conditional probability tables (CPTs).

The BN is adaptive and able to update given evidence on the state of belief for the structure and performance prediction of the model. Eq. (3.1) represents the conditional independence for a random set of risk variables $U = \{Y_1, \dots, Y_n\}$, indicates joint probability distribution $P(U)$, and is based on the chain rule (Moradi et al., 2022): Hence,

$$P(U) = \prod_{i=1}^n P(Y_i | P_y(Y_i)) \quad (3.1)$$

where $P_y(Y_i)$ represents a parent node. Eq (2) shows the probability of Y_i ;

$$P(Y_i) = \sum_{U \setminus Y_i} P(U) \quad (3.2)$$

In Eq (3.2), the summation operation is performed on all variables except Y_i .

Bayes' theorem can be used to calculate the posterior probability of an event as soon as new information is available. Such new information is called evidence (E). Evidence is new operational data, including the occurrence or non-occurrence of an event, as shown in Eq. (3.3).

$$P(U|E) = \frac{P(U, E)}{P(E)} = \frac{P(U, E)}{\sum_U P(U, E)} \quad (3.3)$$

BN is a clear visualization of cause-effect relationships among various risk factors and allows updating them based on evidence (Sajid et al., 2018). BNs are valuable tools for assessing internal

corrosion failure because they effectively represent the complex interrelationships among the influencing factors of corrosion in subsea pipelines, such as operating parameters, design parameters, fluid chemistry, etc. A study develops a BN model for corrosion by considering different information, such as expert knowledge, analytical corrosion models, and published literature (C. Liu et al., 2021). In a BN model, we can include multiple corrosion models to estimate the failure probability of corrosion defects. However, the resulting model will become too complicated for analysis. Asset failure is a complex phenomenon with many unknown influencing factors, including the inherent complexity of pipelines and external factors. Therefore, the resultant network becomes a challenging visualization.

It is quite burdensome to construct and deal with Bayesian networks having large sizes of CPTs, and their analysis becomes a challenge. For an extended and large Bayesian network, the model assessment poses additional challenges to computation. Therefore, a traditional Bayesian network technique is limited in scope and inefficiently handles too many risk variables in a single BN model. One of the logical and appropriate alternatives is to break down the complex network into smaller subnetworks and then connect fragmented sub-models to develop a complete system model. It is called an object-oriented Bayesian network (OOBN) (Yang et al., 2017), and the analysis of OOBN over a time frame is called Dynamic OOBN (DOOBN). An illustrative example of it is shown in Fig.3.2. Using the methodology explained in Fig.3.1, a detailed DOOBN is developed like the one presented in Fig.3.2 is designed for a pipeline. The details of the DOOBN are given in a subsequent section.

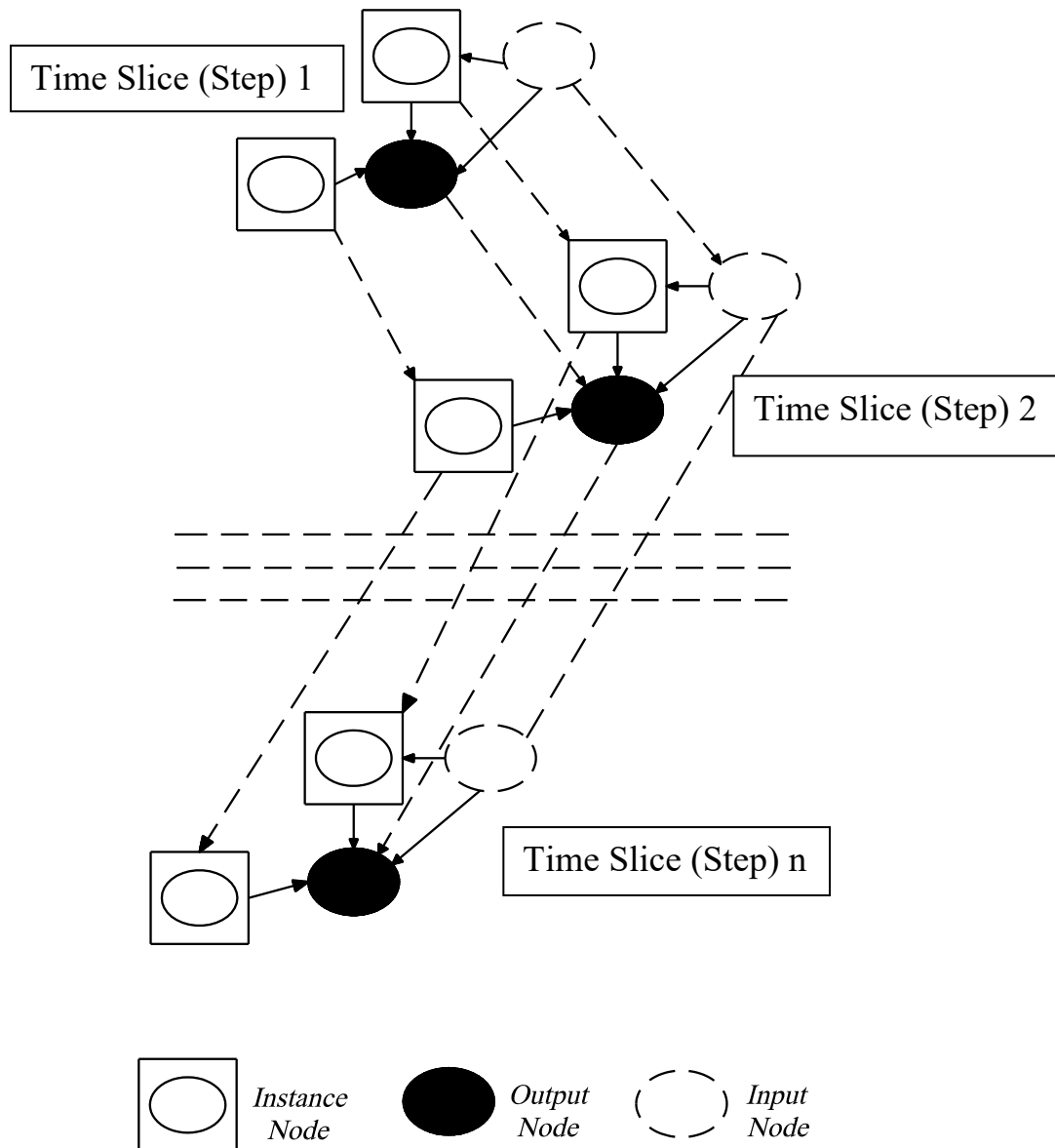


Figure 3. 2: A graphical representation of a DOOBN

Application of the DOOBN

The DOOBN model is developed for a segment (near a platform) of a subsea pipeline (design Life: 25 years; carbon steel: DNV OS F101 grade 450 (SAW); pipe internal diameter 479.4 mm; pipe outer diameter 514.4 mm, thickness 17.5 mm; pigging design: intelligent pig), the operating temperature is from 28 to 45°C, and the operating pressure is about 120 to 160 Bar. The asset failure

is assessed over a 10-year time frame with the key influencing parameters, and the probabilistic characteristics of the pipeline are illustrated through a public repository (Dao et al., 2022) in table 3.2 in the Appendix.

Step 1: Define the subsea system, collect operational and monitoring data from the system

The data collected in this step consist of operating temperature, pressure, composition, material, and external parameters for subsea pipelines. These parameters are defined and monitored based on their mechanical and operational properties, followed by data collection on the corroding asset.

Step 2: Collect data to identify threats and link the data with the threats

Due to internal corrosion, the asset failure risk assessment model has five categories: MIC, UDC, erosion, localized, and uniform corrosion. A detailed literature search was performed to identify and categorize risk variables for each category. For example, in MIC, bacteria presence, operating conditions, MIC control, wetting factors, and water conditions were major risk factors. For UDC modeling, the major factors were deposit formation, oxygen depletion, fluid chemistry, and operating parameters (Sloley, 2020). We considered geometry change, presence of solid particles, water cut, and diameter change in the erosion category as major risk factors. Localized corrosion is subjected to the major factors of galvanic cells, temperature, pH, flow velocity, anodic film, and chloride presence. The Uniform corrosion category has major risk factors of temperature, H₂S, conditions, and CO₂ level. Major risk factors were further classified, and details are discussed in the results and discussion section. In total, 94 influencing factors were identified in this step.

Step 3: Construct an OOBN framework and analyze the data

In this step, we are developing a mathematical model in the OOBN framework to manage the safety and integrity of a subsea pipeline, as discussed in the case study. The developed model will be tested and applied for case studies.

In detail, using the causal relationships, Bayesian subnetworks of MIC, UDC, erosion, localized, and uniform corrosion were developed. Directional links of risk factors were constructed in AgenaRisk Desktop software. One of the primary differences between the conventional BN model and OOBN is the presence of instance nodes and encapsulation in an OOBN. An instance node shows an abstraction of a segment of a Bayesian network which can be used to represent the structure (Sajid et al., 2020). In contrast, encapsulation allows for the transmission of all properties of one Bayesian subnetwork to another. The tool AgenaRisk helped to specify instance nodes for each sub-Bayesian model. The linking and embedding of each Bayesian subnetwork resulted in an OOBN. Similar to the regular BN model, the data in OOBN can be updated as new information becomes available.

Step 4: Expert knowledge elicitation

In this step, the expert knowledge elicitation technique was used to assign marginal probabilities and to develop conditional probability tables (CPTs) for each link identified in step 3. The expert knowledge elicitation technique allows the inclusion of experts' subjective knowledge in probability distribution values for each risk variable (Hassan et al., 2022). Probability data used in the parent nodes and conditional probability tables (CPTs) of the BN model is based on experts' opinions. Experts in this study are a group of researchers led by a senior university professor. The group is actively engaged in research and development on corrosion.

This procedure helps in the statistical inference of OOBN analysis. It is pertinent to mention here that although experts' judgments are subjective, these are made as objectively and carefully as scientifically possible (O'Hagan, 2019). Consistent with the literature, the group of experts was composed of researchers actively engaged in corrosion research and development projects (Bolger, 2018). It is acknowledged that the use of CPTs in this study is to exhibit the proposed method, and the data may not match with any industrial operations.

Step 5: OOBN inference and scenario analysis to estimate potential asset failure

In this step, we converted OOBN into a dynamic model by considering time slices for ten-time steps. The one-year increment was provided to understand the variations over time. Different scenarios were developed, and OOBN inferences were made. Details of each scenario and developed OOBN are provided in the results and discussion section of this paper.

The current study proposed a robust and dynamic probabilistic model for the asset failure assessment of offshore pipelines affected by internal corrosion. A DOOBN is developed to capture and incorporate the key influential factors that trigger internal corrosion and cause asset failure. The proposed model can explore interdependencies of associated risk factors, which can help to assess the likely impact of the internal corrosion mechanism on the pipeline. The asset failure rate is mapped into a dynamic format to predict internal corrosion propagation. The essence is to understand the long-term influence and propagation of internal corrosion in an asset. The results of this study can help to develop management strategies for proactive treatment of internal corrosion and save costs associated with an asset failure due to internal corrosion.

Step 6: Model validation

The proposed model is validated using the k-fold cross method in this step. The use of this validation method assisted in understanding the accuracy and robustness of the proposed model. Various studies have applied the k-fold cross method; for example, see (Geroldinger et., 2021; Marcot & Hanea, 2021; Sajid, 2021). Validation steps include compiling a database of 100 samples with known input nodes and analyzing the response of the output node (asset failure). The random dataset was divided into ten equal segments to identify the k-value, as recommended in the literature (Marcot & Hanea, 2021). The first ten parts of the data were set aside, and the rest was used to parametrize. The model was tested using other datasets, and model results were compared with known outcomes. The procedure was repeated for all ten parts of the datasets. GeNIe academic version from Bayes fusion was used as a software tool to develop random datasets and perform model validation. These steps' outcomes were the nodes' accuracy and receiver operating characteristic (ROC) curves.

3.5 Results and Discussions

For internal corrosion, the results of Bayesian subnetwork models of OOBN are presented in Figs.3.3 to 3.8. These figures indicate key risk factors contributing to the asset's failure. It is pertinent to mention here that the results and analysis of this actual study demonstrate the operationalization of the methodology and hence do not represent any actual situations. These sub-model details are illustrated in tables 3.1.1 to 3.1.6, presented in Appendix.

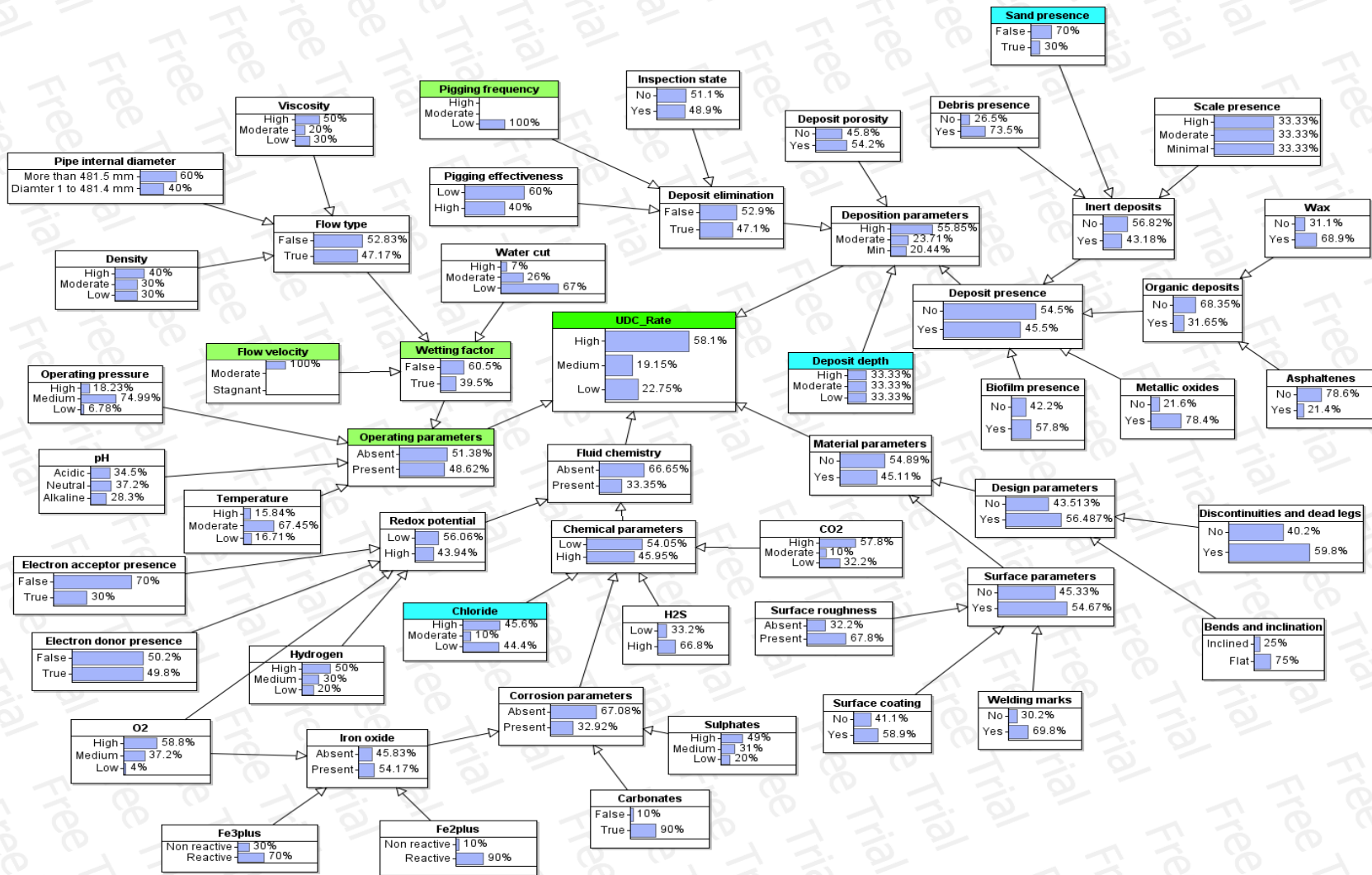


Figure 3. 3: A Bayesian subnetwork model for UDC

Fig.3.3 represents the Bayesian sub-network for UDC, and it shows the interdependencies of various factors under the category of UDC. It shows the interactions among the deposition and material parameters, their propagative influence on the UDC, and the interactions of material, operating, and deposition parameters. The UDC model has been developed considering four key intermediate nodes: deposition, operating, material parameters, and fluid chemistry. A detailed analysis of the UDC model reveals that inert deposits, organic, metallic oxides, and biofilm influence deposit presence. Risk factors of inert deposits are influenced by three factors: debris, sand, and scale, while wax and asphaltenes cause organic deposits. The simultaneous influences of deposit presence, deposit porosity, and deposit elimination contribute to deposition parameters. The effectiveness and frequency of pigging (a utility that removes unwanted materials in a pipeline, such as wax) are associated with the inspection that significantly eliminates deposits. Fig.3.3 also indicates that the operating parameters of the pipeline depend upon pH, temperature, operating pressure, and wetting factor. It has been observed that the wetting factor is the major influencing factor, including water cut, flow velocity, and flow type. The internal pipe diameter, density, and viscosity of the fluid influence flow type. The presence of an electron acceptor and electron donor and the concentration of oxygen and hydrogen influence the occurrence chances of redox potential. A simultaneous presence of oxygen, Fe^{2+} , and Fe^{3+} leads to iron oxide formation. Iron oxide, carbonate, and sulphates contribute to the corrosion parameter, which combines with CO_2 , H_2S , and chloride, creating chemical parameters. As is shown in Fig.3.3, the collective presence of the chemical parameter and the redox potential defines fluid chemistry. The design parameters consist of discontinuities, dead legs, bends, and inclination, while the combination of surface roughness, surface coating, and welding marks influence surface parameters in UDC. A connection between the surface and design parameters of pipelines relates to the material

parameter factor. The model shows that the deposition parameters are the most probable cause of the UDC rate.

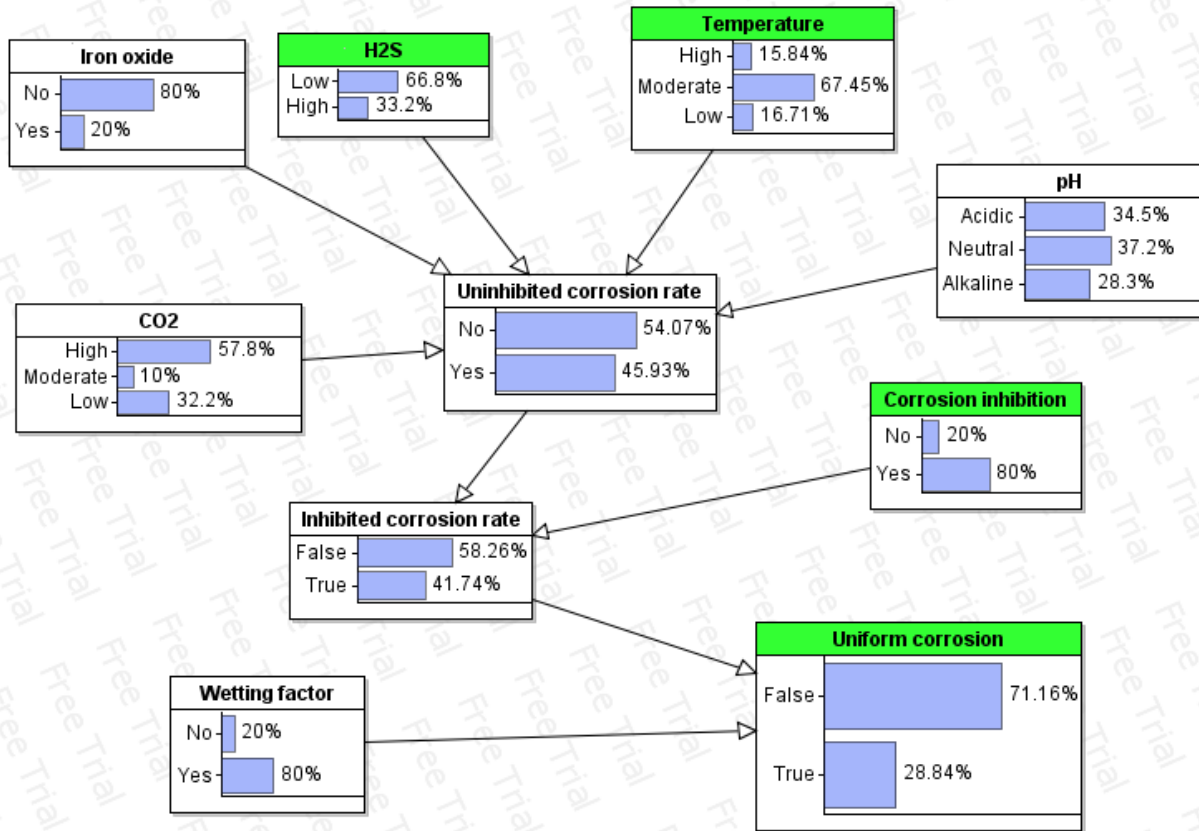


Figure 3. 4: A Bayesian subnetwork for uniform corrosion

Fig.3.4 indicates the Bayesian sub-network for uniform corrosion. It shows two major influencing factors, wetting and inhibited corrosion, that contribute to uniform corrosion. The wetting factor is affected by flow factors such as fluid properties (flow velocity), density, viscosity, and water cut. Uniform corrosion characteristics are significant in the presence of an uninhibited corrosion rate. The CO₂, H₂S, temperature, pH, and iron oxide concentration on the pipeline surface calculate the uninhibited corrosion rate. Results show that if there is CO₂ present, the precipitation of FeCO₃ on the material surface forms a dense film that acts as a protective corrosion film.

However, in the presence of both CO_2 and H_2S , FeS film is developed instead of FeCO_3 . At a low temperature, the precipitation of FeS is easier than that of FeCO_3 .

On the other hand, the precipitation rate of FeCO_3 increases at a high temperature. Besides the impact of inhibited corrosion on uniform corrosion, the wetting factor intrudes with the development of the inhibitor film and tends to remove this film. This action will decrease inhibitor efficiency and increase the uniform corrosion rate on the metal surface of a pipeline. Uniform corrosion can lead to asset failure in the form of a pipeline rupture, and ultimately it can halt the transportation of fluid inside the pipeline. Therefore, the uniform corrosion mechanism needs careful treatment.

Fig.3.5 shows the Bayesian sub-network for localized corrosion caused by UDC rate and galvanic cells. It illustrates that the collective presence of wetting cut and deposit presence affects the UDC rate. Under specific dewing conditions or top of the line corrosion, localized corrosion occurs when acid vapours or CO_2 (carried by water) condense on the top surface of a pipe (J. Li et al., 2022). Also, deposit presence, flow velocity, and corrosion inhibition are associated with localized inhibitors when the fluid flow velocity is maximum (100%). Five major factors contribute to a galvanic cell: localized inhibitor, chloride, temperature, passive film, and anodic film. An electrical connection between two dissimilar metals within an electrolyte solution results in a galvanic cell. The anode is the metal that is corroded, while the other uncorroded metal is the cathode. The interconnections between anodic and passive films and chloride are indicated in Fig.3.5. The H_2S is the key influencing factor of the anodic film. At the same time, pH and temperature are predominant influences of the passive film.

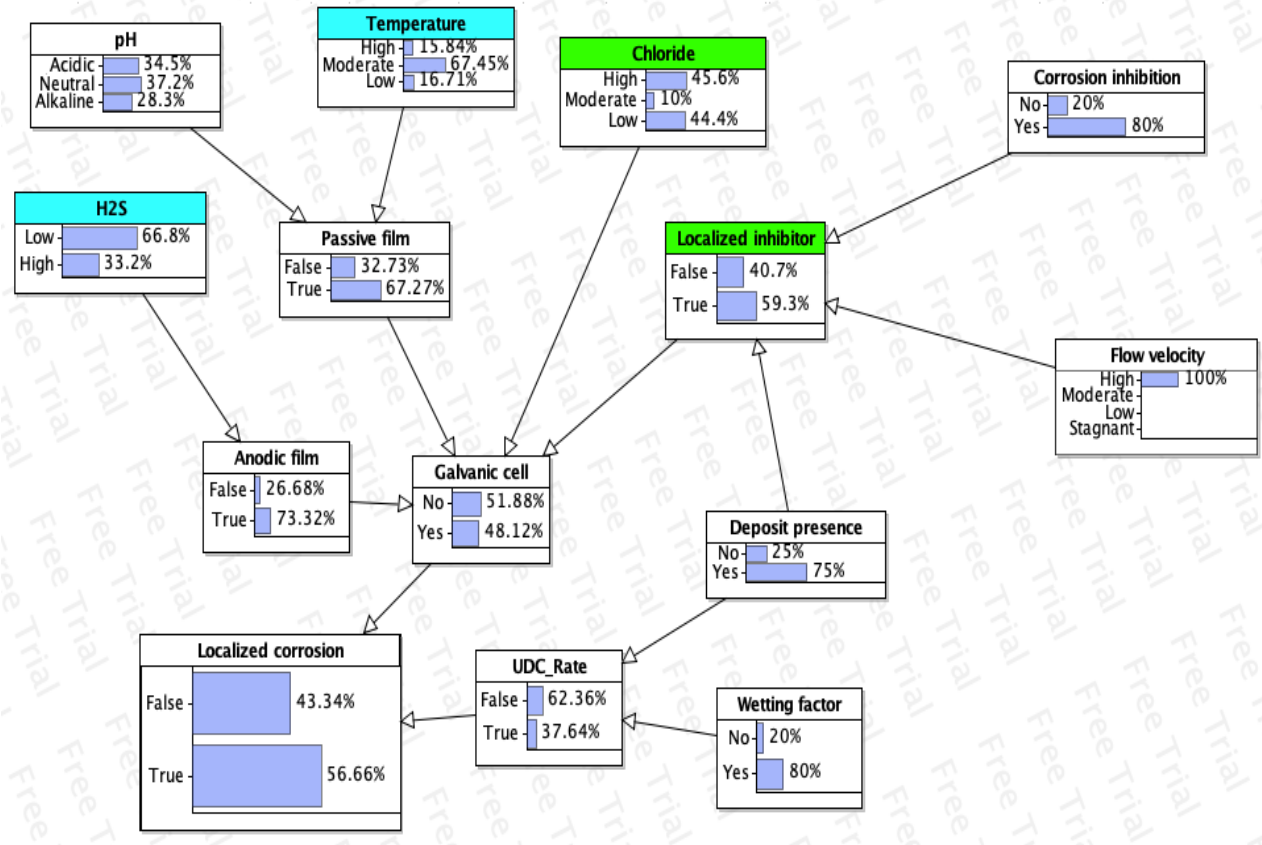


Figure 3. 5: Bayesian network for localized corrosion

Fig. 3.6 is a Bayesian sub-network for erosion. It represents the impact of three key factors, geometry change, water cut, and solid particles, on the erosion of the pipeline, as is also highlighted in the literature. With the simultaneous occurrence of water cuts and solid particles in the fluid, the surface of pipelines will be damaged. In addition, the erosion rate is significantly higher with geometry changes in pipelines, including valves, diameter change, bends and inclination, and T-pieces.

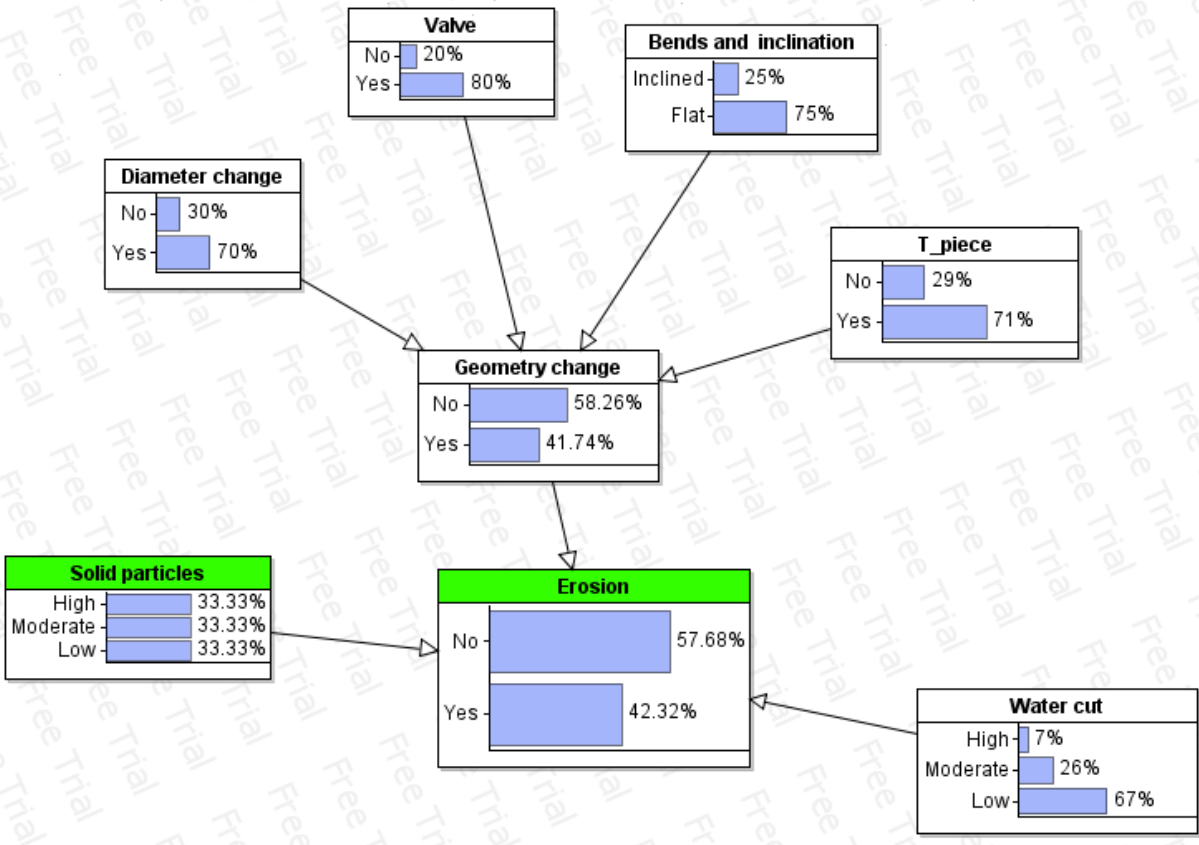


Figure 3. 6: A Bayesian subnetwork model for erosion

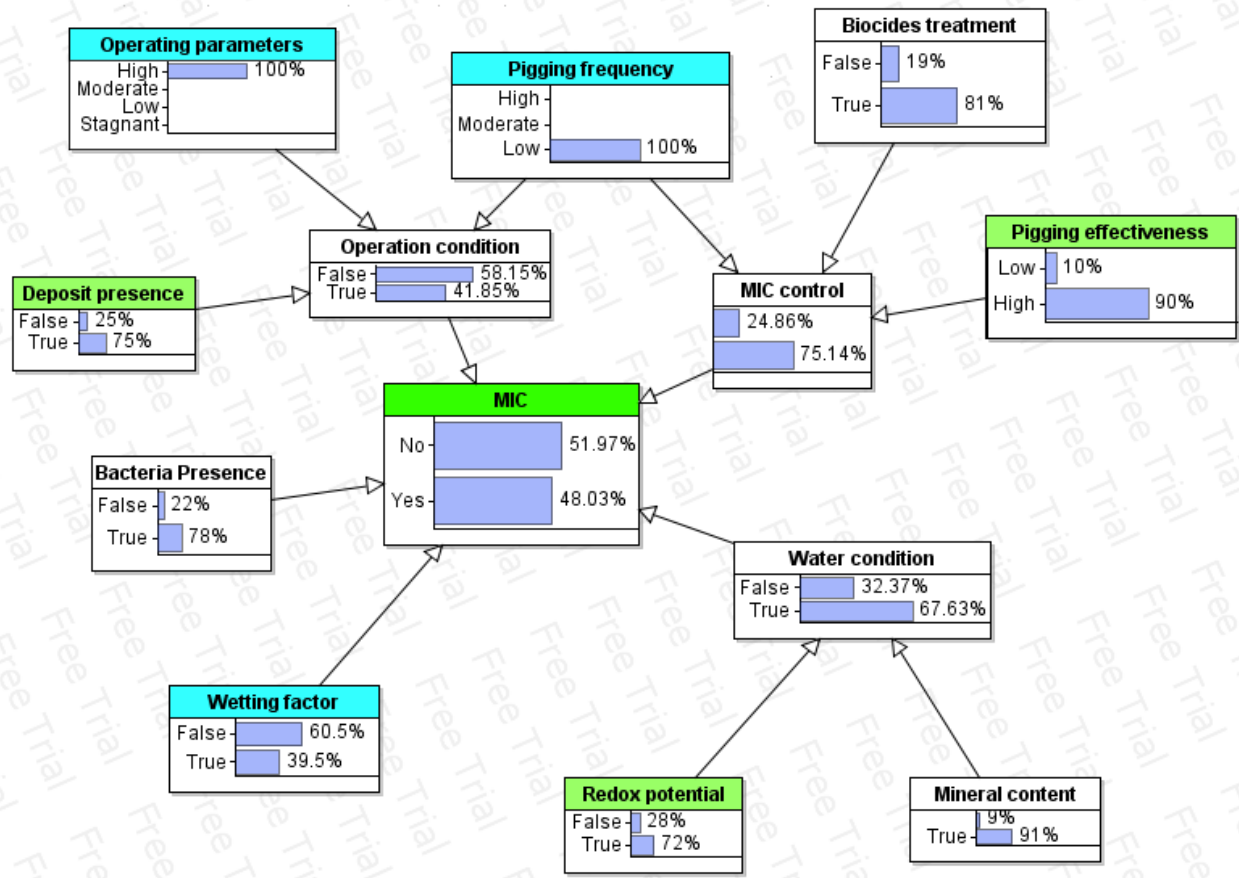


Figure 3. 7: A Bayesian subnetwork model for MIC

Fig.3.7 is a Bayesian sub-network of MIC. It shows the influence of MIC is affected by five dominant factors: water condition, operation condition, bacteria presence, wetting factor, and MIC control. The high redox potential and mineral content in water significantly affect the water condition. The contact of water with a metal surface can also contribute substantially to MIC. There are higher chances of MIC when the wetting factor has low flow velocity. There are high chances for MIC in dead legs and other settling locations in a pipeline. The MIC control is associated with the effectiveness and frequency of pigs in the pipeline and biocides treatment. The bacteria may colonize a pipeline, and its contamination is quite challenging to eliminate.

Consequently, all water for hydro testing must be appropriately treated. As shown in Fig.3.7, the frequency of pigs involves two main factors of MIC: MIC control and operation condition. The operating parameter change and deposits' presence affect MIC operation, significantly increasing influent bacteria activities. Bacteria occur naturally in all seawater and are occasionally introduced into pipelines during hydro tests or reservoir fluids by water injection. Generally, bacteria, known by the collective term Sulphate Reducing Bacteria (SRB), can cause corrosion under complex operating parameters. There are high probabilities of a high MIC rate due to SRB or other types of bacteria (nitrate-reducing and acid-producing bacteria). Pipeline bacteria can develop sulphates under complicated operating conditions, and the bacterial colony can cause UDC. The results indicate that the probability of the occurrence of MIC is quite high.

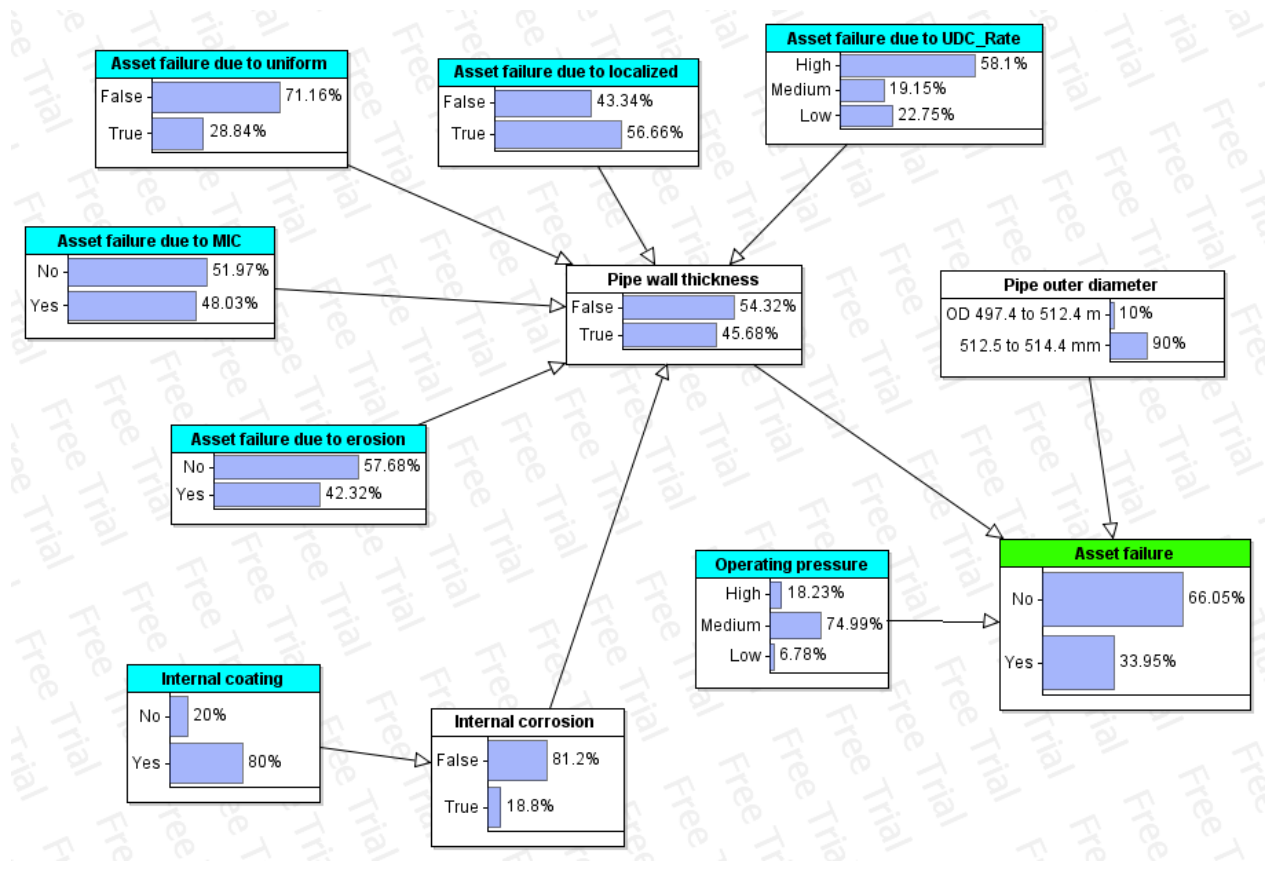


Figure 3. 8: A Bayesian subnetwork model for asset failure of a gas pipeline

Fig.3.8 shows a combined effect of uniform corrosion, UDC, MIC, localized corrosion, and erosion on pipe wall thickness. The Bayesian sub-network in Fig.3.8 shows that loss of pipe wall thickness directly causes asset failure. It shows that a decreased pipe wall thickness leads to the asset's failure. It is pertinent to mention that the outer diameter of a pipe and operating pressure directly influence asset failure. A DOOBN shows the variations in asset failure over time.

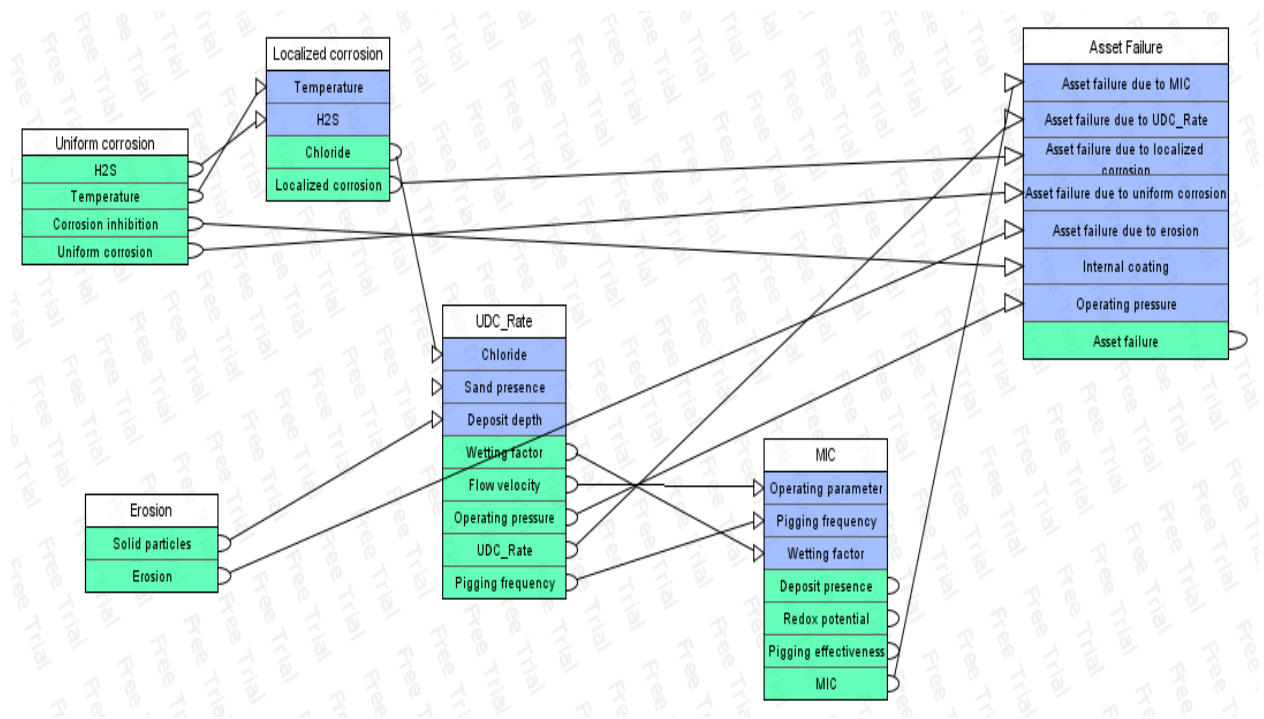


Figure 3. 9: OOBN for asset failure due to internal corrosion of oil and gas pipeline

Fig.3.9 illustrates the OOBN for internal corrosion, which consists of Bayesian sub-networks of uniform corrosion modeling, localized corrosion modeling, MIC modeling, erosion modeling, UDC modeling, and asset failure modeling (corrosion risk of pipelines) for internal corrosion of a pipeline. OOBN represents Bayesian sub-networks for each internal corrosion mechanism and incorporates instance nodes. OOBN has also helped avoid the repetitive tasks of creating identical

structures and cumbersome probability tables. The relationships and interdependency of each risk instance node are implanted in the model as objects. In Fig.3.9, internal nodes are hidden or ‘encapsulated’, and only ‘visible’ nodes are input and output nodes. Encapsulation of many factors and visibility of a few factors are characteristics of an OOBN. Based on the OOBN, probability updating is performed at regular intervals to predict the asset failure probability. The detail of the nodes of the OOBN model is presented in table 3.1.

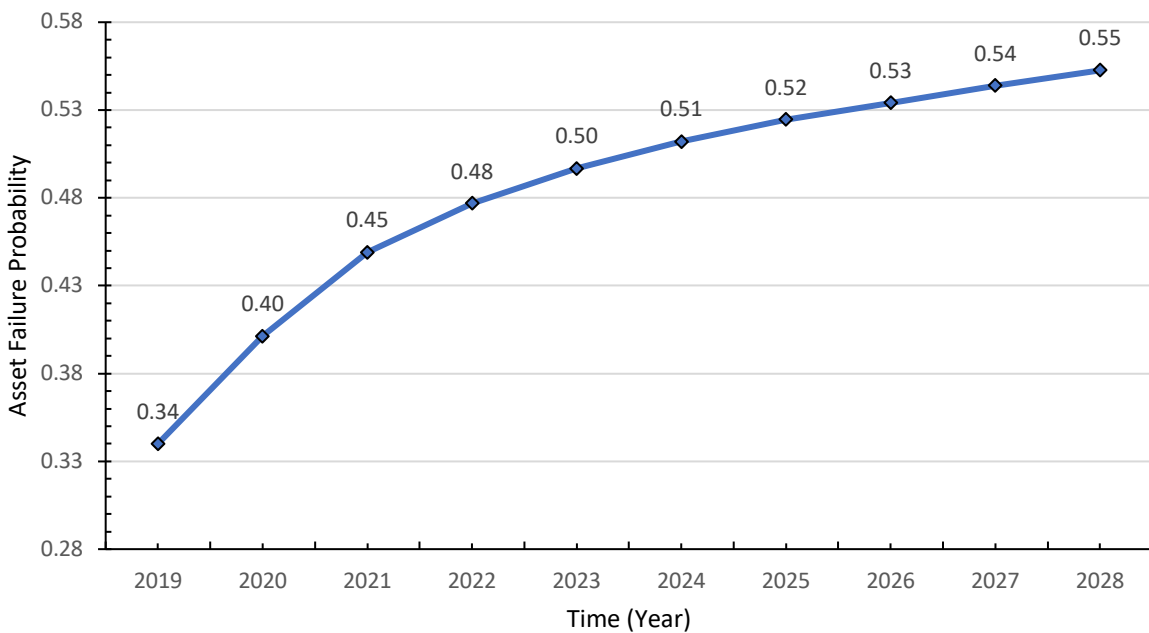


Figure 3. 10: A DOOBN indicating the asset failure over time due to internal corrosion

Fig.3.10 indicates the results of DOOBN for asset failure. It shows that the likelihood of asset failure is 0.34 (34%) in the year 2019 due to the loss of pipe wall thickness, as indicated in Fig. 9. The likelihood of asset failure in 2020 and 2023 are increased to 0.40 (40%) and 0.50 (50%), respectively. After this trend, there is a steady increase in asset failure; in 2028, the likelihood of asset failure will reach 0.55 (55%). These results can help management to develop plans to prevent further corroding of the asset over time.

Sensitivity analysis was performed to understand how the variations of different parameters affect asset failure. Sensitivity analysis also helps to prioritize different events based on their influence on the likelihood of asset failure. For this study, three scenarios were chosen to perform sensitivity analysis. Scenario 1 shows the variations in asset failure due to pressure changes. Scenario 2 indicates the variations in asset failure due to changes in wall thickness over time, and Scenario 3 shows the effect of the outer diameter on asset failure. For each scenario, the probability of occurrence of the variable under study was set to one while the likelihood of the other events remained unchanged, and its influence on asset failure was studied. The results of all three scenarios are presented in Fig.3.11.

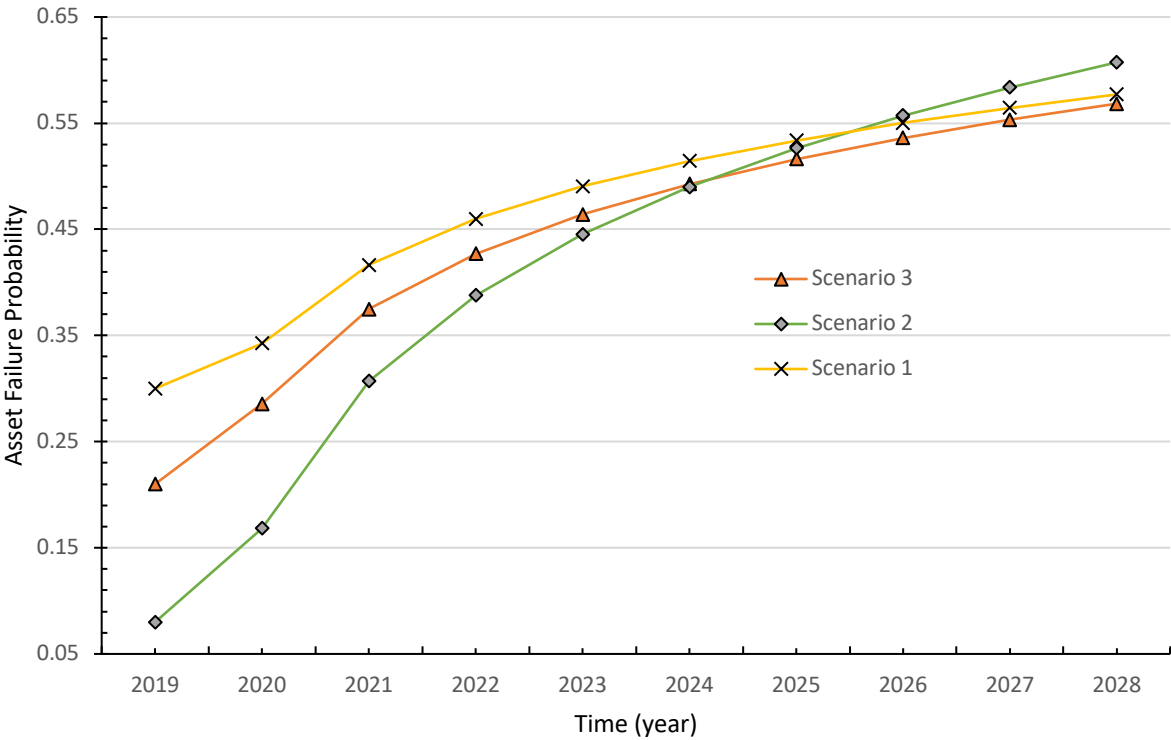


Figure 3. 11: Variations of three scenarios over time in the study

Results show that at the start of 2019, asset failure has the least likelihood of failure due to wall thickness (scenario 2), and there are the highest chances of asset failure due to variations in the

operating pressure inside the pipe. This result agrees with published work in the literature; for example, see (Aulia et al., 2019). Due to its significant contributions to the failure of pipelines, DNV-RP-F101 has categorized it as a basis for assessing corrosion defects. Corrective and preventative measurements can be adapted to minimize the risk of asset failure due to pressure variations inside the pipeline. The maximum allowable operational/operating pressure (MAOP) is one of the methods that can be implied for this purpose (Okodi et al., 2020). The variables linked through directed arcs in DOOBN evolve over the ten slices. The predicted failure probability provided the likelihood prediction of asset failure until 2028. Results identify that with the passage of time, variations in outer diameter, wall thickness, and pressure changes cause an increase in the likelihood of asset failure. In 2028, the probability of asset failure due to changes in wall thickness is higher than that of changes in the outer diameter of the pipeline and internal pressure changes. One of the primary reasons for such results could be that, in the absence of any preventive and corrective actions, the internal corrosion reduces the pipeline wall thickness, leading to asset failure. Results also identified that asset failure due to pressure variations has a slightly higher chance (57.70%) of causing asset failure in 2028 than because of a change in the outer diameter of the pipeline, where the likelihood is 56.68%. The proposed model is an exploratory tool to predict pipeline asset failure due to the interaction of MIC, UDC, erosion, and uniform and localized corrosion. The model captures the non-linear interactions between these influencing factors and provides the failure of assets in different time slices. The dynamic model finds its applications in offshore oil and gas industries, where it can further enhance the forecasting and monitoring of asset failure propagation. In future work, it is recommended to study the extent of corrosion damage based on the dynamic model in this study.

Model validation

Model validation is one of the critical steps in the DOOBN learning process. The model accuracy and ROC curve results of the validation are discussed in this section. The accuracy value represents the model's correctness in model validation. It is described in terms of a percentage or likelihood value. In this study, the model's accuracy in predicting the correct value of the asset failure node was 0.9322 (93.22%). The interpretation of these results is that the model successfully predicted 839 out of 900 records for each of the DOOBN's ten-time steps. Fig.3.12 shows the accuracy of individual time steps.

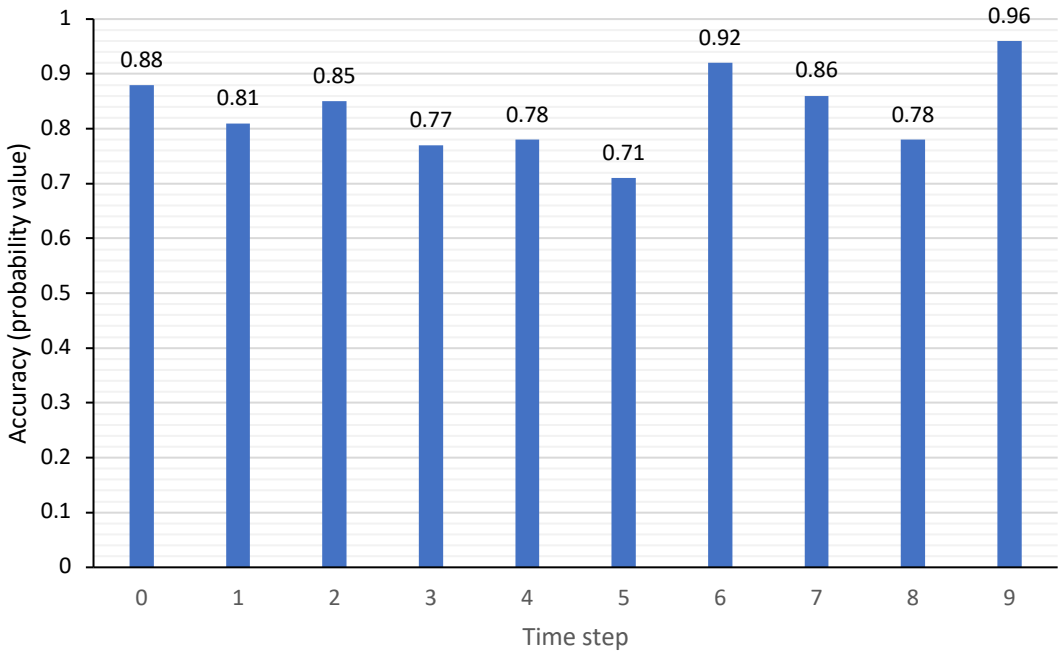


Figure 3. 12: Accuracy of the proposed model for each time step.

Accuracy is represented in probability values ranging from 0 to 1.

Fig.3.12 shows that time step 9 has the highest accuracy of 0.96 (96 percent accuracy) while time step 5 has the least accuracy of 0.71. The receiver operating characteristic (ROC) curve is a graphical representation of the relationship between the false positive rate (1-specificity) and the

true positive rate (sensitivity). The effectiveness of the response variable, asset failure, is measured by the area under the ROC curve (AUROC). While AUROC's ideal value is 1, a random guess will result in a value of 0.5 (Bewick et., 2004). This finding suggests that a value above 0.5 and closer to 1 denotes a better judgment. High true positive values are indicated by an increase in AUROC, demonstrating that model results are reliable. Fig.3.13 shows the ROC curve of the response variable in this study.

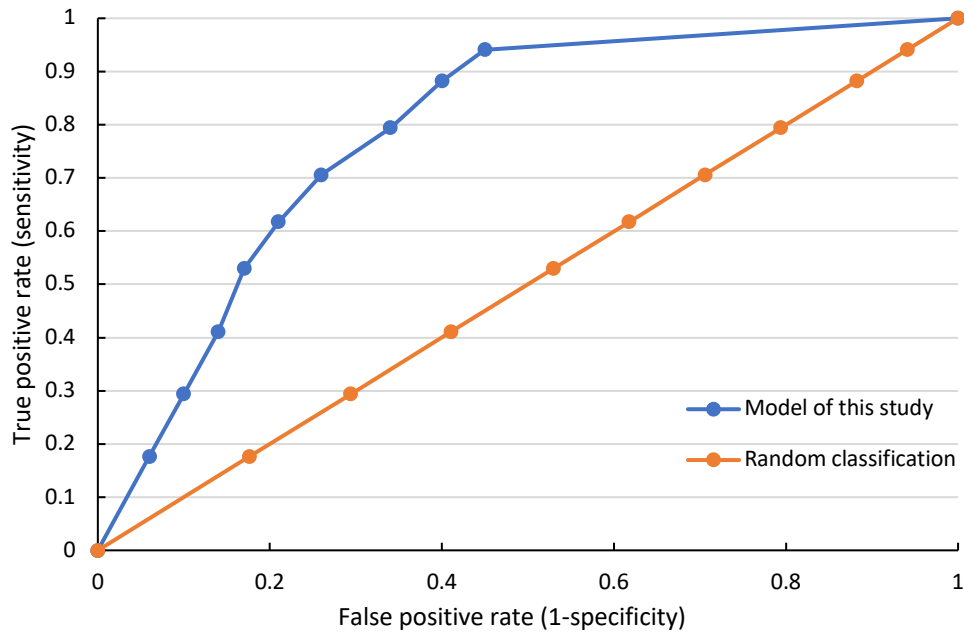


Figure 3. 13: Validation of the DOOBN model in this study

In Fig.3.13, random classification is a diagonal line. It indicates a hypothetical classifier for the ROC baseline curve, and classifiers below this denote the worthlessness of data and indicate that data is worse. For a model to be useful, the classifier values of the model should be above the random classifier diagonal, and AUROC should be closer to 1. Results in Fig.3.13 show that the

DOOBN model shows better performance and that results are reliable. The AUROC for the model is 0.9322, indicating that the data used, and the model results are reliable.

3.6 Conclusions

In this study, we developed a mathematical model for risk assessment of asset failure due to internal corrosion in a gas pipeline. We proposed our model based on the OOBN technique, which included five different corrosion mechanisms in the study. These are internal corrosion due to UDC, uniform corrosion, localized corrosion, erosion, and MIC. The OOBN also helped overcome the computational limitations of regular BN dealing with an extensive network. The technique consisted of breaking complex networks into small, interconnected fragments called Bayesian sub-network models. The OOBN was transformed into a DOOBN by analyzing the asset failure over time. The study identified 94 risk factors contributing to asset failure due to internal corrosion. It is concluded that among the five categories of internal corrosion in our case study, UDC has the highest contribution to causing inner deterioration, followed by MIC, while uniform corrosion has the least contribution to internal corrosion. The study also concluded that the outer diameter of the pipeline and operating pressure significantly influence asset failure. It concluded that the use of DOOBN helped to understand the variations in internal corrosion probabilities over time. In future work, it is recommended to develop maintenance management actions based on the results of this study.

Data availability statement

The DOOBN presented in this article and the pipeline's data are available through a public data repository Mendeley at: <https://data.mendeley.com/datasets/g5h5gktwnd/1>.

3.7 Appendix

Table 3. 1: OOBN for asset failure due to internal corrosion of oil and gas pipeline

Parameters		Sub criteria	State	Discretization Values
3.1.1 A Bayesian subnetwork model for UDC (Fig.3.4)				
1	UDC rate (mm/year)	Operating parameter; Fluid chemistry; Material parameter; Deposition parameter	High	$2 \leq \text{UDC rate} < 5$
			Moderate	$1 \leq \text{UDC rate} < 2$
			Low	UDC rate < 1
2	Operating parameter	Temperature; pH; Operating pressure; Wetting factor	Absent	CPT
			Present	
3	Temperature (T), °C		High	$60^\circ\text{C} \leq T$
			Moderate	$30^\circ\text{C} \leq T < 60^\circ\text{C}$
			Low	$T < 30^\circ\text{C}$
4	pH		Acidic	$6 \leq \text{pH}$
			Neutral	$5 \leq \text{pH} < 6$
			Alkaline	$4 \leq \text{pH}$
5			High	$100 \leq \text{OP}$
			Moderate	$10 \leq \text{OP} < 100$

	Operating pressure (OP), Bar		Low	OP < 10
6	Wetting factor	Water cut; Flow velocity; Flow type	False	CPT
			True	
7	Water cut (WC), %		High	$30 \leq WC < 100$
			Moderate	$15 \leq WC < 30$
			Low	WC < 15
8	Flow type (FT), m/s	Density; Pipe internal diameter; Viscosity	High	$2 \leq FT < 3$
			Moderate	$1 \leq FT < 2$
			Low	$0.1 \leq FT < 0.5$
			Stagnant	$0 \leq FT < 0.1$
9	Density		High	Case dependent
			Moderate	
			Low	
10	Pipe internal diameter (mm)		More than 481.5mm	Database
			Diameter 1 to 481.4mm	
11			High	Case dependent

	Viscosity, cp		Moderate	
			Low	
12	Fluid chemistry	Redox potential; Chemical parameter	Absent	CPT
			Present	
13	Redox potential	Electron acceptor presence; Electron donor presence; O ₂ ; Hydrogen	Low	CPT
			High	
14	Electron acceptor presence		False	Case dependent
			True	
15	Electron donor presence		False	Case dependent
			True	
16	O ₂ , ppm		High	$100 \leq O_2$
			Moderate	$10 \leq O_2 < 100$
			Low	$O_2 < 10$
17	Hydrogen		High	Unknown
			Moderate	
			Low	

18	Iron oxide	Fe2plus; Fe3plus; O ₂	Absent	CPT
			Present	
19	Fe2plus (Fe ²⁺), ppm		Non-reactive	$0 \leq \text{Fe}^{2+} < 30$
			Reactive	$30 \leq \text{Fe}^{2+} < 100$
20	Fe3plus (Fe ³⁺), ppm		Non-reactive	$0 \leq \text{Fe}^{3+} < 40$
			Reactive	$40 \leq \text{Fe}^{3+} < 100$
21	Corrosion parameter	Iron oxide; Carbonates; Sulphates	Absent	CPT
			Present	
22	Chemical parameter	Chloride; H ₂ S; Corrosion parameter; CO ₂	Low	CPT
			High	
23	Chloride (Cl), ppm		High	$30,000 \leq \text{Cl}$
			Moderate	$500 \leq \text{Cl} < 30,000$
			Low	$0 \leq \text{Cl} < 500$
24	H ₂ S, ppm		Low	$0 \leq \text{H}_2\text{S} < 50$
			High	$50 \leq \text{H}_2\text{S} < 1000$

25	CO ₂ , Bar		High	$10 \leq \text{CO}_2 < 100$
			Moderate	$1 \leq \text{CO}_2 < 10$
			Low	$0 \leq \text{CO}_2 < 1$
26	Material parameter	Surface parameter; Design parameter	No	CPT
			Yes	
27	Surface parameter	Surface; Surface coating; Welding marks	No	CPT
			Yes	
28	Surface		Absent	Pipeline operator
			Present	
29	Surface coating		No	Pipeline operator
			Yes	
30	Welding marks		No	Pipeline operator
			Yes	
31	Design parameter	Bends and inclination; Discontinuities and dead	No	CPT
			Yes	
32	Bends and inclination		Inclined	Pipeline operator
			Flat	
33	Discontinuities and dead		No	Pipeline operator
			Yes	

34	Organic deposits	Wax; Asphaltenes	No	CPT
			Yes	
35	Wax		No	Database
			Yes	
36	Asphaltenes		No	Database
			Yes	
37	Inert deposits	Scale presence; Sand presence; Debris presence	No	CPT
			Yes	
38	Scale presence		High	Depends on the product type
			Moderate	
			Low	
39	Sand presence		False	Asset specific parameters
			True	
40	Debris presence		No	Asset specific parameters
			Yes	
41		Inert deposits (as above);	No	CPT

	Deposit presence	Organic deposits (as above); Metallic oxides; Biofilm presence; Deposition parameter	Yes	
42	Deposition parameter	Deposit elimination; Deposit depth; Deposit porosity; Deposit presence (as above)	High	CPT
			Moderate	
			Low	
43	Deposit porosity		No	Case dependent
			Yes	
44	Deposit elimination	Inspection state; Pigging effectiveness; Pigging frequency	False	CPT
			True	
45	Inspection state		No	Pipeline operator
			Yes	
46	Pigging effectiveness		Low	Pipeline operator
			High	
47	Pigging frequency		High	- More than once in 4 weeks
			Moderate	

			Low	- Once 12 weeks - Less than once in 48 weeks
48	Metallic oxides		No	Unknown
			Yes	
49	Biofilm presence		No	Unknown
			Yes	
3.1.2. A Bayesian subnetwork for uniform corrosion (Fig.3.5)				
50	Uniform corrosion	Inhibited corrosion rate; Wetting factor	False	CPT
			True	
51	Inhibited corrosion rate	Uninhibited corrosion rate; Corrosion inhibition	CPT	CPT
52	Corrosion inhibition		No	Unknown
			Yes	
53	Internal corrosion mitigation	Corrosion inhibition; Internal coating	False	CPT
			True	
54	Uninhibited corrosion rate	Iron oxide; H ₂ S; CO ₂ ; Temperature; pH	No	CPT
			Yes	

3.1.3. Bayesian network for localized corrosion (Fig.3.6)				
55	Localized corrosion	Galvanic cell; UDC rate	False	CPT
			True	
56	UDC rate	Deposit presence; Wetting factor	High	CPT
			Medium	
			Low	
57	Galvanic cell	Anodic film; Passive film; Chloride; Localized inhibitor	No	CPT
			Yes	
58	Localized inhibitor	Corrosion inhibition; Flow velocity	False	CPT
			True	
59	Anodic film		False	Unknown
			True	
60	Passive film		False	Unknown
			True	
3.1.4. A Bayesian subnetwork model for erosion (Fig.3.7)				
61	Erosion corrosion	Solid particles; Water cut; Geometry change	No	CPT
			Yes	

62	Solid particles		High	Depends on the product type
			Moderate	
			Low	
63	Geometry change	Valve; Bends & inclination; T_piece; Diameter change	No	CPT
			Yes	
64	Diameter change		No	Unknown
			Yes	
65	T_piece		No	Pipeline operator
			Yes	
66	Valve		No	Pipeline operator
			Yes	
3.1.5. A Bayesian subnetwork model for MIC (Fig.3.8)				
67	MIC (mm/year)	Operating parameter; Bacteria Presence; Wetting factor; Water condition; MIC control	No	CPT
			Yes	
68	Operating parameter	Deposit presence; Operating parameter;	False	CPT
			True	

		Pigging frequency		
69	Bacteria Presence		False	Unknown
			True	
70	Water condition, ppm	Redox potential; Mineral content	False	CPT
			True	
71	MIC control	Pigging frequency; Biocides treatment; Pigging effectiveness	False	CPT
			True	
3.1.6. A Bayesian subnetwork model for asset failure of a gas pipeline (Fig.3.9)				
72	Asset failure	Operating pressure; Pipe outer diameter; Pipe wall thickness	No	CPT
			Yes	
73	Pipe outer diameter, mm		OD 497.4 to 512.4	Database
			512.5 to 514.4 mm	
74	Pipe wall thickness	Asset failure due to; UDC_Rate (UDC rate) Asset failure due to uniform corrosion (Uniform corrosion); Asset failure due to localized corrosion (Localized corrosion); Asset failure due to erosion (Erosion); Asset failure due to MIC (MIC).	False	CPT
			True	
CPT: Based on conditional probability tables developed by experts' knowledge elicitation (Step 4).				

Table 3. 2: Case history parameters in the DOOBN model

Important Parameters	Value
Temperature (T), °C	28-45°C
pH	Up to 5.31
Operating pressure (OP), Bar	120 - 140 Bar
Water cut (WC), %	Moderate
Flow type (FT), m/s	15 -30
Density	Up to 1025 kg/m ³
Pipe internal diameter (mm)	479.4 mm
Viscosity, cp	1.8- 5 cp
Fluid chemistry	Experts' knowledge
Electron acceptor presence	N/A
Electron donor presence	N/A
O₂, ppm	N/A
Hydrogen	N/A
Fe₂plus (Fe²⁺), ppm	N/A
Fe₃plus (Fe³⁺), ppm	N/A
Chloride (Cl), ppm	Up to 6540 ppm
H₂S, ppm	Up to 20
CO₂, Bar	Up to 100
Surface	N/A
Surface coating	N/A
Welding marks	N/A
Bends and inclination	Flat
Discontinuities and dead	Yes
Wax	High
Asphaltenes	High

Scale presence	Moderate
Sand presence	Less sand
Debris presence	N/A
Deposit porosity	N/A
Inspection state	Yes
Pigging effectiveness	Good
Pigging frequency	Intelligent pig Less than once in 48 weeks
Metallic oxides	N/A
Biofilm presence	N/A
Corrosion inhibition	N/A
Anodic film	N/A
Passive film	N/A
Solid particles	High
Diameter change	N/A
T-piece	Yes
Valve	Yes
Bacteria Presence	High
Pipe outer diameter, mm	514.4 mm

Table 3. 3: The operational summarized data of the gas pipeline during six years

Value	Temperature (°C)	Pressure (Bar)	Flow Rate (MMSCMD)
Minimum	25.62	0	0
Maximum	56.79	156	10.46
Mean	45.89	140	5.53

CHAPTER 4

4 A Bayesian approach to under-deposit corrosion assessment in oil and gas pipelines

4.1 Preface

*A version of this chapter has been submitted to **the Journal of Process Safety and Environmental Protection** (Under review). I am the primary author along with the Co-authors, Faisal Khan, Yahui Zhang, Rioshar Yarveisy, Shams Anwar, and Hai H. Ngo. I developed the conceptual framework for the model and carried out the literature review. I prepared the first draft of the manuscript and subsequently revised the manuscript based on the co-authors' and peer review feedbacks. Co-author Faisal Khan helped in the concept development and testing the model, reviewing, and revising the manuscript. Co-author Rioshar Yarveisy assisted in development and data analysis of systematic review paper and reviewing the manuscript. Co-author Shams Anwar assisted in the literature review and review the manuscript. Co-author Hai H. Ngo provided help in idea preparation of research activities and data curation. Co-author Yahui Zhang contributed to implementing the concept and reviewing the manuscript. Co-author Zaman Sajid contributed to implementing the concept and reviewing the manuscript.*

4.2 Abstract

Under-deposit corrosion (UDC) and microbiologically influenced corrosion under deposits (UD-MIC) have increasingly been identified as severe forms of localized corrosion threatening the integrity of pipelines. This work utilizes a knowledge-based, semi-quantitative Bayesian approach to capture UDC and UD-MIC susceptibility and severity. This article proposed a Bayesian Network framework to study susceptibility to UDC and UDC corrosion rate. The effective corrosion rate is introduced as a measure to combine the susceptibility and corrosion rate. This

measure could identify high-risk locations by assessing the probable corrosion rate while highlighting the pipeline's vulnerability to deposit settlement. Four case studies of pipeline failures due to UDC illustrate the framework's validity. A case study for a sweet gas pipeline is adapted to explore the model's robustness in assessing cases with low probabilities of UDC occurrence. The gas pipeline data, the corrosion key performance indicators spanning six years, general information on the pipeline, and the Bayesian network are made publicly available through a repository.

Keywords: Under deposit corrosion; MIC; Bayesian method; Bayesian Network; Pipeline

4.3 Introduction

Pipelines serve as the primary means of oil and gas transportation worldwide (Alves & Lima, 2021; Foorginezhad et al., 2021; Biezma et al., 2020) emphasizing the importance of integrity management in the sector. The statistics in the oil, gas, and chemical process industries, point out that 70% of all mechanical integrity failures are related to piping. In the United States, the Pipeline and Hazardous Materials Safety Administration (PHMSA) reported 5709 major pipeline accidents from 1998 to 2017, with corrosion failure accounting for 20% of the accidents (PHMSA, 2017). The destructive internal corrosion of the multiphase pipelines caused \$203 million in losses in 2017. In addition to causing great economic loss when pipelines are damaged, they also pose a major environmental threat. As a result, risk-based pipeline integrity management programs are increasingly used to mitigate the environmental, societal, and financial risks of operating these assets. The pipeline integrity management programs call for accurate modeling of corrosion progress as the main time-dependent hazard (Cruz et al., 2022; Khan et al., 2021).

A severe type of localized degradation is under deposit corrosion (UDC) (Alamri, 2020). UDC refers to the development and progression of corrosion under or in the vicinity of accumulated deposits due to the creation of micro-environments with different corrosion-related characteristics

(Gósi et al., 2022). Under specific operational conditions, particles carried by the flow gather and form deposits at the six o'clock position of pipelines. Water may be in the same position depending on the terrain and other operational parameters. In the presence of water, these deposits create isolated local micro-environments with characteristics vastly different from those of the bulk fluid. Under the deposits, zones with different electrochemical potentials form and cause corrosion. In addition to these conditions, the deposits prevent the corrosion products from dispersing. The collected metallic corrosion products can potentially exacerbate the corrosion progress.

Despite developing various methods for experimental assessment and studying UDC, the knowledge of the phenomenon and its mechanisms is still growing. The relatively slow progress in understanding UDC is due to the difficulties of monitoring corrosion-related activities under the deposits (Sliem et al., 2021). Furthermore, UDC attack impacts the surface based on many known mechanisms. These mechanisms materialize depending on various environmental, operational, and deposit-related parameters. For instance, most cases of UDC occurrence are associated with microbiologically influenced corrosion (MIC).

MIC is the exacerbated degradation progress of metallic materials in the presence of microorganisms. The MIC attack sheltered by deposits is called UD-MIC hereafter. In the oil and gas industry, UDC represents a significant risk to the integrity of carbon steel pipelines. The formation of solid deposits provides rich conditions for microorganisms to grow (Ryu and Yoon, 2021). Thus, addressing microbiological and deposit-related factors in the combined UD-MIC corrosion process is crucial for understanding its mechanism. Considering the limited literature on the UD-MIC phenomenon, this research article adapts the influencing factors by incorporating the specific conditions brought about by deposits. Insufficient knowledge about the mechanisms and interactions causing the phenomenon compels the practitioners to use knowledge-based and

subjective modeling. Moreover, missing data necessitates implementing probabilistic approaches to deal with uncertainty. Reliability of oil and gas pipelines are integral part of system safety and there are many factors which effect the system reliability. The interdependencies of these factors have not been explored previously. The novel methodology presented in this study contributes by developing an interconnected network which shows the interdependencies and influencing factors that contribute to the asset degradation due to UDC and UDC-MIC. Thus, this work utilizes a Bayesian network (BN) to assess susceptibility to UDC and UD-MIC and provides a semi-quantitative measure of the severity of expected corrosion rates, relying on available knowledge of these phenomena. Even though to our knowledge, this approach has not been applied to modeling UDC, the BN is one of the most used tools for modeling MIC (Yazdi et al., 2021). In this study, the probabilistic BN modeling is applied because of mainly three reasons. First, the BN model help to develop directional relationships among different variables of corrosion rates. These directional relationships develop a network which can be studied probabilistically to capture and evaluate the likely impact of corrosion on system susceptibility. Second, the develop network can update values of its states when new information (evidence) becomes available. This aspect important in corrosion studies. Third, BN model helps to predict the likelihood of each possible causes that contribute to pipeline failure. In this way, one can assess the most critical risk factor in corrosion of oil and gas pipelines.

The BN proposed in this work first assesses which UDC or UD-MIC mechanisms are likely to occur, then provides a semi-quantitative measure of expected rates and combines the two to provide an effective UDC rate. The model's viability is evaluated against case histories of UDC-related accidents. Furthermore, a case study focused on a sweet, dry gas pipeline illustrates the model's robustness. In addition to the Bayesian network proposed here, the corrosion key

performance indicators of the gas pipeline from 2015 to 2020, including product specifications, are made publicly available through a repository (Dao et al., 2022).

Bayesian networks (BNs)

Bayesian networks (BNs) are widely used for safety and risk analysis because they incorporate complicated causal relationships and present them graphically (Meng et al., 2022; Sajid et al., 2017, 2020). A BN structure can be defined subjectively (knowledge-driven) by relying on the expert's experience with variables and their correlation (Dawuda et al., 2021; Mamudu et al., 2021). Many researchers have used BNs to reflect corrosion-related phenomena with various levels of uncertainty (Abubakirov et al., 2020). The research concerning MIC has relied on discrete Bayesian networks (Adumene, Khan, Adedigba, and Zendejboudi, 2021), continuous Bayesian networks (Yazdi et al., 2021), dynamic bayesian networks (Bougofa et al., 2021; Sajid, 2021), and data-driven approaches relying on Bayesian inference for structural learning (Kamil et al., 2021). Applicability of these methods ranging from data-driven models to subjective knowledge-based networks depends on data availability.

As directed acyclic graphs, BNs are composed of nodes representing variables and arcs representing causal links between them. The CPTs specify how the parent nodes affect their children by assigning probability values to them (Meng et al., 2023). By definition, BNs represent the probability distributions $P(U)$ associated with variables $U = \{A_1 \dots A_n\}$, such that the probability distributions have conditional independence and are connected through a chain as shown in equation (4.2).

$$P(U) = \prod_{i=1}^n P(A_i | P_a(A_i)) \quad (4.1)$$

where, $P_a(A_i)$ are the parents of A_i in the Bayesian Network, and $P(U)$ represents the properties of the BN (Kamil et al., 2021; Khakzad et al., 2013).

BNs rely on the Bayes theorem, where the prior probability of occurrence of nodes (parameters) can be updated using new information. This principle shown in equation (4.3) can be utilized to either predict the probability of occurrence of a child given its parents or update the prior probabilities of parents given their child. The probability of the form $P(\text{outcome} | \text{event})$ is calculated in a predictive analysis, which indicates the likelihood of an accident occurring based on knowledge about the outcome of a primary event (Kamil et al., 2023; Sajid, 2021).

$$P(U|E) = \frac{P(U, E)}{P(E)} = \frac{P(U, E)}{\sum_U P(U, E)} \quad (4.2)$$

4.4 The Proposed Model

UDC occurrence depends on the accumulation of solids and water in the six o'clock position of the pipelines. Under the deposits, conditions promoting various corrosion degradation and inhibiting mechanisms may exist (Anwar et al., 2022; Jawwad and Mohamed, 2020). The widespread co-occurrence of UDC and MIC under the deposits necessitates UD-MIC inclusion in models involved with UDC. The complexity and uncertainty of the phenomena related to UDC and the specificity of conditions leading to its occurrence require probabilistic approaches. Here, a Bayesian network is adapted to model the damage-causing mechanisms and conditions leading to UDC together to observe the joint impact of these aspects on the degradation rates.

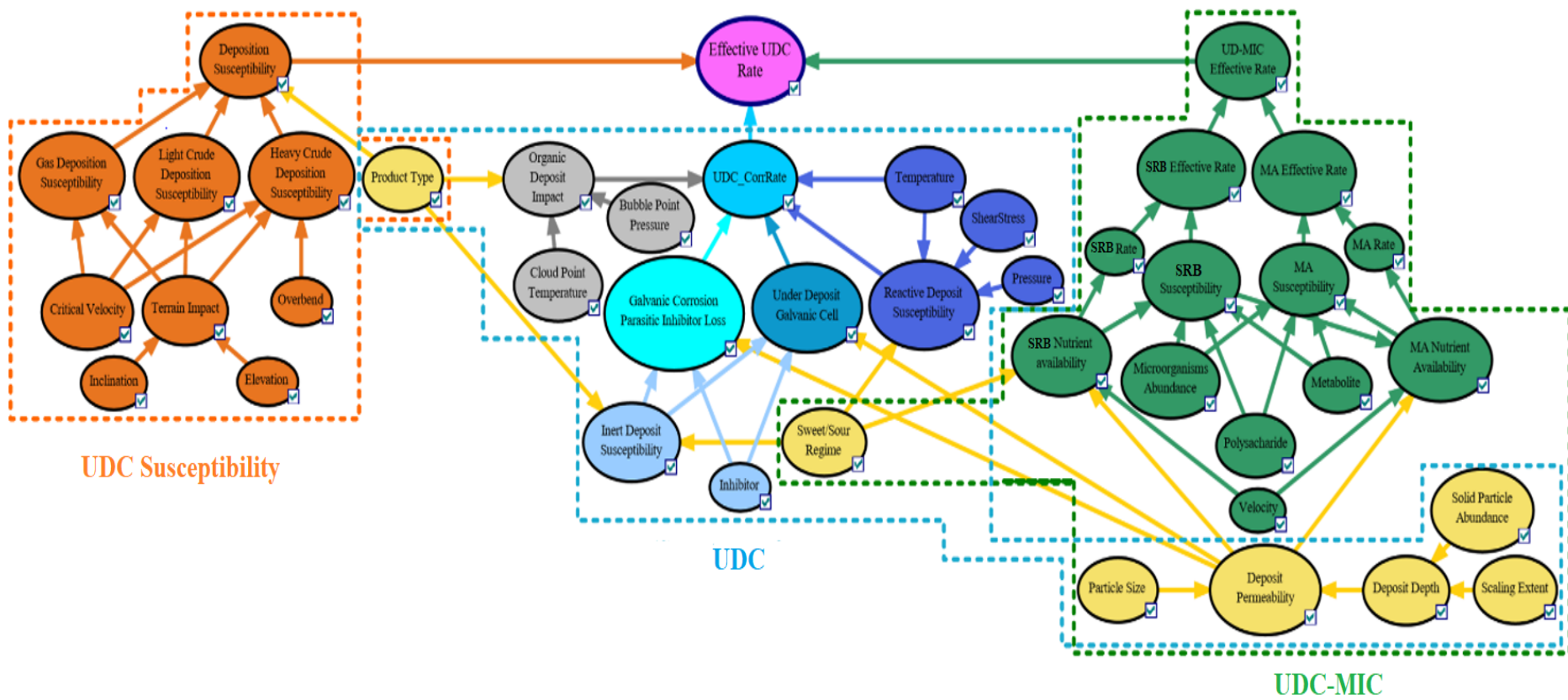


Figure 4.1: Overview of the UDC effective corrosion rate model for oil and gas pipelines

This section presents the proposed Bayesian network model for UDC assessment in oil and gas pipelines. Fig. 4.1 shows an overview of the BN. Each of the submodels is distinguishable by the distinct color of its nodes. The model comprises three main modules:

(1) UDC: The available literature suggests UDC occurs as galvanic cells forming under or around the deposits. The conditions which influence the formation of galvanic cells and the severity of damage that follows depend on the deposit's characteristics. The UDC submodel is concerned with this aspect. The UDC submodel assesses the corrosion rates expected from various damage-causing mechanisms under the deposits. UDC rate is assessed by choosing the mechanism with the highest UDC rates. This submodel's components are illustrated by the nodes isolated using the dashed blue line in Fig. 4.1 and discussed in detail in the section.

(2) UD-MIC: MIC occurrence and severity are influenced by the presence of sessile microorganisms, sufficient nutrients, and protection from the environment. UD-MIC occurrence is also dependent on the deposit characteristics, i.e., porosity. The UD-MIC submodel's nodes are marked by the green dashed line in Fig. 4.1. The UD-MIC network is presented in section below, and the background understanding supporting the network's structure is presented in the UD-MIC section. This submodel assesses the susceptibility to MIC occurrence and possible degradation rates separately. UD-MIC submodel assesses the possibility of MIC occurrence based on biotic parameters and combines it with the observed corrosion rates obtained from literature to provide the MIC effective rate. The MIC effective rate is the summation of effective rates of sulfate-reducing bacteria (SRB), and methanogenic archaea (MA). This variable works like the effective UDC rate discussed in more detail below.

(3) UDC Susceptibility: It was mentioned that UDC occurrence is related to the accumulation of deposits and water at the 6 o'clock position of pipelines. The conditions promoting deposition

are related to the terrain and design of the pipeline. The probability of deposit accumulation is assessed in the UDC susceptibility submodel highlighted by the orange dashed line in Fi and discussed in more detail in UDC susceptibility.

This section briefly explores the Bayesian Networks and then discusses the mentioned submodels in detail. The model nodes' details are presented in the appendixes, and the BN is shared through the repository (Dao et al., 2022) to provide more information on the conditional probability tables (CPTs). This model aims to calculate the *Effective UDC* rate by combining the UDC and UD-MIC rates to reflect mechanisms causing the highest rates. Lastly, the effective UDC rate is calculated as the product of the deposition susceptibility and the mechanism with the highest threat, as shown in equation (4.1). In Bayesian networks, the sum of the probabilities of each node's states should be unity. Therefore, in cases where deposition susceptibility is not 100%, the effective UDC rate's probabilities will not add up to unity. The remainder is added to the lowest observable state for effective rate, i.e., outstanding ($< 0.02 \text{ mm/year}$).

$$UDC_{effective} = \text{deposition susceptibility} \times \max(UDC, UDMIC) \quad (4.3)$$

4.5 Model results

UDC Submodel

A localized corrosion process develops and progresses under or around the formed deposits on a metallic surface, known as under deposit corrosion (UDC). A significant threat in the oil and gas industry is that carbon steel pipelines will fail due to UDC. UDC is not a specific corrosion type; rather, the occurrence of specific conditions leading to escalated degradation through activation of different galvanic corrosion or MIC mechanisms. These conditions are connected to deposit type, characteristics, and environmental parameters. This section first explores the deposit types and

their impact on the corrosion severity. Then it will discuss the UDC mechanisms individually. Lastly, the UDC aspect of the BN model is presented and discussed.

Deposit types: Deposits accumulated in pipelines significantly impact the observed corrosion rates, as they could exacerbate or inhibit them. Deposits can impact corrosion rates by creating micro-environments with different environmental parameters from the bulk fluid (Sliem et al., 2021; Subramanian et al., 2022). Considering UDC is not a specific corrosion type explainable by a single mechanism (Askari et al., 2019), the corrosion-causing mechanisms under the deposits depend on the deposit's nature.

Most of the literature (Obot, 2021; Östürk and Sevimoğlu, 2021; Sliem et al., 2021) categorizes deposit types into organic and mineral, yet this section divides them into three types: inert deposits, reactive deposits and organic deposits .

Inert deposits: Inert deposits are inorganic deposits that cannot facilitate electrochemical reactions. Inert deposits contribute to UDC by creating different aeration zones and limiting inhibitor diffusion to the metal surface. Therefore, this article adopts an approach similar to that of many other researchers (Lynch, 2019; Makar, 2000), where UDC occurrence is linked to inhibitor presence. The source of inert deposits is either hydrates or particles from the formation. Therefore, as shown in Fig. 4.2, two factors influence the system's susceptibility to the accumulation of inert deposits, i.e., the product type and the system's sourness level.

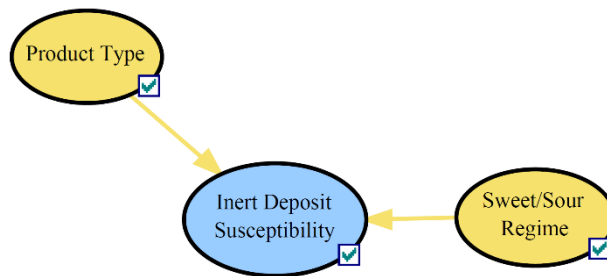


Figure 4.2: The inert deposit susceptibility submodel

The model in Fig. 4.3 relates the occurrence of UDC mechanisms to inert deposit and inhibitor presence and reflects their characteristics (porosity and permeability) to the severity of UDC and UD-MIC mechanisms. There, the deposit's particle size and depth impact the amount of inhibitor loss in addition to diffusion mechanisms. Subsequently, the permeability of the deposits determines which corrosion mechanism is likely to occur.

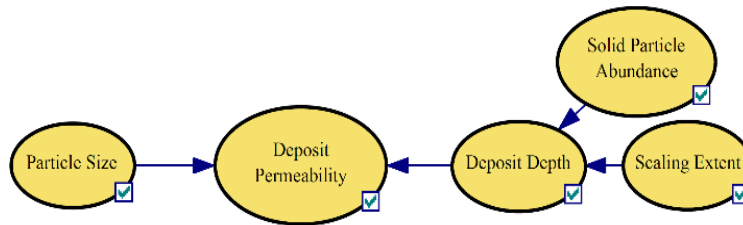


Figure 4.3: The deposit permeability aspect of the UDC model

Here the influence of inert deposits is modeled as a diffusion barrier against inhibitor and nutrient penetration to the metal surface. The permeability of the deposition is the consequence of deposit depth and particle size. Larger particles result in higher diffusion rates and, consequently, higher corrosion rates under the deposits. Scaling extent involves undissolved, or inert water precipitates chipped off from the pipe walls. Details on the nodes and their states are presented in appendix table 4.9.

Reactive deposits: As shown in Fig. 4.4, the parameters influencing the formation of corrosion product layers are pressure and temperature. Furthermore, shear stress influences the product layer's adherence to the pipe wall. On the other hand, sour environments form a range of iron sulfide products, many of which are highly corrosive.

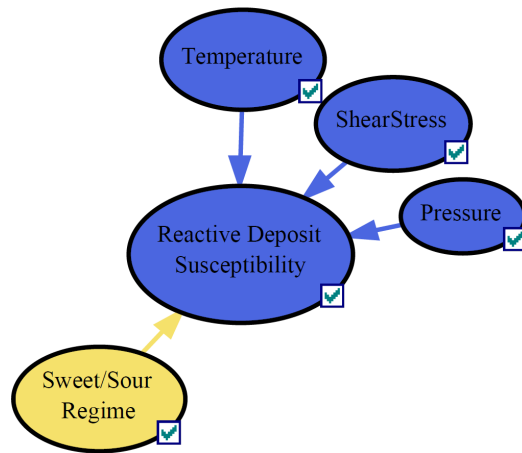


Figure 4.4: Reactive deposit susceptibility submodel

In Fig. 4.4, reactive deposit susceptibility concerns loose and undissolved reactive solids. Therefore, the reactive deposit susceptibility is defined to reflect higher probabilities in the case of sour environments with higher than moderate temperatures where sulfide scales form, but the pressure and shear stresses are low enough, so they do not form hardy scales. These conditions increase the probability of corrosion product formation while allowing dispersion, as they cannot adhere to the walls. Details of the sub model are presented in table 4.10 of the appendix.

Organic deposits: The organic deposits formed on metal surfaces are either living organisms (biofouling) or non-living substances precipitated by crude oil (Finch et al., 2017). Organic deposits in oil and gas pipelines are crude oil precipitates, e.g., wax and asphaltene, or could be biofilm, the bacterial community inside an exopolysaccharide matrix (De Cesare et al., 2020; Irajii and Ayatollahi, 2019). Since, biofilm mostly forms at the interface between microorganisms (planktonic bacteria) and surface materials, the scope of this work is concerned with UDC and UD-MIC and does not consider biofilms and focuses on wax and asphaltene only.

Waxes are long-chain, normal alkane compounds, while asphaltenes are large molecules comprising polyaromatic and heterocyclic aromatic rings with side branching. It should be noted that these organic deposits are an issue only present in crude oil, where wax deposition is observed when dealing with most crudes, but asphaltene-related issues are rare in comparison (G. A. Mansoori et al., 2007; Q. Wang et al., 2020).

As shown in Fig. 4.5, the deposition mechanism of wax is driven by temperature, pressure, and hydrocarbon composition. The wax deposition tendency and rate can be assessed using cloud point, which depends on temperature and pressure and is calculated based on solid-liquid equilibria.

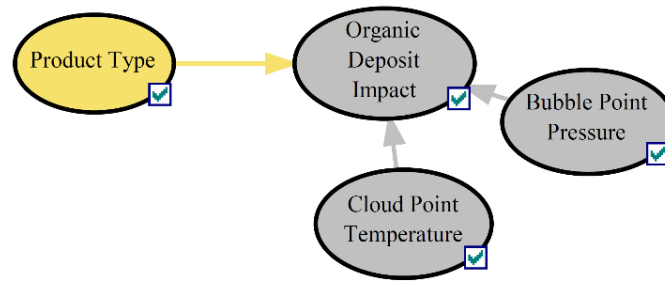


Figure 4.5: Organic deposit impact submodel

Although asphaltene and wax are vastly different in precipitation and mitigation, the interest is in their inhibitive role here. Two simplified parameters, cloud and bubble points, are used to assess organic deposition susceptibility, and the respective corrosion rates are set to the minimum in case of its occurrence.

As illustrated in Fig. 4.5, the organic deposit's impact is influenced by bubble point pressure, representing asphaltene, and the cloud point temperature, representing wax deposition. Lastly, due to the instability of asphaltene in heavy crudes and the lack of these substances in gas, the product

type also influences the organic deposit's capacity to inhibit corrosion. The details of the sub model's components are presented in appendix table 4.11.

UDC mechanisms

In this section, two UDC mechanisms used in the proposed model are explained. The two mechanisms are involved in galvanic corrosion due to inhibitor loss or the formation of different aeration zones. Galvanic corrosion due to parasitic inhibitor loss: In processes with high water cut, where the formation of ionic paths between the area covered under the deposit and uncovered metal is possible, a mechanism similar to crevice corrosion could occur. In this mechanism, the different chemistries under and around the deposition site give rise to the galvanic force required for electron transfer between the internal anode (under the deposits) and external cathode (bare metal) surrounding it (Netto et al., 2005; Subramanian, 2018).

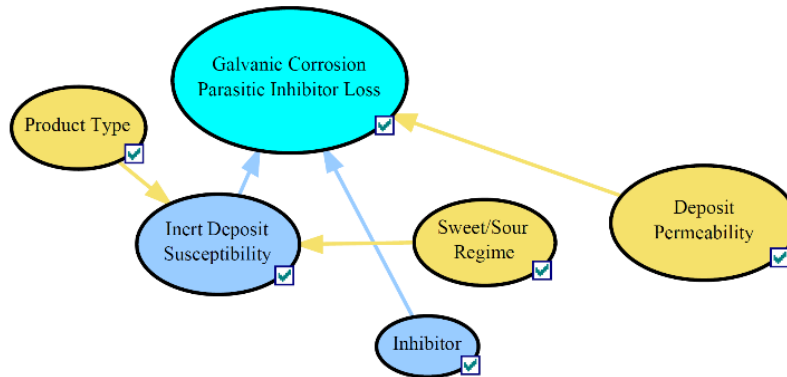


Figure 4.6: Influence diagram for the galvanic corrosion due to parasitic inhibitor loss mechanism

Although UDC occurrence is pertinent to inhibitor application, the use of suitable inhibitors informed by inhibitor performance under deposit tests is proven capable of mitigating these phenomena. This is achieved by successfully increasing inhibitor dosage to cover the increased

area and applying appropriate inhibitors. Therefore, it should be noted that the inhibitor node in this model suggests using an inhibitor without measures to mitigate UDC.

Galvanic corrosion due to parasitic inhibitor loss occurs when the deposit is impermeable. Impermeable deposits maximize the difference between the microenvironment and the bulk fluid. Details of this mechanism's BN nodes are presented in appendix table 4.12.

Under-deposit galvanic cell: In this case, both anodic and cathodic sites are located under the deposits. These electrochemically different areas may establish due to irregularities in deposit particles sequentially creating different chemistries in each other's vicinity. In this mechanism, the deposit is permeable enough for the inhibitor to reach the metal surface, but the grains prevent it from reaching some areas. This results in zones with different potentials close to each other, resulting in galvanic corrosion under the deposits.

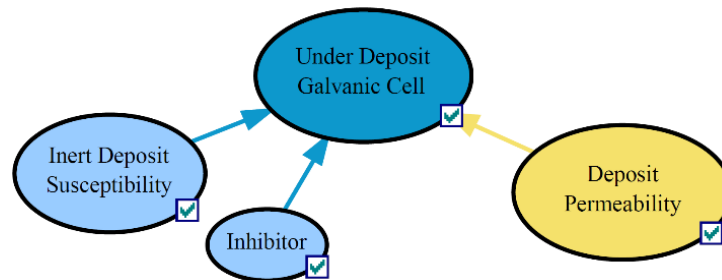


Figure 4. 7: Influence diagram of the under deposit galvanic cell mechanism's components

From Fig. 4.7, it can be observed that this mechanism shares the same parents as the previous UDC mechanism. Galvanic cells under the deposit become predominant under the same conditions as the previous mechanism with one difference: Here, permeable deposits promote corrosion. The higher the amount of biocide reaching the bare metal, the higher the electrochemical potential difference compared to the zones it cannot reach, and consequently, higher corrosion rates.

UDC corrosion rate: The UDC corrosion rate depends on the observed corrosion rates of individual mechanisms.

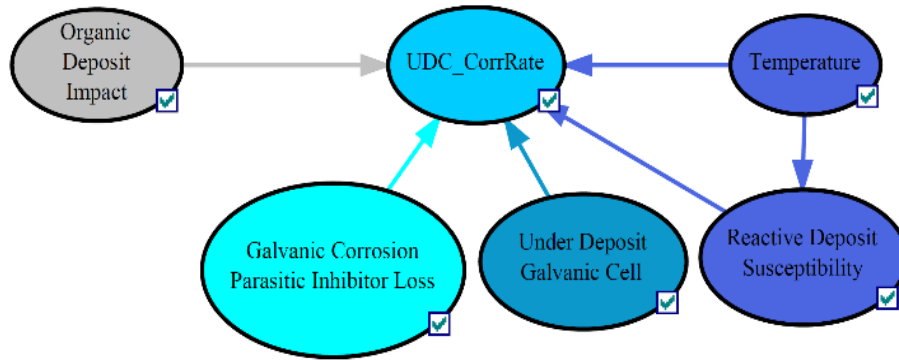


Figure 4.8: Overview of factors influencing UDC

Here, the expected corrosion rate of the UDC submodel is defined as the maximum of the corrosion rates observed by the two mechanisms mentioned above. Furthermore, the exacerbating impacts of reactive deposit's presence and temperature directly influence the UDC corrosion rate. Higher temperatures significantly increase the observed corrosion rates (Ayello et al., 2014; X. Chen et al., 2021). Moreover, the corrosion products have a similar impact with less severity. Lastly, conditions leading to wax and asphaltene deposition inhibit corrosion under the deposits. Considering that removal of wax deposits is easier compared to the hardy deposits, including asphaltene, the inhibiting effect of mixed wax and asphaltene deposits is assumed to be higher. Details of this aspect of the submodel are not presented as the UDC-CorrRate's discretization is similar to the mechanism's nodes and presented in table 4.12, table 4.13 of the appendix, and other nodes were discussed earlier.

UD-MIC Submodel

The submodel presented in this section aims to assess the effective rate of UD-MIC in the presence of methanogenic archaea and sulfate-reducing microorganisms. This model considers the susceptibility and possible degradation rates due to MIC and provides a semi-quantitative severity measure, the effective UD-MIC rate. This measure provides the means to assess the probability of

MIC occurrence due to the system's susceptibility and the probabilities of occurrence of different degradation rates simultaneously. This model avoids involving biological parameters unless necessary and focuses on operational parameters tangible for and available to practitioners.

The complexity of the MIC-related phenomena necessitates providing a background supporting the point of view implemented in modeling them. This section tries to provide a rationally structured background about the general living conditions of microorganisms, taxa involved in MIC, resources required for the attack to occur, MIC indicators, and mechanisms involved in MIC.



Figure 4.9: Overview of the UD-MIC BN's influence diagram

Fig. 4.9 illustrates the influence diagram of the UD-MIC submodel's Bayesian network. Mechanisms through which microorganisms damage metallic materials are many and still debated. The effect of MIC to accelerate corrosion rate is presented clearly. As the widespread occurrence of SRB and MA and deposits, the model is only focused on the bacterial groups involved in SRB and MA.

First, the concept of biofilm and how organisms active inside a biofilm escalate corrosion are discussed. Later, the mechanisms specific to each microorganism and the syntrophic relation between the SRB and MA are discussed.

SRB in the presence of electron donors and sulfate can cause MIC by producing H_2S . The reaction of carbon steel with the biogenic H_2S results in the production of Fe_xS_y , which can be oxidized to form elemental sulfur, another highly corrosive substance. Contrary to all SRB's ability to cause MIC has only been observed in the presence of specialized SRB (Q. Wang et al., 2021; R. Zhao et al., 2022). MA obtain the electrons required to form methane from carbon dioxide by the dissolution of iron. Dissolution of iron results from electron consumption by sulfate reduction, where a conductive deposit (siderite) provides the electron required for the methanogenesis (Venzlaff et al., 2013; Y. Yuan et al., 2022).

The model reflects the influencing parameters in modeling the two MIC mechanisms for MA and SRB. Both mechanisms are modeled using a similar structure where their effective rates are the product of the possibility of the microorganism's activity in the system and their respective corrosion rates. Lastly, the UD-MIC effective rate results from summing the SRB and MA effective rates. The nodes and structure of the network are motivated and discussed in more detail. The importance of including the biofilm in modeling MIC was discussed, and it was highlighted that the model devises the deposition permeability so it can reflect the role of the biofilm. Here,

the deposition permeability acts the same as the UDC model. Meanwhile, the permeability role is rather different. In the UD-MIC submodel, increased permeability results in increased microorganic activity as greater amounts of the nutrient are made available to the microorganisms, resulting in higher corrosion rates.

The difference between the two microorganism's nutrient availability structures are the sweet/sour regime nodes for the SRB and the SRB activity node for the MA. SRB activity is possible in the presence of sulfate. On the other hand, the SRB activity provides the nutrient for methanogens in their syntropic relationship. Therefore, SRB presence in the system improves the nutrient availability to MA. The details of nodes in sub model of UD-MIC are presented in table 4.14.

Fluid velocity is included in the MIC model, its role is more concerned with its limiting impact on the microorganic activity as a nutrient and oxygen carrier rather than the preventive factor for MIC initiation. Nutrient availability for both microorganisms has a similar structure, which is impacted by deposit permeability and velocity. Where deposit permeability and flow velocity are limiting factors for nutrition transfer. As mentioned, permeable deposits result in favorable conditions for microbial activity as they allow more nutrients and water through. Moreover, increasing flow velocities also result in increased nutrient availability.

UDC susceptibility Submodel

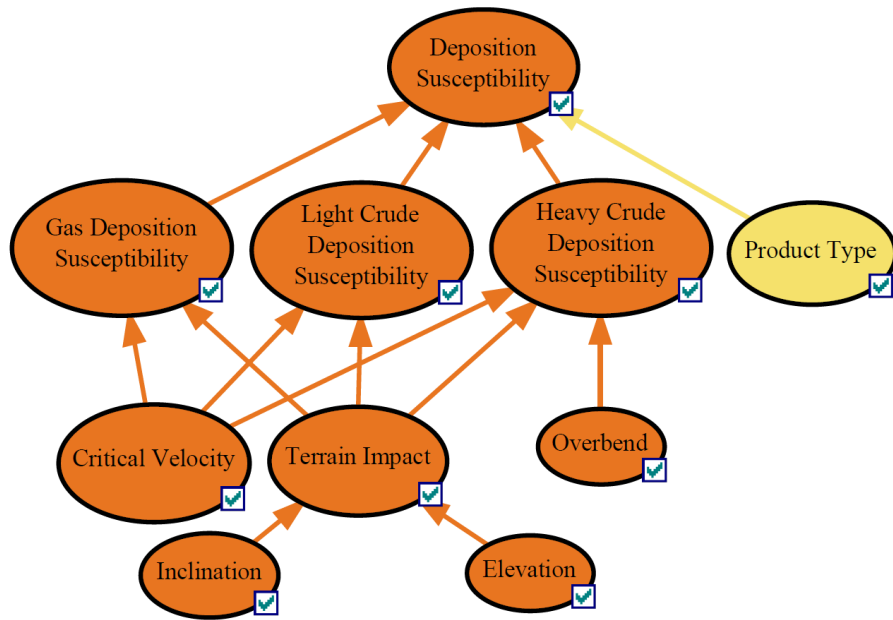


Figure 4.10: The deposition susceptibility assessment submodel

Corrosion requires three components, an anode, a cathode, and an electrolyte containing a reducible species which connects the electrodes (Torkzaban et al., 2008). Oil and gas pipelines’ metallic surfaces can act as cathode and anode when zones with different electrochemical potentials form under or around the deposits (Luo et al., 2021; Pang, Wang, Lu, et al., 2021). Hence, the presence of an electrolyte creating the connection between the two electrodes is the missing component from an electrochemical cell. The susceptibility to UDC pertains to the co-occurrence of the electrolyte with solid deposits. The deposition susceptibility submodel is shown in Fig. 4.10, its nodes are presented in table 4.8 of the appendix.

Product type impacts the deposition mechanisms and consequently affects the probability of favorable conditions for UDC. The pipeline’s terrain plays a pivotal role in possible locations for deposition and water collection. The terrain’s potential for deposition is assessed using two parameters, inclination and elevation. Areas susceptible to deposition are local minima and flat, while sloped and elevated positions have a lower chance of deposition. In the model, a section is

assumed flat if its inclination is less than 5%, and it is considered to be the local minima if it is lower than the sections preceding and coming after it.

The flow's capacity to remove accumulated solids is defined using the critical velocity parameter, implying that velocities less than the required amount by the practitioner's understanding will lead to deposition. The areas close to and downstream from overbends tend to become deposition zones and present signs of corrosion irrespective of the terrain impact on water accumulation. The accumulation of such particles wetted with micro-water is thought to be the cause of corrosion immediately after overbends in large diameter heavy crude carrying pipelines.

4.6 Discussions

Four case histories with varying levels of uncertainty focused on different aspects of the model are adapted. The model is then applied to an offshore gas pipeline case study. The parameters used to simulate the conditions discussed in the case histories are presented in table 4.15 of the Appendix. An overview of the case histories and the assessment results using the BN are presented and discussed in this section. Probability data used in the parent nodes and conditional probability tables (CPTs) of BN model is based on experts' opinions. Experts in this study are a group of researchers led by a senior university professor. The group is actively engaged in research and development on corrosion.

Case 1: Microbial-induced corrosion of subsea pipeline in the Gulf of Suez

This case history represents the leakage of a 17-kilometer, 24-inch, crude carrying, API-5L XS-60 subsea pipeline with a wall thickness of 0.75 inches. As shown on the seabed profile of the pipeline in **Error! Reference source not found.**, failure has occurred on a low and flat area preceding a relatively steep slope. The pipeline carries medium crude with API gravity of 29, water content of 80%, and average paraffin content of 10%. The pipeline is treated with continuous corrosion and

scale inhibitor injections. The information obtained from corrosion monitoring systems suggests corrosion rates of 3 MPY (~0.08 mm/year) with no bacterial activity or indication of scaling or organic deposits.

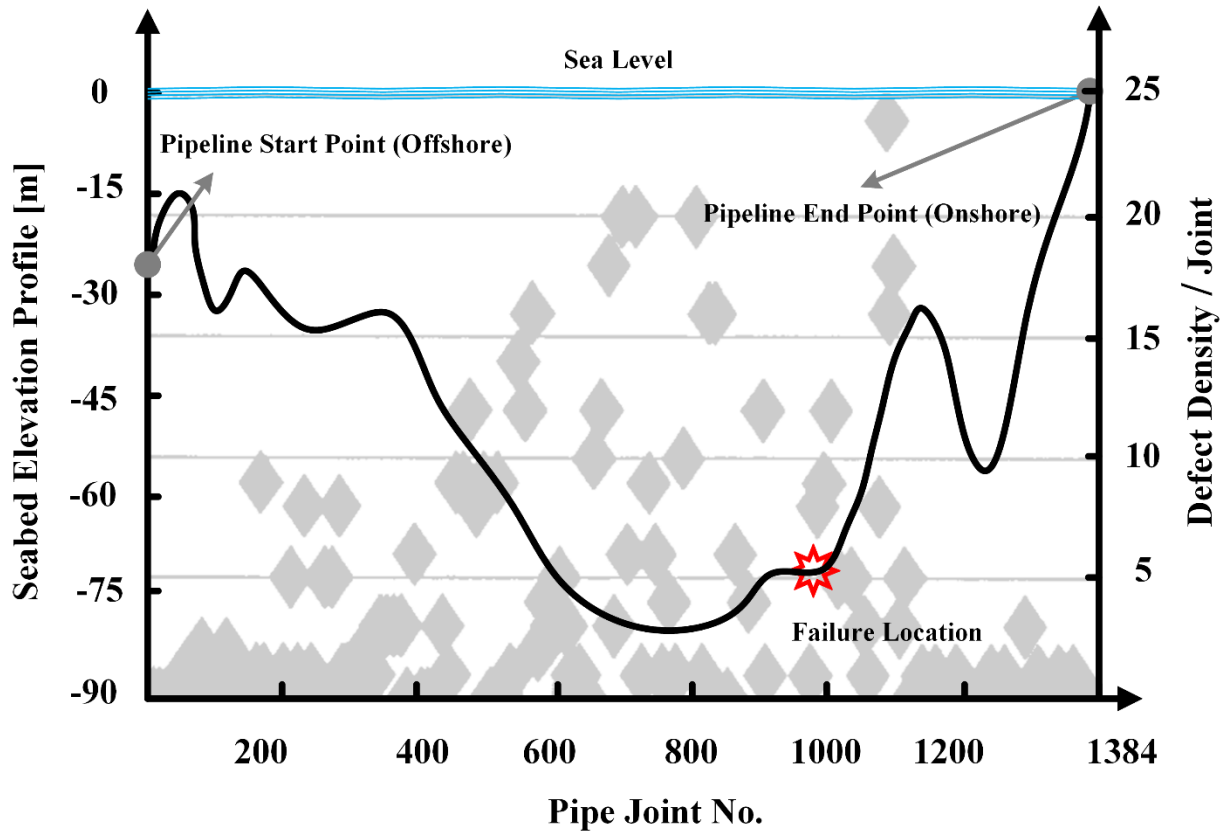


Figure 4.11: The pipeline’s seabed elevation profile and the defect densities on pipe joints, adapted from (El-Raghy et al., 2000)

The failure occurred as five leaks, all in the six o’clock position on an 860-meter-long segment of the pipeline. The post-accident ultrasonic pigging of the pipeline revealed severe metal loss resulting in an 80% wall-thickness reduction on 530 joints spanning over 7 km. Fig. 4.11 illustrates the seabed profile of the pipeline superposed over the defect densities detected by the ultrasonic tool. It can be observed that severe corrosion occurs at the mid-section of the pipeline while the offshore and onshore sides of it are in relatively good condition. The authors report severe metal

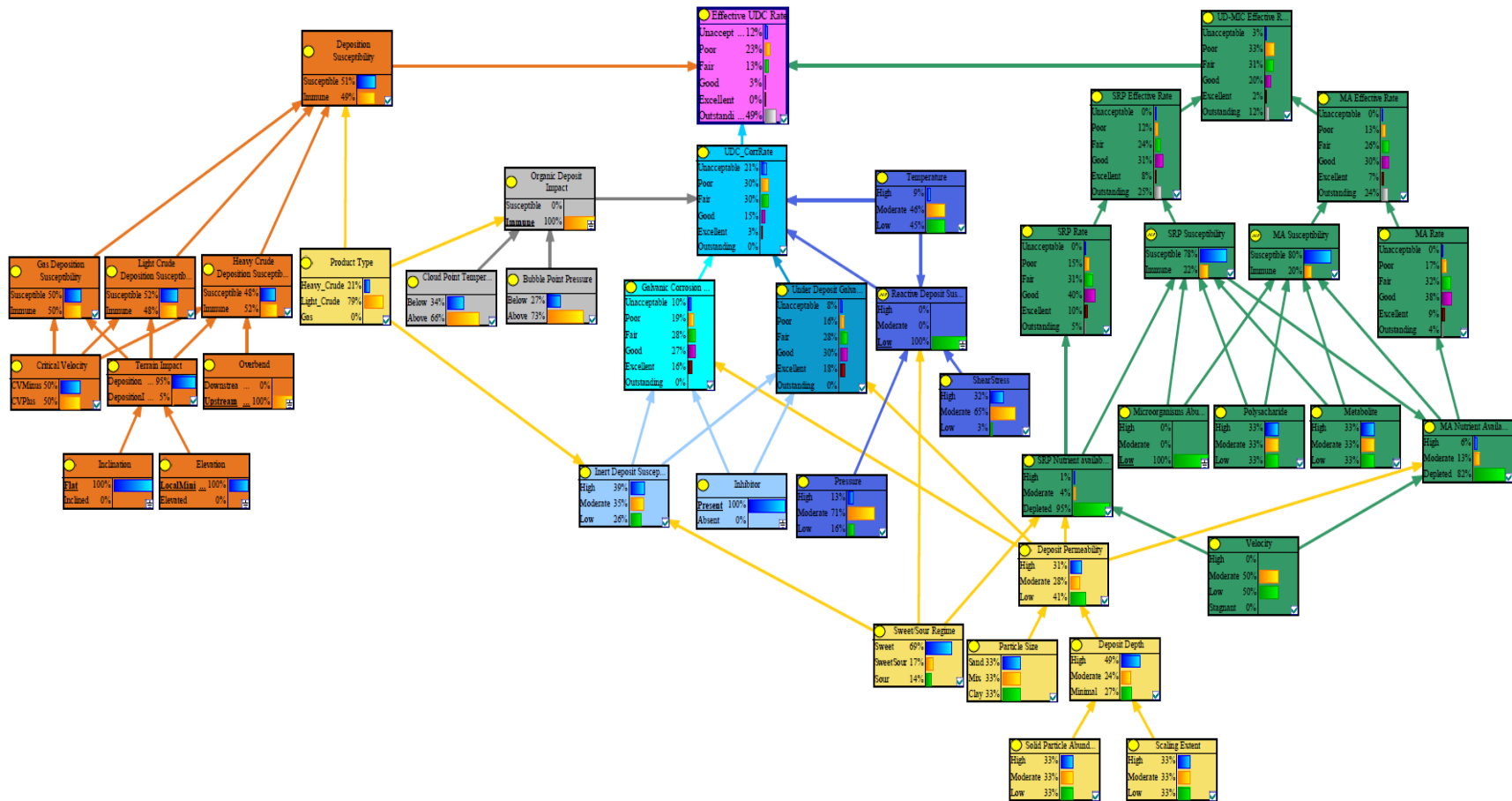
loss in the same section where channeling corrosion (a severe form of UDC) is the predominant feature while the two sides show minor degradation.

The failure is mostly due to deficiencies in the corrosion monitoring program, such as:

- (1) Absence of a microbial monitoring program in a field challenged by a long history of souring following water injection;
- (2) Absence of a frequent pigging program to battle scaling and deposition;
- (3) Absence of inline inspections ;
- (4) Absence of biocide treatment.

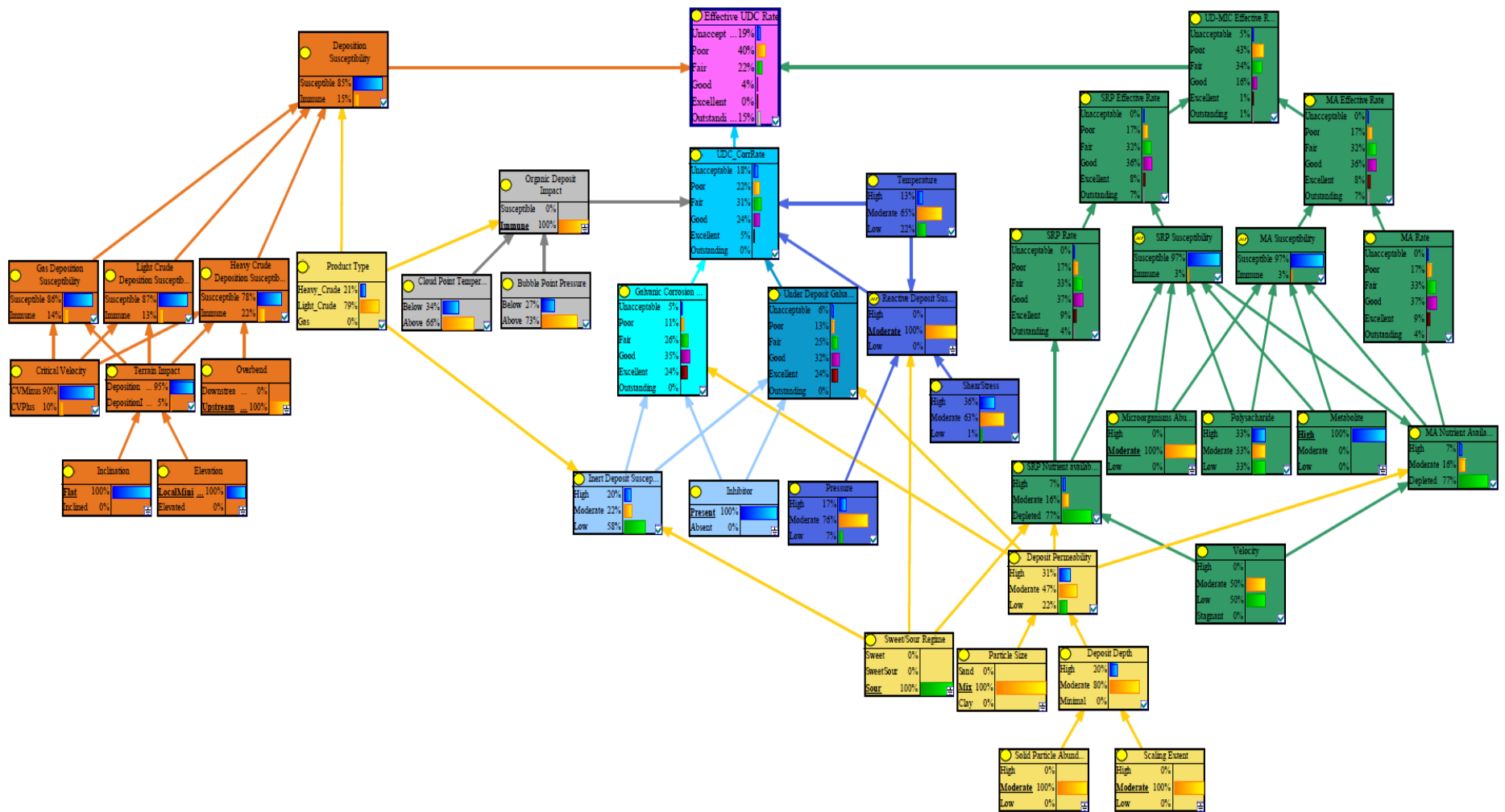
The mentioned deficiencies resulted in this unexpected accident. Here the case history is modeled twice, first relying on the incomplete and uncertain information available to the operator before the accident, and second using the information gathered from the accident analysis.

Fig. 4.12 illustrates the implementation of the two sets of parameters used to compare the impact of different uncertainty levels on the consistency of the assessment results. Due to the pipeline's age and lack of inline inspection, the authors have not provided corrosion rates. Therefore, the comparison is focused on severities rather than validating the corrosion rates.



(a) With incomplete information based on the accident analysis results

Figure 4.12: Results of effective corrosion rates assessment of the Gulf of Suez crude pipeline failure



(b) With information based on the accident analysis results

Figure 4.13: Results of effective corrosion rates assessment of the Gulf of Suez crude pipeline failure

Table 4.1: The effective corrosion rates assessed using data with different levels of uncertainty

Effective UDC Rate	Probability of Occurrence (%)	
	Incomplete Information	Accident Analysis Information
Unacceptable	12	19
Poor	23	40
Fair	13	22
Good	3	4
Excellent	0	0
Outstanding	49	15

Table 4.1 illustrates the probability of observing different corrosion rates at the failure location. The incomplete data suggest a 50% chance of no UDC occurrence. In contrast, its occurrence is likely to result in poor, fair, or unacceptable corrosion rates in the same order, where the likelihood of corrosion rates between 1-5 mm/year is twice as high as in other cases. At the same time, relying on complete information results in an 85% chance of occurrence, where the possibility of observing corrosion rates between 1-5 mm/year is once again dominant. The probability of poor effective corrosion rates based on incomplete information is almost half when complete information is used.

The results suggest a wrong sense of safety when deciding based on the faulty data available to practitioners before the accident, even if UDC was considered. Meanwhile, the complete dataset provides insight into both the severity and the high probability of UDC occurrence. Furthermore,

incomplete data suggests galvanic corrosion due to parasitic inhibitor loss as the predominant mechanism, while complete information concerns bacterial activity and UD-MIC.

Case 2: Pitting corrosion failure analysis of a wet gas pipeline

This case history revolves around a 4.2-kilometer multiphase (gas, condensate, and water) buried gathering pipeline with a wall thickness of 11.4 millimeters, which failed after two years of service due to unpredicted pitting in the six o'clock position. ILI data obtained from the Magnetic flux leakage (MFL) tool and later direct inspections suggest severe pitting in four locations. The elevation map shown in Fig.4.13 reveals the locations of pitting and failure on the elevation profile of the pipeline.

Despite the authors not implicating UDC as the corrosion failure mode, they mention the formation of stratified flow in severe pitting and failure locations and the presence of scaling and corrosion products in a nominally H₂S-free sweet environment. Examining the elevation profile of the pitting and failure locations suggests the sites are local minima. The presence of significant amounts of water, in addition to the previously mentioned factors, motivates handling this case as UDC. Moreover, no biotic data is presented, and the model is set to reflect this aspect.

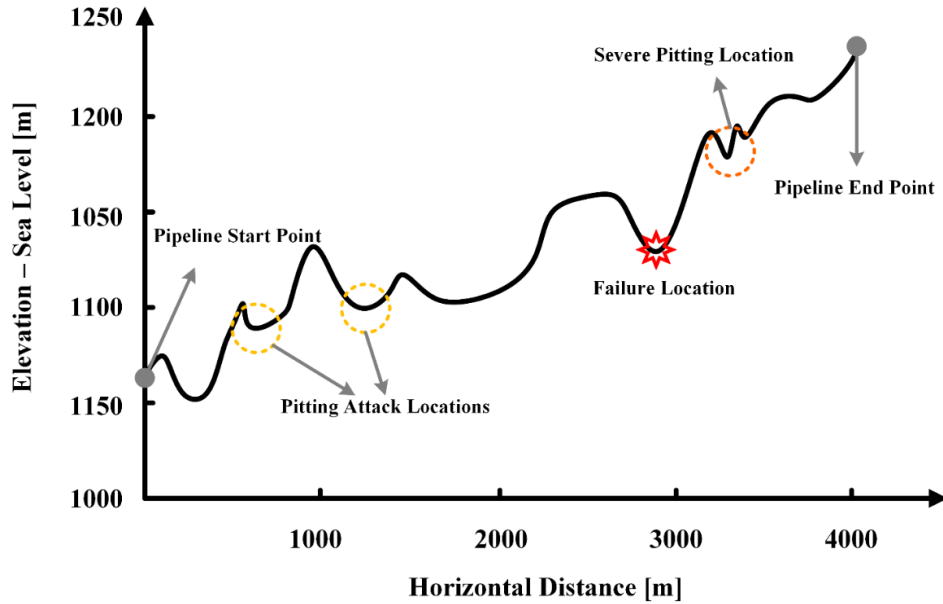


Figure 4.14: Pipeline elevation profile obtained from MFL tool adapted from (H.Mansoori et al., 2017)

Fig 4.14 illustrates the results of implementing this case history in the UDC BN, and table 4.2 presents an overview of effective UDC rate probabilities. It is observed that the highest probable effective corrosion rates are greater than 5mm/year. This observation agrees with the corrosion rates causing the failure, whose average corrosion rates were approximately 5.7 mm/year. Furthermore, the distribution of effective corrosion rates suggests that more than 50% of the observations would be above 1 mm/year and 90% above 0.5 mm/year. Focusing on the other two locations of damage accumulation, shown with yellow and orange circles in Fig 4.14, reveals their location to be similar to the failure location. Reviewing the model's results and comparison with ILI information of the line suggests the distribution of the effective rates is also representative of the 657 defects found in the pipeline.

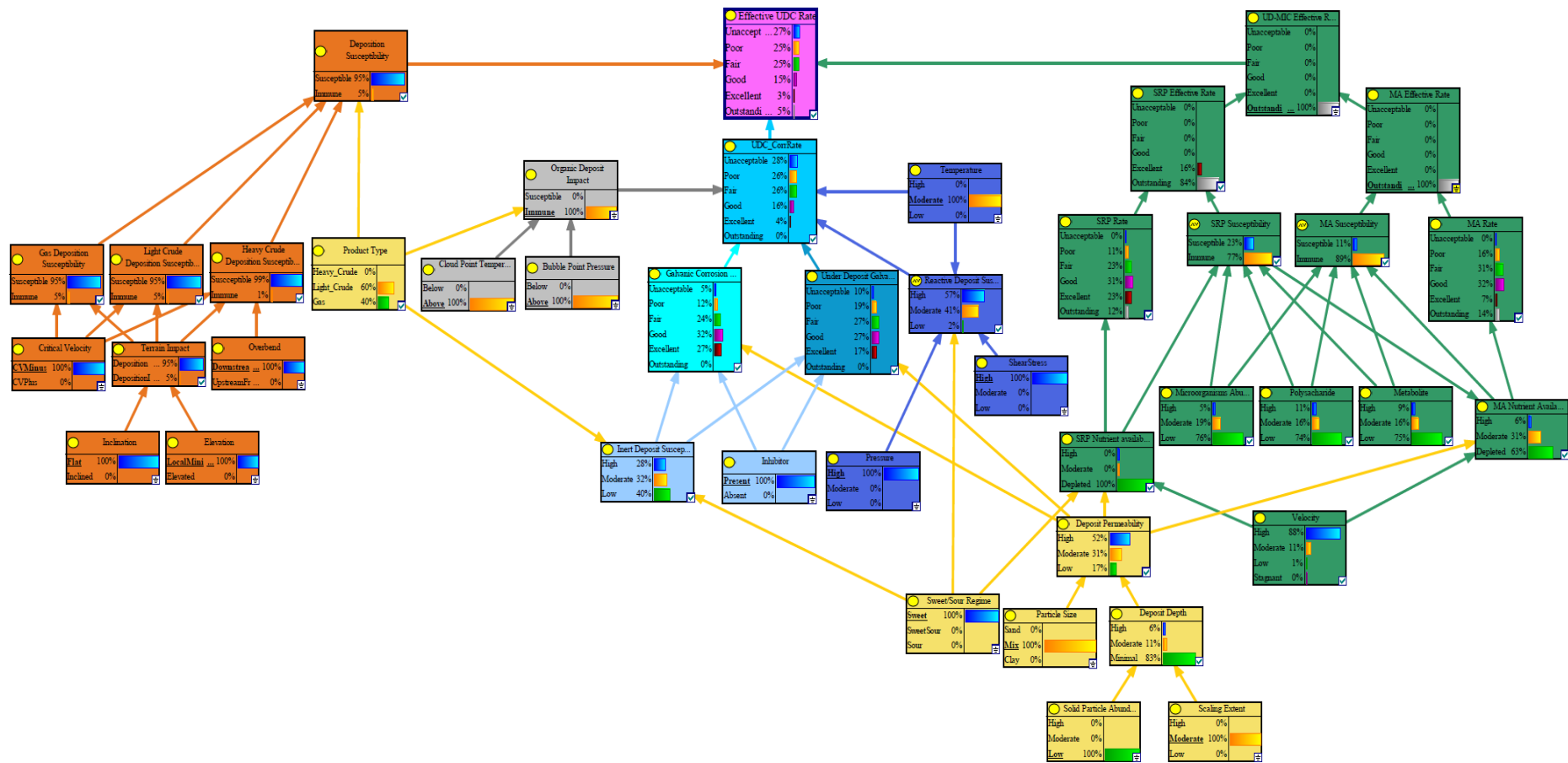


Figure 4. 15: Wet gas pipeline effective UDC rate assessment

Table 4.2: Effective UDC rates and their respective probabilities of occurrence

Effective UDC Rate	Probability of occurrence (%)
Unacceptable	27
Poor	25
Fair	25
Good	15
Excellent	3
Outstanding	5

Case 3: Under deposit corrosion in a subsea water injection pipeline

This case history concerns an API 5L X-60, 10-inch, 3.95 km water injection pipeline with an outside diameter of 10 inches and a nominal wall thickness of 12.7 millimeters. After four years of service, the premature pipeline failure occurred at the six o'clock position as two leaks were caused by channeling corrosion.

The pipeline has been treated with oxygen scavengers, corrosion inhibitors, and biocides. The injected sea water is reported to have high levels of chloride and more than average sulfate content with a concentration of 2860 ppm. In addition to calcium scales, iron oxides, sulfides, and magnesium oxide were detected at the damage location. The authors report moderate SRB counts at 10³ CFU/ml range. The authors report flow velocities less than required for reentraining the deposits and loosely adhered corrosion product layers. The loose products result from low temperature, low pressure, and low shear stress environments resulting in a higher probability of detachment and deposition.

Fig. 4.15 and table 4.3 illustrate the BN implementing this case history and the corresponding effective UDC rates. The results suggest that corrosion rates are distributed in poor to fair intervals, with a slightly higher chance of corrosion rates being between 1-5 mm/year. In this case study, similar to the authors' conclusions, the damage is due to microbial activity. The model shows that the corrosion rates related to UDC mechanisms are mostly in the 0.1-0.5 mm/year interval. Furthermore, from a susceptibility to deposition aspect, this pipeline is 87% likely to be impacted by UDC-related mechanisms.

Table 4.3: The BN representing the subsea water injection pipeline's case history

Effective UDC Rate	Probability of occurrence (%)
Unacceptable	6
Poor	36
Fair	34
Good	10
Excellent	0
Outstanding	13

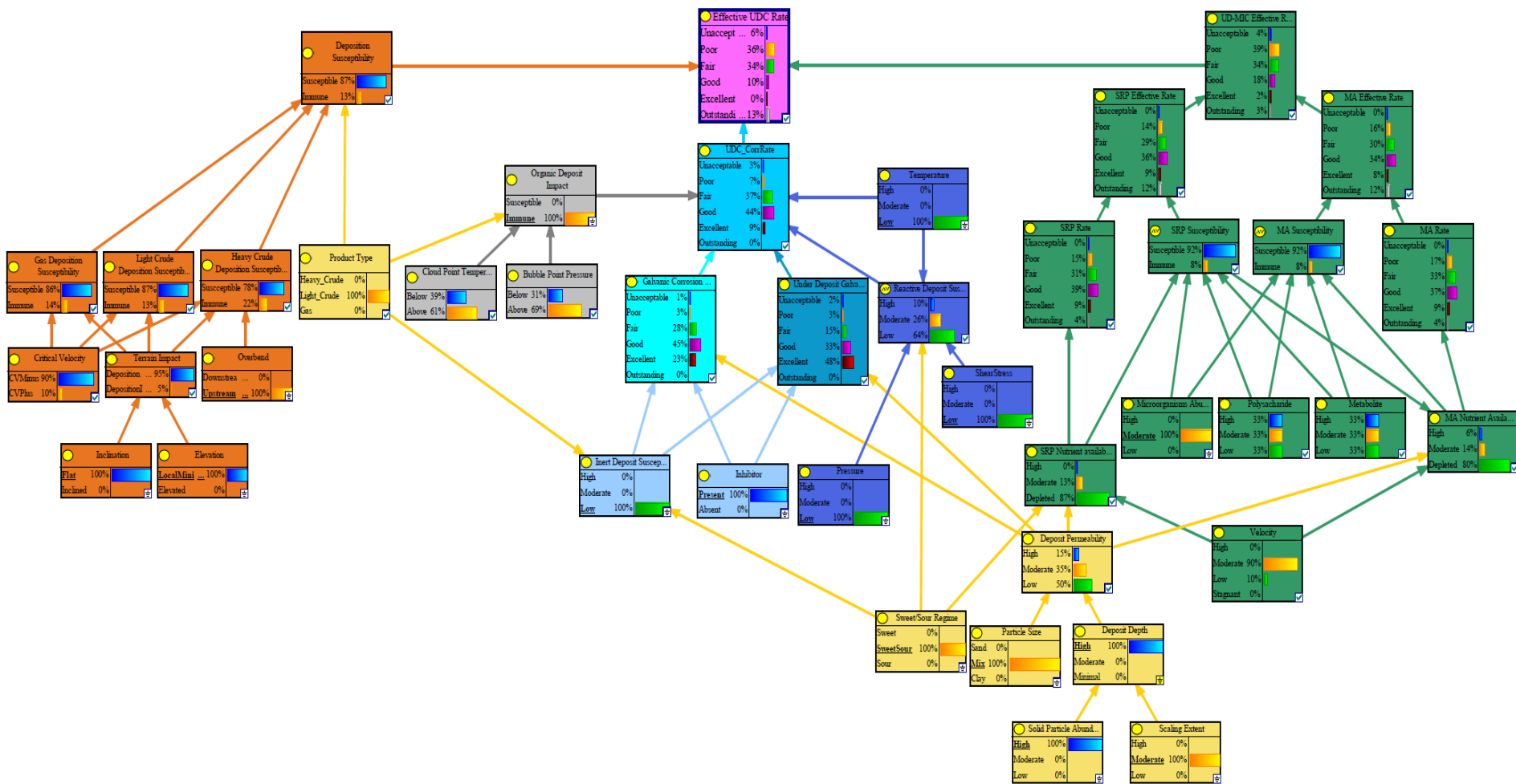


Figure 4.16: Overview of the UDC BN implementing information from the subsea water injection pipeline failure

Case 4: Failure in outlet piping in a high-pressure wet crude production trap

This case study revolves around two failed large diameter pipes, i.e., a 20-inch standby piping and a 24-inch bypass line of a production trap at a gas-oil separation plant (Alabbas, 2017). The pipes with an initial thickness of approximately 9.5 millimeters experience massive leaks after being in service for two years. The author provides evidence that the excessive corrosion rates were due to bacterial activity in the presence of inert deposits and active corrosion products. The microbiological data from the qPCR analysis of dry samples collected from the part suggest the abundance of MIC-causing taxa, including SRB, SRA, APB, and MA.

Even though the case history provides limited quantitative data on corrosion products, qualitative terms are transferred to the model to assess the model's performance with highly uncertain information. It was mentioned that the product type reflects the solid content and viscosity of the product, which sequentially affect the deposition susceptibility and inert deposit abundance. Here, to simulate water's impact, this fluid is modeled by relying on characteristics of light crude.

The results of the BN shown in Fig. 4.16 are presented in table 4.4. It can be observed that the most likely corrosion rates to be observed are between 1-5mm/year, which is the result of microbial activity and UDC mechanisms. This assessment agrees with the average corrosion rate of 4.7 mm/year. The 27% probability of observing unacceptable rates above 5mm/year suggests a higher density of observations in this region.

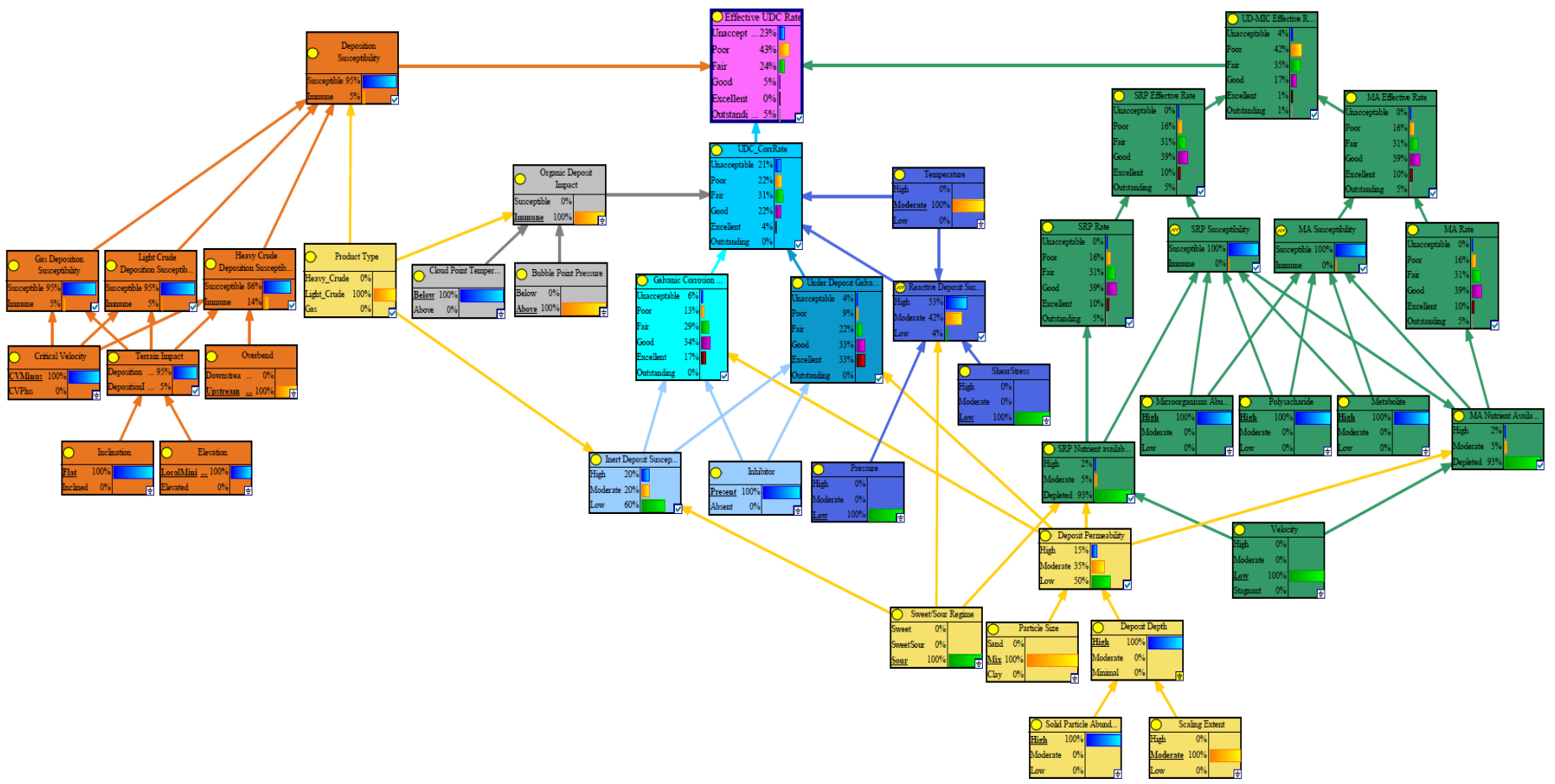


Figure 4.17: Overview of BN evaluating effective corrosion rates for the crude product traps

Table 4.4: Effective UDC rates based on information from the wet crude product traps case study

Effective UDC Rate	Probability of occurrence (%)
Unacceptable	27
Poor	43
Fair	24
Good	5
Excellent	0
Outstanding	5

Case study: Dehydrated gas pipeline

The case study implemented here concerns a gas transmission pipeline tie-in section. At the time of the inspection utilized here, the pipeline had been operating for six years. The pipeline carries processed gas with negligible water cut. The gas is not treated with chemicals except for negligible amounts of mono-ethylene glycol (MEG) for hydrate formation prevention, which has been leftover from earlier stages.

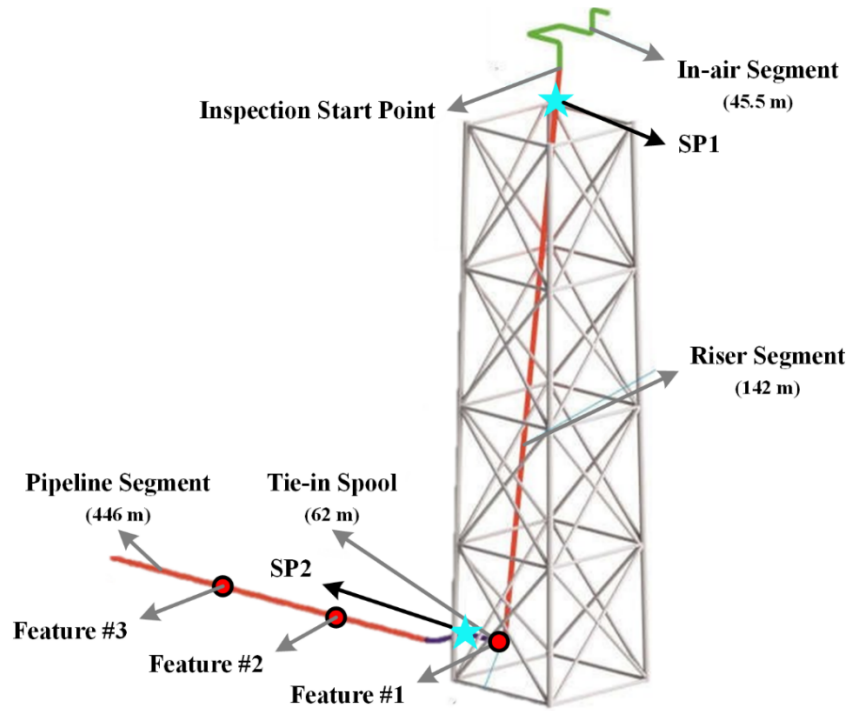


Figure 4.18: Inspected pipeline segment's schematic

The pipeline segment that was inspected using the phonon diagnostics technique (PDT) and the approximate location of the detected features is shown in Fig. 4.18. The design pressure of the pipeline is 160 (Barg), its operating temperature is 46°C, and it is constructed using submerged arc-welded (SAW) DNV OS F101 steel grade 450. Table 4.5 represents summary statistics of the gas's CO₂, water, and H₂S content over six years and the operational parameters, temperature, pressure, and daily flow rates.

Table 4. 5: Six-year-long data summary statistics for the export gas

	Gas Parameters			Operational Parameters		
	Water Dew Point (°C)	H2S (ppmv)	CO2 (%mole)	Temperature (°C)	Pressure (Barg)	Flow Rate (MMSCMD)
Minimum	-50	0.01	3.18	25.62	0	0
Maximum	-10	10	5.38	56.79	156	10.46
Mean	-23.5	2.6	4.1	45.89	140	5.53

Table 4.6 shows that the three features with depths of less than 10% pipe wall thickness have been identified on sections with a nominal wall thickness of 17.5 millimeters. The associated corrosion rate with the most severe of the three pits is approximately 0.3 millimeters per year, while the results of the randomized ultrasonic inspection suggest a maximum corrosion rate of 0.07 millimeters/year.

Table 4.6: Overview of the corrosion features identified

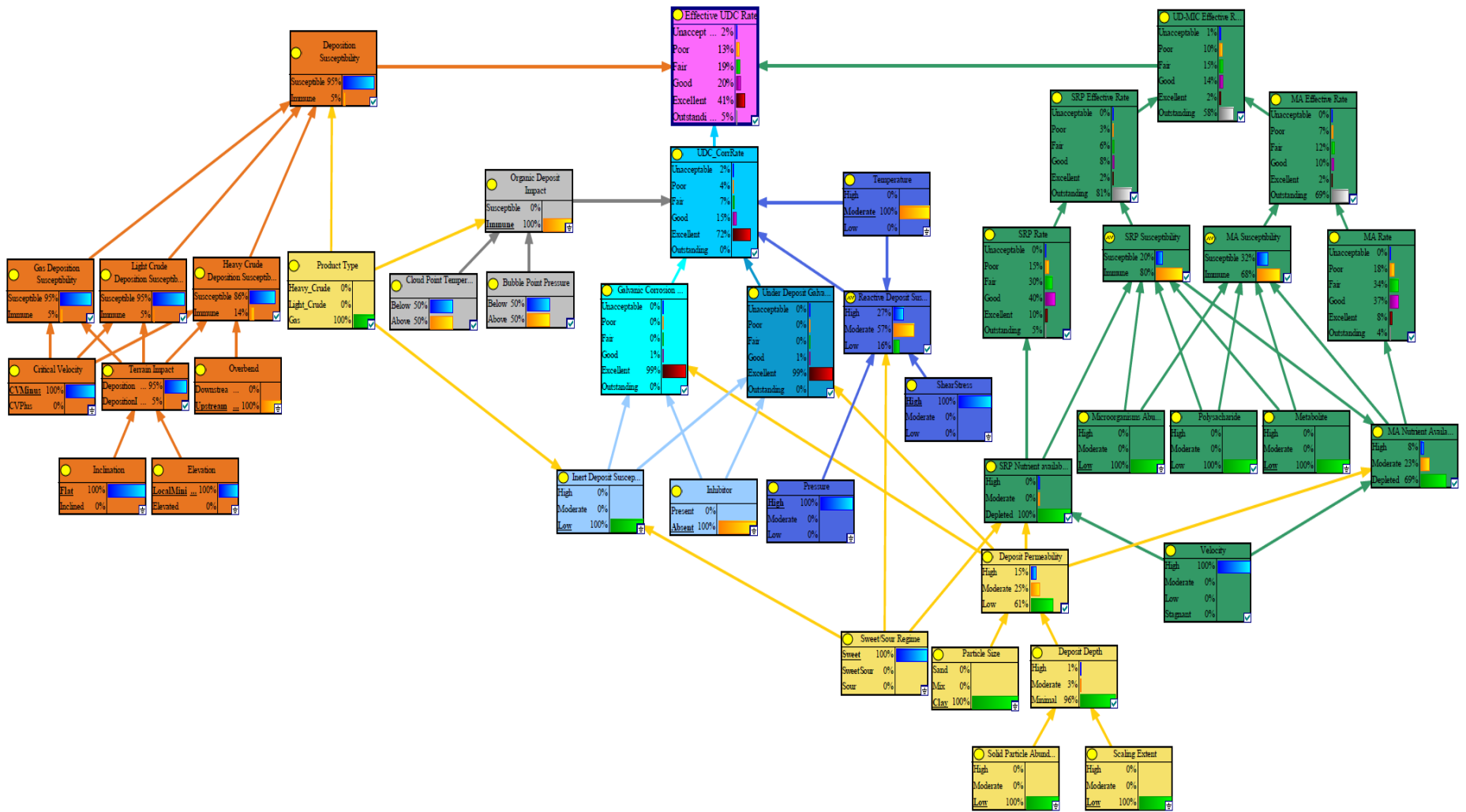
Feature ID	Distance (m)	Length (mm)	Width (mm)	Depth (%)	Feature Depth
1	142.4	870	1615	10	1.75
2	269.1	1650	1615	10	1.75
3	371.7	1820	1615	10	1.75

The BN model assesses the UDC effective rate in two locations on the pipeline segment marked by stars in Fig. 4.18. Each location is simulated with two flow rates to explore the impact of shear force’s ability to restrain the settled particles following a shutdown. Fig 4.18 shows the two cases concerned with the location close to “feature #1,” and table 4.7 presents the effective UDC rates.

Table 4.7: Overview of the effective UDC rates simulated for two points on the pipeline segment

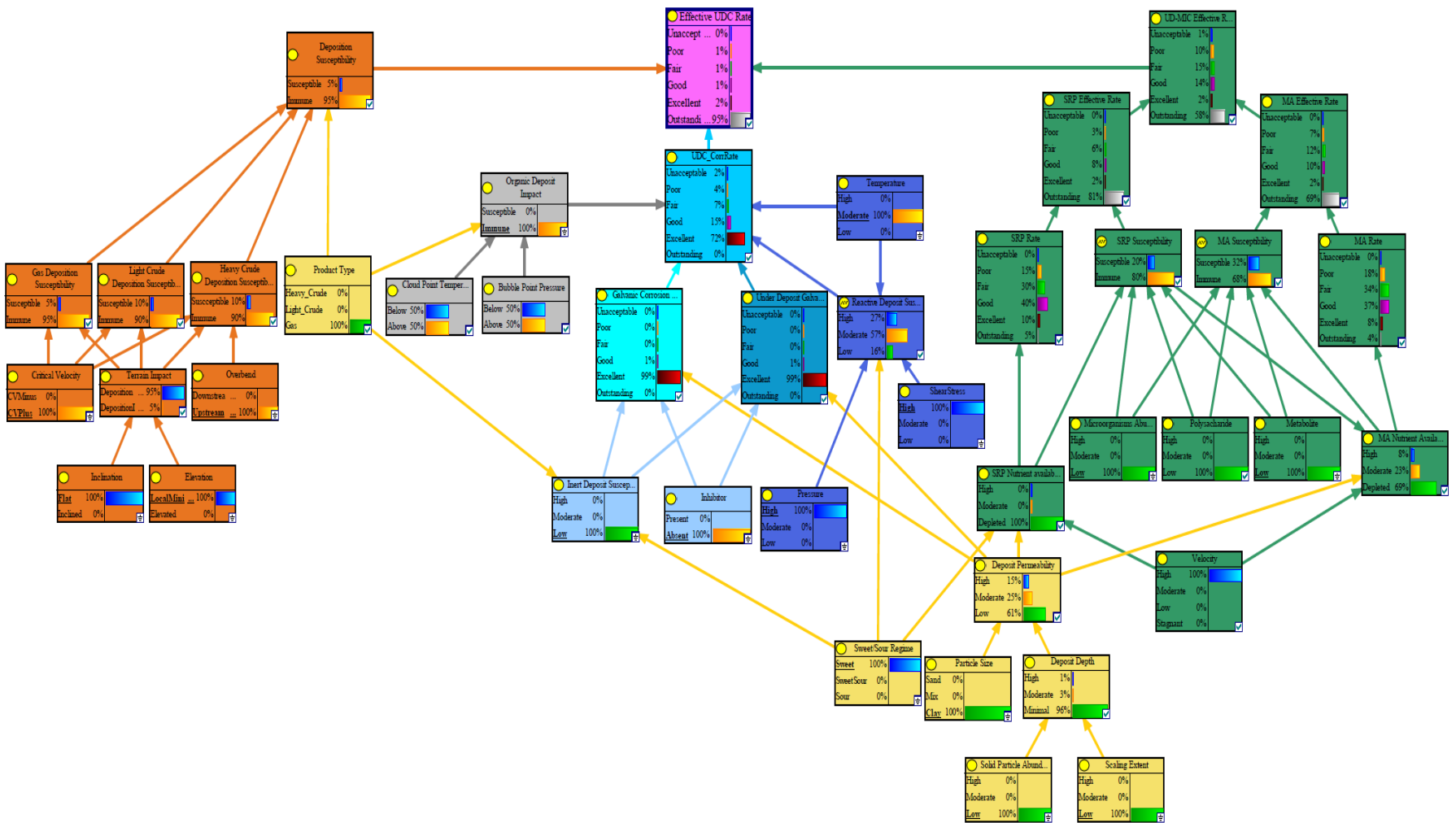
Effective UDC Rate	Probability of Occurrence (%)			
	SP1		SP2	
	High Flow Rate	Low Flow Rate	High Flow Rate	Low Flow Rate
Unacceptable	0	1	0	2
Poor	0	3	1	13
Fair	0	4	1	19
Good	0	5	1	20
Excellent	1	9	2	41
Outstanding	99	78	95	5

Considering the short distance between the two points, the only varying aspect when implementing parameters is the elevation and the inclination. From table 4.7, it can be seen that due to its low location and flatness, the tie-in spool is associated with higher effective UDC rates compared to the location near the in-air segment. Furthermore, it can be seen that if the shear forces are not strong enough, this section is prone to UDC occurrence even in the presence of low numbers of particles. Due to the low humidity of the fluid, the rates are likely to be less than 0.1 millimeters/year. Lastly, results from the first simulated point (SP1) suggest the highly unlikely occurrence of UDC with high-enough flow rates, while the chances of observing corrosion rates lower than 0.1 millimeters are close to 90% when dealing with lower than critical velocity flow rates.



(a) With velocities lower than the critical velocity

Figure 4.19: Overview of the BN implementation of the tie-in pool area



(b) Sufficiently-high velocities

Figure 4.20: Overview of the BN implementation of the tie-in pool area

4.7 Conclusions

This article discusses the complexities of assessing UDC in detail, aiming to assess susceptibility to its various mechanisms. Moreover, this article tries to provide a tangible measure for practitioners to assess the severity of possible UDC attacks by combining the observed degradation rates and susceptibility to them. This measure is introduced as the “*effective UDC rate*.” The effective UDC rate simultaneously combines the rates expected from each mechanism with susceptibility to deposition. Each mechanism’s associated corrosion rates are also the result of combining their expected corrosion rates with susceptibility to them. The implemented case histories and case studies suggest the proposed BN is sufficiently capable of predicting the corrosion rates range and damage severity distribution. Exploring the extreme case of a gas pipeline supports the BN’s robustness as it shows its ability to assess UDC extremes with agreeable accuracies. Lastly, the model is developed with quantitative analysis in mind. Hence, applying data-driven Bayesian networks as data becomes available provides the capacity for further progress.

Data availability statement

The UDC Bayesian network presented in this article and the gas pipeline’s data are available through a public repository (Dao et al., 2022). The repository is accessible to the reviewers through the following link: <https://data.mendeley.com/drafts/vdxdz56h7p>.

4.8 Appendixes

Table 4. 8: The node descriptions and discretization ranges of the UDC susceptibility model

	Node ID	State	Discretization Values
1	Inclination	Flat	$Slope < 5\%$
		Sloped	$Slope > 5\%$
2	Elevation	Local Minima	Based on elevation profile
		Not	
3	Critical velocity	CV Minus	Case dependent
		CV Plus	
4	Overbend	Downstream From	Based on the elevation profile
		Upstream From	

Table 4. 9: Deposit permeability submodel descriptions and discretization ranges

	Node ID	State	Discretization Values
1	Particle Size	Sand	$> 50 \mu m$
		Mix	$> 10 \mu m, < 50 \mu m$
		Clay	$< 10 \mu m$
2	Solid Particle Abundance	High	Depends on the product type and Asset specific parameters
		Moderate	
		Low	
3	Scaling Extent	High	Depends on the product type and Asset specific parameters
		Moderate	
		Low	
4	Deposit Depth	High	$> 8 \text{ mm}$
		Moderate	$3-8 \text{ mm}$
		Low	$< 3 \text{ mm}$
5	Deposit Permeability	High	Propagated from parent nodes
		Moderate	

Low

Table 4. 10: Reactive deposit susceptibility submodel's nodes, states, and discretization values

Node ID	States	Discretization Values	
1	Temperature	High	> 60 °C
		Moderate	>30 °C , <60 °C
		Low	<30 °C
2	Pressure	High	>100Barg
		Moderate	>10 Barg , <100 Barg
		Low	<10 Barg
3	Shear Forces	High	Asset specific
		Moderate	
		Low	
4	Sweet/Sour Regime	Sweet	0-49 ppm H ₂ S
		Sweet/Sour	50-500 ppm H ₂ S
		Sour	>500 ppm H ₂ S

Table 4. 11: The organic deposit's inhibiting impact submodel components

Node ID	State	Discretization
1	Bubble Point Pressure	Asset Specific
2	Cloud Point Temp.	Asset Specific
3	Product Type	Asset Specific
4	Organic Deposit Impact	Inferred

Table 4. 12: Details of the galvanic corrosion due to parasitic inhibitor loss mechanism's submodel

Node ID	State	Discretization	
1	Sweet/Sour Regime* ^A	Sweet	0-49 ppm H ₂ S
		Sweet/Sour	50-500 ppm H ₂ S
		Sour	>500 ppm H ₂ S
2	Inhibitor	Present	Asset Specific
		Absent	
3	Inert deposit Susceptibility	High	Inferred
		Moderate	
		Low	
4	Galvanic Corrosion Parasitic Inhibitor loss* ^B	Outstanding	<0.02 mm/y
		Excellent	0.02-0.1 mm/y
		Good	0.1-0.5 mm/y
		Fair	0.5-1
		Poor	1-5
		Unacceptable	>5

*^A Discretization based on Shell Design and Engineering practices (DEP) criteria for fluid services

*^B The corrosion rate discretization is based on typical inhibiting chemistry performance ratings in the oil and gas industry.

Table 4. 13: . The under deposit galvanic cell mechanism's node properties and discretization

Node ID	State	Discretization	
1	Under deposit Galvanic Cell	Outstanding	<0.02 mm/y
		Excellent	0.02-0.1 mm/y
		Good	0.1-0.5 mm/y
		Fair	0.5-1
		Poor	1-5
		Unacceptable	>5

Table 4. 14: The UD-MIC submodel's properties

	Node ID	State	Discretization
1	Velocity	High	>1 m/s
		Moderate	0.1-1 m/s
		Low	<0.1 m/s
		Stagnant	0 m/s
2	MA Nutrient Availability	High	500 ppm
	SRB Nutrient Availability	Moderate	10-500 ppm
		Depleted	<10 ppm
3	Microorganism Abundance	High	$> 10^6$
		Moderate	$10^4 - 10^6$
		Low	$< 10^4$
4	Polysaccharide	High	Case dependent
		Moderate	
		Low	
5	Metabolite	High	Case dependent
		Moderate	
		Low	
6	SRB Rate	Outstanding	<0.02 mm/y
	MA Rate	Excellent	0.02-0.1 mm/y
	SRB Effective Rate	Good	0.1-0.5 mm/y
	MA Effective Rate	Fair	0.5-1
	UD-MIC Effective Rate	Poor	1-5
		Unacceptable	>5
7	SRB Susceptibility	Susceptible	Inferred
	MA Susceptibility	Immune	

Table 4. 15: Case history parameters as implemented in the model.

Node ID	Case histories	
	Case 1– missing information	Case 1 – complete
Product Type	Medium crude: API-29	Medium crude: API-29
Sweet/Sour Regime	Souring history No planktonic SRB	Souring history High bacterial count
Solid Particle Abundance	No organic deposit Slight increase in iron	Organic deposits Iron sulfide, oxides Sand
Scaling Extent	None	NA
Particle Size	N/A	Mix (sand, corrosion products)
Elevation	Low	Low
Inclination	Flat	Flat
Overbend	Preceding	Precedingf
Critical Velocity	NA	NA
Bubble Point Pressure	NA	NA
Cloud Point Temperature	NA	NA
Inhibitor	10 ppm amine based	10 ppm amine based
Pressure	NA	NA
Temperature	NA	NA
Shear Stress	NA	NA
Velocity	NA	NA
Microorganism Abundance	Low/Insignificant Planktonic population	Moderate (SRB) enumeration Sessile
Polysaccharide	NA	NA
Metabolite	NA	Present
Node ID	Case histories	
	Case 2	Case 3

Product Type	Multiphase	Water
Sweet/Sour Regime	Sweet	NA
Solid Particle Abundance	Low	Unknown > 5 μm filtered out
Scaling Extent	Moderate	Low
Particle Size	Mix	< 5 μm
Elevation	Low	Low
Inclination	Flat	Flat
Overbend	NA	NA
Critical Velocity	Below	Below
Bubble Point Pressure	NA	NA
Cloud Point Temperature	NA	NA
Inhibitor	Present	Present
Pressure	113 bar	~103 bar
Temperature	46 °C	35
Shear Stress	High	Moderate
Velocity	NA	0.53-0.93 m/s
Microorganism Abundance	NA	Moderate
Polysaccharide	NA	Present
Metabolite	NA	Present

Node ID	Case histories
	Case 4
Product Type	Crude oil
Sweet/Sour Regime	Sour
Solid Particle Abundance	High
Scaling Extent	Moderate
Particle Size	Mix
Elevation	Low

Inclination	Flat
Overbend	NA
Critical Velocity	NA
Bubble Point Pressure	NA
Cloud Point Temperature	NA
Inhibitor	NA
Pressure	~3.5 bar
Temperature	35-46 °C
Shear Stress	Low
Velocity	Low
Microorganism Abundance	High
Polysaccharide	NA
Metabolite	NA

CHAPTER 5

5 Dynamic Bayesian network model to study under-deposit corrosion

5.1 Preface

*A version of this chapter has been published in the **Reliability Engineering & System Safety**, 109170, 2023. I am the primary author along with the Co-authors, Zaman Sajid, Faisal Khan, and Yahui Zhang. I developed the conceptual framework for the failure assessment model and carried out the literature review. I prepared the first draft of the manuscript and subsequently revised the manuscript based on the co-authors' and peer review feedback. Co-author Zaman Sajid provided support in implementing the concept and testing the model. Co-author Faisal Khan helped in the concept development, design of methodology, reviewing, and revising the manuscript. Co-author Yahui Zhang provided fundamental assistance in validating, reviewing, and correcting the model and results. The co-authors also contributed to the review and revision of the manuscript.*

5.2 Abstract

This paper develops theoretical and mechanistic aspects of under-deposit corrosion (UDC) into a dynamic model and compares UDC progression and mitigation with current industrial practices. A Dynamic Bayesian Network (DBN) model is developed to understand different risk factors and their interdependencies in UDC and how the interaction of these risk factors leads to asset failure due to UDC. The DBN uses available UDC theory and transforms it into a probabilistic framework. The study compares DBN results from the general theory of UDC (based on the theory and mechanism of UDC) to industrial practices. The corrosion mechanism is represented in a Bayesian

probabilistic framework involving solid deposits, flow velocity, operating pressure, under-deposit galvanic cell, chloride, pH, partial pressure of CO₂, mono-ethylene glycol, and operating temperature. The Monte Carlo simulation (MCS) is used to characterize the stochastic properties of UDC. The proposed model assesses the asset failure probability over five years of continuous operation. DBN results show that they are consistent with failure probabilities data reported by the industry. Results also reveal that the pipeline wall thickness, outer pipe diameter, tensile strength, and operating pressure are critical contributors to UDC rate and asset failure likelihood. The results of this study are crucial for the inspection and maintenance schedule of pipelines affected by UDC.

Keywords: Under deposit corrosion (UDC); Dynamic Bayesian Network; Solid deposits; CO₂ corrosion mechanism; Asset Failure Probability

5.3 Introduction

The UDC, a type of localized corrosion in pipelines, has been reported to be a critical contributor to sudden system failure across the energy, oil and gas, and marine industries (Liengen et al., 2014; Sørensen et al., 2012). Many studies have reported the detrimental consequences of under-deposit pitting corrosion for oil and gas pipelines (Q. Wang et al., 2021; Sliem et al., 2021; Suarez et al., 2019). The morphology of UDC is complex and unclear, resulting in unpredictable characteristics that limit their monitoring, treatment, and mitigation (Almahamedh, 2015; Ossai et al., 2015).

UDC is corrosion occurring beneath a steel surface (Dao et al., 2023; Alamri, 2020; Hoseinieh et al., 2016). Increased corrosion is observed under solid deposits under the horizontal lines (Ohtsu et al., 2002). The nature of the environmental, characteristic, and operational factors could further enhance the high rate of degradation of the steel pipelines. Depending on their potential impact and mode, these degradation-instigating factors can be classified into organic, inorganic, and mixed deposits (B. He et al., 2015; Obot, 2021b). How these factors interact and lead to asset

failure is still unclear. There have been observations of complex solid mixes of sand, clay, wax, asphaltenes, hydrates, and corrosion products forming in subsea pipelines (Ali et al., 2018; Z. Wang et al., 2020). However, the formation processes of these deposits are not well studied, and which factors are the most critical are still unknown. These deposits present a wide range of structures and compositions, which makes them extremely difficult to analyze and mitigate (Östürk and Sevimoğlu, 2021; Tong et al., 2022). Deposits are frequently linked to UDC because of their remarkable capacity to adsorb corrosion, while inhibitors promote microbial metabolism and development (Durnie et al., 2005; Y. Liu et al., 2014). However, no systematic model is available to explain the interconnections of various risk factors that influence UDC.

The fluid transported through pipelines carries particles. Under an operating environment, these particles gather and form deposits of different porosity at the six o'clock position in the pipelines. For gas pipelines, the water droplet or condensation provides a supportive environment for the deposit. Moreover, corrosion products, such as metallic products, are collected and could increase the rate of UDC. The deposits are further classified based on their sources, porosity, and fluid type. The likely interaction among the under-deposit, biofilm, and failed pigging process contributes to the premature failure of the fluid lines of the well. Understanding the influence of multivariate interactions on the under-deposit-induced failure of oil and gas pipelines is essential. Furthermore, industrial practices and theories to deal with UDC have never been linked in current literature.

This study proposes integrating mechanistic and probabilistic models for UDC behavior and aims to predict the failure likelihood of a gas pipeline suffering UDC. The mechanical structure describes the physics and concepts of UDC formation, while probabilistic properties are used to define the corrosion response parameters. Results of the theoretical approach are compared with industrial data using a stochastic approach. In this study, the stochastic process is Monte Carlo

simulation (MCS), performed on a limit state function (LSF) using industrial data. The approach is tested on an under-deposit-induced corroding gas pipeline, and a failure profile is developed. The model offers a predictive tool for failure assessment and finds its applications in developing guidelines for the integrity management of critical assets in oil and gas operations. Section 1 of this paper provides an introduction and current literature addressing corrosion mechanisms and UDC based on different techniques. It also discusses the novelty and state-of-the-art contributions of the present study. Section 2 outlines the details of a dynamic Bayesian network (DBN) for asset failure analysis. Section 3 proposes the novel methodology and its application to an industrial case study. Section 4 provides results and discussion, and the last section concludes this work.

5.4 Literature review

UDC is a pitting corrosion type complicated to detect, predict, and prevent (Bhandari et al., 2015; Shekari et al., 2017a; J. Zhao, 2014). Oil and gas pipelines suffering from UDC can lead to asset failure. Therefore, understanding the multiple mechanisms and interactions of different risk factors in UDC is vital to address asset integrity.

Many attempts have been made to model the UDC mechanism using various techniques and methods. A recent study presented a three-D electrochemical probe design to visualize dynamically changing and complex internal pipeline corrosion. The experimental testing and validation of the study show that the proposed probe design is an effective tool for understanding different influencing factors affecting corrosion. This study helps understand multi-mechanism and multi-phase localized corrosion in the industrial environment. (Laleh et al., 2023).

Another study used a probabilistic approach called Bayesian Probabilistic Network (BPN) to understand the interaction of UDC and MIC mechanisms (Adumene et al., 2022). Researchers used BPN to structure the interaction and propagation of UDC and MIC risk factors. The study

assessed the failure's impact on human lives and the environment and estimated the economic loss using the expected utility and perfumed consequence analysis. The proposed BPN model captured the complex interaction between UDC and MIC mechanisms that led to predicting leak failure probability and consequence analysis.

A study examined the characteristics and compositions of scales formed at various depths in oil-producing wells. Researchers used analytical techniques to study the UDC mechanism, including X-ray spectroscopy, optical microscopy, transmission electron microscopy, scanning electron microscopy, and X-ray diffraction (Y. Yang et al., 2021). The study revealed that the corrosion under the scale surface is diversified. Work also analyzed the influence of environmental factors, including chlorine, steel microstructure, calcium, oxygen content, and multi-phase flow, on the corrosion mechanism and formation of scale. The findings of this study helped to understand scale formation and UDC mechanism in oil production wells.

A review study on UDC provided detailed theoretical mechanisms and processes behind UDC. It also discussed mitigation techniques to mitigate UDC in the oil and gas industries. Investigation revealed that no single mechanism could explain UDC since it is based on the type of deposits and different alloys and corrosive species involved in the UDC process. The study identified various risk factors in an inhomogeneous and highly resistive environment that lead to UDC. It emphasized for a study to consider such parameters in understanding the UDC mechanism (Sliem et al., 2021). Obot provided the basic definition and mechanism of UDC and its different types of deposits (Obot, 2021b). It also identified different approaches to mitigate UDC in the oil and gas pipelines. The study helped to understand the complex relationship between corrosion mechanism and deposit structure and the association of UDC with MIC. The study was limited to explaining theoretical concepts.

Wang and Melchers examined the long-term UDC of carbon steel pipes and identified that combined MIC and UDC cause channeling corrosion (Wang & Melchers, 2017). Their study performed laboratory experiments to analyze pitting depth and morphology and identified that interactive effects of UDC and MIC led to localized corrosion. In contrast, the intensity of localized corrosion is increased due to the addition of nitrogen. This study helped to understand the formation of channeling corrosion in injection pipelines located in offshore waters. This work identified that deposits are a critical factor in triggering UDC. This factor can also develop favorable conditions for microbiological activity and hence has the potential to promote MIC.

From the available literature, understanding the UDC mechanisms and interdependencies of risk factors is currently restricted (Obot, 2021a; Place et al., 2009). Thus, the critical interacting risk factors that lead to UDC have not been examined in much detail. Furthermore, many studies are based on studying a combined mechanism of MIC and UDC. However, compared to MIC, understanding the UDC mechanism and its interrelated risk factors has received much less attention in the literature, even though, as indicated in the literature review above, it has been reported as a dominating corrosion cause in the oil and gas industries. Limited studies on the UDC mechanism are based on studying one or two risk factors in UDC and have limited scope and applications. Assessment of UDC-induced failure demands a more profound comprehension of stochastic behavior displayed by UDC and its influential parameters, which subsequently influence failure prediction. Thus, an effective risk assessment requires the establishment of a dynamic model. The dynamic framework will be able to capture the time-dependent behavior of UDC and its key characteristics to forecast complicated failure causes, failure propensity, and failure-related outcomes. Therefore, this study aims to develop a model for non-linear interactions among UDC risk factors. Using a Bayesian Network approach, it estimates the dynamic behavior of the

probability of asset failure. Results of the probabilistic model are compared with industrial data using a stochastic approach, i.e., MCS and risk profiles are compared. The findings of this study help investigate how time dependent UDC influences the likelihood of failure and dynamic behavior of UDC.

5.5 Dynamic Bayesian Network (DBN) for Asset Failure Analysis

A Bayesian Network (BN) is a probabilistic method used for accident modeling in various fields of study (Adumene, Khan, Adedigba, & Zendejboudi, 2021; Sajid et al., 2017a; Taleb-Berrouane et al., 2021; Y. Yang et al., 2017). A BN risk model also assists in identifying critical direct and indirect factors that lead to an accident (Khakzad et al., 2011; Taleb-berrouane et al., 2018). BN is a probabilistic technique that can graphically represent the causal interrelations between variables. It qualitatively and quantitatively describes the intricate relationship (Bensi et al., 2013; Hassan et al., 2022; Moradi et al., 2022).

The probability of an event in a BN is presented in eq. (1).

$$P(X|Y) = \frac{P(Y|X).P(X)}{P(Y)} \quad (5.4)$$

where:

$P(X|Y)$ is the conditional probability of event X, given that event Y takes place.

$P(Y|X)$ represents the conditional probability of event Y, given that X takes place.

$P(X)$ and $P(Y)$ are the prior probabilities of events X and Y, respectively, and indicate marginal probabilities.

A “static” BN model is mapped into a “dynamic” model DBN to monitor the degradation of pipelines in real time. DBN shows the conditional independence for a set of random variables in a

time slice $t = (1, \dots, n)$ (Sajid et al., 2020; Sajid, 2021). Fig. 1 (a) shows a static BN model considering four random variables, and Fig. 1 (b) shows n slices of a DBN.

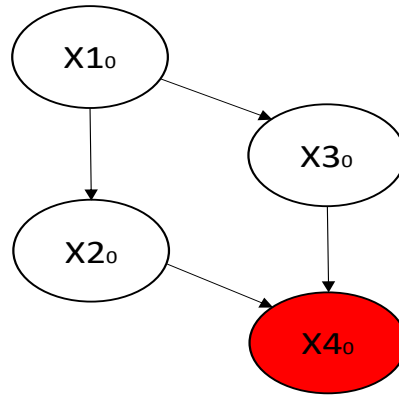


Figure 5. 1(a): A static BN

X1 is the root node, X2 and X3 are the intermediate nodes, and X4 is the leaf node.

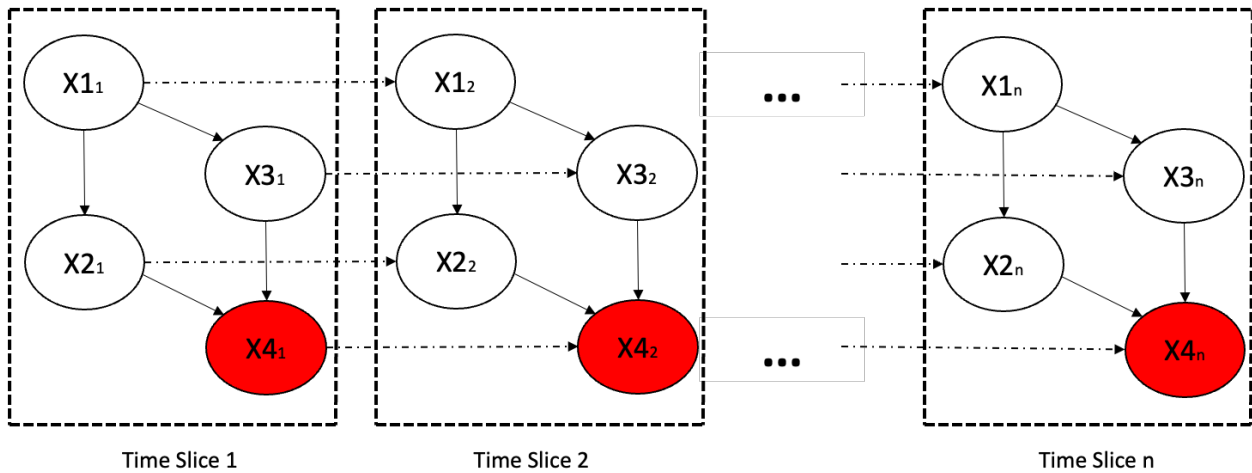


Figure 5. 1 (b): A graphical of a DBN over n steps

This study aims to compare the performance and results of the DBN model with industrial data using a stochastic approach called MCS. The DNV-RP-F-101 method (As, 2015; Tee and Pesinis, 2017; Witek, 2016) is applied in this study to compute failure pressure (burst pressure) for a pipeline in an industrial case study. The stochastic approach calculates the defect depth due to UDC over time. This study uses MCS to estimate an asset's probability of failure (PoF) due to

UDC. MCS considers statistical probability distributions of input parameters. Industrial data is used as an input to the stochastic model. The predicted defect depth is modeled as a linear function where parameters are derived from this literature (Caleyo et al., 2009; Sahraoui and Chateauneuf, 2016; Witek et al., 2018). The scope of this study is limited to the influence of UDC on defect depth. A corroded pipeline typically fails or becomes unreliable through a burst or a small leak (C. Liu et al., 2021; Okodi et al., 2020). This effect is due to high internal pressure, mainly considered a random variable (Amaya-Gómez et al., 2019; Witek, 2016; Zhang and Zhou, 2013). Therefore, variables in MCS are random. The input data is adopted from an oil and gas industry field. Industrial data was discretized and analyzed for five years, and results were compared with DBN time slices for five years.

5.6 The applications of DBN – an industrial case study

A gas transmission pipeline has been operating for five years, and its PoF is studied by proposing a novel methodology using a case study. The gas has negligible amounts of mono-ethylene glycol (MEG) for hydrate formation prevention. The pipe material is a submerged arc-welded (SAW) DNV-RP-F101 steel grade 450 with a normal diameter of 810 mm. The pipeline operating pressure is 16 MPa, and the tensile strength is 535 MPa. UDC affected and corroded the gas pipeline during its five years of operation. The relative defect depth is studied using UDC concepts and theory, and the PoF of the pipeline is computed. Its comparison is made using industrial data on pipe wall thickness having a nominal wall thickness of 10 mm. The focus is to estimate the likelihood of asset failure over five years.

5.7 The Analysis Methodology

Fig.5.2 sketches the proposed methodology in this study. It consists of four steps, as discussed in this section.

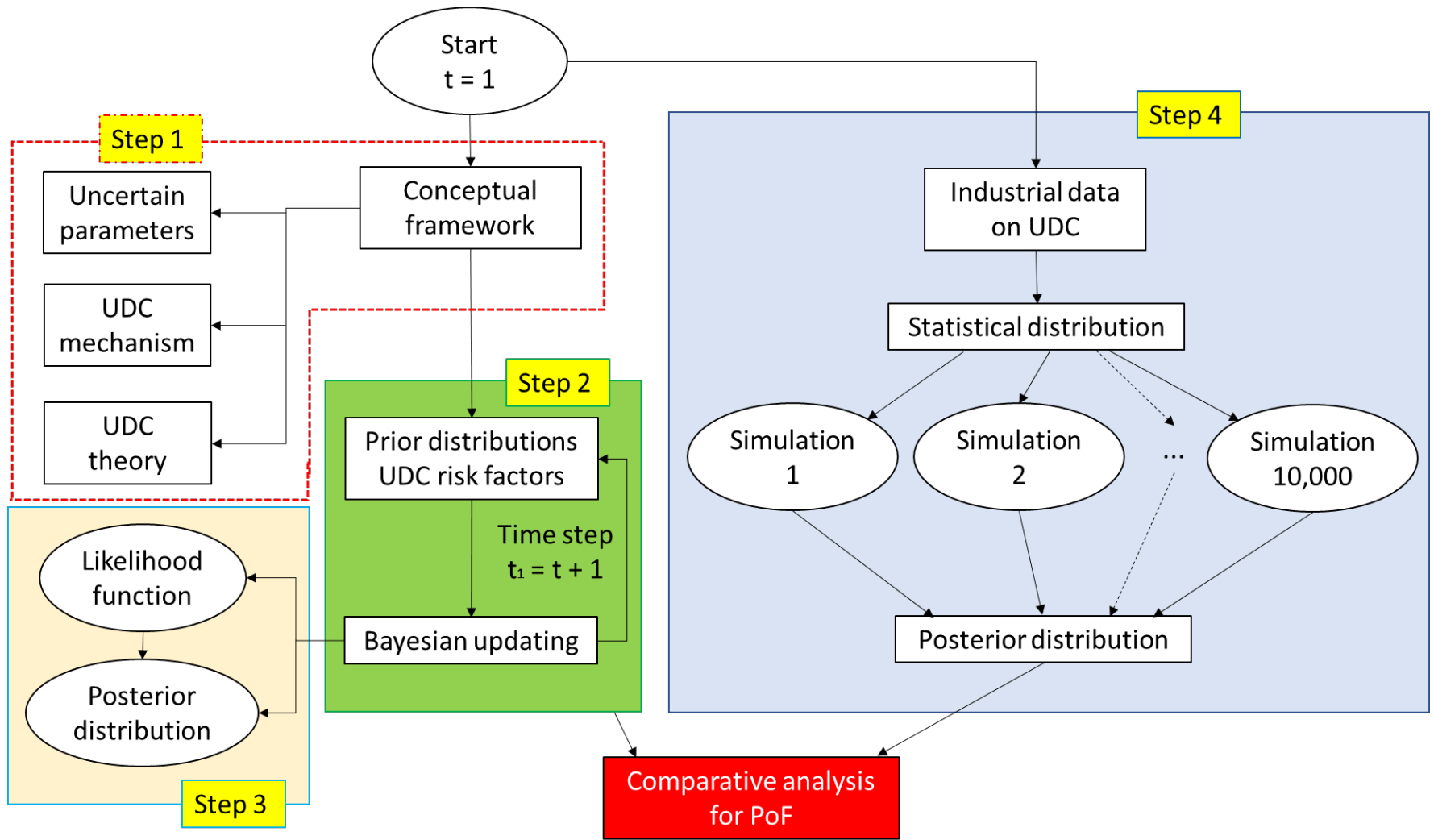


Figure 5. 2: A schematic view of the methodology for the case study

Step 1: Development of a qualitative Bayesian Network (BN) model

As a first step, a qualitative BN model was constructed. The BN model was based on the available UDC mechanism, concepts, and theory discussed in this paper's introduction. This step resulted in a graphical model representing corrosion parameters' interdependencies and the mechanism behind UDC.

Step 2: Dynamic probabilistic framework for UDC

The output from step 1 was transformed into a quantitative dynamic probabilistic framework called a DBN. This goal was achieved in two steps: (a) structural learning (related to the structure of the static BN model) and (b) parameter learning (related to probabilistic values). Structure learning was performed through experts' inputs, who pointed out links between nodes. Experts in this study have vast experience in corrosion research and development. Structural learning provided the interdependencies among risk factors and was the outcome of step 1. Parameter learning defined the marginal probabilities and conditional probability tables (CPTs) of nodes in the DBN. These details are provided in the Appendix. Experts' opinions were taken to assign probabilistic values, between 0 to 1 to each node in the developed structure of the BN model. In a DBN, the change in variables was considered time-dependent and studied for five years, as discussed in the case study. Therefore, prior probability distributions are defined at the first-time step ($t=0$), a similar approach was adopted from child nodes at $t=0$, and the developed DBN model was run for five years. The outcome of this step was the temporal BN model, which provided the changes in quantitative variables based on time. GeNIe software by Bay Fusion, LLC was used as a tool to construct, and Bayesian inference was performed as discussed in step 3.

Step 3: Risk-based Bayesian Inference

In this step, Bayesian inference was made using the temporal aspects of DBN in step 2. A GeNie tool allowed updating probabilistic beliefs of five-time steps. It resulted in the posterior probabilities of each node in the Bayesian model. The result of this step was the probability of failure (PoF) of the pipeline due to UDC. The PoF in this study is defined as the asset's failure due to the influence of defect depth corroded from UDC.

Step 4: Model validation from industrial data and results comparison

In this step, the results from step 3 were validated using industrial data. This step helped to understand the accuracy and robustness of the DBN in predicting PoF due to UDC. Validation of DBN was performed using a stochastic approach. This approach has been used in previous studies (Hasan et al., 2012; Vanaei et al., 2017; Witek, 2018). Using the DNV-RP-F-101 method, the limit state function (LSF) was simulated as follows:

PoF for the corroded pipeline in terms of time (T) is presented below:

$$P_F(T) = P[\text{LSF}(\vec{X}, T) \leq 0] = \int_{\text{LSF}(\vec{X}) \leq 0} f(X_i, T) dx_i \quad (5.2)$$

Where: $P_F(T)$ – failure pressure of pipeline in terms of time, [MPa]

LSF = the remaining capacity - operating pressure P_{op}

LSF = $P_F - P_{op}$, and PoF = $P(\text{LSF} \leq 0)$

- If $\text{LSF} > 0$, the pipeline has no failure and is safe for operation.
- Otherwise, there are chances for pipeline failure when defect depth exceeds 80% of the thickness of the pipeline wall.

The $P_F(T)$ of a pipeline with time was presented as follows:

$$P_F(T) = \frac{2t f_u \left(1 - \frac{d(T)}{t}\right)}{(D-t) \left(1 - \frac{d(T)}{tM(T)}\right)} \quad (5.3)$$

Where:

The length correction factor $M(T)$ was computed from the relationship below:

$$M(T) = \sqrt{1 + 0.31 \left(\frac{L(T)^2}{Dt} \right)} \quad (5.4)$$

t – wall thickness (mm); f_u – tensile strength (MPa); $d(T)$ - defect depth $d(T)$ at time T ; D - pipe outer diameter (mm).

According to (Arakere et al., 2021), the dimensions of the fundamental pipe factors are shown in Fig.5. 3.

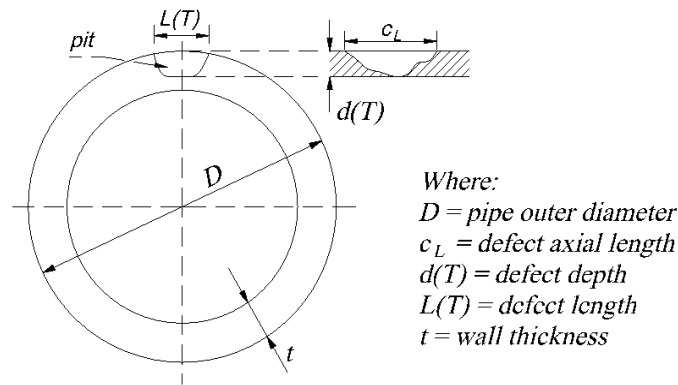


Figure 5. 3: The corroded pipe dimensions

Using equations (5.2) and (5.3), MCS was performed to assess the PoF for the pipeline due to growing UDC. Industrial data were used as input to the model. The study used industrial data for in-line inspection of pipe wall corrosion and determined the experimental mean values such as d_{mean} (defect depth or loss in wall thickness). Similar to other studies, radial corrosion growth (c_d) and axial (c_L) were taken as constants.

For the corrosion growth model available in the literature (Qin et al., 2015), the estimated defects at time T were calculated as follows:

$$d(T) = d_{mean}(0) + c_d \cdot T \quad (5.5)$$

Where:

$d(T)$ - defect depth.

According to (Vanaei et al., 2017), the predicted maximum pit depth (d_p) was estimated as a linear function of the growth rate of UDC, \dot{d} as shown below:

$$d_p(T) = d_{mean}(0) + \dot{d}t \quad (5.6)$$

$$\dot{d} = \frac{d_2 - d_1}{T_2 - T_1} \quad (5.7)$$

where d_2 and d_1 are loss in wall thickness at year 1 (T_1) and year 2 (T_2), respectively. The analysis was performed up to year 5 (T_5), and MCS, a schematic diagram shown in Fig. 4, was run for 10,000 iterations. In this work, Oracle® Crystal Ball software was used to perform MCS.

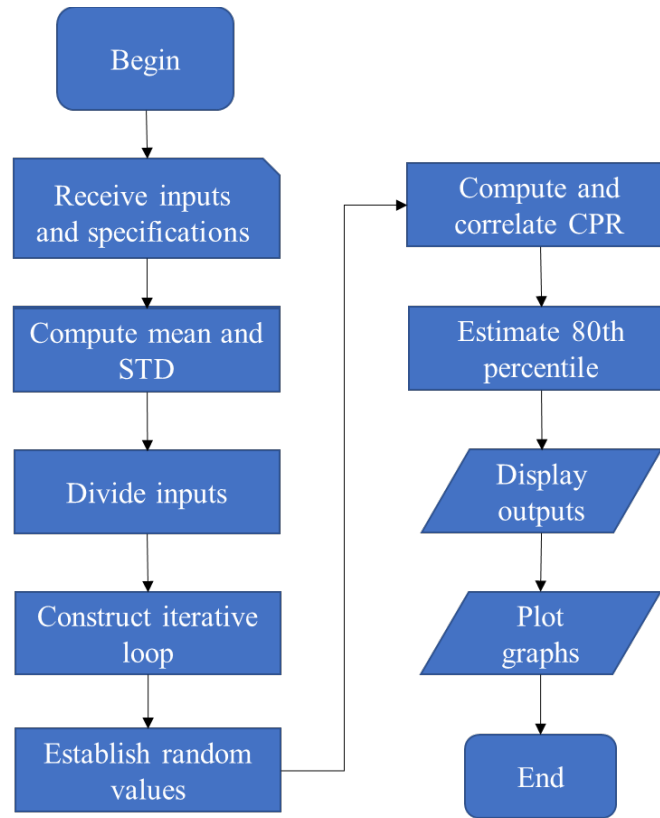





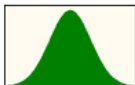


Figure 5. 4: A framwork of the MSC process

The data used in the MCS is shown in Table 5.1.

Table 5. 1: Details of parameters and their associated distributions in MCS

Parameter	Symbol	Value	Distribution
Outer diameter (mm)	D	810	 Normal (Mean = 810, St. Dev. = 50.80)
Tensile Strength (Mpa)	f_u	535	 Lognormal (Location = 0, Mean = 535, St. Dev. = 53.50)

Wall thickness (mm)	t	10	 Normal (Mean = 10 St. Dev. = 1.43)
Defect depth (mm)	d	1.2	 Normal (Mean = 1.2 St. Dev. = 0.32)
Defect length (mm)	L	45	 Normal (Mean = 45 St. Dev. = 4.51)
Operating pressure (MPa)	POP	16	 Normal (Mean = 16 St. Dev. = 1.40)
Probability of failure	$PoF = PF - POP$		

The MCS results were compared with outcomes in step 3 and are discussed in the next section.

5.8 Results and Discussion

Fig.5.5 shows a qualitative BN model for UDC based on the UDC mechanism and concepts. It shows contributing factors of UDC that lead to asset failure. Results in Fig. 5.5 show that organic, inorganic, and mixed deposits influence suspended deposits which affect solid deposits. Results of the BN model in Fig.5.5 show that solid deposits, the shearing force of the pipeline, and the under-deposit galvanic cell influence the UDC corrosion rate. The interdependency model of the UDC mechanism shows that three factors affect under-deposit galvanic cells: chloride, MEG, and pH of

the fluid flowing in the pipeline. The pH of the fluid is influenced by operating temperature, and P_{CO_2} and MEG act as UDC inhibitor and reduces the risk of hydrate formation.

Model results show that operating pressure influences pipeline failure and shearing force. In addition, the flow velocity of the fluid is also an influencing factor in shearing forces, and flow velocity affects solid deposits. The qualitative BN model of UDC in Fig.5.5 shows that the UDC corrosion rate contributes to the loss of pipe wall thickness and affects the defect length. The loss in pipe wall thickness is influenced by defect depth, and the combination of defect length and depth influences burst pressure. Two risk factors, namely steel grade and outer diameter (OD) of the pipeline, also contribute to its burst pressure. Results show that operating and burst pressures are the main influencing factors for pipeline failure.

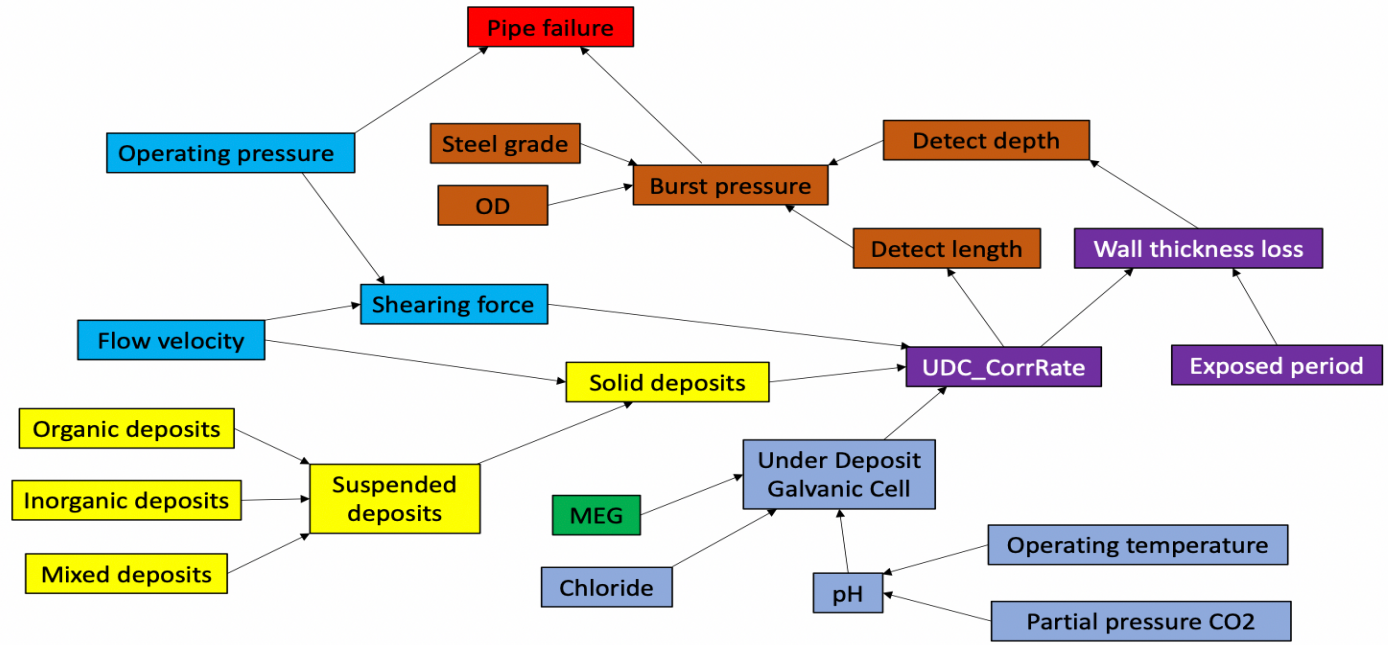


Figure 5. 5: BN model of UDC asset failure for subsea pipelines

Fig.5.5 shows the resultant BN model, which also captures and incorporates the key influential factors that trigger UDC and lead to asset degradation. The prediction of the asset failure mechanism due to UDC is challenging. It is because of the complexity and unstable characteristic of the influential factors. However, the results of the BN model help to understand the interdependencies of risk factors and provide a propagation path that best describes the pipeline's degradation. The results of Bayesian sub-models are discussed here.

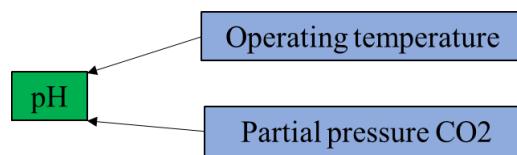


Figure 5. 5 (a): Bayesian subnetwork of the environmental aspect of the UDC asset failure model

Fig.5.5 (a) is a Bayesian subnetwork of environmental parameters. It shows that UDC is influenced by environmental parameters like pH, temperature, and partial pressure of CO₂ (PCO₂). Specifically, the processes of electrochemical, crystallization, transport of solid deposits, and other corrosion factors are considerably affected by temperature and PCO₂. An increase in PCO₂ causes an increase in surface pH, and the pH decreases as the precipitation of FeCO₃ occurs. At a constant pH of the solution, the increase in PCO₂ causes more increased precipitation of FeCO₃ compared to the UDC rate. The presence of under deposits is permeable enough for the inhibitor to reach the metal surface. It results in zones with different potentials close to each other, resulting in galvanic corrosion under the deposits, and is presented in Fig.5.5 (b). Results show that understanding the effect of solid deposits on the UDC process and its mechanism in the presence of corrosion inhibitors can help to develop corrosion mitigation strategies.

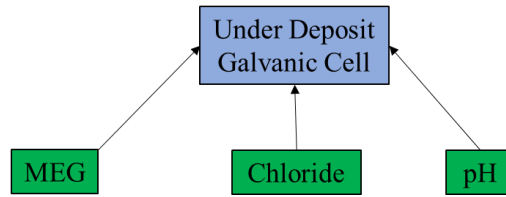


Figure 5. 5 (b): Bayesian subnetwork of under-deposit galvanic cell impact

Fig.5. 5 (b) shows a Bayesian subnetwork of a galvanic cell, which illustrates that galvanic cells under the deposit become predominant in the presence of pH, chlorides, and MEG. In gas pipelines, water content is the most crucial risk factor in determining the speed of the UDC rate and UDC mechanism. High-water contents cause an electrochemical mechanism where the UDC rate is high. MEG can absorb water and makes water unavailable to form hydrate. Therefore, the presence of MEG influences the solubility of the corrosive products in the water phase and can significantly inhibit the UDC rate.

A lower amount of MEG inhibitor can lead to higher electrochemical potential difference, increasing the UDC rate. On the other hand, an increase in MEG on carbon steel causes a slight likely rise in HCO_3^- concentration. As explained in the dynamic analysis results, the different amounts of HCO_3^- concentration show other trends over time. As the pH reaches more than six and FeCO_3 solubility is low, the reaction kinetics of FeCO_3 precipitation and protective film formation is accelerated. The galvanic contact between the corrosion product and surface metal can increase iron dissolution by increasing the cathodic reaction. The effects of chlorides are linked to the penetration of passive oxide films on carbon steels to cause pitting. The chlorides in a sour production environment can lead to a localized breakdown of the protective film on carbon steel pipe. Chlorides are a primary culprit of damage to protective films, as they increase corrosion rate. Corrosive production systems can cause corrosion to occur faster, especially if chlorides are present and the pH of the water is under five.

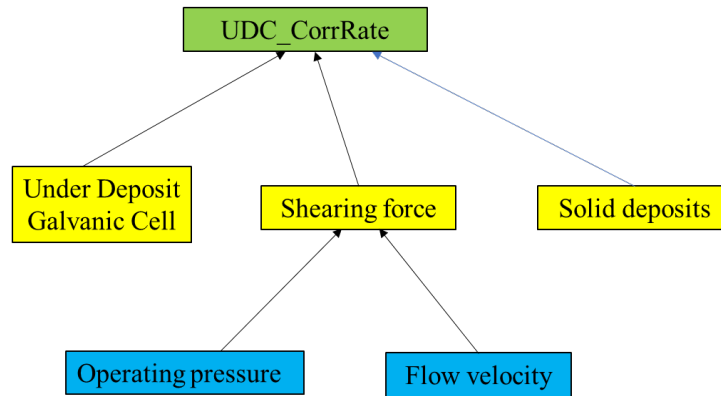


Figure 5. 5 (c): Bayesian subnetwork for UDC rate

Results of the Bayesian subnetwork model of the UDC rate are shown in Fig. 5.5(c). It indicates that the under-deposit galvanic cell, the shearing force, and solid deposits influence the UDC corrosion rate. The collective presence of the flow velocity and high operating pressure can affect the distribution of the aqueous phase (and corrosion inhibitor), in which corrosion occurs, and the hydrodynamic shearing force at the pipe wall. Flow velocity affects the mass transfer of corrosive species to the pipe wall and corrosion products from the pipe wall. If free gas is present, higher pressures increase P_{CO_2} , reducing the aqueous phase's pH and thereby increasing the corrosion rate. If no free gas is present, no more CO_2 can dissolve into the solution as the pressure increases. Therefore, pumping a liquid to higher pressure does not affect the corrosivity of the fluid. Solid deposits are key prevailing factors that cause severe corrosion. They ascertain the influencing operating parameters and the corresponding UDC rate in steel pipelines.

The adhesion of the product layer to the pipe wall is affected by shearing force. Sour environments, on the other hand, develop a variety of iron sulfide products, and most of them are highly corrosive. In processes with high shearing force, where the formation of ionic paths between the area covered under the deposit and uncovered metal is possible, a mechanism similar to crevice corrosion could occur (Senatore et al., 2018; Q. Wang et al., 2021).

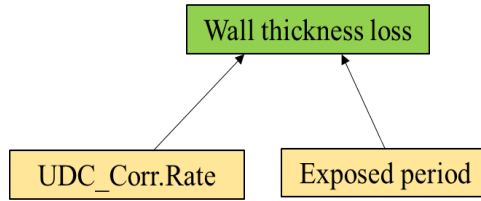


Figure 5. 5 (d): Bayesian subnetwork of wall thickness loss

A Bayesian subnetwork of wall thickness loss is presented in Fig. 5.5 (d). After an exposed period, UDC can cause wall thickness loss. The wall thickness loss rate is based on the UDC corrosion rate.

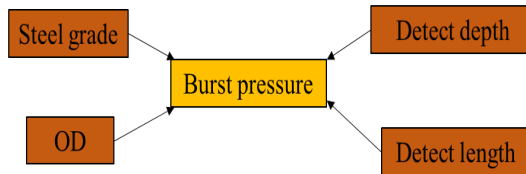


Figure 5. 5 (e): Bayesian subnetwork of burst pressure

The Bayesian subnetwork model in Fig.5. 5 (e) demonstrates the importance of the pipeline's outer diameter (OD), steel grade, defect length, and defect depth of UDC on burst pressure, also called failure pressure. The available failure pressure models are deterministic and assess corrosion defects' severity based on nominal values such as the internal pipeline pressure loading (POP) and pipeline capacity, i.e., failure pressure of the pipeline (PF). This result is in accordance with the available literature (Caleyo et al., 2002).

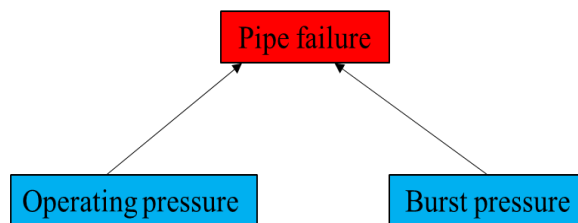


Figure 5. 5 (f): Bayesian subnetwork model for asset failure

Results of the Bayesian subnetwork for asset failure are presented in Fig. 5.5 (f). It indicates that PoF is the difference between burst pressure, P_F , and operating pressure, P_{OP} . Direct or alternating current at localized locations of an asset can produce UDC. The results of DBN illustrate the corrosion propagation profile of the asset over time and are presented in Fig. 5.6.

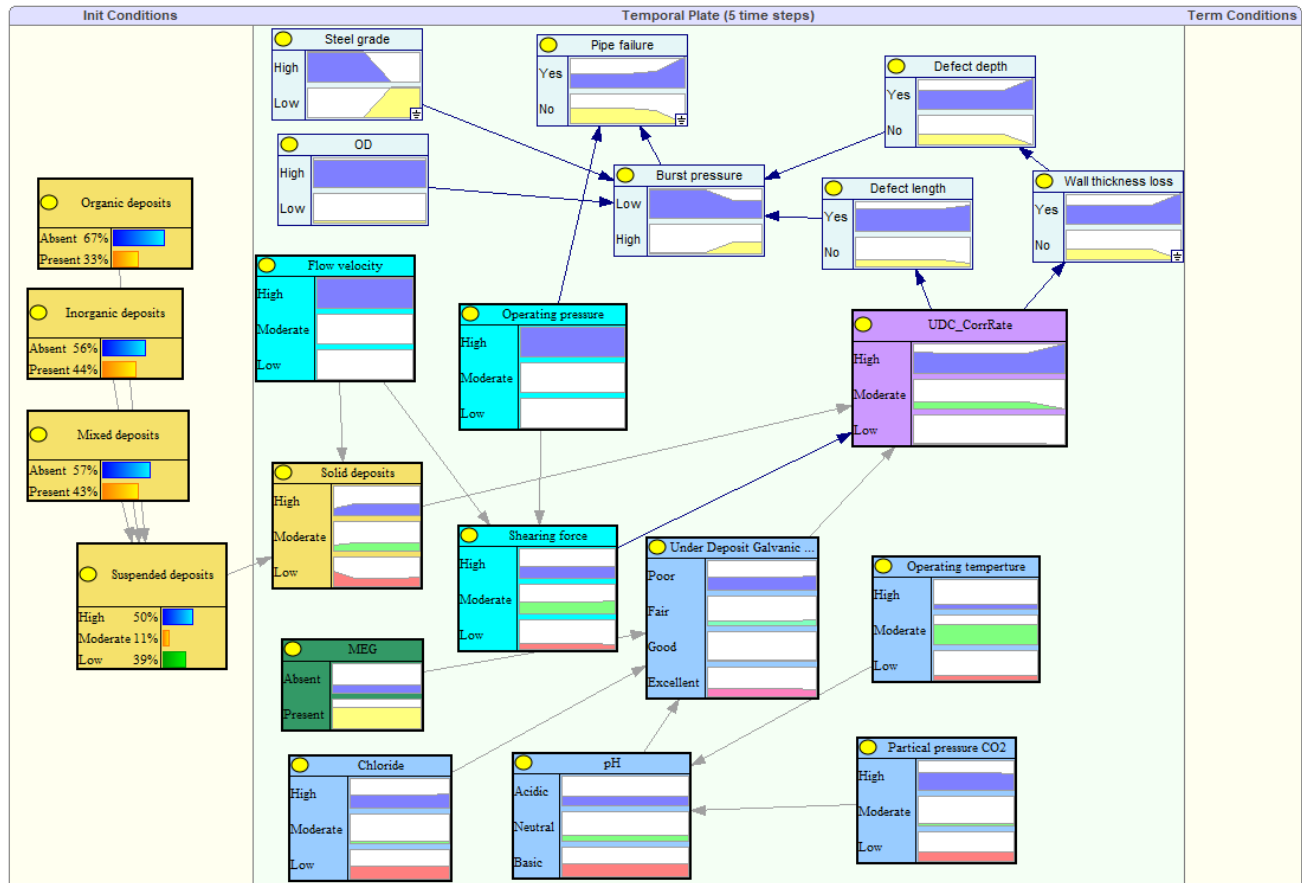


Figure 5. 6: DBN result for pipe failure (PoF), simulation developed in Genie Software

All risk factors in the DBN lie in two regions: initial conditions and temporal plate. Variables in initial conditions are those variables with values that do not change with time. In other words, these variables are static rather than dynamic. The variables in the temporal plate have their values change over time. The red bar of a variable in the temporal plate indicates a low state, a green bar indicates a moderate state, and a blue bar indicates a high state of a given variable.

Each risk factor in Fig. 5.6 has a probability density function which indicates the relative likelihood of that variable. Based on the state of the variable, it can take on a random value. In Fig. 6, each directed arc indicates the direction of the causal relationship. It shows the probabilistic relationship among risk factors of UDC that lead to the PoF of the asset. The probabilistic results of the UDC mechanism help to understand in-depth the impact of different risk factors in UDC that lead to asset failure. The probabilistic results show that the occurrence probability of suspended deposits is based on the occurrence probabilities of organic, inorganic, and mixed deposits. This result indicates that out of three states of suspended deposits, high, medium, and low, the probability of having high-suspended deposits is high. Results show four under-deposit galvanic cell parameters: poor, fair, good, and excellent. The probabilistic results indicate that $P(\text{Under deposit galvanic cell} = \text{poor}/\text{MEG, Chloride and pH}) = 0.45$ and $P(\text{Under deposit galvanic cell} = \text{excellent}/\text{MEG, Chloride and pH}) = 0.30$. This result shows that there is a high possibility of the UDC corrosion rate being low, and this reduces the PoF. The effect of shearing force on the UDC rate is a function of the velocity of the fluid and operating pressure. The result shows that the probability of high shearing force is 0.40, and the likelihood of wall thickness loss is 0.62. Results of DBN indicate that the wall thickness loss increases with the increase in shear forces over time, and the results do not influence the presence or absence of MEG. The dynamic result shows that the rise in shearing forces reduces the performance of the MEG inhibitor. These results demonstrate the importance of wall thickness loss due to UDC in assessing the integrity and reliability of an asset. It provides a well-informed early warning guide on the necessity for proactive asset condition monitoring.

The results of industrial data analysis use a limit state function to assess the PoF of the asset. The results of MCS are presented as a cumulative density function (CDF) of the PoF shown in Fig. 5.7.

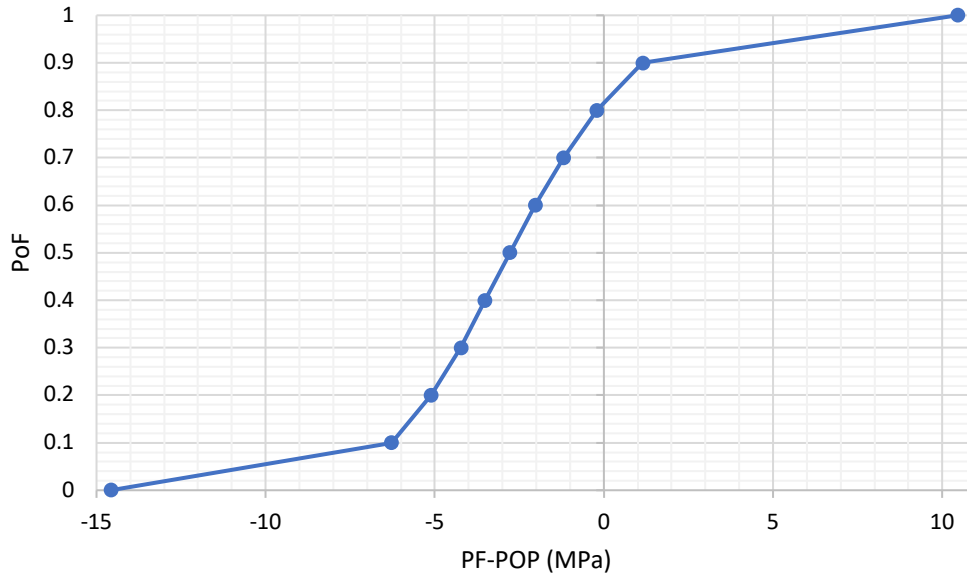


Figure 5. 7: CDF of PoF

The x-axis indicates PF-POP, the limit state function (LSF) used in this study. A negative value of LSF shows that operating pressure is higher than failure pressure, which may lead to a damaged pipeline due to UDC. Y-axis shows the probability of failure and ranges from 0 to 1. Where 0 indicates no chance of pipeline failure and 1 shows the 100% certainty of pipeline failure.

Fig. 5.7 shows that the pressure may vary from -15 MPa to 11 MPa. These results help report PoF at different failure pressures. Fig. 7 also helps to analyze the distribution of failure pressure. From deterministic calculations, the difference between failure and operating pressures (LSF) is -2.69 MPa. Negative pressure indicates that the operating pressure is higher than the failure pressure, and the pipeline can burst due to UDC. The occurrence of limit state function $LSF > 0$ is computed by analyzing Fig. 7 for positive numbers. Results show that the certainty of $LSF > 0$ is 18.32%. It

means there are 81.68% ($100\% - 18.32\% = 81.68\%$) chances of pipeline failure, i.e., $P(LSF \leq 0) = 0.8168$.

A comparison of the DBN model and industrial data is presented in Fig.5.8. It shows that the limit state functions $d(T)$ and $d(L)$ increase with time, the defect depth increases with time, and this reduces the wall thickness over time. Therefore, there is an increase in the loss of wall thickness.

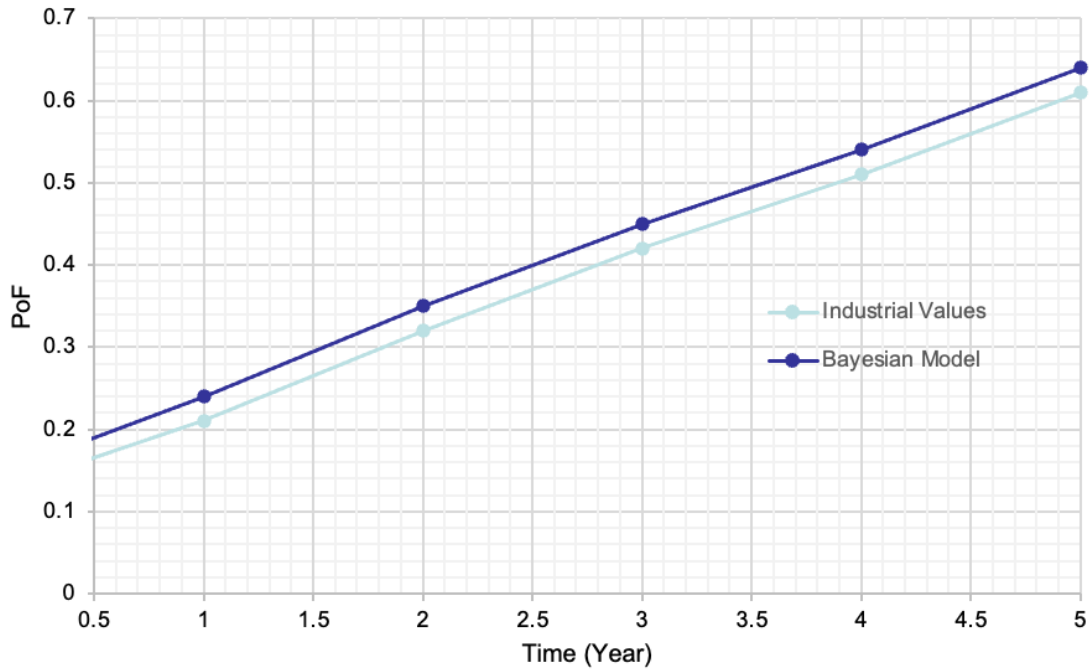


Figure 5. 8: Comparison of dynamic Bayesian Network and Industrial data

Results in Fig. 5.8 are plotted between time on the x-axis and PoF (probability of failure) on the y-axis. Fig. 5.8 shows that both industrial values and results of the BN model have a linear and similar trend of PoF over time. It confirms that the theoretical model results are consistent with industrial practices. As shown in Fig.5.8, there are minor discrepancies, but they are closer to each other at all five years. Since the results computed from DBN are based on the structural learning of DBN, which is based on the UDC mechanism, theory, and concepts, they are considered an approximate assessment of PoF rather than an actual and accurate assessment. In contrast, the

results of MCS are based on actual industrial data. The comparative results show that the dynamic model can achieve reliable and reasonable results similar to the industrial data. The results of this study can be used to develop a maintenance schedule to mitigate UDC. Change in burst pressure of an operational pipeline depends on the loss of metal wall thickness and increased computed defect depth.

Sensitivity analysis

Sensitivity analysis helps to understand key input parameters that influence the model output. Fig. 5.9 shows the correlation of different parameters in MCS to PF-POP. It shows a positive correlation of PF-POP with t and f_u , which is interpreted as the increase in t and f_u leading to a rise in PF-POP and a decrease in t and f_u , causing a reduction in PF-POP. The correlation of PF-POP with POP , l , d , and D is negative, which indicates that a decrease in these variables will increase the value of PF-POP.

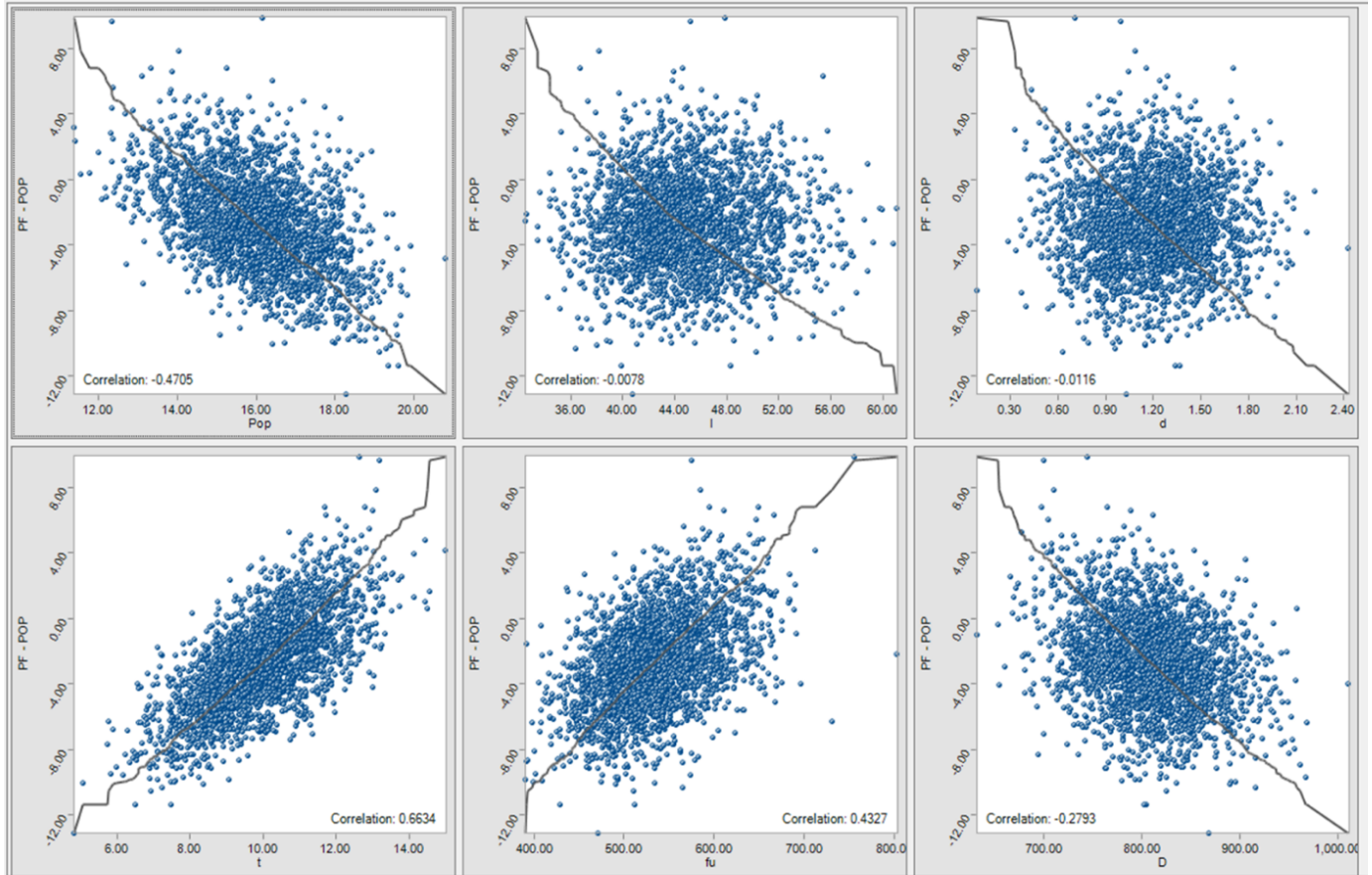


Figure 5.9: Correlation of MCS parameters in the UDC model

The DBN model for the UDC analysis shows six key factors. Their contributions towards PoF are demonstrated in Fig. 5.10. It shows that higher pipe wall thickness and tensile strength enhance the pipeline's integrity. Their contributions are 46.8% and 20.3%, respectively. Results in Fig. 5.10 also indicate that a decrease in POP and pipe outer diameter causes compromises in the integrity of the pipeline, and their contributions are 23.9% and 9%, respectively. It shows that pipeline wall thickness and operating pressure are critical elements in the UDC rate. The results of this study are valuable for oil and gas industries to develop mitigation and maintenance plans to avoid asset losses due to UDC.

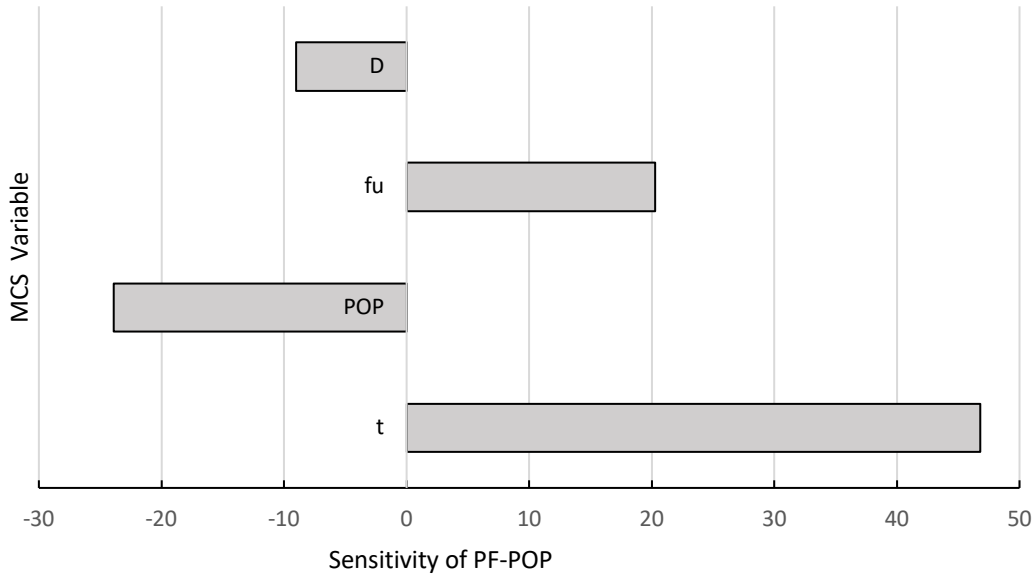


Figure 5. 10: Results of sensitivity analysis

This figure shows the impact of MCS variables on PF-POF. A positive value indicates an increase in a limited state function, and a negative value shows a decrease in a limited state function.

5.9 Conclusions

UDC in pipelines poses severe risks to transporting fluid in oil and gas industries. UDC involves different mechanisms which are based on the nature of the deposits involved, field conditions (iron sulfide, microorganisms, sand, waxes, asphaltenes), operational parameters (temperature, operating pressure, burst pressure), and the chemistry (chemical reactions in UDC) involved. In this study, the UDC mechanism is modeled using a DBN approach. The network approach of DBN helps to understand the key risk factors in the UDC mechanism and their interdependencies that lead to corroding a pipeline in the oil and gas industry and ultimately costing billions of dollars to the industry. A temporal aspect of DBN is utilized to understand the variations and nature of the UDC mechanism over five years. The outcomes of this study reveal that the theoretical model

supports practical observations. The study also highlights the importance of understanding the physical characteristics of the solid deposits (depth, formation, and composition), solution chemistry (pH, oil, water contents), and corrosion formation mechanism (precipitation, diffusion, MIC) in UDC.

The study also concludes that pipe wall thickness and pipe tensile strength significantly reduce the PoF and increase asset reliability. The study identifies that the theoretical model of DBN is consistent with actual industrial data. Hence, DBN is a reliable tool for oil and gas industries to monitor, control and mitigate UDC in their pipeline systems. This work can help to develop the reliability and maintenance schedule of the pipelines in the subsea industry. It can support the selection of optimal inspection intervals so that PoF can be maintained within an acceptable range and mitigated through regular maintenance. For future work, performing an economic risk analysis integrated with UDC DBN is recommended. It will help to understand the most cost-intensive risk factors contributing to the high cost of asset damage due to UDC.

5.10 Appendix

Sr. No.	Nodes	States	Probability values
1	Organic deposits	Absent	0.6667
		Present	0.3333

2	Inorganic deposits	Absent	0.5600
		Present	0.4400

3	Mixed deposits	Absent	0.5700
		Present	0.4300

4	Suspended deposits	Organic deposits	Absent				Present			
		Inorganic deposits	Absent		Present		Absent		Present	
		Mixed deposits	Absent	Present	Absent	Present	Absent	Present	Absent	Present
		High	0.1000	0.8500	0.4000	0.7500	0.1000	0.7000	0.6000	0.9500
		Moderate	0.1000	0.1000	0.2000	0.0100	0.2000	0.0500	0.2000	0.0050
		Low	0.8000	0.0500	0.4000	0.2400	0.7000	0.2500	0.2000	0.0450

5	Steel grade	High	0.7800
		Low	0.2200

6	OD	High	0.9200
---	----	------	--------

		Low	0.0800
--	--	-----	--------

7	Flow velocity	High	1.0000
		Moderate	0.0000
		Low	0.0000

8	Solid deposits	Flow velocity	High			Moderate			Low		
		Suspended deposits	High	Moderate	Low	High	Moderate	Low	High	Moderate	Low
		High	0.4000	0.5000	0.0100	0.6000	0.4000	0.1000	0.7000	0.5000	0.3333
		Moderate	0.3000	0.3000	0.0500	0.2000	0.3000	0.5000	0.2000	0.2000	0.3333
		Low	0.3000	0.2000	0.9400	0.2000	0.3000	0.4000	0.1000	0.3000	0.3333

9	MEG	Absent	0.3000
		Present	0.7000

10	Chloride	High	0.4560
		Moderate	0.1000
		Low	0.4440

		Burst pressure	High	Low
--	--	----------------	------	-----

11	Pipe failure	Operating pressure	High	Moderate	Low	High	Mode rate	Low
		Yes	0.4400	0.8800	0.7800	0.7700	0.3240	0.1200
		No	0.5600	0.1200	0.2200	0.2300	0.6760	0.8800

12a	Burst pressure	Defect depth	Yes							
		Defect length	Yes				No			
		Steel grade	High		Low		High		Low	
		OD	High	Low	High	Low	High	Low	High	Low
		Low	1.0000	0.8800	0.7300	0.4200	0.9000	0.9900	0.8200	0.7800
		High	0.0000	0.1200	0.2700	0.5800	0.1000	0.0100	0.1800	0.2200

12b	Burst pressure	Defect depth	No							
		Defect length	Yes				No			
		Steel grade	High		Low		High		Low	
		OD	High	Low	High	Low	High	Low	High	Low
		Low	0.9000	0.9800	0.5500	0.6100	0.8800	0.5600	0.1900	0.6600
		High	0.1000	0.0200	0.4500	0.3900	0.1200	0.4400	0.8100	0.3400

13	Operating pressure	High	0.9900
		Moderate	0.0100
		Low	0.0000

14	Shearing force	Operating pressure	High			Moderate			Low		
		Flow velocity	High	Moderate	Low	High	Moderate	Low	High	Moderate	Low
		High	0.4	0.15	1.11E-16	0.1	0.05	0.05	0.05	0.01	0.03
		Moderate	0.4	0.65	2.00E-01	0.2	0.05	0.05	0.1	0.05	0.01
		Low	0.2	0.2	0.8	0.7	0.9	0.9	0.85	0.94	0.96

15	pH	Operating temperature	High			Moderate			Low		
		Partial pressure CO2	High	Moderate	Low	High	Moderate	Low	High	Moderate	Low
		Acidic	0.7000	0.6000	0.0000	0.4000	0.3500	0.2000	0.4500	0.2000	0.0300
		Neutral	0.2000	0.2000	0.2000	0.3000	0.1500	0.2000	0.2500	0.1000	0.0100
		Basic	0.1000	0.2000	0.8000	0.3000	0.5000	0.6000	0.3000	0.7000	0.9600

	pH	Acidic
--	----	--------

16a	Under Deposit Galvanic Cell	Chloride	High		Moderate		Low	
		MEG	Absent	Present	Absent	Present	Absent	Present
		Poor	0.5000	0.5000	0.2000	0.2000	0.0001	0.0001
		Fair	0.3500	0.3500	0.2000	0.2000	0.0010	0.0010
		Good	0.1000	0.1000	0.3500	0.3500	0.0100	0.0100
		Excellent	0.0500	0.0500	0.2500	0.2500	0.9889	0.9889

16b	Under Deposit Galvanic Cell	pH	Neutral					
		Chloride	High		Moderate		Low	
		MEG	Absent	Present	Absent	Present	Absent	Present
		Poor	0.0001	0.0001	0.0001	0.0001	0.7000	0.7000
		Fair	0.0010	0.0010	0.0010	0.0010	0.2000	0.2000
		Good	0.0100	0.0100	0.0100	0.0100	0.0800	0.0800
Excellent	0.9889	0.9889	0.9889	0.9889	0.0200	0.0200		

16c	Under Deposit Galvanic Cell	pH	Basic					
		Chloride	High		Moderate		Low	
		MEG	Absent	Present	Absent	Present	Absent	Present
		Poor	0.7000	0.7000	0.7000	0.7000	0.7000	0.7000

		Fair	0.2000	0.2000	0.2000	0.2000	0.2000	0.2000
		Good	0.0800	0.0800	0.0800	0.0800	0.0800	0.0800
		Excellent	0.0200	0.0200	0.0200	0.0200	0.0200	0.0200

17	Partial pressure CO2	High	0.5780
		Moderate	0.1000
		Low	0.3220

18	Operating temperature	High	0.1584
		Moderate	0.6745
		Low	0.1671

19	Defect depth	Wall thickness loss	Yes	No
		Yes	1.0000	0.0000
		No	0.0000	1.0000

20	Defect length	UDC CorrRate	High	Moderate	Low
		Yes	0.8800	0.5600	0.0200
		No	0.1200	0.4400	0.9800

21	Wall thickness loss	UDC_CorrRate	High	Moderate	Low
		Yes	0.8800	0.0200	0.1900
		No	0.1200	0.9800	0.8100

22a	UDC_ CorrRate (Under Deposit Galvanic Cell Poor)	Solid deposits	High			Moderate			Low		
		Shearing force	High	Moderate	Low	High	Moderate	Low	High	Moderate	Low
		High	0.9100	0.9800	0.1200	0.8800	0.4300	0.5500	0.7800	0.7800	0.7800
		Moderate	0.0800	0.0000	0.7800	0.0700	0.5200	0.4000	0.2200	0.2200	0.2000
		Low	0.0100	0.0200	0.1000	0.0500	0.0500	0.0500	0.0000	0.0000	0.0200

22b	UDC_ CorrRate (Under Deposit Galvanic Cell Fair)	Solid deposits	High			Moderate			Low		
		Shearing force	High	Moderate	Low	High	Moderate	Low	High	Moderate	Low
		High	0.8800	0.9800	0.8800	0.7800	0.9900	0.8900	0.8800	0.5600	0.4500
		Moderate	0.1000	0.0100	0.1200	0.2200	0.0000	0.0900	0.0900	0.4000	0.5000
		Low	0.0200	0.0100	0.0000	0.0000	0.0100	0.0200	0.0300	0.0400	0.0500

22c	UDC_ CorrRate (Under Deposit Galvanic Cell Good)	Solid deposits	High			Moderate			Low		
		Shearing force	High	Moderate	Low	High	Moderate	Low	High	Moderate	Low
		High	0.4300	0.4300	0.5600	0.3400	0.8800	0.2200	0.4500	0.8800	0.7300
		Moderate	0.4700	0.3700	0.1000	0.6600	0.0000	0.5600	0.3200	0.0000	0.1600

		Low	0.1000	0.2000	0.3400	0.0000	0.1200	0.2200	0.2300	0.1200	0.1100
--	--	-----	--------	--------	--------	--------	--------	--------	--------	--------	--------

22d	UDC_ CorrRate (Under Deposit Galvanic Cell = Excellent)	Solid deposits	High			Moderate			Low		
		Shearing force	High	Moderate	Low	High	Moderate	Low	High	Moderate	Low
		High	0.4300	0.4300	0.5600	0.3400	0.8800	0.2200	0.4500	0.8800	0.7300
		Moderate	0.4700	0.3700	0.1000	0.6600	0.0000	0.5600	0.3200	0.0000	0.1600
		Low	0.1000	0.2000	0.3400	0.0000	0.1200	0.2200	0.2300	0.1200	0.1100

CHAPTER 6

6 Risk assessment of oil and gas pipelines failure in Vietnam

6.1 Preface

*A version of this chapter is published in the **International Journal of Engineering and Technology (IJET)**, ISSN: 1793-8236 (Online); DOI: 10.7763/IJET. I am the primary author along with the Co-authors, Zaman Sajid, and Yahui Zhang. I and Zaman conducted the research prepared, the first draft of the manuscript, and analyzed the data, then subsequently revised the manuscript. Co-author Yahui Zhang helped in analyzing the data and revising the paper. All authors had approved the final version.*

6.2 Abstract

Pipelines in the oil and gas industry have been used as one of the most practical and inexpensive methods for large-scale oil and gas transportation. In harsh operating conditions, these pipelines are susceptible to failure, which causes leakage of oil and gas and a significant impact on the environment and economy. Therefore, operational failure risk in oil and gas pipelines is of utmost significance. This paper proposes a model to study the risk assessment of natural gas release in onshore gas pipelines in Vietnam. The methodology analyzes the causes of the failure of the gas pipeline by integrating fault tree analysis (FTA) and fuzzy theory. Monte Carlo simulation is used to evaluate the level of uncertainty. The study identifies 21 risk factors that lead to the failure of the pipelines. The results of a case study on two pipelines in Vietnam reveal that the risk of pipeline failure due to rupture is higher than the failure risk due to puncture. Results also show that corrosion is the least dominating factor in pipeline failure. However, it carries catastrophic consequences.

The stochastic analysis provides risk profiles at different levels. The study recommends using a copper alloy as a construction material to prevent pipeline failure.

Keywords: Operational failure risk; Risk of leakage; Fault tree analysis; Fuzzy logic; Gas pipeline failure; Monte Carlo simulation

6.3 Introduction

Energy is the foundation of modern industry and the sustainable development of the economy. The energy consumption of natural gas has increased rapidly in recent years, which has led to significant growth in the natural gas industry. Thus, achieving a high production rate has gained a lot of attention. However, an essential part easily ignored in the natural gas industry and transportation needs to be more focused on. As the natural gas consumer market becomes more mature, pipeline transportation, especially large volume, and remote distance transportation has become a popular topic worldwide (Aziz et al., 2021; C. Chen et al., 2021; Nandi et al., 2022). Natural gas is produced at a production site, or natural gas could be at a treatment plant, at a gas distribution center, or for industrial operations. Sometimes it is also called a gas transmission pipeline. On land, the main transport method is through natural gas pipelines. Natural gas pipeline transportation has the benefits of fast construction, low transportation cost, less land occupation, high safety performance, large oil and gas transportation volume, less transportation loss, no waste water emission, small leakage risk, little environmental pollution, little impact by adverse climate, easy management, a small amount of equipment maintenance, and remote centralized monitoring (Fadiran et al., 2019; Nong et al., 2020). Based on its use, there are three gas transmission pipelines: gathering pipeline, gas transmission pipeline, and gas distribution pipeline(Lam & Zhou, 2016;

Ríos-Mercado & Borraz-Sánchez, 2015). Gas gathering pipeline: the pipeline from the wellhead of the gas field to the gas treatment plant.

Accidents in natural gas or oil pipelines may cause fatality and substantial economic loss (W. Wang et al., 2022). Thus, this study aims to develop a risk assessment methodology for the failure of oil and gas pipelines due to different factors. A fault tree analysis (FTA) is conducted to evaluate risk and associated components of risks. This conference paper uses a fuzzy method to transform the linguistic expressions of experts into subsequent failure probabilities.

The most crucial part of the FTA is to transfer a physical system into a well-organized, structured, logical probabilistic diagram utilizing quantitating the abstract concepts towards the miscellaneous events that might contribute to the downfall of a system (Badida et al., 2019; Xie et al., 2021). In the developed fault tree (FT), one can explicitly observe the various branches (certain specific causes) leading to one specified top event of interest. AND and OR gates are the two basic logic gates, and the hazard analysis done previously can be used to generate the TOP events.

In this study, Crystal Ball (CB) software, developed by Oracle, is used as a tool to perform Monte Carlo simulation (MCS). The MCS predicts all possible results for a specific situation, uses charts to summarize the analysis, and displays the probability of each outcome (da Silva et al., 2019; Das et al., 2018). In addition to describing statistics, trend graphs, and related variable assignments, sensitivity analysis is also conducted.

6.4 Risk analysis of natural gas pipeline operation

Risk of oil and gas pipelines corrosion

Corrosion occurs due to the susceptibility of oil and gas pipelines to external environmental factors. In detail, pipelines in areas near high temperatures, cold day and night temperature differences are more significant; pipeline acid alkali, rain, and snow can lead to oil and gas pipeline corrosion. Before the pipeline is typically put into use, although the pipeline maintenance managers have made some preparations in advance, it also will be from corrosion. Because the pipeline is buried in the underground soil all year round, the pipe outside the area of the natural environment, temperature, and moisture changes will corrode on oil and gas pipeline. And because of the pipeline material selection, the construction technology, and the methods used during construction, this has a direct relationship with the corrosion of the pipeline. In addition, oil and gas resources contain a variety of chemical substances, and all kinds of chemical components are more complicated and varied. For example, the hydrogen sulfate element in oil and gas resources can cause specific chemical reactions during transportation. It can change the crystal lattice of the oil and gas pipeline interior, which directly leads to a significant reduction in the corrosion resistance of the pipeline (J. Chen et al., 2021).

Risk of leakage in pipelines

Because oil and gas pipelines have been put into use and have a long working life, they are also affected by various factors such as the local natural climate and environment, construction technology, and pipeline material. As a result, in addition to the corrosion of oil and gas pipelines, leakage occurs. Once the oil and gas pipeline leaks, it will directly cause economic losses, and more serious will cause pollution and damage to the natural ecological environment.

Risk of weather conditions

During the pipeline construction, various climates, such as high temperatures, severe cold, frost, rain, snow, dense fog, cold waves, and storms, will be encountered. Such climatic conditions not

only cause serious harm to the body of the construction workers but also reduce the efficiency of the staff, slow down the construction process, and have a particular impact on the machinery and equipment and the construction work.

Oversight of oil pipelines management

First, there will be illegal buildings around the oil pipeline. The existence of these illegal buildings will significantly affect the maintenance of the pipeline. Secondly, before the pipeline is laid, facilitating the pipeline laying may satisfy all the demolition requirements, which will produce a large amount of cash impact. At the same time, to save money, inferior materials will be chosen in the pipeline.

In this work, Crystal Ball software will simulate sensitivity analysis, input the basic event probability, and measure the sensitivity of important factors that affect the top event. After FTA, the primary events' probabilities are obtained. The next step is to input them all in the spreadsheet with Excel and then import data into Crystal Ball software to perform a series of sensitivity analysis operations. Thus, the probability density function (PDF) of the top event and the cumulative distribution function (CDF) is obtained, and the most important influencing factors affecting the top event are analyzed. The average and basic deviations of the top event and the base event are also attained. All the things that have been done by CB aim to identify the most critical factors in the pipeline risk analysis.

6.5 Methodology

Case Study

This case study represents the leakage of the objected two transmission pipelines in Vietnam named line 1 and line 2. The two lines, buried underground, are now submerged in the water due

to diverting the fluvial river in the vicinity. The water is 1.5m to 6m deep, and the submerged length accounts for one-fourth of its total length. The following is the basic information about the two objected pipelines' condition. The designed pressure for line 1 is 10 MPa with a diameter of 711 mm and a length of 43.8 km. The designed pressure and diameter for line 2 are the same as line 1 but with a length of 43.4 km.

The application of Crystal Ball software to reevaluate the risk of the underwater pipelines and make comparisons in terms of different aspects. Due to the original position of the pipelines, no extra protection measurements were implemented, and risk analysis is required in case of the rupture or burst of the pipelines. The top event is the gas release caused by rupture and puncture (Hedlund et al., 2019; S. Yuan et al., 2019) (Lu et al., 2015). To have an explicit visual comparison between the precedent method used and the new method, including the Crystal Ball, the FT developed in the previous project will be simplified, and the corresponding occurrence likelihood of each simplified event will still be considered as the original one.

Step 1: Defining System

The study begins with defining the potential failure of a natural gas transmission underwater pipeline in one of the metropolises in a rural area in Vietnam.

Components operating and failure modes: two lines are investigated in this study. The buried environment of these two lines was radically changed, and the pipelines are now submerged due to the waterway realignment. Statistically, the maximum water level is up to 6 meters, and the submerged length underwater accounts for one-fourth of the total length with no supplementary anti-erosion and anti-corrosion protection which may lead to hang risk and finally yield rupture or puncture.

System boundary conditions: the gas release caused by rupture and puncture is considered the study's top event for the FTA. The underwater situation is confronted; therefore, the intermediate events for the FT can be corrosion, wrong operation, fatigue, etc. The number of primary events is cut down to 21 for simplicity.

Step 2: FT construction and analysis

The FT is constructed. The procedures are presented in Appendix. The probabilities of each primary event are given in Appendix, developed based on the judgment of different prestigious safety experts. The qualitative and quantitative FTA were combined with the Crystal Ball software results, which are discussed in the results section.

Step 3: Conversion from FTA to Crystal Ball analysis

Based on the above method, we obtain the deterministic top-event probability. However, obtaining historical data under actual conditions is impossible, and there are errors in the deterministic probability of many basic events. Using the crystal ball software to analyze the probability. The PDF of the top event (Gas release) and the CDF are obtained and analyzed at a confidence interval of 95%, and the most important influencing factors affecting the top event are analyzed. The average and basic deviations of the top event and the basic event are also obtained. For this simulation, 10,000 trials are applied to forecast the top event. Import the data from the FTA into an Excel spreadsheet and set the Standard deviation as ten percent of the corresponding basic event probability. Data from this step is presented in Appendix.

Step 4: Use of logic gates and defining assumptions

Probabilities of top and intermediate events were calculated using logic gates in an FTA. In FTA, logic gates deal with deterministic relationships. Each basic event has a certain failure probability based on experience and previous data. After analyzing the accidents that happened in the pipelines, according to the principle of determining the FT top event, select “Gas release” as the top event. The top event and intermediate events can be calculated by using the equation of the OR and AND gates (Taleb-Berrouane et al., 2020). For the OR logic gate, the equation is shown below

$$P = P(X_1) + P(X_2) + \dots + P(X_n) = \sum_{i=1}^n P(X_i) \quad (6.1)$$

For the AND logic gate, the equation is shown below

$$P = P(X_1) \times P(X_2) \times \dots \times P(X_n) = \prod_{i=1}^n P(X_i) \quad (6.2)$$

The “mean” value is set to the same number as the probability, and then the standard deviation is set as ten percent of the corresponding basic event probability. The green color of the cell indicates assumptions, as shown in Table 3. This step is repeated for all input data sets. The model's output is the top event, “Gas Release” and is defined as a forecast in CB. The color of the cell turns blue, indicating an output. Simulation is repeated in 10,000 trials, and simulation is run. Input data of top and intermediate events and assumptions defined in CB are presented in table 6.1 and table 6.2 of the appendix.

6.6 Results and discussions

The constructed FT is shown in Figure 6.1. It can be seen that the number of primary events is 21, and their contributions to the top events are displayed by virtue of ‘AND’ and ‘OR’ gates.

The results after performing the analysis are presented below. The unreliability value is 0.02429, which means the probability of gas release in these underwater pipelines is 0.02429. The frequency

of the top event is 0.02675, and expected number remains the same as the frequency, whereas the CFI is 0.02742. The probability of failure and frequency can be used as the input for the risk assessment tool (Excel coding). The value of the importance of GT2 (0.7296) is much higher than that for GT1 (0.2704); thus, the rupture (GT2) of the underwater pipelines is more likely to happen as compared to the puncture (GT1), which means more attention should be placed on the measurements to prevent the rupture of the pipelines instead of puncture of the pipelines. Because these measurements can largely reduce the probability of failure of the top event. As shown in FTA, the minimum cut sets are GT1, and GT2, corresponding to the Q value is 0.0066 and 0.01781, respectively. The gate time profile result indicates that the unreliability does not change with time.

The risk assessment tool is then supplemented to assess the risk of the gas release. The severity level is taken as major as the released gas can cause an explosion or fire, given the ignition source, and the environment may be contaminated.

The probability from the FTA is 0.02429, so the impact likelihood is considered unlikely; therefore, the risk is medium and needs to be remedied, after which the residual risk is low because the severity level is lowered to 2 with the supplemented additional measurement, such as crossing the pipelines and cover the surface with a copper alloy to prevent the pipelines from being corroded.

The results from the Crystal Ball simulations at 95-percentile show that the probability of gas release from the oil and gas pipeline ranges between 0.02272 to 0.02689. Results of sensitivity analysis show the defect in both pipelines are the most significant factor, contributing to 37.8% of releasing gas, while the fluid impact is only 7.5%. This study analyzes all the natural gas and oil pipeline situations, essential installations, and factors affecting the gas release event. Using the FTA as the core, the deterministic calculation method is used to calculate the probability of the event, and the Monte Carlo simulation is performed using the crystal ball software. The simulation

is a normal distribution. After 10000 trials, the mean value of the top event is 0.024782, the Median Value is 0.024770, and the Standard Deviation of the top event is 0.001084. The maximum and minimum occurrence probabilities of the top event are 0.028545 and 0.0208806. Results also show that the 90th percentile is 0.023379. The probability of top events and intermediate events solved the uncertainty that may arise without historical data. The probability of the top event ranges from 0.02272 to 0.02689 with a certainty of 95%. Through analysis, the main factors affecting the gas release incident are the Defect of pipe (type 1 and 2), fluid impact, and dredging.

6.7 Conclusions

Natural gas or oil release accidents of underwater transmission pipelines had constantly happened over the past few years, which are deemed as the most critical factor affecting the economic growth and ocean environment; hence, in order to prevent accidents from arising, an effective risk assessment is necessary to mitigate or eliminate the potential hazards. In this case study, the data, especially the risk characteristics, from the previous case study on the underwater pipelines in Vietnam were used to construct a simplified FT by regarding some intermediate events as the basic events from which the input data for the subsequent Crystal Ball simulation were generated. FTA and Crystal Ball simulation results show that a comprehensive understanding of the hazards that may cause the gas release in the underwater pipelines can be drawn out so additional protection measurements can be implemented in time.

The FTA is an advantageous and convenient risk assessment method where each primary event and its contribution to the top event are listed explicitly. Nonetheless, determining the most significant hazards amongst these miscellaneous events is challenging, so taking the most imperative measurements to alleviate or even rule out the hazards might be challenging. Given the predicament that a safety engineer in oil and gas industries might have, a combination of FTA and crystal ball

simulation was applied in this case study by which the most sensitive factor (event) can be found in basic event sensitivity figure and the most likely tope event probability can be obtained from forecast frequency view. Using only one risk assessment method to deal with unpredictable working situations is monotonous and unreliable; thus, the recommendation is made that various risk assessment methods should be used when dangerous conditions are confronted with the best predicting results.

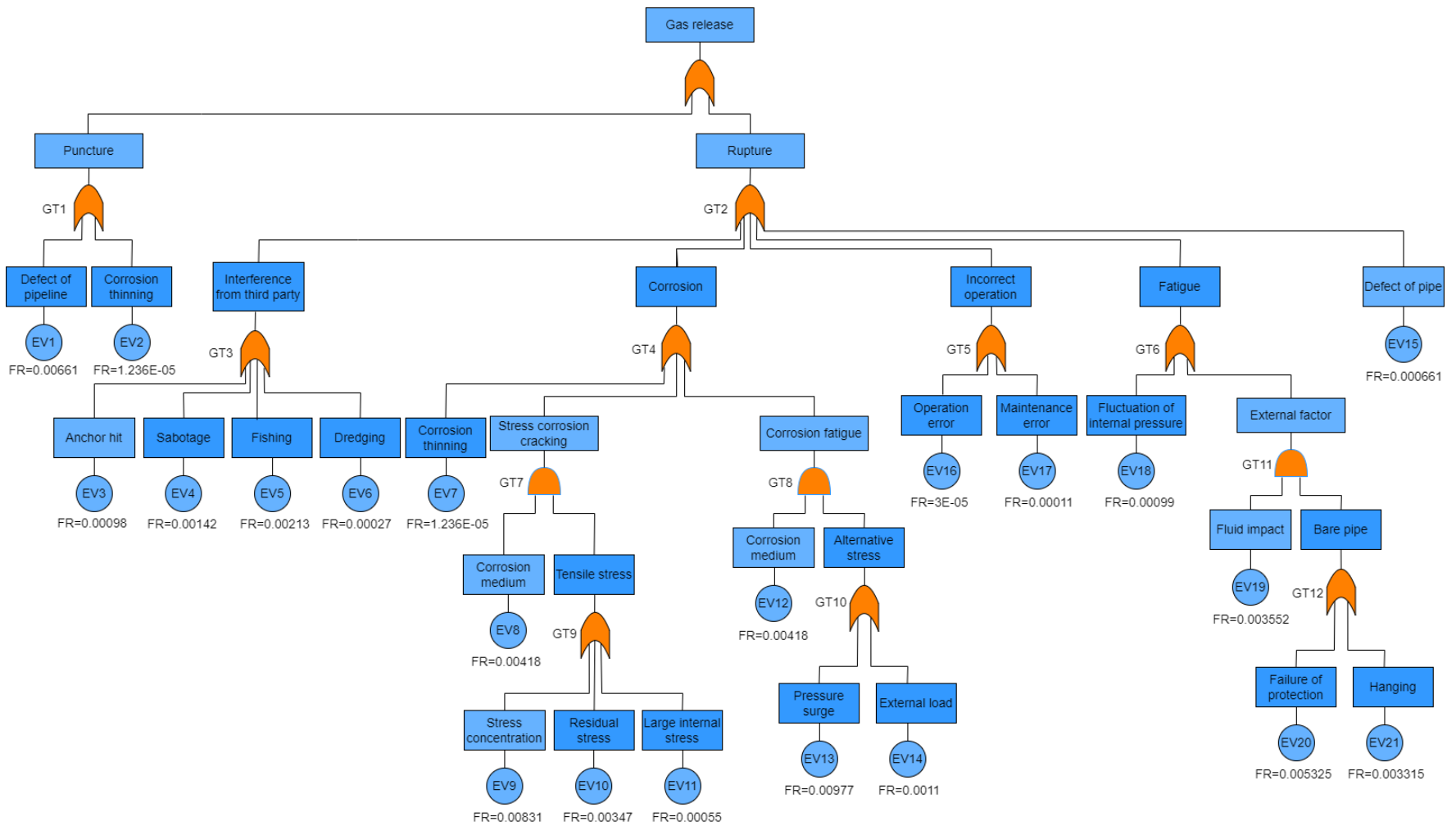


Figure 6. 1: FT of the underwater pipelines

6.8 Appendix

Table 6. 1: List all the primary events for the construction of the FT

EV	Detailed description	Failure rate
1	A defect is a deviation from the original pipeline configuration	0.00661
2	The diameter of the pipe is thinned because of corrosion	0.00001236
3	Pipeline interfering due to ship anchor	0.00098
4	Pipeline interference due to sabotage	0.00142
5	Pipeline interference due to fishing	0.00213
6	Pipeline interfering due to river dredging	0.0027
7	The diameter of the pipe is thinned because of corrosion	0.00001236
8	Pipeline corrosion (because of corrosion medium number 1)	0.00418
9	Pipeline crack corrosion (stress concentration)	0.00831
10	Pipeline crack corrosion (residual stress)	0.00347
11	Pipeline crack corrosion (high internal stress)	0.00055
12	Pipeline corrosion (corrosion medium number 2)	0.00418
13	Pipeline fatigue corrosion (pressure surge)	0.00977
14	Pipeline fatigue corrosion (external load)	0.0011
15	A defect in a deviation from original pipeline configuration	0.00661
16	Pipeline failure (incorrect operation)	0.00003
17	Pipeline failure (inappropriate maintenance)	0.00011
18	Pipeline fatigue (internal pressure fluctuation)	0.00099
19	Pipeline fatigue (fluid impact)	0.03552
20	Pipeline fatigue (protection failure)	0.05325
21	Pipeline fatigue (hanging)	0.03315

Table 6. 2: Probability of Top and Intermediate events

EV#.	Top and Intermediate events	Probability
TP	Gas release	0.0247706240
GT1	Puncture	0.0066223600
GT2	Rupture	0.0181482640
GT3	Interference from third party	0.0072300000
GT4	Corrosion	0.0001093360
GT5	Incorrect operation	0.0001400000
GT6	Fatigue	0.0040589280
GT7	Stress corrosion cracking	0.0000515394
GT8	Corrosion fatigue	0.0000454366
GT9	Tensile stress	0.0123300000
GT10	Alternative stress	0.0108700000
GT11	External factor	0.0030689280
GT12	Bare pipe	0.0864000000

CHAPTER 7

7 Safety Analysis of Blended Hydrogen Pipelines using Dynamic Object-oriented Bayesian Network

7.1 Preface

*A version of this chapter is submitted to the **International Journal of Hydrogen Energy** (Decision in Process). I am the primary author along with the Co-authors, Zaman Sajid, Faisal Khan, and Yahui Zhang. I wrote original draft, Software, Review & editing, and developed the Methodology, Formal analysis, Conceptualization, Data curation. I prepared the first draft of the manuscript and subsequently revised the manuscript based on the co-authors' and peer review feedback.*

Co-author Zaman Sajid provided support in Writing – review & editing, Supervision, Software, Methodology, Formal analysis, Data curation. Co-author Faisal Khan helped in writing – review & editing, Supervision, Methodology, Formal analysis, Conceptualization. Co-author Yahui Zhang provided fundamental assistance in Writing – review & editing, Supervision, Methodology, Formal analysis. The co-authors also contributed to the review and revision of the manuscript.

7.2 Abstract

Energy demand is increasing rapidly while traditional fossil fuel resources are depleting. Hydrogen is considered a promising alternate fuel. The safety of hydrogen transportation is a key issue that warrants greater attention, primarily to determine how existing pipelines of natural gas transportation can be used for hydrogen transportation. This study has proposed a safety analysis model using the physics and mechanistic approach of hydrogen-associated degradation. A dynamic Object-Oriented Bayesian network (OOBN) model is proposed to study the mechanisms

and physics of failure with hydrogen-associated degradation. The proposed model is explained using an industrial case study. Results show that low-strength steel is less susceptible to hydrogen-associated degradation than high-strength steel pipes for hydrogen transportation. Moisture, internal stress, and loss of metal ductility are key safety aspects that require detailed attention. The results of dynamic OOBN also indicate that hydrogen release probability follows a non-linear behaviour dependent on the type of metal and operating conditions. The study identifies the controlling corrosion rate, which can ensure the safety of blended hydrogen pipelines. The study finds its application in hydrogen production and transportation operations.

Keywords: Hydrogen release, Hydrogen pipelines, OOBN, Hydrogen embrittlement, Hydrogen stress cracking, Hydrogen transportation.

7.3 Introduction

Modern industry and sustainable economic development are based on energy (Bull, 2001; Matzen et al., 2015; Patel et al., 2022). The usage of natural gas, carbon-based energy sources, and other fossil fuels has increased the level of carbon dioxide and gas emissions in the atmosphere of the earth, which has raised the average world temperature (Sharma & Ghoshal, 2015). Implementing environmentally clean hydrogen with flexible transportation of energy and feedstock in the clean energy industries can help reduce global warming (Bull, 2001; Layzell et al., 2020).

In the industrial sector, hydrogen can be produced using the conventional steam reforming method from hydrocarbon feedstocks, such as natural gas, liquefied petroleum gas (LPG), and naphtha, or using technology developed in refineries such as catalytic reforming (CCR), propane dehydrogenation (PDH), and others (dehydrogenation of propane) (Xiang et al., 2022).

Currently, about 96% of hydrogen is produced from non-renewable sources, with natural gas making up 48%, reforming 30%, and coal providing 18%. Only about 4% is produced by

electrolysis (Pareek et al., 2020). Sustainable methods of hydrogen production from renewable sources need to be developed to solve the problem of fossil fuel depletion and carbon dioxide depletion (Oliveira et al., 2021).

Fig.7.1 shows the three main conversion routes (Anwar et al., 2021; Bull, 2001; Matzen et al., 2015) to create hydrogen: hydrogen is produced from water and electricity, fossil fuels, and biomass feedstocks. The modes of hydrogen delivery by pipelines are also presented in Fig.7.1.

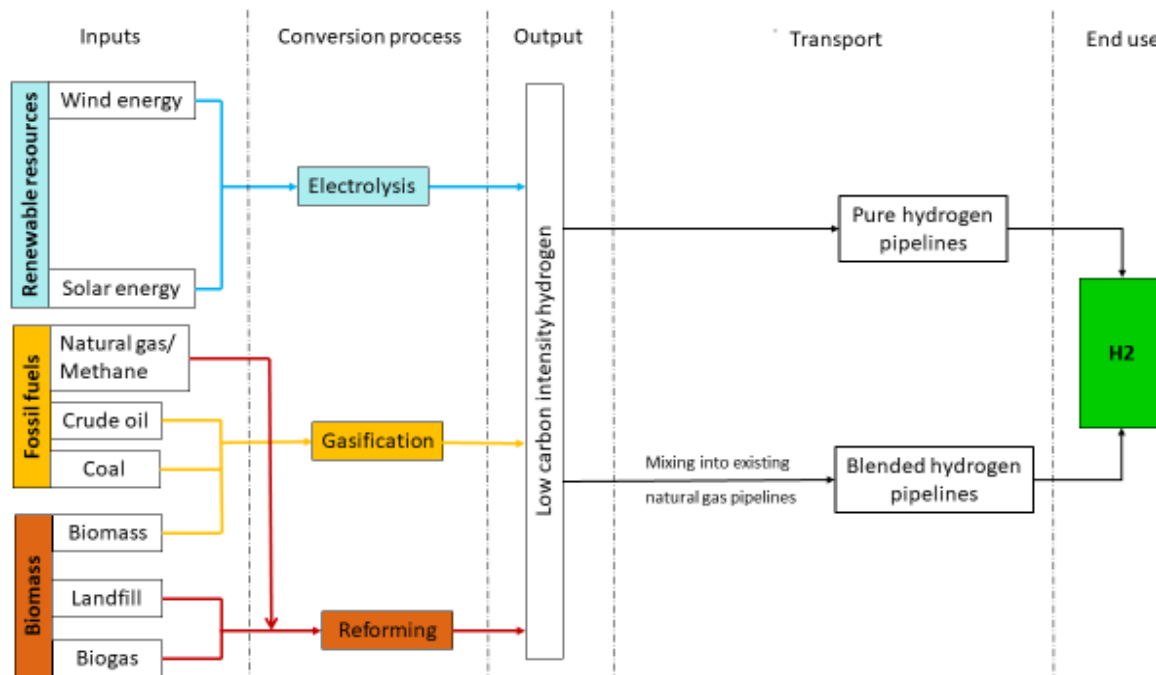


Figure 7. 1: Hydrogen production and delivery

It is essential to reduce the usage of fossil fuels for the continual transformation of the energy system to accommodate the reduction of greenhouse gas emissions. Thus, countrywide hydrogen supply chain analysis is receiving special attention from scientific researchers.

A dearth of transportation systems hinders the growth of the hydrogen industry. It is conceivable to transmit a mixture of hydrogen and natural gas (H2NG) using existing natural gas pipelines, due to the high cost of establishing specialized infrastructure (Cerniauskas et al., 2020; J. Liu et

al., 2021; Yoon et al., 2022). However, the safe transportation of hydrogen is a big challenge, and no models are available to assess the risk of hydrogen release in the production system and during its transportation.

Safety analysis of hydrogen production systems and transportation pipelines is essential since many countries are engaging in constructing pipeline networks for hydrogen to meet their energy needs. For example, in Europe, 1,100 to 1,770 kilometers of a hydrogen pipeline network has been established. By 2040, there is a plan to have 40,000 kilometers of hydrogen pipelines in Europe. Similarly, in the United States, 2,500 active hydrogen pipelines have been reported. Moreover, Canada has invested in several hundred kilometers of hydrogen pipelines. One of the prominent applications of this work is the fuel transmission pipelines between Canada and the United States (Okunlola et al., 2022). There are nearly 120,000 km long pipelines between the two nations to transport crude oil and natural gas. Also, there are 48-km hydrogen pipelines connected near Edmonton for Saskatchewan and a 30-km pipeline grid for hydrogen production in Ontario (M. A. Khan et al., 2021; Marin et al., 2010).

With the contemporary trend of the hydrogen industry today, there is a need to understand how to make an existing natural gas infrastructure safe for a hydrogen pipeline.

Transporting hydrogen in pipelines is much more energy intensive than natural gas transportation. Hence, there is a possibility of needing longer hydrogen pipelines (H. Wang et al., 2022). It is believed that in 2050 the quantity of hydrogen produced and transported will be ten times that of today. A huge pipeline network is required to transport all this energy. At the moment, this is not likely because liquefying hydrogen consumes 20% of the energy content of the hydrogen itself (Sharma & Ghoshal, 2015).

The two most viable ways for delivering hydrogen through natural gas pipelines are hydrogen mixing and reassigning natural gas pipelines for the transportation of pure hydrogen. Recent studies show significant barriers to reducing greenhouse gas emissions when natural gas is blended with hydrogen. These barriers are primarily due to technical blending constraints and challenges with the hydrogen separation process. However, combining hydrogen delivery pipelines can cut costs by at least 60% (Cerniauskas et al., 2020). Furthermore, it is necessary to assess the influence of a hydrogen component on the transport process in order to ensure the practicality, safety, and cost-effectiveness of using an existing natural gas pipeline to transfer blended H₂NG. Produced hydrogen will be transmitted to users as a gas (Yoo et al., 2021). In order to deliver hydrogen, this study will focus on blended hydrogen pipelines (Erdener et al., 2022).

It is crucial to conduct safety management and analysis of H₂NG transmission pipelines because of the gas's large volume and high pressure. Using pipelines to transport hydrogen poses potentially major safety issues. Blended hydrogen pipelines are easily corroded and cracked, and leakage accidents lead to equipment damage; if the leakages occur, explosions can occur; then, the failures can be catastrophic. To conduct safety management on the H₂NG pipelines and avoid various types of safety accidents, it is essential to understand the hydrogen degradation mechanism to improve the safety of H₂NG transmission.

Blended hydrogen pipeline systems

In practice, large-scale hydrogen production facilities might not be located close to a natural gas field; as a result, hydrogen might be injected at various pressurization facilities (J. Liu et al., 2021). The separation between pressure stations grows as the hydrogen fraction increases. Overpressure develops when the original pressure stations' configuration is kept.

Using intermediate gas injection, the inlet pressure of pressurization stations was decreased to the gas injection point. As shown in the figure below.

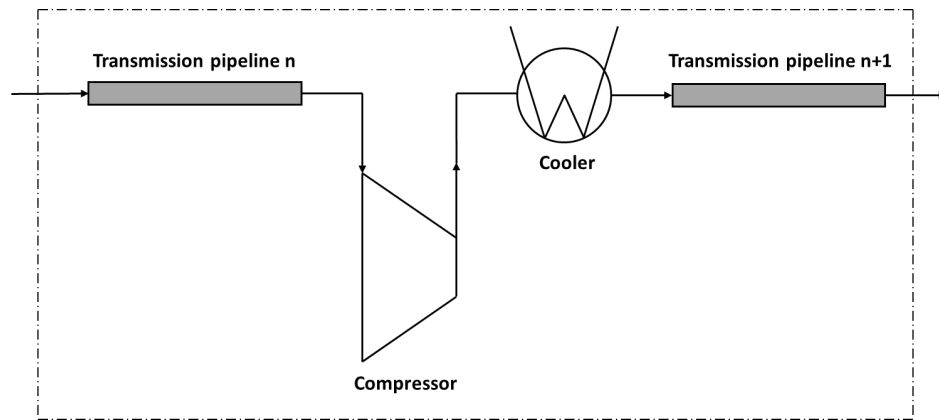


Figure 7. 2: The structure of equipment in a pressurization station

Gaseous hydrogen flows through pipes with a high pressure at the inlet to a lower pressure at the outlet (Y. Zhang et al., 2022). However, during the transmission process, the operating pressure in the natural gas pipeline decreases. To create a pressure differential, increasing the pressure lost through friction compressor stations is necessary. These friction compressor stations, namely pressurization stations, are often erected every 100 to 500 km along the length of H₂NG pipelines.

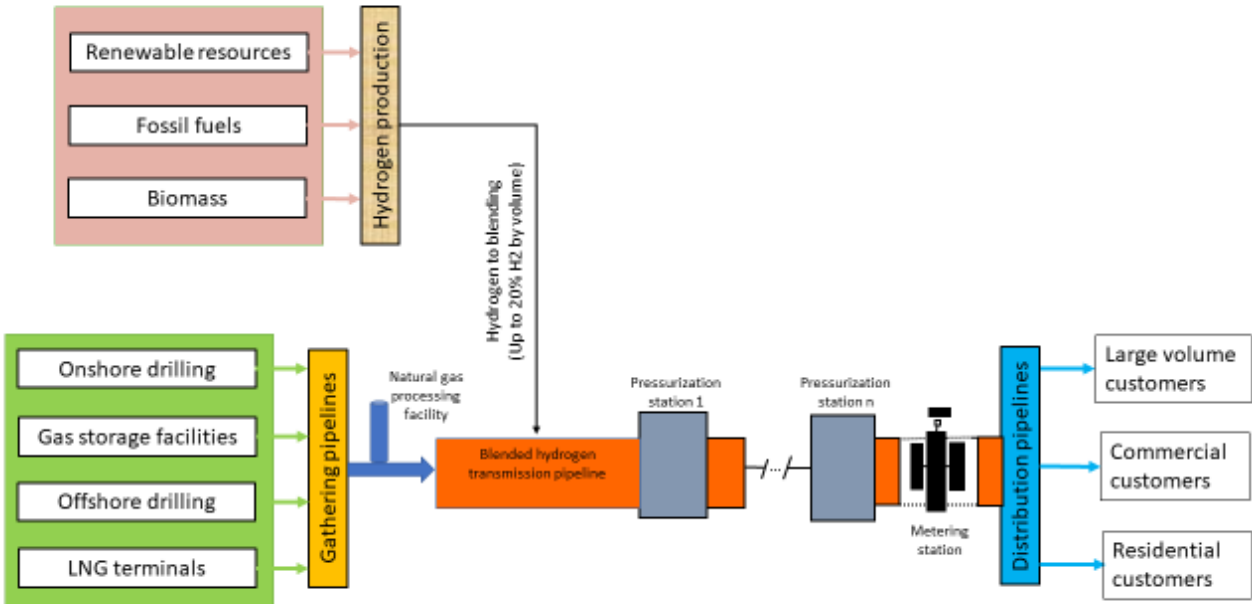


Figure 7. 3: Structure of a hydrogen pipeline transport system

It is predicted that using existing natural gas pipes for hydrogen transportation rather than building and installing new ones will result in capital cost savings of between 75 and 90 percent.

In addition, existing natural gas pipes are frequently built with identical specifications and regulations. Thus, when using these pipelines to transport hydrogen, to reuse current natural gas pipelines, only minor alterations are needed to reduce hydrogen embrittlement and qualify them for hydrogen transmission.

The lifetime of the pipelines will be shortened by transporting hydrogen through existing natural gas pipelines, due to an increase in material degradation. Thus, replacing compressor stations is necessary to convert existing natural gas pipelines for hydrogen transmission.

Hydrogen must be initially compressed for transport to be financially feasible because of its low volumetric mass density. Therefore, gas compressors are crucial components of hydrogen transportation, storage, and liquefaction.

The pipelines that will serve as the foundation of the potential hydrogen network include both recently constructed (40%) and moderately worn (60%) ones (Melaina et al., 2013; Yoon et al., 2022).

The considerable rise in gas outlet temperature during gas compression is an unintended side effect. The larger the compression ratio, the more pronounced this effect will be. The hot gaseous flow is pumped directly into blended hydrogen pipeline systems' compressor stations without gas cooling equipment. As a result, a high injection temperature can have an impact on a pipe section's pressure loss. We examined how a pipeline section's gas inlet temperature affected the pressure loss that resulted during pipeline transport, to delve deeper into the associated effects.

It is of considerable significance to carry out safety management and analysis of H2NG transmission pipelines because of the large volume and high pressure of gas (F. Yang et al., 2021). Therefore, using pipelines to transport hydrogen poses potentially major safety issues. Blended pipelines are easily corroded. Cracking, and leakage accidents lead to equipment damage (F. Yang et al., 2021); if leakages occur, explosions can occur, and then the failures can be catastrophic.

Hydrogen-associated degradation mechanisms

Hydrogen embrittlement (HE) and stress-corrosion cracking (SCC) are two main types of hydrogen damage to metallic materials such as steels (S. P. Lynch, 2007). Fig. 7.4 summarizes the mechanism behind hydrogen degradation.

Hydrogen embrittlement (HE)

HE is regarded as a hazardous hydrogen transit failure. Atomic hydrogen may enter and be absorbed on the surface of a pipeline by a very intricate mechanism. The procedure consists of four phases; the first is hydrogen enrichment of the surface layer. The second is hydrogen's

migration through metal, and the third is hydrogen's highly intricate interactions with other materials, which ultimately result in hydrogen damage.

Hydrogen-enhanced localized plasticity (HELP) and hydrogen-enhanced decohesion (HEDE) (Djukic et al., 2016, 2019; Polyanskiy et al., 2022) are two distinct HE mechanisms in steel and pipelines (Djukic et al., 2015).

While HEDE is thought to be hydrogen adsorbed at fracture tips and hydrogen separated at grain boundaries and particle-matrix interfaces, HELP is thought to entail hydrogen atmospheres around dislocations and impediments in the plastic zone before cracks form.

Hydrogen stress corrosion cracking (SCC)

SCC is common in metallic materials, such as steels and stainless steels. Although the wall thickness loss due to SCC is negligible, it causes a significant loss of mechanical strength of the materials.

It is hard to detect SCC in the early period. Cracks develop while the equipment is working. Thus, SCC is the main cause of the sudden collapse of structures, leading to catastrophic failures.

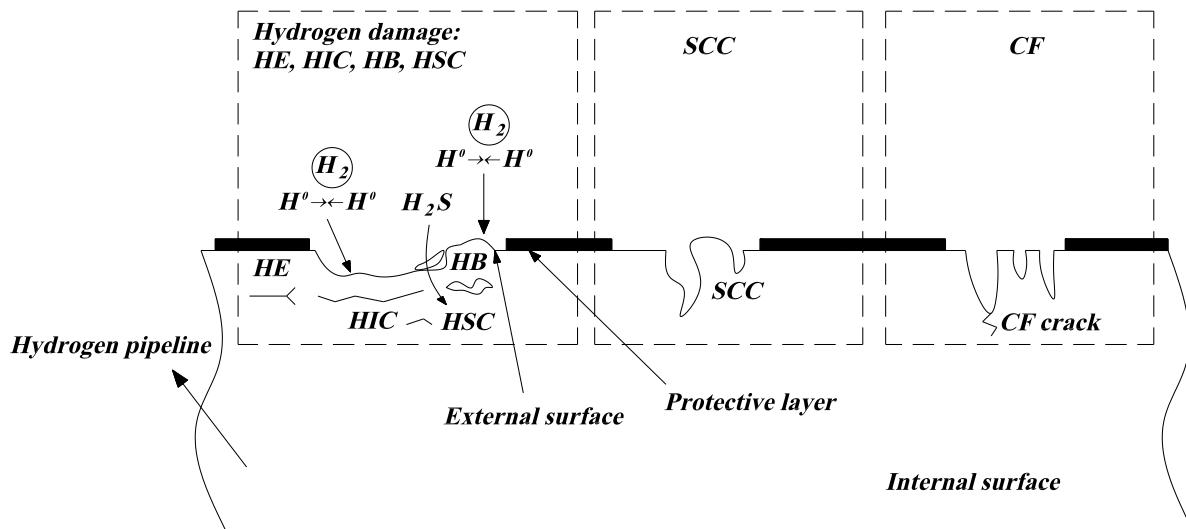


Figure 7. 4: Hydrogen-associated degradation mechanisms

Hydrogen blistering (HB)

Internal stress causes hydrogen blisters to form. The delamination of the pipeline's wall thickness caused by hydrogen diffused on the surface of a hydrogen pipeline causes bulgings on that surface while no external stress is being applied (Martin & Sofronis, 2022; Wasim & Djukic, 2022).

Hydrogen-induced cracking (HIC) or hydrogen-assisted cracking (HAC)

HIC and HB have a close relationship (X. Li et al., 2021). In pipelines, HIC or HAC, cold cracking, delayed cracking, or under-bead cracking can lead to leaks, ruptures, pipe replacement, and lost revenue. All factors such as the construction materials, welding technique, and climatic conditions can affect hydrogen cracking. However, their interdependencies are unknown.

Hydrogen stress cracking (HSC)

HSC is a type of hydrogen damage induced by galvanism, which incites cracking on the materials of hydrogen pipelines. HSC can result in the development of gas chambers and the breaking of pipeline steel material into various layers (Ge et al., 2020; Nguyen et al., 2021). The diffused hydrogen on the surface of hydrogen pipelines recombines into molecular hydrogen, resulting in delamination. The presence of internal hydrogen delamination of hydrogen pipelines causes HSC. Another type of HSC is sulfide stress cracking (SSC) (Ramirez et al., 2008). Diffused hydrogen accumulates on the external surface of steel pipelines, causing the initiation of brittle failures due to SSC.

Corrosion fatigue (CF)

Damage to pipes caused by the application of cyclic stresses is known as fatigue (Nanninga et al., 2010; Popov et al., 2018; Ronevich & San Marchi, 2017). Tiny cracks caused by fatigue can lead to leaks when they combine to form a larger crack. By combining this cyclic stress with the stress

concentrators present on the external surface of the pipeline surface in diverse corrosion conditions and under deposit damage, such as pits and fissures, CF fracture initiation is made more likely.

This work studies the safety aspects of hydrogen transportation using hydrogen mechanisms and operational parameters. Using an industrial case study, a dynamic model is proposed to study the variations in the susceptibility of hydrogen over time. The introduction section provides details of different mechanisms in hydrogen transportation; the methodology section outlines the steps of the proposed methodology; the results and discussion section provides the study results and examines them with an application. The conclusion section concludes the major findings of the study.

7.4 The proposed model

The steps involved in the development of the proposed model are shown in Fig.7.5, and a step-by-step explanation is provided below.

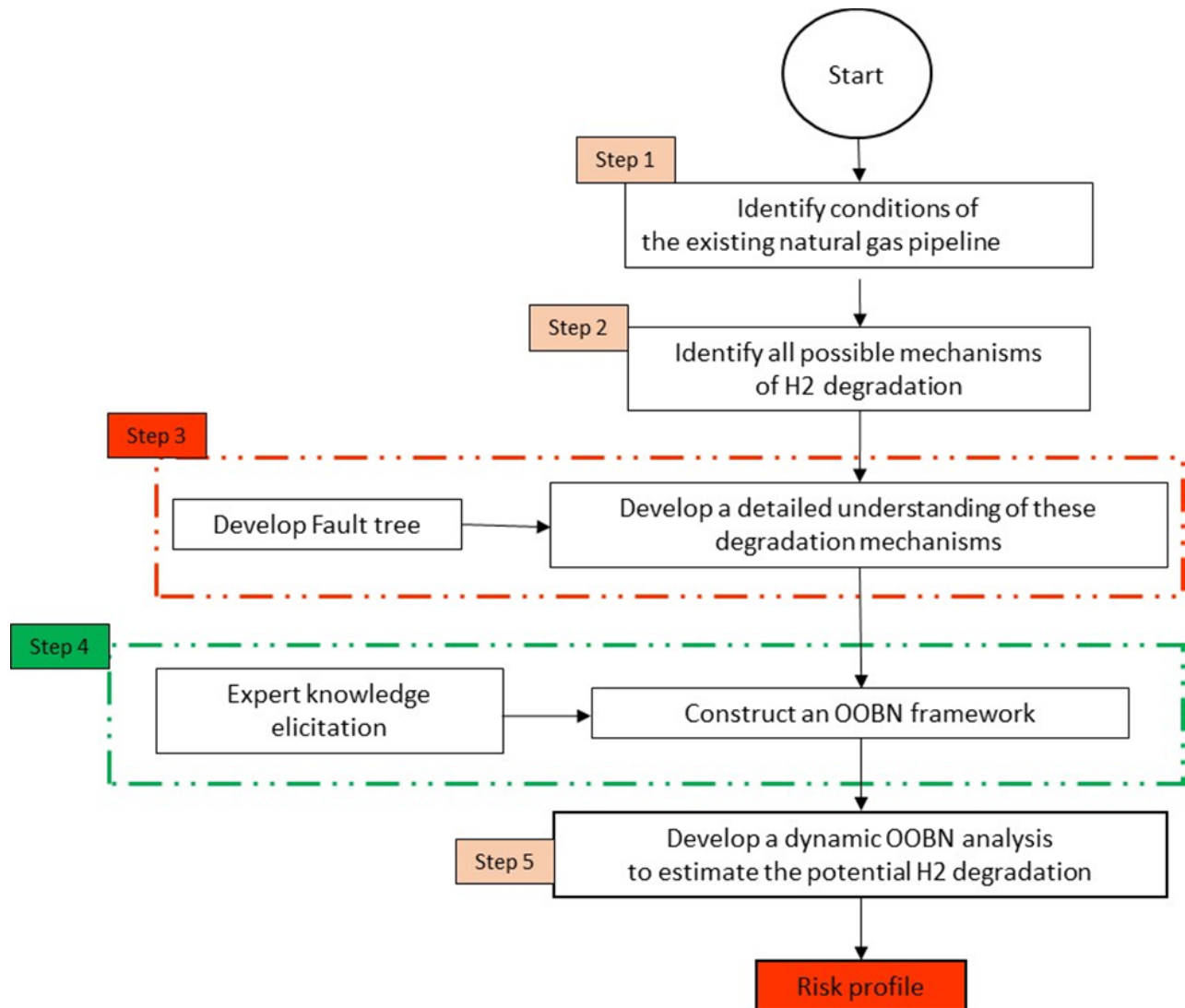


Figure 7. 5: Proposed methodology for hydrogen transportation mechanism

BNs have the property of being directed acyclic graphs (DAG). Each node in a BN model indicates a risk factor or uncertain variable, and arcs are used to represent the causal relationships among nodes (Sajid et al., 2017b). The BN model's conditional probability tables (CPTs) indicate the strength of relationships among nodes (Sajid, 2021).

The BN model is adaptive, which means as soon as new information, called a belief, becomes available, the state or belief of a node can be updated. This updating mechanism does not need any

structural changes and it does not affect the predictive abilities of the model. A random set of risk variables $U = \{Y_1, \dots, Y_n\}$, shown in Eq. (1), has conditional independence. It shows the joint probability distribution, indicated as $P(U)$, and is developed using the chain rule, as indicated in the literature (F. Khan et al., 2021; Sajid et al., 2018; Taleb-berrouane et al., 2018; Yazdi, Khan, Abbassi, et al., 2022).

$$P(U) = \prod_{i=1}^n P(Y_i | P_y(Y_i)) \quad (7.1)$$

where, $P_y(Y_i)$ shows a parent node and Y_i is a child node.

The probability of a child node (Y_i) is indicated in Eq. 7.2.

$$P(Y_i) = \sum_{U \setminus Y_i} P(U) \quad (7.2)$$

Eq (7.2) shows the addition of all variables except Y_i .

In BN models, Bayes' theorem is used to compute the posterior probability of an event based on new operational data of information. New information indicates the existence or non-existence of an event and is named as evidence (E), as indicated in Eq. (7.3).

$$P(U|E) = \frac{P(U, E)}{P(E)} = \frac{P(U, E)}{\sum_U P(U, E)} \quad (7.3)$$

BNs show the cause-effect relationships among nodes in a graphical manner, which helps to visualize links among the nodes (Sajid et al., 2017b, 2018). BN modeling technique has been applied in various fields of study. While a BN model can be used to study interdependencies of various factors, the resultant graphical model becomes too complex to understand and analyze. As indicated previously, the phenomena of hydrogen transportation are too complex; therefore, using

BN will provide a limited understanding of its mechanism, and BN model visualization will be a challenge (Borgheipour et al., 2021; Y. Chang et al., 2019; Mohammadfam & Zarei, 2015).

Furthermore, the construction and handling of large CPTs is another challenge. Therefore, traditional BN has limited scope and is inefficient for studying a large number of variables. An alternate approach is to divide or break down the network into small Bayesian subnetworks and connect them. This advanced-level approach is called an object-oriented Bayesian network (OOBN), and analyzing the OOBN over time is called Dynamic OOBN (DOOBN) (Sajid et al., 2020; Sarwar et al., 2018; Weidl et al., 2005). An example of it is shown in Fig. 7.6.

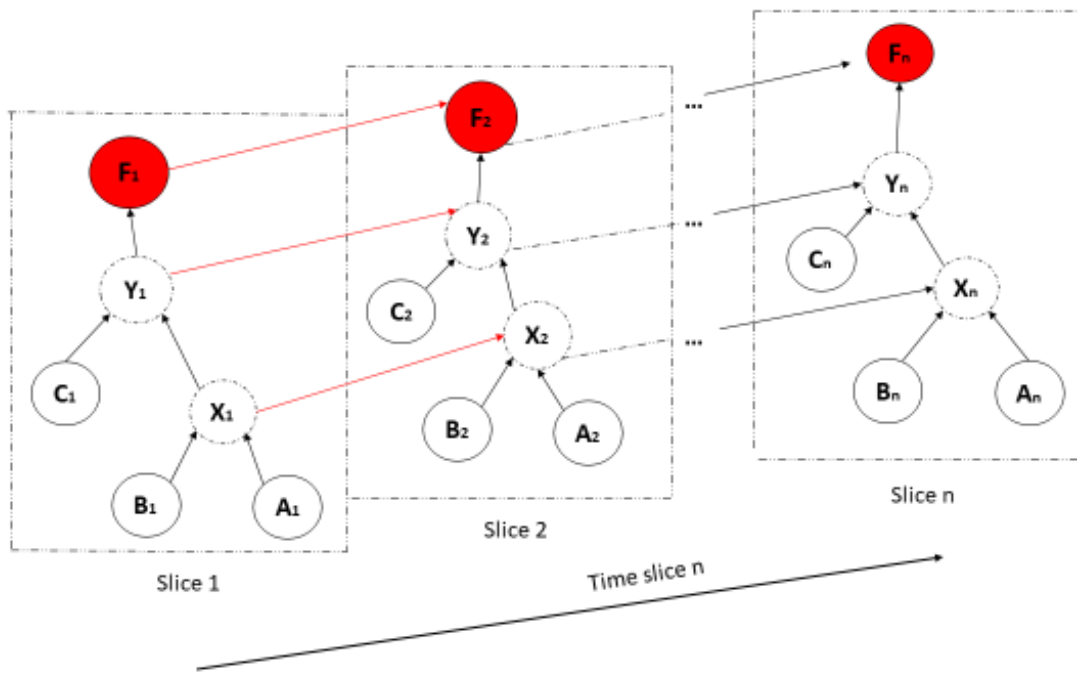


Figure 7. 6: A graphical representation of a DOOBN

A dynamic OOBN model is developed for an H2NG pipeline of an existing natural gas pipeline. The natural gas pipeline is made of low-strength carbon steel (X52 or lower) pipe and has been designed to work for 50 years. The pipeline is 914.4 mm in diameter and 0.0178 mm in fracture

toughness. The hydrogen pipeline has a total length of 1500 km, and one compressor station is placed every 500 km. The transmission pipeline operates at pressures from 70 to 100 bar. The suction pressure of the inlet compressor (bar) is 16 bar, and the discharge pressure of the inlet compressor (bar) is 70 bar. The operating pressures of gaseous hydrogen flow are from 70 to 100 bar. The gas is liquefied to -253°C , and the operating temperature of the H₂NG pipeline is from -253°C to -162°C .

Step 1: Identify conditions of the existing natural gas pipeline

Existing natural gas pipes are frequently built with identical specifications and regulations. When using these pipelines to transport hydrogen, only minor alterations are needed to reduce hydrogen embrittlement and qualify them for hydrogen transmission. In this step, a detailed literature review was conducted to identify the conditions of existing natural gas pipelines and determine how those could be adopted for hydrogen transportation. These involve understanding pigging, or cleaning and drying (moving a pipeline scraper through the pipelines while applying compressed dry air); displacement purging (to remove gaseous and other contaminants using inert nitrogen gas); monitoring and inspection to find and fix defects, cracks, or leaks in pipelines; and repair of outdated equipment, such as worn-out valves.

Step 2: Identifying all possible mechanisms of H₂ degradation

In this step, all possible mechanisms of hydrogen degradation were identified. Also included are how hydrogen permeates to metal surfaces, what mechanism it follows, and what control strategies are present.

Step 3: Understanding degradation mechanisms using fault tree

In this step, the risk factors identified in the last two steps were connected using available theoretical knowledge, and a fault tree was constructed. The fault tree consists of top events (risk of hydrogen release), intermediate events (conceptual and theoretical risk factors in hydrogen transportation mechanisms), and basic events (risk factors that cannot be further divided (Borghepour et al., 2021; Khakzad et al., 2011)). Fig.7 presents the constructed fault tree with its basic events shown in table 7.1.

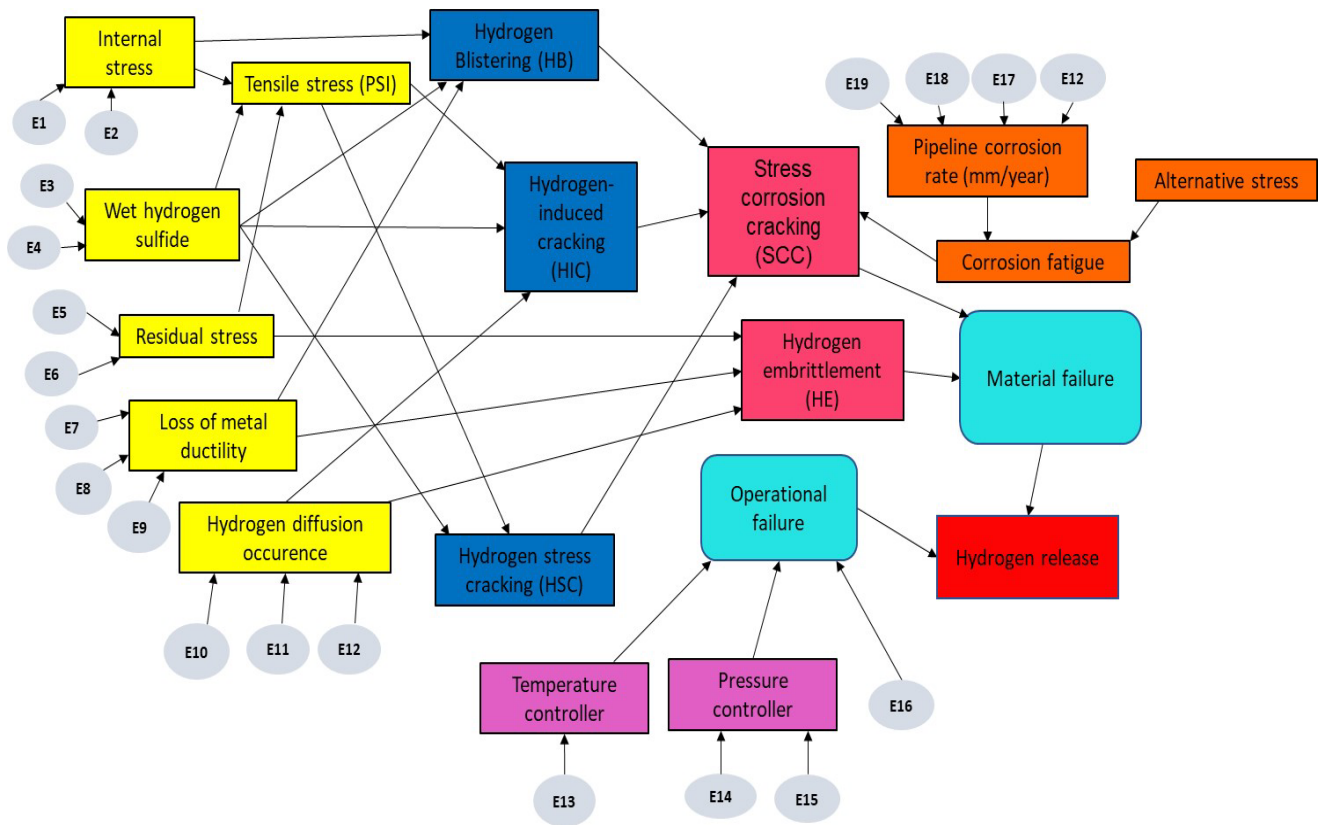


Figure 7. 7: Fault tree of hydrogen degradation mechanism

Table 7. 1: The basic events for hydrogen release

Evidence	Names
E1	Pipe wall thickness (mm)
E2	Operating pressure (bar)
E3	Moisture contents
E4	pH level
E5	Mechanical load (N)
E6	Particle mass loss (%)
E7	Fracture toughness (kJ/m ²)
E8	Pipe defects
E9	Weld defect
E10	Hydrogen permeation
E11	Operating temperature (C)
E12	Cathodic protection
E13	Cooling operation installed
E14	Safety valve installed
E15	Compressors
E16	Maintenance frequency
E17	Presence of oxygen
E18	H ₂ S corrosion
E19	Flow velocity (m/s)

Step 4: Constructing OOBN

The output of step 4 was used to develop the OOBN framework for hydrogen release. The details of the steps involved in developing OOBN are available in previous work. Since this work is a foundation for studying the hydrogen release risk, there is no information available on probabilities

and interconnectivity of risk factors in the OOBN model. In this scenario, the structure of OOBN was developed using output from step 4, and an expert elicitation technique was used to develop probabilistic data.

Step 5: Dynamic OOBN analysis and sensitivity analysis

In this step, the static OOBN model developed in step 4 was converted into dynamic OOBN using the time domain. AngenaRisk software was used to perform analysis on dynamic OOBN. The outcome of this step was the risk of potential hydrogen release. The risk profile consisted of the time and probability of hydrogen release, which was analyzed for ten years, starting in 2023. A sensitivity analysis was performed to identify critical parameters for the safety of blended hydrogen in the natural gas pipeline. Using AngenaRisk software, the influence of risk parameters on hydrogen release was assessed, and results were discussed.

7.5 Results and Discussion

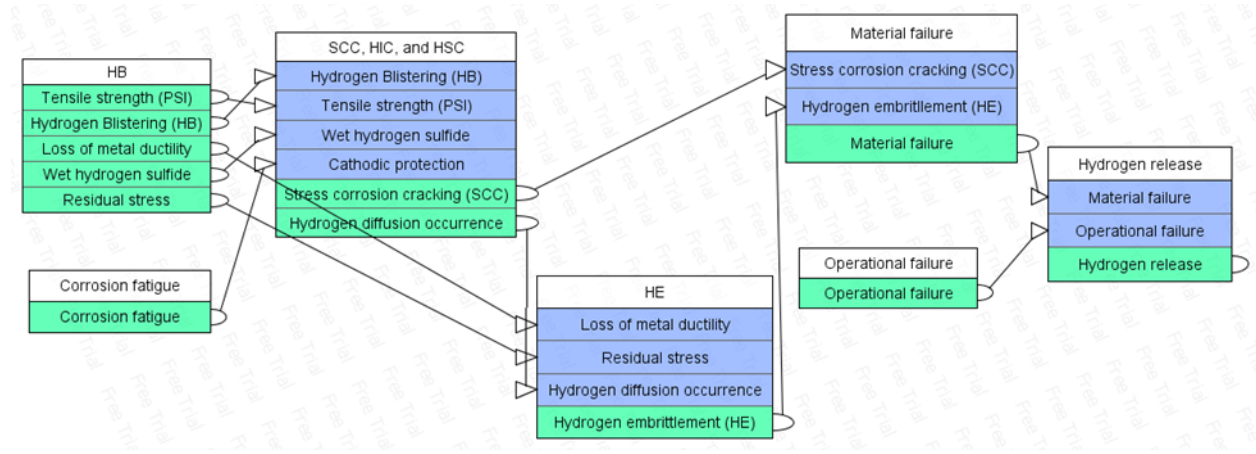


Figure 7. 8: Hydrogen release OOBN model

Fig.7.8 illustrates the OOBN for hydrogen release, which consists of Bayesian sub-networks of hydrogen blistering (HB) modeling, hydrogen corrosion cracking (SCC) modeling, hydrogen

embrittlement (HE) modeling, corrosion fatigue (CF) modeling, material failure modeling, operational failure modeling, and hydrogen release modeling for a blended hydrogen pipeline.

OoBN represents Bayesian sub-networks for hydrogen damage mechanisms and incorporates instance nodes. OoBN helps to avoid the repetitive tasks of creating identical structures and cumbersome probability tables. The relationships and interdependencies of each risk instance node are implanted in the model as objects in Fig.7.8. In this figure, internal nodes are hidden, or 'encapsulated', and the only 'visible' nodes are input and output nodes. Encapsulation of many factors and visibility of a few factors are characteristics of an OoBN. Based on the OoBN, probabilities, updating is performed at regular time intervals to predict the hydrogen release probability. The details of the nodes of the OoBN model are presented in the appendix.

Bayesian subnetwork models of OoBN are presented in Figs. 7.9 to 7.15 for hydrogen release. These figures indicate key risk factors contributing to the failure of the hydrogen pipeline and the subsequent release of hydrogen. It is pertinent to mention here that the results and analysis of this study demonstrate the operationalization of the methodology and hence do not represent any actual situations. These sub-models details are illustrated in the appendix.

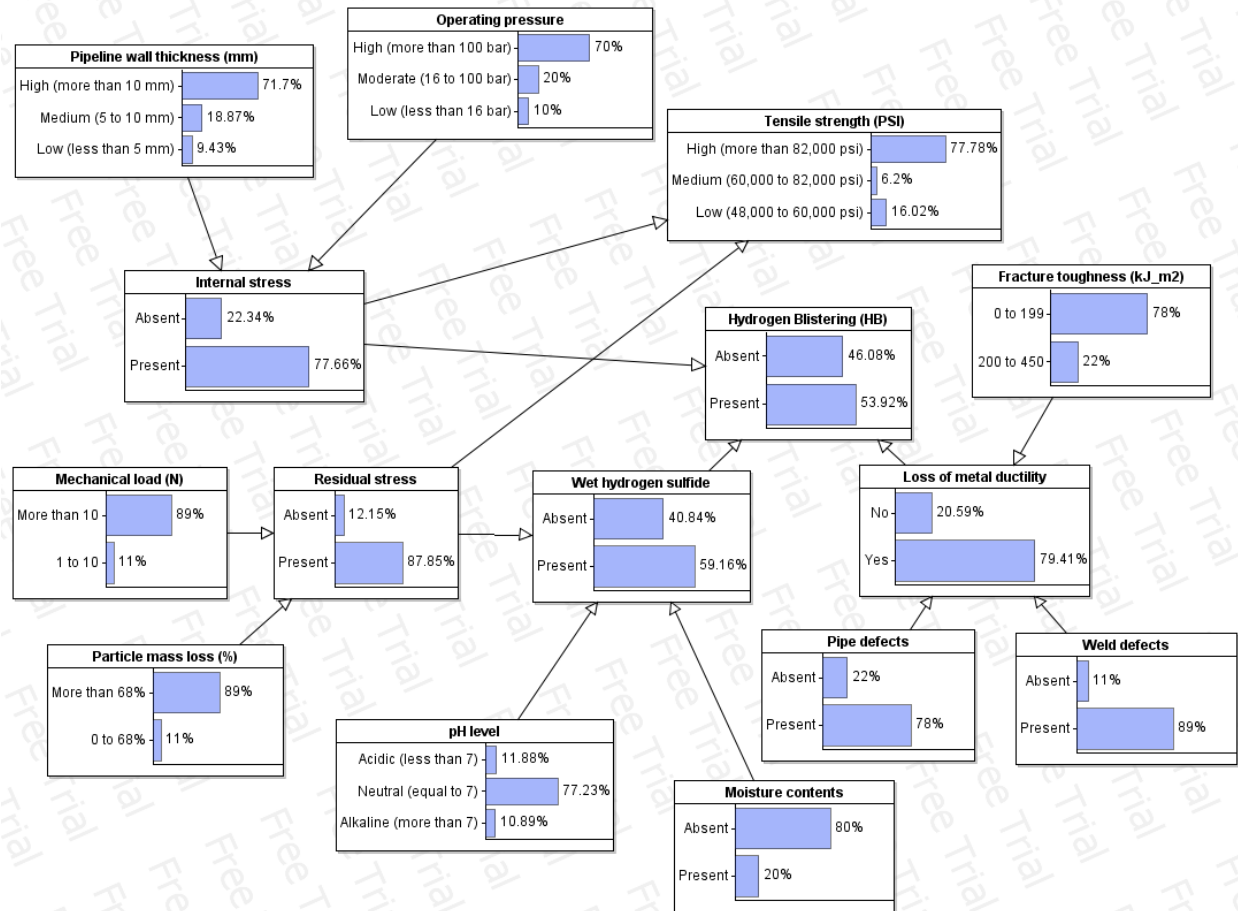


Figure 7. 9: Hydrogen blistering (HB) submodel

Fig.7.9 represents the Bayesian sub-network for HB and shows the interdependencies of various factors under the category of HB. It shows the interactions among material characteristics and the component of the hydrogen pipeline's influence on the HB. The HB model provides three key intermediate nodes: internal stress, wet hydrogen, and loss of metal ductility. An analysis of the HB model reveals that fracture toughness, pipe defects, and weld defects influence the loss of metal ductility. The pipe wall thickness and operating pressure influence the internal stress risk factor. Moisture contents and pH level influence the level of wet hydrogen sulfide, while the residual stress of the hydrogen pipeline depends upon mechanical load and particle mass loss. The

model in Fig.7.9 also indicates a connection between the residual stress and internal stress of hydrogen pipelines.

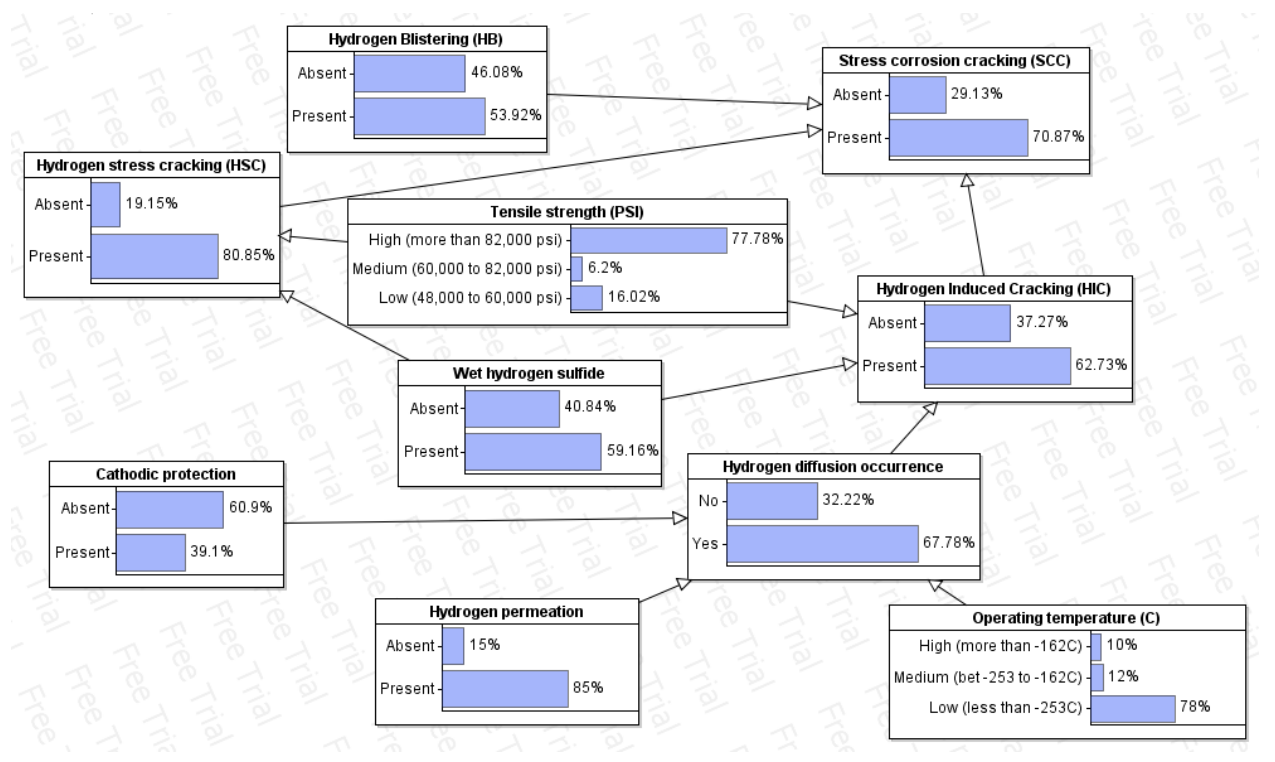


Figure 7. 10: Hydrogen corrosion cracking (SCC) submodel

Fig.7.10 indicates the Bayesian sub-network for SCC. It shows the interactions of HB, HIC, and HSC that lead to SCC. The mechanism of HB has been described earlier. Results show that the HIC factor is affected by tensile strength, wet hydrogen sulfide, and hydrogen diffusion occurrence. In the presence of cathodic protection, hydrogen permeation, and the operating temperature, hydrogen diffuses on the surface of hydrogen pipelines. The simultaneous presence of wet hydrogen sulfide and tensile strength not only leads to HIC but also causes HSC. Therefore, wet hydrogen sulfide and tensile strength predominantly influence SCC. Tensile stresses and numerous corrosion processes work together to cause SCC on sensitive materials, especially in high-strength steels. SCC takes years from crack initiation to failure, leading to sudden brittleness

on most metallic materials. Results of dynamic OOBN show that the cracks propagate very quickly. SCC is a fracture due to the combined effects of tensile stress and a corrosive environment. Therefore, SCC is more likely to occur in hard-welded zones and high-strength metallic materials. The weld will be a weak area for this cracking, as it is for SCC, because the majority of this failure mode's failures occur along the weld line. The interaction of stress and strain is linked to the mode of cracking. SCC first appears on the surface of the metals from small holes, weld defects, and pipe defects. SCC usually initiates from the bottom of pitting holes; then, the cracks propagate and develop at a stable rate, ending the propagation of cracks and broken pieces of pipe and other debris. Due to interactions between various hydrogen components in hydrogen pipelines, SCC is frequently vulnerable to HB, HIC, HSC, and corrosion fatigue. This result is consistent with the literature (Wasim & Djukic, 2022; H. Zhang & Tian, 2022). HIC can disperse across the metal of the weld or the heat-affected zone and often takes place at stress concentrations, such as the weld's root. Three separate events, hydrogen in the weld, a broken susceptible microstructure, and tensile stress acting on the weld, must co-occur for HIC to occur. Hydrogen cracking will not occur if one or more of these conditions are absent. Hydrogen causes fracture and fatigue in metals.

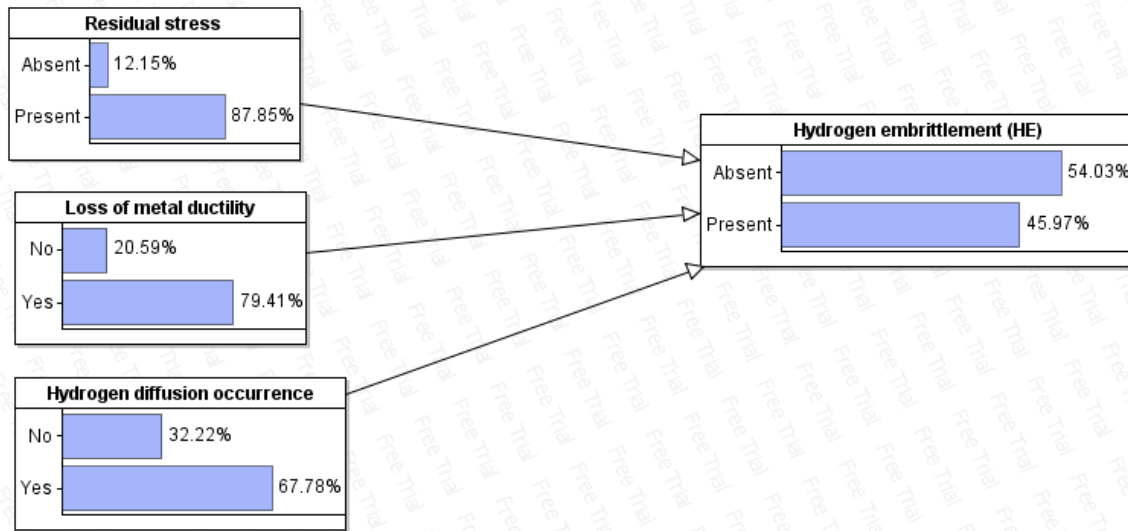


Figure 7. 11: Hydrogen embrittlement (HE) submodel

Fig.7.11 is a Bayesian sub-network for HE. It encapsulates the impact of residual stress, loss of metal ductility, and hydrogen diffusion occurrence on the hydrogen transportation pipeline. Metals are used to make pipes more brittle when hydrogen atoms are introduced to the substance. The ductility of metals is substantially decreased in hydrogen gas. Additionally, hydrogen significantly reduces the metal's ability to fracture and speeds up the formation of fatigue damage, which causes HE. The transitory hydrogen diffusion and accumulation around the crack tips are influenced by multiple factors, namely composition, defect density, microstructure, impurity concentration under precisely defined parameters, hydrogen charging condition, pressure, temperature, and stress level (local hydrogen concentration). It is possible to define HE as the degradation of the mechanical properties of most metallic materials. This distinguishes it from other hydrogen damage mechanisms. Results show that the hydrogen damage mechanism HE involves the degradation of mechanical properties of materials, such as loss of ductility and tensile strength, resulting in a reduction in the material's toughness and fracture resistance. As a consequence, due to the presence of this dissolved hydrogen and other hydrogen damages, subcritical cracking is produced.

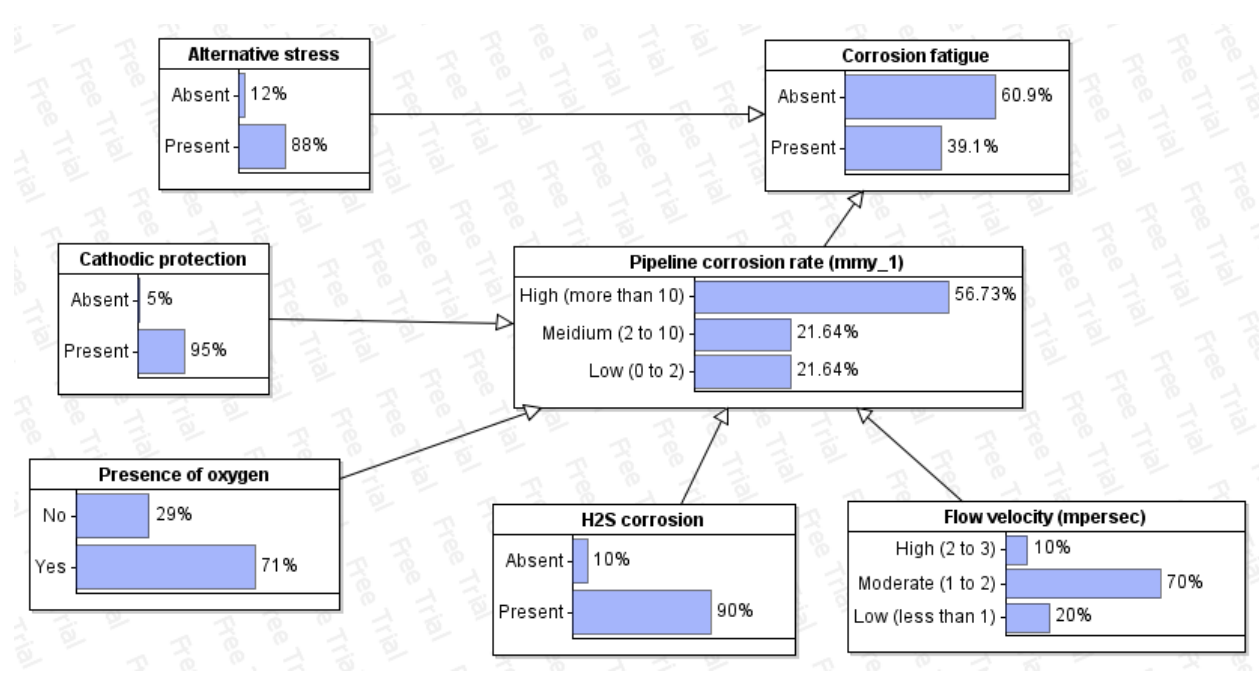


Figure 7. 12: Corrosion fatigue (CF) submodel

The Bayesian sub-network in Fig.7.12 shows that the CF is affected by alternative stress and the pipeline corrosion rate. The presence of oxygen, H2S corrosion, flow velocity, and cathodic protection increases the corrosion rate in the hydrogen pipeline.

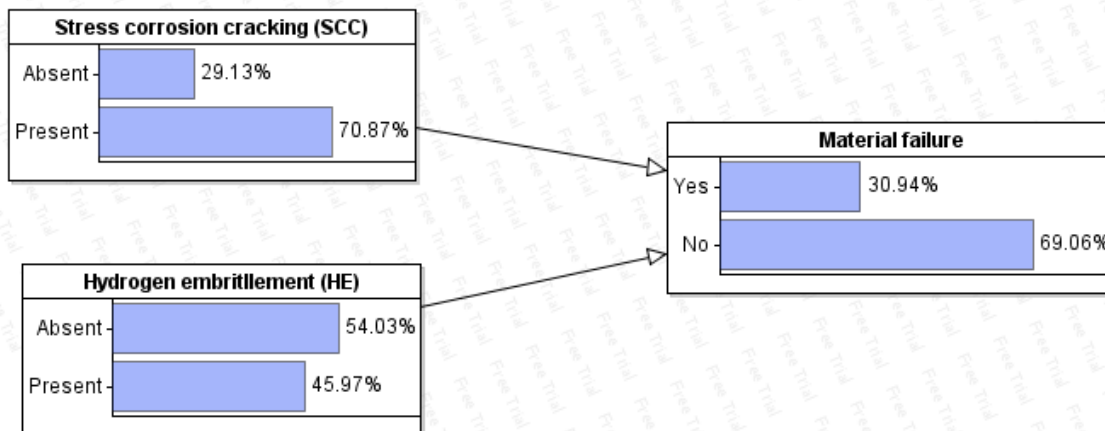


Figure 7. 13: Material failure submodel

Fig.7.13 is a Bayesian sub-network of material failure. It shows that the material failure is due to stress corrosion cracking (SCC) and hydrogen embrittlement (HE).

Fig.7.14 shows the interdependencies of various factors under the category of operational failure. It shows the interactions among the temperature and pressure controller factors, their propagative influence on the failure of the operating hydrogen pipeline, and the effectiveness and frequency of maintenance. As is shown in Fig.14, the collective presence of the compressors and safety valve installation influences the pressure controller. The temperature controller failure is associated with the cooling operation having been installed directly.

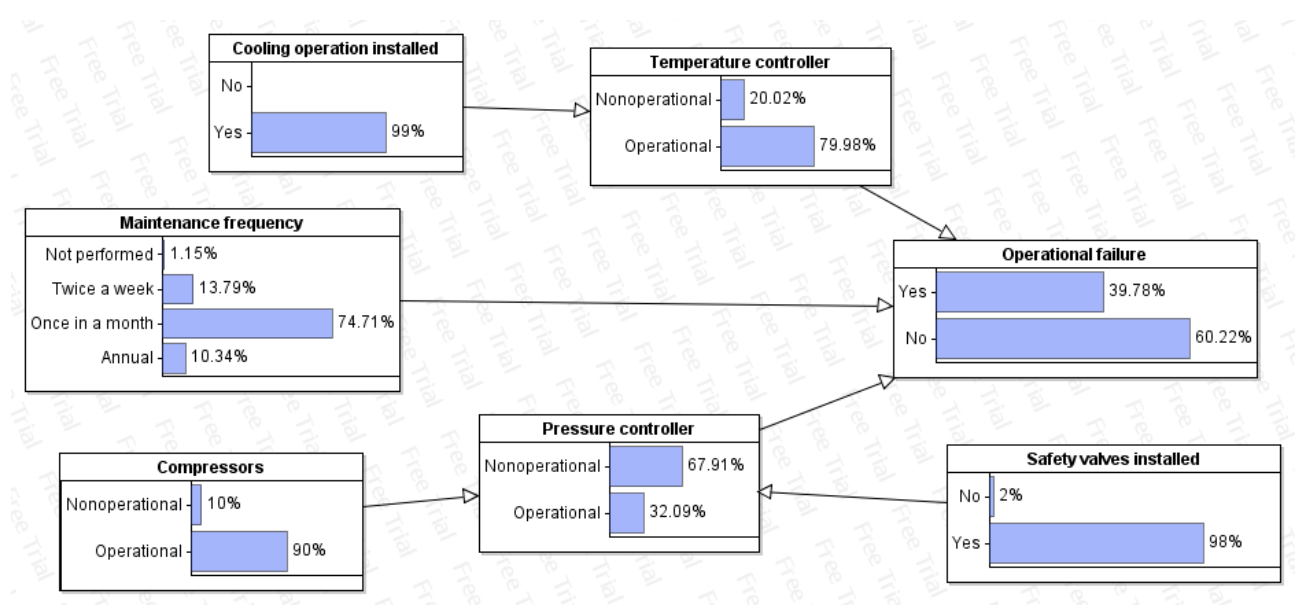


Figure 7. 14: Operational failure submodel

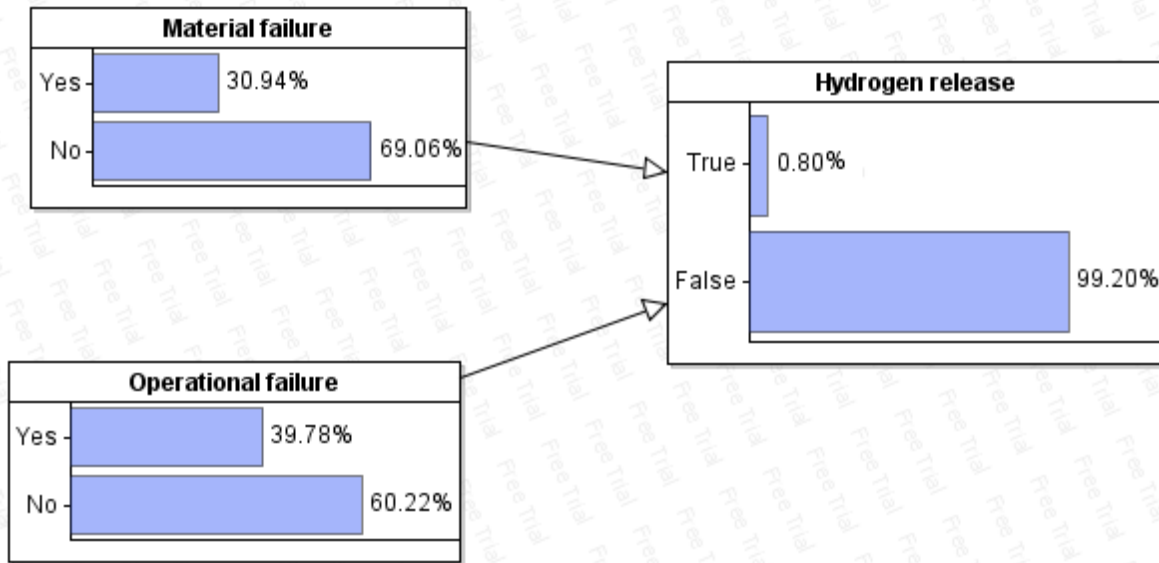


Figure 7. 15: Hydrogen release submodel

Fig.7.15 shows the combined effect of material failure and operational failure on hydrogen release. The Bayesian sub-network in Fig.15 shows that hydrogen release is due to the failure of the construction material in the hydrogen transportation pipeline and the operational failure to transport hydrogen. A DOOBN, shown in Fig.7.15, indicates the variations of these risk factors over time and indicates how the probability of hydrogen release changes over time.

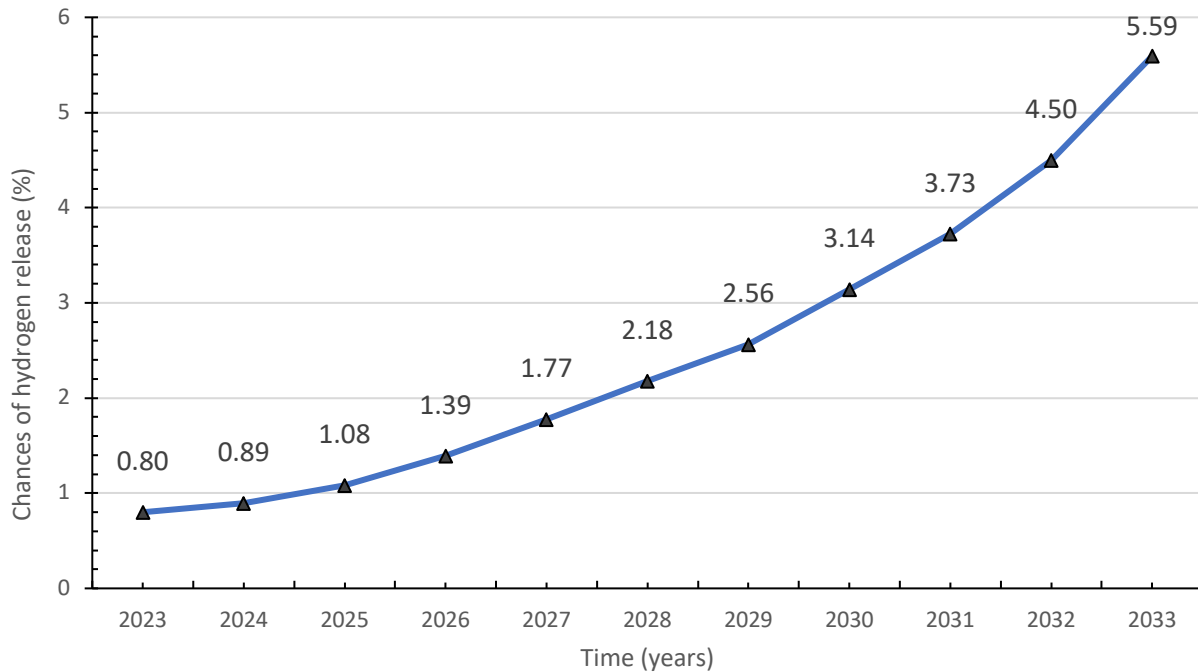


Figure 7.16: Chances of hydrogen release over time

Fig.7.16 shows the probability of a hydrogen leak over ten years starting in 2023. The time-dependent probability demonstrates the usability of this work. Results show that the change in the probability of hydrogen release over time is a non-linear trend. There is a slow yet significant degradation in the initial years, and in the later years, the leak probability grows exponentially. The reason for this trend is the higher degradation in later years as the system ages and the operational conditions remain the same. This indicates a sharp increase in hydrogen leak probability with time. The majority of these pipelines are made of carbon steel or stainless steel, having a diameter ranging from 4 to 48 inches. This study shows that high-strength steels in natural gas transmission are prone to hydrogen embrittlement, while low-strength steel is recommended for hydrogen pipelines. A study has shown that the use of high-strength steel instead of low-strength steel can save 10% to 40% on the cost (Briottet et al., 2012). However, high-strength steels in hydrogen transportation have increased chances of degradation than low-strength steel

due to hydrogen attack and HE. Results of sensitivity analysis indicate three main contributions which are critical to the safety of the blended hydrogen pipeline. Those are corrosion, material failure, and operational failure. Fig. 7.17 shows the top three parameters for each domain that can affect the safety of the blended hydrogen pipeline with the existing natural gas pipeline.

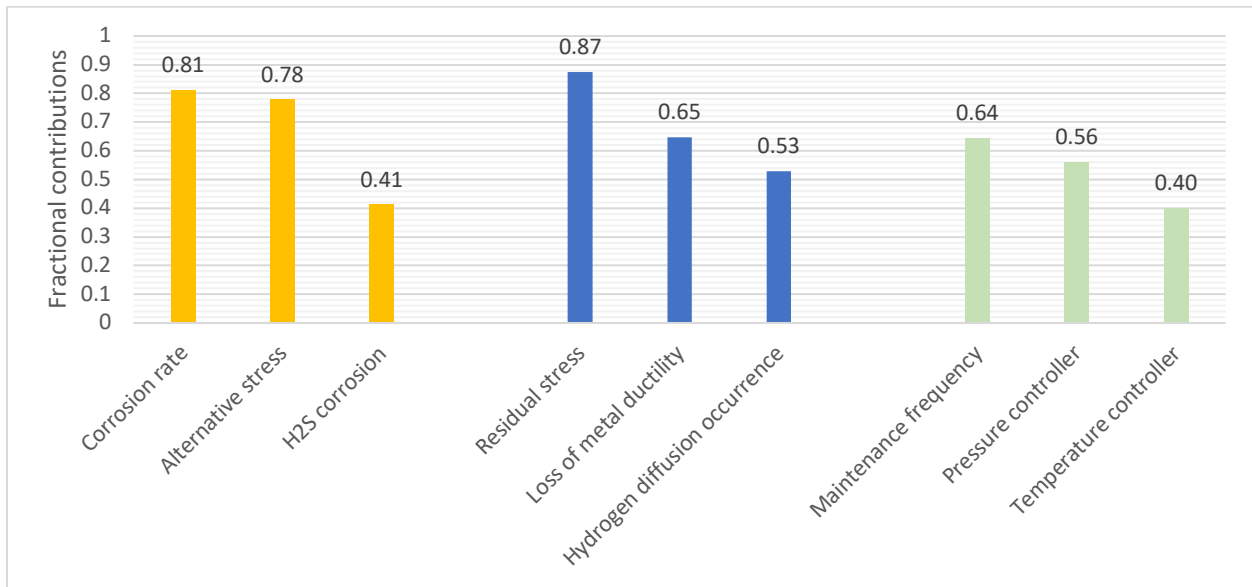


Figure 7.17: Results of sensitivity analysis

The yellow colour indicates corrosion mechanism, blue colour indicates risk factors in material failures, and green colour indicates risk factors in operational failure. Results are shown for the top three contributors.

Results of sensitivity analysis indicate that the corrosion rate is the most critical factor in the safety of the pipeline being corroded and has an 81% contribution, followed by alternative stress (78%) and H2S corrosion (41%). In the category of material failure, residual stress (87%) is the most significant contributor to the safety of the blended hydrogen pipeline, followed by loss of metal ductility (65%) and hydrogen diffusion occurrence (53%). Results of sensitivity analysis show that

maintenance frequency has the highest contribution (64%) in ensuring safe hydrogen operations, followed by the pressure controller (56%) and temperature controller (40%).

7.6 Conclusions

This study provides a methodological framework for assessing the likelihood of hydrogen release in transportation pipelines. A dynamic OOBN is developed to study the safety of hydrogen transportation pipelines over time. The results indicate that, unlike natural gas pipelines, the safe operation of hydrogen pipelines is more challenging. The use of the hydrogen mechanism in the model building process indicates that due to the small size of hydrogen molecules, there are safety issues associated with hydrogen transportation, and they require a careful leak management system. Results indicate that the probability of hydrogen release is sluggish in the first three years of operation, and then there is a sudden increase in its release. Such a trend is associated with the degradation of pipelines over time. The study also concludes that low-strength steel pipelines are less prone to embrittlement and hydrogen attack than high-strength steel. Therefore, the study recommends using low-strength steel for hydrogen transportation. Further research is recommended to assess how predictive maintenance can help to increase the safety of hydrogen pipelines.

7.7 Appendix

Variables	States
Particle mass loss (%)	Zero to 68
	More than 68
Mechanical load (N)	1 to 10
	More than 10
pH level	Acidic (pH < 7)
	Neutral (pH = 7)
	Alkaline pH > 7
Moisture contents	Present
	Absent
Operating pressure (OP), Bar	High (100 < OP)
	Moderate (16 < OP < 100)
	Low (OP < 16)
Pipe wall thickness (PW), mm	High (PW > 10)
	Medium (5 < PW < 10)
	Low (PW < 5)
Internal stress	Present
	Absent
Flow velocity (FV), m/s	High (2 < FV < 3)
	Moderate (1 < FV < 2)
	Low (1 < FV)
H ₂ S corrosion	Present
	Absent
Pipeline corrosion rate (CR), mm/year	High (CR > 10)
	Medium (2 < CR < 10)
	Low (0 < CR < 2)
Present of oxygen	Yes
	No
Alternative stress	Present

	Absent
Corrosion fatigue	Present
	Absent
Tensile strength (TS), PSI	High (TS>82,000)
	Medium (60,000<TS<82,000)
	Low (48,000<TS<60,000)
Cathodic protection	Present
	Absent
Hydrogen Blistering (HB)	Present
	Absent
Wet hydrogen sulfide	Present
	Absent
Residual stress	Present
	Absent
Fracture toughness (FT), kJ/m ²	200 to 450
	0 to 200
Pipe defect	Present
	Absent
Weld defect	Present
	Absent
Hydrogen permeation	Present
	Absent
Operating temperature (OT), C	High (OT > -162)
	Medium (-253 C<OT< -162)
	Low (OT< -253)
Flow control installed	Yes
	No
Safety valve installed	Yes
	No
Compressors	Operational

	Non-operational
Maintenance frequency	Not performed
	Twice a week
	One a month
	Annual
Cooling operation installed	Yes
	No
Pressure controller	Operational
	Non-operational
Loss of metal ductility	Yes
	No
Hydrogen diffusion occurrence	Yes
	No
Hydrogen-induced cracking (HIC)	Present
	Absent
Hydrogen stress cracking (HSC)	Present
	Absent
Stress corrosion cracking (SCC)	Present
	Absent
Hydrogen embrittlement (HE)	Present
	Absent

CHAPTER 8

8.1 Summary

The proposed methodology of this study is briefly provided as the following steps:

- (i) The data are collected by inspection, measurement, and fluid analysis, including pressure, operating temperature, material, composition, and external factors for subsea pipelines. These factors are determined and supervised according to their mechanical and operational characteristics with the corroding asset data collection;
- (ii) The collected information related to operational parameters is categorized, and processed into probabilistic methods for predicting the dependencies and relationships;
- (iii) The failure characteristics are defined based on discretized wall thickness, regression model using actual data to generate results, then compare the results with a probabilistic model to predict the UDC defect propagation to a system failure;
- (iv) The corrosion parameters' interdependencies and the mechanism behind UDC are represented by their probability distributions. A quantitative dynamic probabilistic framework is obtained to predict the system reliability considering the interrelationship among failure of the asset due to the influence of defect depth corroded from UDC;
- (v) Strikingly, the probability of failure of pipelines due to UDC is validated by a stochastic approach using industrial data, which helps to test the accuracy and robustness of the risk-based probabilistic model in predicting failure of pipeline system due to UDC;

(vi) Based on understanding of existing natural gas pipelines, a simple logical diagram is developed to identify all possible mechanisms of hydrogen degradation of blended hydrogen pipelines;

(vii) A dynamic probabilistic model to study the mechanisms and physics of failure of the hydrogen-blended pipeline is proposed to identify, assess, and evaluate failure scenarios of H₂ transportation through oil and gas pipelines.

The Bayesian Networks (BNs) technique is a probabilistic inference tool for prediction and reasoning under uncertainty. BNs are widely used for safety and risk analysis because they incorporate complicated causal relationships and present them graphically. A BN structure can be defined subjectively (knowledge-driven) by relying on the expert's experience with variables and their correlation. The conditional dependencies among the parent and child nodes are described by the conditional probability table (CPT).

BN is a powerful and flexible probabilistic technique that can graphically represent the causal interrelations between variables and quantitatively represent this intricate relationship.

The intrinsic complexity of pipelines and outside roots are just two of the countless unidentified contributing elements to the complicated phenomena of asset failure. The resulting network then presents a demanding visualization problem. An alternate approach is to divide or break down the network into small Bayesian subnetworks and connect them. Specifically, to deal with cumbersome probability tables of traditional Bayesian networks, an object-oriented Bayesian network (OOBN) is developed to oversee the offshore pipeline's integrity and safety. In OOBN, probabilities, updating is performed at regular time intervals to predict the failure probability. Analyzing the OOBN over time is called Dynamic OOBN (DOOBN).

Suffering from UDC, the deterioration of pipelines will increase with exposure time resulting in strength loss and system failure. At this time, the safety of the system is dependent on the management of its remaining strength and useful life. To manage UDC with multiple induced assets, Monte Carlo simulation (MCS) and sensitivity analysis are proposed. The following safety analyses for exploring the above important aspects are briefly described.

Monte Carlo simulation informed the Bayesian network

The Monte Carlo simulation (MCS) is used to assess baseline UDC under conditions driven by operational parameters. The simulation results are used in structural learning to decide the influence of various parameters on the UDC rate. The structural learning portion of the model relates the operational parameters to the UDC rate. Additional parameters such as mitigation and those not included in the empirical models are added based on expert judgment to achieve a complete model. In this study, the MCS is used to characterize the stochastic properties of asset failures.

Sensitivity analysis

Sensitivity analysis is used to understand key input parameters that influence the model output.

Results of sensitivity analysis indicate the main contributions which are critical to the safety of the pipeline. It also shows the top parameters for each domain that can affect the safety of the pipeline.

The results are valuable for oil and gas industries to develop mitigation and maintenance plans to avoid asset losses due to UDC.

8.2 Conclusions

The main highlights and conclusions obtained from the working thesis are summarized as the following:

1. The results provide a diagnostic of the internal corrosion mode and UDC, particularly based on monitoring normal and abnormal parameters.
2. The estimated likelihoods would help prioritize action to prevent and control UDC before the failure stage.
3. Bayesian Network can provide theoretical knowledge which can be compared to industrial data. It is helpful when one lacks industrial data for the study.
4. A dynamic probabilistic model to study the mechanisms and physics of failure of the hydrogen-blended pipeline is proposed to identify, assess, and evaluate failure scenarios of H₂ transportation through oil and gas pipelines.

8.3 Recommendations

The present thesis focused on developing a mathematical model to manage the safety and integrity of conventional pipelines, then mapping into the safety of hydrogen pipelines. According to the conducted objectives, the ongoing works should be recommended as below:

1. An economic risk analysis integrated with UDC DBN is recommended to understand the most cost-intensive risk factors contributing to the high cost of asset damage due to internal corrosion and UDC in particular.
2. The recommendation is made that advanced various risk assessment methods for pipelines should be used when dangerous conditions are confronted with the best-predicting results.
3. Further research is recommended to assess how predictive maintenance can help to increase the safety of hydrogen pipelines.
4. A techno-economic analysis also is recommended for ongoing work.

9 References

- Abubakirov, R., Yang, M., & Khakzad, N. (2020). A risk-based approach to determination of optimal inspection intervals for buried oil pipelines. *Process Safety and Environmental Protection*, *134*, 95–107.
- Adumene, S., Islam, R., Dick, I. F., Zarei, E., Inegiyemiema, M., & Yang, M. (2022). Influence-Based Consequence Assessment of Subsea Pipeline Failure under Stochastic Degradation. *Energies*, *15*(20), 7460.
- Adumene, S., Khan, F., & Adedigba, S. (2020). Operational safety assessment of offshore pipeline with multiple MIC defects. *Computers and Chemical Engineering*, *138*.
<https://doi.org/10.1016/j.compchemeng.2020.106819>
- Adumene, S., Khan, F., Adedigba, S., & Zendejboudi, S. (2021). Offshore system safety and reliability considering microbial influenced multiple failure modes and their interdependencies. *Reliability Engineering & System Safety*, *215*, 107862.
- Adumene, S., Khan, F., Adedigba, S., Zendejboudi, S., & Shiri, H. (2021). Dynamic risk analysis of marine and offshore systems suffering microbial induced stochastic degradation. *Reliability Engineering & System Safety*, *207*(March 2021), 107388.
<https://doi.org/10.1016/j.ress.2020.107388>
- Al-Yaari, M. (2011). Paraffin wax deposition: mitigation & removal techniques. *SPE Saudi Arabia Section Young Professionals Technical Symposium*.
- Alabbas, F. M. (2017). MIC case histories in oil, gas, and associated operations. In *Microbiologically Influenced Corrosion in the Upstream Oil and Gas Industry* (pp. 499–516). CRC Press.
- Alabbas, F. M., & Mishra, B. (2013). Microbiologically influenced corrosion of pipelines in the oil & gas industry. *Proceedings of the 8th Pacific Rim International Congress on Advanced*

Materials and Processing, 3441–3448.

- Alamri, A. H. (2020). Localized corrosion and mitigation approach of steel materials used in oil and gas pipelines – An overview. *Engineering Failure Analysis*, 116, 104735. <https://doi.org/https://doi.org/10.1016/j.engfailanal.2020.104735>
- Ali, W., Duong, P. L. T., Khan, M. S., Getu, M., & Lee, M. (2018). Measuring the reliability of a natural gas refrigeration plant: Uncertainty propagation and quantification with polynomial chaos expansion based sensitivity analysis. *Reliability Engineering & System Safety*, 172, 103–117.
- Allan, K., Obeyesekere, N., Fell, D., Brown, T., & Bluth, M. (2012). Field sidestream testing to evaluate the effectiveness of chemicals to mitigate under deposit corrosion. *NACE - International Corrosion Conference Series*, 6, 5055–5069.
- Almahamedh, H. H. (2015). Under-Deposit Caustic Corrosion on Sodium Carbonate Pipeline. *Procedia Engineering*. <https://doi.org/10.1016/j.proeng.2015.08.026>
- Alves, D. T. S., & Lima, G. B. A. (2021). Establishing an onshore pipeline incident database to support operational risk management in Brazil-Part 2: Bowtie proposition and statistics of failure. *Process Safety and Environmental Protection*, 155, 80–97.
- Amaya-Gómez, R., Sánchez-Silva, M., Bastidas-Arteaga, E., Schoefs, F., & Munoz, F. (2019). Reliability assessments of corroded pipelines based on internal pressure—A review. *Engineering Failure Analysis*, 98, 190–214.
- Ameh, E. S., Ikpeseni, S. C., & Lawal, L. S. (2017). A review of field corrosion control and monitoring techniques of the upstream oil and gas pipelines. *Nigerian Journal of Technological Development*, 14(2), 67–73.
- Andreini, M., Gardoni, P., Pagliara, S., & Sassu, M. (2019). Probabilistic models for the erosion

- rate in embankments and reliability analysis of earth dams. *Reliability Engineering & System Safety*, 181, 142–155.
- Anwar, S., Khan, F., Zhang, Y., & Djire, A. (2021). Recent development in electrocatalysts for hydrogen production through water electrolysis. *International Journal of Hydrogen Energy*, 46(63), 32284–32317.
- Arabnejad, H., Mansouri, A., Shirazi, S. A., & McLaury, B. S. (2015). Development of mechanistic erosion equation for solid particles. *Wear*, 332, 1044–1050.
- Arakere, A., Rodriguez, M., Oostendorp, D., Swamy, P., McStravick, R., & Bridges, A. (2021). An Approach to Optimize the Wall Thickness of In-Service Pipelines. *CORROSION 2021*.
- Argenti, F., Landucci, G., Reniers, G., & Cozzani, V. (2018). Vulnerability assessment of chemical facilities to intentional attacks based on Bayesian Network. *Reliability Engineering & System Safety*, 169, 515–530.
- As, D. N. V. (2015). *Corroded pipelines*. DNV-RP-F101.
- Askari, M., Aliofkhaezai, M., & Afroukhteh, S. (2019). A comprehensive review on internal corrosion and cracking of oil and gas pipelines. *Journal of Natural Gas Science and Engineering*, 71, 102971.
- Aulia, R., Tan, H., & Sriramula, S. (2019). Prediction of Corroded Pipeline Performance Based on Dynamic Reliability Models. *Procedia CIRP*, 80, 518–523.
<https://doi.org/https://doi.org/10.1016/j.procir.2019.01.093>
- Ayello, F., Jain, S., Sridhar, N., & Koch, G. H. (2014). Quantitive assessment of corrosion probability-a Bayesian network approach. *Corrosion*, 70(11), 1128–1147.
- Aziz, N., Tanoli, S. A. K., & Nawaz, F. (2021). A programmable logic controller based remote pipeline monitoring system. *Process Safety and Environmental Protection*, 149, 894–904.

- Badida, P., Balasubramaniam, Y., & Jayaprakash, J. (2019). Risk evaluation of oil and natural gas pipelines due to natural hazards using fuzzy fault tree analysis. *Journal of Natural Gas Science and Engineering*, *66*, 284–292.
- Bensi, M., Der Kiureghian, A., & Straub, D. (2013). Efficient Bayesian network modeling of systems. *Reliability Engineering & System Safety*, *112*, 200–213.
- Bhandari, J., Khan, F., Abbassi, R., Garaniya, V., & Ojeda, R. (2015). Modelling of Pitting Corrosion in Marine and Offshore Steel Structures - A Technical Review. *Journal of Loss Prevention in the Process Industries*, *37*(December 2018), 39–62. <https://doi.org/10.1016/j.jlp.2015.06.008>
- Borgheipour, H., Tehrani, G. M., Eskandari, T., Mohammadi, O. C., & Mohammadfam, I. (2021). Dynamic risk analysis of hydrogen gas leakage using Bow-tie technique and Bayesian network. *International Journal of Environmental Science and Technology*, *18*(11), 3613–3624.
- Bougofa, M., Taleb-Berrouane, M., Bouafia, A., Baziz, A., Kharzi, R., & Bellaouar, A. (2021). Dynamic availability analysis using dynamic Bayesian and evidential networks. *Process Safety and Environmental Protection*, *153*, 486–499.
- Briottet, L., Batische, R., de Dinechin, G. de, Langlois, P., & Thiers, L. (2012). Recommendations on X80 steel for the design of hydrogen gas transmission pipelines. *International Journal of Hydrogen Energy*, *37*(11), 9423–9430.
- Brown, B., & Moloney, J. (2017). 15 - Under-deposit corrosion. In A. M. B. T.-T. in O. and G. C. R. and T. El-Sherik (Ed.), *Woodhead Publishing Series in Energy* (pp. 363–383). Woodhead Publishing. <https://doi.org/10.1016/B978-0-08-101105-8.00015-2>
- Bull, S. R. (2001). Renewable energy today and tomorrow. *Proceedings of the IEEE*, *89*(8), 1216–

1226.

- Caleyo, F., Gonzalez, J. L., & Hallen, J. M. (2002). A study on the reliability assessment methodology for pipelines with active corrosion defects. *International Journal of Pressure Vessels and Piping*, 79(1), 77–86.
- Caleyo, F., Velázquez, J. C., Valor, A., & Hallen, J. M. (2009). Probability distribution of pitting corrosion depth and rate in underground pipelines: A Monte Carlo study. *Corrosion Science*, 51(9), 1925–1934.
- Cerniauskas, S., Junco, A. J. C., Grube, T., Robinius, M., & Stolten, D. (2020). Options of natural gas pipeline reassignment for hydrogen: Cost assessment for a Germany case study. *International Journal of Hydrogen Energy*, 45(21), 12095–12107.
- Chang, Y.-C., Woollam, R., & Orazem, M. E. (2014). Mathematical Models for Under-Deposit Corrosion. *Journal of The Electrochemical Society*, 161(6), C321–C329. <https://doi.org/10.1149/2.034406jes>
- Chang, Y., Zhang, C., Shi, J., Li, J., Zhang, S., & Chen, G. (2019). Dynamic Bayesian network based approach for risk analysis of hydrogen generation unit leakage. *International Journal of Hydrogen Energy*, 44(48), 26665–26678.
- Chawla, V., Gurbuxani, P. G., & Bhagure, G. R. (2012). Corrosion of water pipes: a comprehensive study of deposits. *Journal of Minerals and Materials Characterization and Engineering*, 11(5), 479–492.
- Chen, C., Li, C., Reniers, G., & Yang, F. (2021). Safety and security of oil and gas pipeline transportation: A systematic analysis of research trends and future needs using WoS. *Journal of Cleaner Production*, 279, 123583.
- Chen, J., Gong, Y., Jiang, T.-H., Pan, A.-X., Wang, S.-H., & Yang, Z.-G. (2021). Failure analysis

- on abnormal leakage of TP321 stainless steel pipe of medium temperature shifting gas in hydrogen production system. *Engineering Failure Analysis*, 125, 105413.
- Chen, X., Li, C., Ming, N., & He, C. (2021). Effects of temperature on the corrosion behaviour of X70 steel in CO₂-Containing formation water. *Journal of Natural Gas Science and Engineering*, 88, 103815.
- Chen, X., Wang, G., Gao, F., Wang, Y., & He, C. (2015). Effects of sulphate-reducing bacteria on crevice corrosion in X70 pipeline steel under disbonded coatings. *Corrosion Science*, 101, 1–11.
- Cheng, Y. F. (2007). Fundamentals of hydrogen evolution reaction and its implications on near-neutral pH stress corrosion cracking of pipelines. *Electrochimica Acta*, 52(7), 2661–2667.
- Cruz, J. P. B., Veruz, E. G., Aoki, I. V., Schleder, A. M., de Souza, G. F. M., Vaz, G. L., de Barros, L. O., Orłowski, R. T. C., & Martins, M. R. (2022). Uniform Corrosion Assessment in Oil and Gas Pipelines Using Corrosion Prediction Models—Part 1: Models Performance and Limitations for Operational Field Cases. *Process Safety and Environmental Protection*.
- da Silva, A. F., Marins, F. A. S., Dias, E. X., & da Silva Oliveira, J. B. (2019). Modeling the uncertainty in response surface methodology through optimization and Monte Carlo simulation: an application in stamping process. *Materials & Design*, 173, 107776.
- Das, S., Bayat, A., Gay, L. F., & Matthews, J. (2018). Productivity analysis of lateral CIPP rehabilitation process using symphony simulation modeling. *Journal of Pipeline Systems Engineering and Practice*, 9(1), 4017032.
- De Cesare, F., Di Mattia, E., Zussman, E., & Macagnano, A. (2020). A 3D soil-like nanostructured fabric for the development of bacterial biofilms for agricultural and environmental uses. *Environmental Science: Nano*, 7(9), 2546–2572.

- Djukic, M. B., Bakic, G. M., Zeravcic, V. S., Sedmak, A., & Rajcic, B. (2016). Hydrogen embrittlement of industrial components: prediction, prevention, and models. *Corrosion*, 72(7), 943–961.
- Djukic, M. B., Bakic, G. M., Zeravcic, V. S., Sedmak, A., & Rajcic, B. (2019). The synergistic action and interplay of hydrogen embrittlement mechanisms in steels and iron: Localized plasticity and decohesion. *Engineering Fracture Mechanics*, 216, 106528.
- Djukic, M. B., Zeravcic, V. S., Bakic, G. M., Sedmak, A., & Rajcic, B. (2015). Hydrogen damage of steels: A case study and hydrogen embrittlement model. *Engineering Failure Analysis*, 58, 485–498.
- Durnie, W. H., Gough, M. A., & De Reus, J. A. M. (2005). Development of corrosion inhibitors to address under deposit corrosion in oil and gas production systems. *NACE - International Corrosion Conference Series*.
- El-Raghy, S. M., Abou El-Leil, H. M., & Ghazal, H. H. (2000). Microbial-induced corrosion of subsea pipeline in the Gulf of Suez. *SPE Production & Facilities*, 15(02), 126–129.
- Erdener, B. C., Sergi, B., Guerra, O. J., Chueca, A. L., Pambour, K., Brancucci, C., & Hodge, B.-M. (2022). A review of technical and regulatory limits for hydrogen blending in natural gas pipelines. *International Journal of Hydrogen Energy*.
- Fadiran, G., Adebusuyi, A. T., & Fadiran, D. (2019). Natural gas consumption and economic growth: Evidence from selected natural gas vehicle markets in Europe. *Energy*, 169, 467–477.
- Fan, T., Liu, Z., Li, M., Zhao, Y., Zuo, Z., & Guo, R. (2022). Development of cost-effective repair system for locally damaged long-distance oil pipelines. *Construction and Building Materials*, 333, 127342.

- Fang, W., Wu, J., Bai, Y., Zhang, L., & Reniers, G. (2019). Quantitative risk assessment of a natural gas pipeline in an underground utility tunnel. *Process Safety Progress*, 38(4), e12051.
- Finch, B. E., Marzoughi, S., Di Toro, D. M., & Stubblefield, W. A. (2017). Phototoxic potential of undispersed and dispersed fresh and weathered Macondo crude oils to Gulf of Mexico marine organisms. *Environmental Toxicology and Chemistry*, 36(10), 2640–2650.
- Foorginezhad, S., Mohseni-Dargah, M., Firoozirad, K., Aryai, V., Razmjou, A., Abbassi, R., Garaniya, V., Beheshti, A., & Asadnia, M. (2021). Recent advances in sensing and assessment of corrosion in sewage pipelines. *Process Safety and Environmental Protection*, 147, 192–213.
- Ge, F., Huang, F., Yuan, W., Peng, Z., Liu, J., & Cheng, Y. F. (2020). Effect of tensile stress on the hydrogen permeation of MS X65 pipeline steel under sulfide films. *International Journal of Hydrogen Energy*, 45(22), 12419–12431.
- Gósi, P., Rátkai, S., Shetty, P., Wirth, R., Maróti, G., Oszvald, F., & Knisz, J. (2022). Prediction of long-term localized corrosion rates in a carbon steel cooling water system is enhanced by metagenome analysis. *Engineering Failure Analysis*, 141, 106733.
- Guo, Y., Zhong, M., Gao, C., Wang, H., Liang, X., & Yi, H. (2021). A discrete-time Bayesian network approach for reliability analysis of dynamic systems with common cause failures. *Reliability Engineering & System Safety*, 216, 108028.
- Gupta, J., Talukdar, M. K., Velusshami, S. K., Sharma, A., & Makkar, S. (2021). Premature Failure of Submarine Well Fluid Lines: A Case Study. *Journal of Failure Analysis and Prevention*, 21(2), 363–369. <https://doi.org/10.1007/s11668-020-01051-0>
- Han, D., Jiang, R. J., & Cheng, Y. F. (2013). Mechanism of electrochemical corrosion of carbon steel under deoxygenated water drop and sand deposit. *Electrochimica Acta*, 114, 403–408.

<https://doi.org/10.1016/j.electacta.2013.10.079>

- Hasan, S., Khan, F., & Kenny, S. (2012). Probability assessment of burst limit state due to internal corrosion. *International Journal of Pressure Vessels and Piping*, *89*, 48–58.
- Hassan, S., Wang, J., Kontovas, C., & Bashir, M. (2022). An assessment of causes and failure likelihood of cross-country pipelines under uncertainty using bayesian networks. *Reliability Engineering & System Safety*, *218*, 108171.
- He, B., Han, P., Lu, C., & Bai, X. (2015). Effect of soil particle size on the corrosion behavior of natural gas pipeline. *Engineering Failure Analysis*, *58*, 19–30.
- He, H., Liu, Z., Wang, W., & Zhou, C. (2015). Microstructure and hot corrosion behavior of Co–Si modified aluminide coating on nickel based superalloys. *Corrosion Science*, *100*, 466–473.
- Hedlund, F. H., Pedersen, J. B., Sin, G., Garde, F. G., Kragh, E. K., & Frutiger, J. (2019). Puncture of an import gasoline pipeline—Spray effects may evaporate more fuel than a Buncefield-type tank overfill event. *Process Safety and Environmental Protection*, *122*, 33–47.
- Heidary, R., & Groth, K. M. (2021). A hybrid population-based degradation model for pipeline pitting corrosion. *Reliability Engineering & System Safety*, *214*, 107740.
- Hoseinieh, S. M., Homborg, A. M., Shahrabi, T., Mol, J. M. C., & Ramezanzadeh, B. (2016). A novel approach for the evaluation of under deposit corrosion in marine environments using combined analysis by electrochemical impedance spectroscopy and electrochemical noise. *Electrochimica Acta*, *217*, 226–241.
- Hou, Y., Aldrich, C., Lepkova, K., & Kinsella, B. (2018). Detection of under deposit corrosion in a CO₂ environment by using electrochemical noise and recurrence quantification analysis. *Electrochimica Acta*, *274*, 160–169.
- Ilman, M. N. (2014). Analysis of internal corrosion in subsea oil pipeline. *Case Studies in*

- Engineering Failure Analysis*, 2(1), 1–8.
- Iraji, S., & Ayatollahi, S. (2019). Experimental investigation on asphaltene biodegradability using microorganism: cell surface properties' approach. *Journal of Petroleum Exploration and Production Technology*, 9(2), 1413–1422.
- Jawwad, A. K. A., & Mohamed, I. K. (2020). The combined effects of surface texture, flow patterns and water chemistry on corrosion mechanisms of stainless steel condenser tubes. *Engineering Failure Analysis*, 109, 104390.
- Kagarise, C., Vera, J. R., & Eckert, R. B. (2017). The importance of deposit characterization in mitigating UDC and mic in dead legs. *NACE - International Corrosion Conference Series*.
- Kamil, M. Z., Khan, F., Halim, S. Z., Amyotte, P., & Ahmed, S. (2023). A methodical approach for knowledge-based fire and explosion accident likelihood analysis. *Process Safety and Environmental Protection*, 170, 339–355.
- Kamil, M. Z., Taleb-Berrouane, M., Khan, F., & Amyotte, P. (2021). Data-driven operational failure likelihood model for microbiologically influenced corrosion. *Process Safety and Environmental Protection*, 153, 472–485.
- Katerina, K., & Gubner, R. (2010). Development of standard test method for investigation of under-deposit corrosion in carbon dioxide environment and its application in oil and gas industry. *CORROSION 2010*.
- Khakzad, N., Khan, F., & Amyotte, P. (2011). Safety analysis in process facilities: Comparison of fault tree and Bayesian network approaches. *Reliability Engineering & System Safety*, 96(8), 925–932.
- Khakzad, N., Khan, F., & Amyotte, P. (2013). Dynamic safety analysis of process systems by mapping bow-tie into Bayesian network. *Process Safety and Environmental Protection*,

91(1–2), 46–53.

Khan, B., Khan, F., Veitch, B., & Yang, M. (2018). An operational risk analysis tool to analyze marine transportation in Arctic waters. *Reliability Engineering & System Safety*, 169, 485–502.

Khan, F., Yarveisy, R., & Abbassi, R. (2021). Risk-based pipeline integrity management: A road map for the resilient pipelines. *Journal of Pipeline Science and Engineering*, 1(1), 74–87. <https://doi.org/10.1016/j.jpse.2021.02.001>

Khan, M. A., Young, C., & Layzell, D. B. (2021). The Techno-economics of hydrogen pipelines. *Transition Accelerator Technical Briefs*, 1(2), 1–40.

Koch, G. (2017). Cost of corrosion. *Trends in Oil and Gas Corrosion Research and Technologies*, 3–30.

Kuang, D., & Cheng, Y. F. (2015). AC corrosion at coating defect on pipelines. *Corrosion*, 71(3), 267–276.

Laleh, M., Xu, Y., & Tan, M. Y. J. (2023). A three-dimensional electrode array probe designed for visualising complex and dynamically changing internal pipeline corrosion. *Corrosion Science*, 211, 110924.

Lam, C., & Zhou, W. (2016). Statistical analyses of incidents on onshore gas transmission pipelines based on PHMSA database. *International Journal of Pressure Vessels and Piping*, 145, 29–40.

Layzell, D. B., Young, C., Lof, J., Leary, J., & Sit, S. (2020). Towards net-zero energy systems in Canada: A key role for hydrogen. *Transition Accelerator Reports*, 2(3).

Li, J., Wang, D., & Xie, F. (2022). Failure analysis of CO₂ corrosion of natural gas pipeline under flowing conditions. *Engineering Failure Analysis*, 137, 106265.

- Li, X., Chen, Q., Li, C., Zhang, X., Tong, G., Cui, P., Lu, L., Ma, Q., Yuan, J., & Fu, A. (2022). Insights into the perforation of the L360M pipeline in the liquefied natural gas transmission process. *Engineering Failure Analysis, 140*, 106566.
- Li, X., Huang, W., Wu, X., Zhang, J., Wang, Y., Akiyama, E., & Hou, D. (2021). Effect of hydrogen charging time on hydrogen blister and hydrogen-induced cracking of pure iron. *Corrosion Science, 181*, 109200.
- Li, X., Jia, R., Zhang, R., Yang, S., & Chen, G. (2022). A KPCA-BRANN based data-driven approach to model corrosion degradation of subsea oil pipelines. *Reliability Engineering & System Safety, 219*, 108231.
- Li, X., Ma, X., Zhang, J., Akiyama, E., Wang, Y., & Song, X. (2020). Review of hydrogen embrittlement in metals: Hydrogen diffusion, hydrogen characterization, hydrogen embrittlement mechanism and prevention. *Acta Metallurgica Sinica (English Letters), 33*, 759–773.
- Liengen, T., Féron, D., Basséguy, R., & Beech, I. (2014). Understanding Biocorrosion: Fundamentals and Applications. In *Understanding Biocorrosion: Fundamentals and Applications*. <https://doi.org/10.1016/C2013-0-16468-9>
- Liu, C., Wang, Y., Li, X., Li, Y., Khan, F., & Cai, B. (2021). Quantitative assessment of leakage orifices within gas pipelines using a Bayesian network. *Reliability Engineering & System Safety, 209*, 107438.
- Liu, J., Teng, L., Liu, B., Han, P., & Li, W. (2021). Analysis of hydrogen gas injection at various compositions in an existing natural gas pipeline. *Frontiers in Energy Research, 9*, 685079.
- Liu, Y., Zhang, Y., & Yuan, J. (2014). Influence of produced water with high salinity and corrosion inhibitors on the corrosion of water injection pipe in Tuha oil field. *Engineering Failure*

Analysis, 45, 225–233.

- Lu, H., Behbahani, S., Azimi, M., Matthews, J. C., Han, S., & Iseley, T. (2020). Trenchless construction technologies for oil and gas pipelines: State-of-the-art review. *Journal of Construction Engineering and Management*, 146(6), 3120001.
- Luo, S., Fu, A., Liu, M., Xue, Y., Lv, N., & Han, Y. (2021). Stress corrosion cracking behavior and mechanism of super 13Cr stainless steel in simulated O₂/CO₂ containing 3.5 wt% NaCl solution. *Engineering Failure Analysis*, 130, 105748.
- Lynch, S. (2019). A review of underlying reasons for intergranular cracking for a variety of failure modes and materials and examples of case histories. *Engineering Failure Analysis*, 100, 329–350.
- Lynch, S. P. (2007). Progress towards understanding mechanisms of hydrogen embrittlement and stress corrosion cracking. *CORROSION 2007*.
- Mahidashti, Z., Rezaei, M., & Asfia, M. P. (2020). Internal under-deposit corrosion of X60 pipeline steel upon installation in a chloride-containing soil environment. *Colloids and Surfaces A: Physicochemical and Engineering Aspects*, 602, 125120.
- Mamudu, A., Khan, F., Zendehboudi, S., & Adedigba, S. (2021). Dynamic risk modeling of complex hydrocarbon production systems. *Process Safety and Environmental Protection*, 151, 71–84.
- Mansoori, G. A., Vazquez, D., & Shariaty-Niassar, M. (2007). Polydispersity of heavy organics in crude oils and their role in oil well fouling. *Journal of Petroleum Science and Engineering*, 58(3–4), 375–390.
- Mansoori, H., Mirzaee, R., Esmailzadeh, F., Vojood, A., & Dowrani, A. S. (2017). Pitting corrosion failure analysis of a wet gas pipeline. *Engineering Failure Analysis*, 82, 16–25.

- Marin, G. D., Naterer, G. F., & Gabriel, K. (2010). Rail transportation by hydrogen vs. electrification—case study for Ontario Canada, I: propulsion and storage. *International Journal of Hydrogen Energy*, 35(12), 6084–6096.
- Martin, M. L., & Sofronis, P. (2022). Hydrogen-induced cracking and blistering in steels: A review. *Journal of Natural Gas Science and Engineering*, 104547.
- Matzen, M. J., Alhajji, M. H., & Demirel, Y. (2015). *Technoeconomics and sustainability of renewable methanol and ammonia productions using wind power-based hydrogen*.
- Mazumder, R. K., Fan, X., Salman, A. M., Li, Y., & Yu, X. (2020). Framework for seismic damage and renewal cost analysis of buried water pipelines. *Journal of Pipeline Systems Engineering and Practice*, 11(4), 4020038.
- Melaina, M. W., Antonia, O., & Penev, M. (2013). *Blending hydrogen into natural gas pipeline networks: a review of key issues*.
- Mohammadfam, I., & Zarei, E. (2015). Safety risk modeling and major accidents analysis of hydrogen and natural gas releases: A comprehensive risk analysis framework. *International Journal of Hydrogen Energy*, 40(39), 13653–13663.
- Moradi, R., Cofre-Martel, S., Droguett, E. L., Modarres, M., & Groth, K. M. (2022). Integration of deep learning and Bayesian networks for condition and operation risk monitoring of complex engineering systems. *Reliability Engineering & System Safety*, 222, 108433.
- Nandi, M., Vyas, N., Vij, R. K., & Gupta, P. (2022). A review on natural gas ecosystem in India: Energy scenario, market, pricing assessment with the developed part of world and way forward. *Journal of Natural Gas Science and Engineering*, 104459.
- Nanninga, N., Slifka, A., Levy, Y., & White, C. (2010). A review of fatigue crack growth for pipeline steels exposed to hydrogen. *Journal of Research of the National Institute of*

Standards and Technology, 115(6), 437.

- Netto, T. A., Ferraz, U. S., & Estefen, S. F. (2005). The effect of corrosion defects on the burst pressure of pipelines. *Journal of Constructional Steel Research*, 61(8), 1185–1204.
- Nguyen, T. T., Heo, H. M., Park, J., Nahm, S. H., & Beak, U. B. (2021). Stress concentration affecting hydrogen-assisted crack in API X70 pipeline base and weld steel under hydrogen/natural gas mixture. *Engineering Failure Analysis*, 122, 105242.
- Nong, D., Nguyen, T. H., Wang, C., & Van Khuc, Q. (2020). The environmental and economic impact of the emissions trading scheme (ETS) in Vietnam. *Energy Policy*, 140, 111362.
- Obot, I. B. (2021a). Under-deposit corrosion on steel pipeline surfaces: mechanism, mitigation and current challenges. *Journal of Bio-and Tribo-Corrosion*, 7(2), 1–14.
- Obot, I. B. (2021b). Under-Deposit Corrosion on Steel Pipeline Surfaces: Mechanism, Mitigation and Current Challenges. *Journal of Bio- and Tribo-Corrosion*, 7(2).
<https://doi.org/10.1007/s40735-021-00485-9>
- Ohtsu, M., Kobayashi, K., Kawazoe, T., Sangu, S., & Yatsui, T. (2002). Nanophotonics: design, fabrication, and operation of nanometric devices using optical near fields. *IEEE Journal of Selected Topics in Quantum Electronics*, 8(4), 839–862.
- Okodi, A., Li, Y., Cheng, R., Kainat, M., Yoosef-Ghodsi, N., & Adeeb, S. (2020). Crack propagation and burst pressure of pipeline with restrained and unrestrained concentric dent-crack defects using extended finite element method. *Applied Sciences*, 10(21), 7554.
- Okoro, A., Khan, F., & Ahmed, S. (2022). A methodology for time-varying resilience quantification of an offshore natural gas pipeline. *Journal of Pipeline Science and Engineering*, 2(2), 100054.
- Okunlola, A., Giwa, T., Di Lullo, G., Davis, M., Gemechu, E., & Kumar, A. (2022). Techno-

- economic assessment of low-carbon hydrogen export from Western Canada to Eastern Canada, the USA, the Asia-Pacific, and Europe. *International Journal of Hydrogen Energy*, 47(10), 6453–6477.
- Oliveira, A. M., Beswick, R. R., & Yan, Y. (2021). A green hydrogen economy for a renewable energy society. *Current Opinion in Chemical Engineering*, 33, 100701.
- Ossai, C. I., Boswell, B., & Davies, I. J. (2015). Pipeline failures in corrosive environments - A conceptual analysis of trends and effects. *Engineering Failure Analysis*, 53, 36–58. <https://doi.org/10.1016/j.engfailanal.2015.03.004>
- Östürk, Ö., & Sevimoğlu, O. (2021). Trace elements microanalysis of metal oxides in deposit formed on combustion chamber surface of landfill gas engine using focused ion beam/scanning electron microscopy technique. *Engineering Failure Analysis*, 123, 105297.
- Pang, L., Wang, Z. B., Lu, M. H., Lu, Y., Liu, X., & Zheng, Y. G. (2021). Inhibition performance of benzimidazole derivatives with different heteroatoms on the under-deposit corrosion of carbon steel in CO₂-saturated solution. *Corrosion Science*, 192, 109841.
- Pang, L., Wang, Z., Emori, W., & Zheng, Y. (2021). Under-Deposit Corrosion of Carbon Steel Beneath Full Coverage of CaCO₃ Deposit Layer under Different Atmospheres. *Journal of Materials Engineering and Performance*, 30, 7552–7563.
- Papavinasam, S., Doiron, A., & Revie, R. W. (2010). Model to predict internal pitting corrosion of oil and gas pipelines. *Corrosion*, 66(3), 35006.
- Pareek, A., Dom, R., Gupta, J., Chandran, J., Adepu, V., & Borse, P. H. (2020). Insights into renewable hydrogen energy: Recent advances and prospects. *Materials Science for Energy Technologies*, 3, 319–327.
- Patel, M., Roy, S., Roskilly, A. P., & Smallbone, A. (2022). The techno-economics potential of

- hydrogen interconnectors for electrical energy transmission and storage. *Journal of Cleaner Production*, 335, 130045.
- PHMSA. (2017). *Data and Statistics*.
- Place, T. D., Holm, M. R., Cathrea, C., & Ignacz, T. (2009). Understanding and mitigating large pipe under deposit corrosion. *Mat. Perf*, 54–61.
- Polyanskiy, V. A., Belyaev, A. K., Polyanskiy, A. M., Tretyakov, D. A., & Yakovlev, Y. A. (2022). Hydrogen Embrittlement as a Surface Phenomenon in Deformed Metals. *Physical Mesomechanics*, 25(5), 404–412.
- Popov, B. N., Lee, J.-W., & Djukic, M. B. (2018). Hydrogen permeation and hydrogen-induced cracking. In *Handbook of environmental degradation of materials* (pp. 133–162). Elsevier.
- Qiao, Q., Cheng, G., Li, Y., Wu, W., Hu, H., & Huang, H. (2017). Corrosion failure analyses of an elbow and an elbow-to-pipe weld in a natural gas gathering pipeline. *Engineering Failure Analysis*, 82, 599–616.
- Qin, H., Zhou, W., & Zhang, S. (2015). Bayesian inferences of generation and growth of corrosion defects on energy pipelines based on imperfect inspection data. *Reliability Engineering & System Safety*, 144, 334–342.
- Ramirez, E., González-Rodríguez, J. G., Torres-Islas, A., Serna, S., Campillo, B., Dominguez-Patiño, G., & Juárez-Islas, J. A. (2008). Effect of microstructure on the sulphide stress cracking susceptibility of a high strength pipeline steel. *Corrosion Science*, 50(12), 3534–3541.
- Ríos-Mercado, R. Z., & Borraz-Sánchez, C. (2015). Optimization problems in natural gas transportation systems: A state-of-the-art review. *Applied Energy*, 147, 536–555.
- Ronevich, J. A., & San Marchi, C. W. (2017). *Assessment of Hydrogen Assisted Fatigue in Steel*

Pipelines. Sandia National Lab.(SNL-NM), Albuquerque, NM (United States).

- Roubos, A. A., Allaix, D. L., Schweckendiek, T., Steenbergen, R. D. J. M., & Jonkman, S. N. (2020). Time-dependent reliability analysis of service-proven quay walls subject to corrosion-induced degradation. *Reliability Engineering & System Safety*, 203, 107085. <https://doi.org/https://doi.org/10.1016/j.ress.2020.107085>
- Ryu, H. K., & Yoon, K. B. (2021). Leak failure at the TP316L welds of a water pipe caused by microbiologically influenced corrosion. *Engineering Failure Analysis*, 122, 105244.
- Sahraoui, Y., & Chateauneuf, A. (2016). The effects of spatial variability of the aggressiveness of soil on system reliability of corroding underground pipelines. *International Journal of Pressure Vessels and Piping*, 146, 188–197.
- Sajid, Z. (2021). A dynamic risk assessment model to assess the impact of the coronavirus (COVID-19) on the sustainability of the biomass supply chain: A case study of a US biofuel industry. *Renewable and Sustainable Energy Reviews*, 151, 111574.
- Sajid, Z., Khan, F., & Veitch, B. (2020). Dynamic ecological risk modelling of hydrocarbon release scenarios in Arctic waters. *Marine Pollution Bulletin*, 153, 111001.
- Sajid, Z., Khan, F., & Zhang, Y. (2017a). Integration of interpretive structural modelling with Bayesian network for biodiesel performance analysis. *Renewable Energy*, 107, 194–203.
- Sajid, Z., Khan, F., & Zhang, Y. (2017b). Integration of interpretive structural modelling with Bayesian network for biodiesel performance analysis. *Renewable Energy*, 107. <https://doi.org/10.1016/j.renene.2017.01.058>
- Sajid, Z., Khan, F., & Zhang, Y. (2018). A novel process economics risk model applied to biodiesel production system. *Renewable Energy*, 118, 615–626.
- Sarwar, A., Khan, F., James, L., & Abimbola, M. (2018). Integrated offshore power operation

- resilience assessment using Object Oriented Bayesian network. *Ocean Engineering*, 167, 257–266.
- Schmitt, G., Schütze, M., & Hays, G. F. (2009). Global needs for knowledge dissemination, research, and development in materials deterioration and corrosion control. *World Corrosion Organization*, 38, 14.
- Senatore, E. V, Taleb, W., Owen, J., Hua, Y., Gomes, J. A. C. P., Barker, R., & Neville, A. (2018). Evaluation of high shear inhibitor performance in CO₂-containing flow-induced corrosion and erosion-corrosion environments in the presence and absence of iron carbonate films. *Wear*, 404, 143–152.
- Shabarchin, O., & Tesfamariam, S. (2016). Internal corrosion hazard assessment of oil & gas pipelines using Bayesian belief network model. *Journal of Loss Prevention in the Process Industries*, 40, 479–495.
- Sharma, S., & Ghoshal, S. K. (2015). Hydrogen the future transportation fuel: From production to applications. *Renewable and Sustainable Energy Reviews*, 43, 1151–1158.
- Shekari, E., Khan, F., & Ahmed, S. (2017a). Economic risk analysis of pitting corrosion in process facilities. *International Journal of Pressure Vessels and Piping*, 157, 51–62.
- Shekari, E., Khan, F., & Ahmed, S. (2017b). Probabilistic modeling of pitting corrosion in insulated components operating in offshore facilities. *ASCE-ASME J Risk and Uncert in Engrg Sys Part B Mech Engrg*, 3(1).
- Shukla, P. K., & Naraian, S. (2017). Under-deposit corrosion in a sub-sea water injection pipeline- A case study. *NACE - International Corrosion Conference Series*.
- Skovhus, T. L., Eckert, R. B., & Rodrigues, E. (2017). Management and control of microbiologically influenced corrosion (MIC) in the oil and gas industry—Overview and a

- North Sea case study. *Journal of Biotechnology*, 256(December 2016), 31–45.
<https://doi.org/10.1016/j.jbiotec.2017.07.003>
- Sliem, M. H., Fayyad, E. M., Abdullah, A. M., Younan, N. A., Al-Qahtani, N., Nabhan, F. F., Ramesh, A., Laycock, N., Ryan, M. P., Maqbool, M., & Arora, D. (2021). Monitoring of under deposit corrosion for the oil and gas industry: A review. *Journal of Petroleum Science and Engineering*, 204(April), 108752. <https://doi.org/10.1016/j.petrol.2021.108752>
- Sørensen, K. B., Thomsen, U. S., Juhler, S., & Larsen, J. (2012). Cost efficient MIC management system based on molecular microbiological methods. *NACE - International Corrosion Conference Series*.
- Suarez, E., Machuca, L., & Lepkova, K. (2019). The role of bacteria in under-deposit corrosion in oil and gas facilities: A review of mechanisms, test methods and corrosion inhibition. *Corrosion and Materials*.
- Subramanian, C. (2018). Localized pitting corrosion of API 5L grade A pipe used in industrial fire water piping applications. *Engineering Failure Analysis*, 92, 405–417.
- Subramanian, C., Ghosh, D., Reddy, D. S., Ghosh, D., Natarajan, R., & Velavan, S. P. (2022). Stress corrosion cracking of U tube heat exchanger used for low pressure steam generation in a hydrogen unit of petroleum refinery. *Engineering Failure Analysis*, 137, 106245.
- Tajallipour, N., Zhu, Z., Teevens, P. J., & Place, T. (2011). Modeling of Solids Deposition for a Heavy Crude Oil Pipeline Using enpICDATM–SRC. *Rio Pipeline Conference*.
- Taleb-Berrouane, M., Khan, F., & Amyotte, P. (2020). Bayesian Stochastic Petri Nets (BSPN)-A new modelling tool for dynamic safety and reliability analysis. *Reliability Engineering & System Safety*, 193, 106587.
- Taleb-Berrouane, M., Khan, F., & Hawboldt, K. (2021). Corrosion risk assessment using adaptive

- bow-tie (ABT) analysis. *Reliability Engineering & System Safety*, 214, 107731.
- Taleb-berrouane, M., Khan, F., Hawboldt, K., Eckert, R., & Skovhus, T. L. (2018). Model for microbiologically influenced corrosion potential assessment for the oil and gas industry. *Corrosion Engineering, Science and Technology*, 1–15.
<https://doi.org/10.1080/1478422X.2018.1483221>
- Tee, K. F., & Pesinis, K. (2017). Reliability prediction for corroding natural gas pipelines. *Tunnelling and Underground Space Technology*, 65, 91–105.
- Thodi, P., Khan, F., & Haddara, M. (2013). Risk based integrity modeling of offshore process components suffering stochastic degradation. *Journal of Quality in Maintenance Engineering*, 19(2), 157–180.
- Tong, K., Bai, X., Fan, Z., Cheng, L., Lyu, J., Han, X., & Qu, T. (2022). Analysis and investigation of the leakage failure on the shale gas gathering and transmission pipeline. *Engineering Failure Analysis*, 140, 106599.
- Torkzaban, S., Tazehkand, S. S., Walker, S. L., & Bradford, S. A. (2008). Transport and fate of bacteria in porous media: Coupled effects of chemical conditions and pore space geometry. *Water Resources Research*, 44(4).
- Vanaei, H. R., Eslami, A., & Egbewande, A. (2017). A review on pipeline corrosion, in-line inspection (ILI), and corrosion growth rate models. In *International Journal of Pressure Vessels and Piping* (Vol. 149, pp. 43–54). Elsevier Ltd.
<https://doi.org/10.1016/j.ijpvp.2016.11.007>
- Venzlaff, H., Enning, D., Srinivasan, J., Mayrhofer, K. J. J., Hassel, A. W., Widdel, F., & Stratmann, M. (2013). Accelerated cathodic reaction in microbial corrosion of iron due to direct electron uptake by sulfate-reducing bacteria. *Corrosion Science*, 66, 88–96.

- Vera, J. R., Daniels, D., & Achour, M. H. (2012). Under deposit corrosion (UDC) in the oil and gas industry: a review of mechanisms, testing and mitigation. *CORROSION 2012*.
- Wang, H., Tong, Z., Zhou, G., Zhang, C., Zhou, H., Wang, Y., & Zheng, W. (2022). Research and demonstration on hydrogen compatibility of pipelines: A review of current status and challenges. *International Journal of Hydrogen Energy*.
- Wang, Q., Ai, M., Shi, W., Lyu, Y., & Yu, W. (2020). Study on corrosion mechanism and its influencing factors of a short distance intermittent crude oil transmission and distribution pipeline. *Engineering Failure Analysis, 118*, 104892.
- Wang, Q., Wu, W., Li, Q., Zhang, D., Yu, Y., Cao, B., & Liu, Z. (2021). Under-deposit corrosion of tubing served for injection and production wells of CO₂ flooding. *Engineering Failure Analysis, 127*, 105540.
- Wang, W., Liu, X., Ma, Y., & Liu, S. (2021). A new approach for occupational risk evaluation of natural gas pipeline construction with extended cumulative prospect theory. *International Journal of Fuzzy Systems, 23*, 158–181.
- Wang, W., Zhang, Y., Li, Y., Hu, Q., Liu, C., & Liu, C. (2022). Vulnerability analysis method based on risk assessment for gas transmission capabilities of natural gas pipeline networks. *Reliability Engineering & System Safety, 218*, 108150.
- Wang, X., & Melchers, R. E. (2017). Long-term under-deposit pitting corrosion of carbon steel pipes. *Ocean Engineering, 133*(May 2016), 231–243.
<https://doi.org/10.1016/j.oceaneng.2017.02.010>
- Wang, Z. B., Pang, L., & Zheng, Y. G. (2022). A review on under-deposit corrosion of pipelines in oil and gas fields: testing methods, corrosion mechanisms and mitigation strategies. *Corrosion Communications*.

- Wang, Z., Zhou, Z., Xu, W., Yang, L., Zhang, B., & Li, Y. (2020). Study on inner corrosion behavior of high strength product oil pipelines. *Engineering Failure Analysis*, *115*, 104659.
- Wasim, M., & Djukic, M. B. (2022). External corrosion of oil and gas pipelines: a review of failure mechanisms and predictive preventions. *Journal of Natural Gas Science and Engineering*, 104467.
- Weidl, G., Madsen, A. L., & Israelson, S. (2005). Applications of object-oriented Bayesian networks for condition monitoring, root cause analysis and decision support on operation of complex continuous processes. *Computers & Chemical Engineering*, *29*(9), 1996–2009.
- Winters, M. A., Stokes, P. S. N., Zuniga, P. O., & Schlottenmier, D. J. (1993). Real-time performance monitoring of fouling and under-deposit corrosion in cooling water systems. *Corrosion Science*, *35*(5–8), 1667–1675.
- Witek, M. (2016). Gas transmission pipeline failure probability estimation and defect repairs activities based on in-line inspection data. *Engineering Failure Analysis*, *70*, 255–272.
- Witek, M. (2018). *Steel pipeline failure probability evaluation based on in-line inspection results*. Department of Power Engineering and Gas Heating Systems.
- Witek, M., Batura, A., Orynyak, I., & Borodii, M. (2018). An integrated risk assessment of onshore gas transmission pipelines based on defect population. *Engineering Structures*, *173*, 150–165.
- Witkowski, A., Rusin, A., Majkut, M., & Stolecka, K. (2017). Comprehensive analysis of hydrogen compression and pipeline transportation from thermodynamics and safety aspects. *Energy*, *141*, 2508–2518.
- Xiang, D., Li, P., & Yuan, X. (2022). Process optimization, exergy efficiency, and life cycle energy consumption-GHG emissions of the propane-to-propylene with/without hydrogen production process. *Journal of Cleaner Production*, *367*, 133024.

- Xie, S., Dong, S., Chen, Y., Peng, Y., & Li, X. (2021). A novel risk evaluation method for fire and explosion accidents in oil depots using bow-tie analysis and risk matrix analysis method based on cloud model theory. *Reliability Engineering & System Safety*, 215, 107791.
- Yang, F., Wang, T., Deng, X., Dang, J., Huang, Z., Hu, S., Li, Y., & Ouyang, M. (2021). Review on hydrogen safety issues: Incident statistics, hydrogen diffusion, and detonation process. *International Journal of Hydrogen Energy*, 46(61), 31467–31488.
- Yang, Y., Khan, F., Thodi, P., & Abbassi, R. (2017). Corrosion induced failure analysis of subsea pipelines. *Reliability Engineering & System Safety*, 159, 214–222.
- Yang, Y., Luo, X., Elsayed, Y. E. A. N., Hong, C., Yadav, A., Rogowska, M., & Ambat, R. (2021). Characteristics of scales and their impacts on under-deposit corrosion in an oil production well. *Materials and Corrosion*, 72(6), 1051–1064.
- Yazdi, M., Khan, F., & Abbassi, R. (2021). Microbiologically influenced corrosion (MIC) management using Bayesian inference. *Ocean Engineering*, 226(September 2020), 108852. <https://doi.org/10.1016/j.oceaneng.2021.108852>
- Yazdi, M., Khan, F., & Abbassi, R. (2022). Operational subsea pipeline assessment affected by multiple defects of microbiologically influenced corrosion. *Process Safety and Environmental Protection*, 158, 159–171.
- Yazdi, M., Khan, F., Abbassi, R., & Quddus, N. (2022). Resilience assessment of a subsea pipeline using dynamic Bayesian network. *Journal of Pipeline Science and Engineering*, 2(2), 100053.
- Yoo, B.-H., Wilailak, S., Bae, S.-H., Gye, H.-R., & Lee, C.-J. (2021). Comparative risk assessment of liquefied and gaseous hydrogen refueling stations. *International Journal of Hydrogen Energy*, 46(71), 35511–35524.
- Yoon, H.-J., Seo, S.-K., & Lee, C.-J. (2022). Multi-period optimization of hydrogen supply chain

- utilizing natural gas pipelines and byproduct hydrogen. *Renewable and Sustainable Energy Reviews*, 157, 112083.
- Yuan, S., Wu, J., Zhang, X., & Liu, W. (2019). EnKF-based estimation of natural gas release and dispersion in an underground tunnel. *Journal of Loss Prevention in the Process Industries*, 62, 103931.
- Yuan, Y., Zhang, G., Fang, H., Su, D., & Wang, F. (2022). Microbial Spatial Distribution and Corrosion Evaluation in Urban Sewer Systems with Different Service Lives. *Engineering Failure Analysis*, 106482.
- Zelmati, D., Bouledroua, O., Hafsi, Z., & Djukic, M. B. (2020). Probabilistic analysis of corroded pipeline under localized corrosion defects based on the intelligent inspection tool. *Engineering Failure Analysis*, 115, 104683.
- Zhang, H., & Tian, Z. (2022). Failure analysis of corroded high-strength pipeline subject to hydrogen damage based on FEM and GA-BP neural network. *International Journal of Hydrogen Energy*, 47(7), 4741–4758.
[https://doi.org/https://doi.org/10.1016/j.ijhydene.2021.11.082](https://doi.org/10.1016/j.ijhydene.2021.11.082)
- Zhang, S., & Zhou, W. (2013). System reliability of corroding pipelines considering stochastic process-based models for defect growth and internal pressure. *International Journal of Pressure Vessels and Piping*, 111, 120–130.
- Zhang, Y., Liu, B., She, X., Luo, Y., Sun, Q., & Teng, L. (2022). Numerical study on the behavior and design of a novel multistage hydrogen pressure-reducing valve. *International Journal of Hydrogen Energy*, 47(32), 14646–14657.
- Zhao, J. (2014). *Risk management for pitting corrosion*. University of Akron.
- Zhao, R., Wang, B., Li, D., Chen, Y., & Zhang, Q. (2022). Effect of sulfate-reducing bacteria from

salt scale of water flooding pipeline on corrosion behavior of X80 steel. *Engineering Failure Analysis*, 106788.

Zvirko, O. I., Savula, S. F., Tsependa, V. M., Gabetta, G., & Nykyforchyn, H. M. (2016). Stress corrosion cracking of gas pipeline steels of different strength. *Procedia Structural Integrity*, 2, 509–516.